Regulation of mitochondrial dynamics in adipose tissue

by

Ciara McCarthy

A thesis submitted in fulfilment of the requirements

for the degree of

Doctor of Philosophy

Molecular Organisation and Assembly of Cells

Doctoral Training Centre, University of Warwick.

July 2014.

Table of contents

List of figures and tables

Chapter 1. Introduction

Chapter 2. Adiposity and mitochondrial dynamics

Chapter 3: Bariatric surgery: effects on markers of mitochondrial fusion and fission expression

Chapter 4: The role of p38 in mitochondrial dynamics

Chapter 5. Molecular modelling of p38 and selection of exemplars of putative p38 isoform selective inhibitors from the AZ compound collection

Acknowledgments

Thank you to my supervisors Dr. Gyanendra Tripathi, Dr. Philip McTernan and Dr. Graeme Robb for their invaluable support, knowledge and guidance over the years. I would also like to thank Dr. Adaikala Antonysunil, Dr. Alison Harte, Dr. Mingzhan Xue, Philip Voyias and Warunee Kumsaiyai for their technical support and Shaun Sabico for his advice and guidance with the statistical analysis of human samples. I would like to thank Dr. Graeme Robb at AstraZeneca for the kinase assay data (Table 5) and for advice and discussions on analysis and presentation of figures for this chapter. I would also like to thank, Dr. Anatoly Shmygol for training and technical assistance in confocal imaging of 3T3 preadipocytes. Finally, to Professor Dmitiris Grammatopoulis,Dr. Hugo van den Berg of the University of Warwick and Dr. Graeme Robb of AstraZeneca for their research suggestions, discussions and advice throughout the PhD.

With regards to samples, I would like to thank Dr. Ioannis Kyrou at the University of Warwick and our collaborators in the Czech Republic, whose cooperation supplied the bariatric surgery adipose tissue samples and fasting glucose and insulin data for this study. The MKK6 (Glu) plasmid for the genetic overexpression work was ordered through Addgene and provided by Roger Davis. Samples for the adiposity study were kindly provided through a collaboration with University Hospital Coventry and Warwickshire. Lastly, many thanks to Dr. Milan Piya and Sean James who helped establish and coordinate the collection of these samples.

Declaration

I declare that this thesis is a record of results obtained by myself and, is composed by myself, unless otherwise stated in the text in the acknowledgments. None of the work has previously been submitted for a higher degree. Sources have been specifically acknowledged by means of reference.

Summary

This thesis advances the understanding of mitochondrial dynamics in adipocytes. Chapter 1 outlines mitochondrial dynamics, health, function and quality control in the context of obesity and T2DM. Chapters 2 and 3 are concerned with characterising mitochondrial dynamics in human abdominal subcutaneous adipose tissue and how the balance of this process may be augmented by adiposity and bariatric surgery. As an extension of this, Chapter 4 explores the potential regulatory role of p38 within adipogenesis in the 3T3-L1 cell line model together with the interplay between p38 and mitochondrial dynamics throughout differentiation. As part of this study, the impact of modulating p38 by chemical means or via the introduction of an overexpression vector was used to investigate the functional consequences of this gene on mitochondrial bioenergetics. The subtle balance of mitochondrial fusion and fusion markers is critical, not only for controlling the abundance and bioenergetic health of mitochondria but also, for overall cellular health. Finally, Chapter 5 extends analysis of the regulatory role of p38 on mitochondrial dynamics through computational modelling of the p38β . From the entire AstraZeneca compound collection, a series of novel and putative p38β inhibitors were selected for further functional assays to assess the effect of these compounds on mitochondrial bioenergetics in 3T3-L1.

Abbreviations

A	Absorbance
AbSc	Abdominal subcutaneous
AbSc AT	Abdominal subcutaneous adipose tissue
Ad	Adipocyte
AT	Adipose tissue
ATP	Adenosine triphosphate
ANOVA	Analysis of Covariance
β-actin	Beta actin
BMI	Body mass Index
BPD	Biliopancreatic diversion
C.E	Coupling efficiency
C/EBP	CCAAT-enhancer-binding protein
C-NMR	Carbon-Nuclear magnetic resonance
CRP	C-reactive protein
CT	Cycle threshold
CVD	Cardiovascular disease
CytB	Cytochrome B
Da	Daltons
dCt	Delta threshold cycle
DEPA	Diethyl pyrocarbinate
dH2O	Distilled water
DMEM	Dulbecco's Minimum Essential Medium
DMSO	Dimethlysulphoxide
DN	Dominant negative
DNA	Deoxyribonucleic acid
DNase	Deoxyribonuclease
dNTPs	Deoxynucleotides triphosphates
DTT	Dithiothreitol
EBI	European Bioinformatics Institute
ECL	Enhanced chemiluminescence
EDTA	Ethylenediaminetetraacetic Acid
ER	Endoplasmic reticulum
FCCP	p-trifluromethoxyphenylhydrazone
GB	Gastric banding
GLUT-4	Glucose-transporter-4
GTP	Guanosine triphosphate
HEPES	4-(2-hydroxyethyl)-1-piperazineethanesulphonic acid
HMW	High molecular weight
H_20	Water
HOMA-IR	Homeostasis Model of Assessment for Insulin resistance

hr	hour
HRP	Horseradish Peroxidase
IMM	Inner mitochondrial membrane
kDa	Kilodaltons
L	Lean (results figures only)
L	Litre
LMW	Lipopolysaccharide
LPS	Low molecular weight
MAPK	Mitogen-activated Kinase
Mfn1/2	Mitofusin 1/2
mg	milligrams
min	minute
ml	milliliter
mm	miliimetres
mM	millimolar
MMPs	Matrix metalloproteases
mRNA	messenger RNA
MS	Metabolic Syndrome
mtDNA	Mitochondrial DNA
mQH_2O	milliQ water (ultra filtered water)
MW	Molecular weight
NaCl	Sodium Chloride
ng	Nanometers
nm	nanograms
nM	nanomolar
nDNA	Nuclear DNA
N.S	non significant
NADH	Nicotinamide adenine dinucleotide
Ob	Obese
OD	Optical density
O.E	Overexpression
Om	Omental
OMM	Outer mitochondrial membrane
Opa1	Optic atrophy 1
Ov	Overweight
PBS	Phosphate buffered saline
PBS-T	Phosphate-buffered Saline containing 0.1% Tween 20
PPAR-γ	Peroxisome Proliferator Activated Receptor gamma
PVDF	Polyvinylidene-fluoride
RIPA	Radio-Immunoprecipitation Assay
RNAi	Ribonucleic acid interference
ROS	Reactive Oxygen Species

RT-PCR	Reverse transcriptase-polymerase chain reaction
qRT-PCR	Quantitative reverse transcriptase polymerase chain reaction
R^2	Correlation coefficient
S.D	Standard Deviation
SDS	Sodium dodecyl sulphate
SDS-PAGE	Sodium dodecyl sulphate-polyacryamide gel electrophoresis
S.E.M	Standard error of the mean
SG	Sleeve gastronectomy
SPSS	Statistical package for the social sciences
SRC	Spare respiratory capacity
TBS	Tris-buffered Saline
TCA	Trichloric acid
TEMED	Tetramethylethelenediamine
T2DM	Type 2 Diabetes Mellitus
TZD	Thiozoladinediones
µg	micrograms
UV	ultraviolet
v/v	Ratio of Volume per Volume
w/v	Weight per Volume
WAT	White adipose tissue
WHO	World Health Organisation
yrs	Years

Chapter 1: Introduction.

1.1 Obesity and T2DM.

1.1.1 *Definition of Obesity and T2DM.*

Obesity is a key contributory factor in the development of insulin resistance (Fernandez-Sanchez, Madrigal-Santillan et al. 2011). The excess accumulation of fat in both overweight (BMI ≥ 25 kg/m^2) and obese (BMI ≥ 30 kg/m^2) individuals results in 2.8 million deaths per year (World Health Organization.). The co-existence of insulin resistance and obesity are known as significant risk factors for the development of Type 2 Diabetes Mellitus (T2DM) (Bastard, Maachi et al. 2006, Abdullah, Peeters et al. 2010).

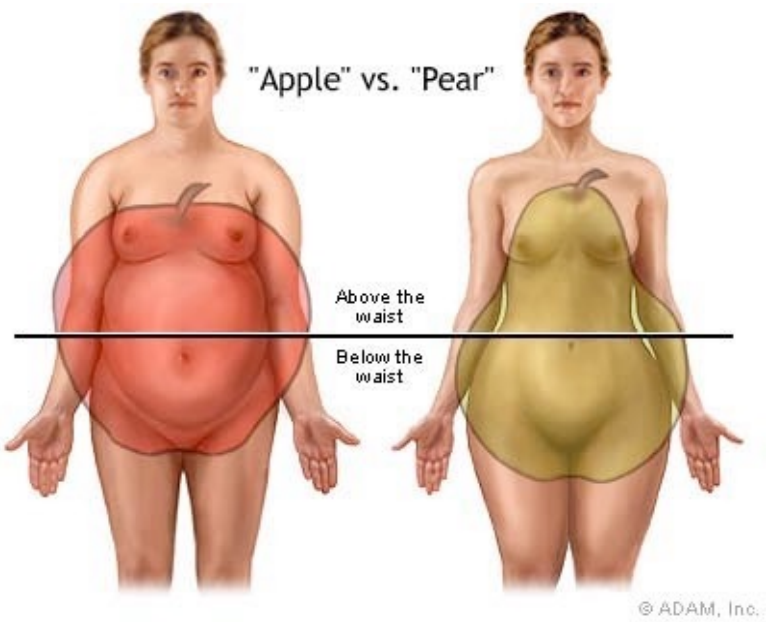

Figure 1.1. Central vs peripheral fat depots. Central fat accumulation (subcutaneous or visceral adipose tissue) is referred to colloquially as an 'apple' shape (left) whilst peripheral deposition of fat (thighs, hips, buttocks) is termed as a 'pear' body type (right). Image taken from http://averaorg.adam.com.

1.1.2. Prevalence and financial impact of obesity.

T2DM accounts for 90% of all diagnosed cases of diabetes (Diabetes UK). T2DM develops by one of two mechanisms, an inability of pancreatic beta cells to produce sufficient insulin or the development of cellular insensitivity to insulin (i nsulin resistance (IR)) (DeFronzo 2004). The consequence of IR is the inability to control blood glucose (Nesher, Della Casa et al. 1987, Covey, Wideman et al. 2006, Bao, Jacobson et al. 2008) and onset of hyperglycaemia (Mah and Bruno 2012). Typically, T2DM develops and is diagnosed in Caucasians over 40 years of age (1994, Sharp, Grunwald et al. 2003, Gujral, Pradeepa et al. 2013). However, in south Asians, T2DM can occur as early as 25 (Diabetes UK). South Asians exhibit a greater tendency than Caucasian cases towards central lipid storage in the abdominal and visceral adipose tissue depots (Morris, Velkoska et al. 2005, Nystad, Melhus et al. 2010, Cai 2013, Ali, Cerjak et al. 2014). Meta-analysis of the risk factors for the development of diabetes, indicate that 80-85% can be explained by obesity (Abdullah, Peeters et al. 2010). Between 1993 and 2011, obesity increased from 13 to 24% in men and 16 to 26% of women (NHS). Together with the trend towards increasing adiposity, cases of diabetes are set to double, in percentage terms, from 5% of the UK population in 2011, to 5 million people (~12% of today's population) (Statistics from World Health Organisation, WHO). In conjunction with the requirement for pharmacological control of diabetes and treatment of obesity, these conditions are often associated with secondary complications including vascular diseases such as coronary artery disease, peripheral vascular disease, renal diseases and ophthalmological disease, which could lead to blindness and peripheral nerve damage causing neuropathy (Sharp, Grunwald et al. 2003). In 2035, the financial cost of treating diabetes and its associated complications is estimated to

reach £39.8 billion (Farzadfar, Finucane et al. 2011). Given the public health burden of diabetes and obesity globally, understanding at a molecular level, the regulation of insulin sensitivity and diabetes, is of vital significance.

1.1.3. *Adipose tissue; central vs peripheral obesity.*

Adipose tissue is the primary storage depot for excess nutritional intake. During conditions of nutrient excess, adipocytes store excess dietary lipids as triglycerides (Rajala and Scherer 2003). Excess dietary intake can be stored centrally (subcutaneous or visceral AT) or in peripheral regions (hips, thighs, buttocks) (Rosen and Spiegelman 2006) (Figure 1.1). Deposition of excess triglycerides centrally is a major risk factor for the onset of metabolic conditions including but not limited to, cardiovascular disease and T2DM (Jung and Choi 2014).

1.1.4. *Adipose tissue remodelling in obesity.*

Adipocytes are capable of cellular remodelling. The inherent flexibility of adipocytes enables them to dynamically increase their number and size in response to conditions of nutrient excess (Lemoine, Ledoux et al. 2012). Adipose tissue remodelling can occur in one of two ways; through increased adipose tissue number (hyperplasia) or volume (hypertrophy) (Figure 1.2). The ability of adipocytes to store excess dietary intake as triglycerides is finite and this capacity differs between individuals (Figure 1.3.) (Scherer 2006, Sun, Kusminski et al. 2011) (Figure 1.3). Once this expansion capacity has been reached, triglycerides must seek new sites of fat deposition (Jung and Choi 2014).

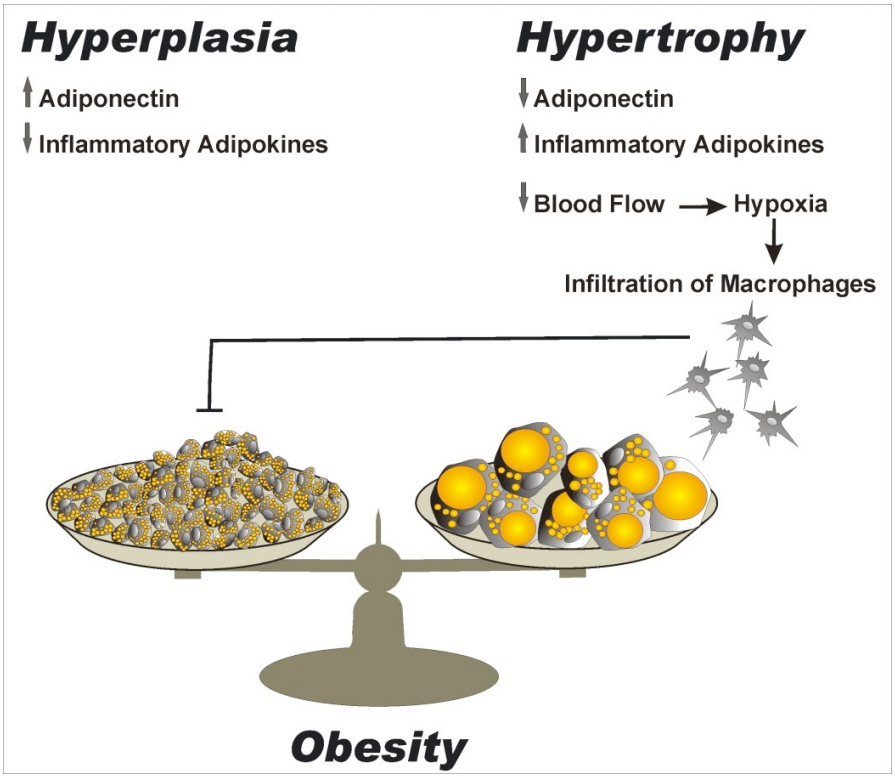

Figure 1.2. Hypertrophy vs Hyperplasia.

Adipose tissue remodelling can occur in one of two ways, through increased adipocyte number (hyperplasia) or volume (hypertrophy)**.** The ability of adipocytes to store excess dietary intake as triglycerides is finite and this capacity differs between individuals (expansion limit). Hyperplasia is accompanied by increased adiponectin secretion and reduction in inflammatory adipokines. Conversely, hypertrophy decreases adiponectin whilst increasing inflammatory adipokines. In obesity, hypertrophy prevails. Figure adapted from Queiroz, J.C. et al. (2009) Arg Bras Endocrinol Metabol.

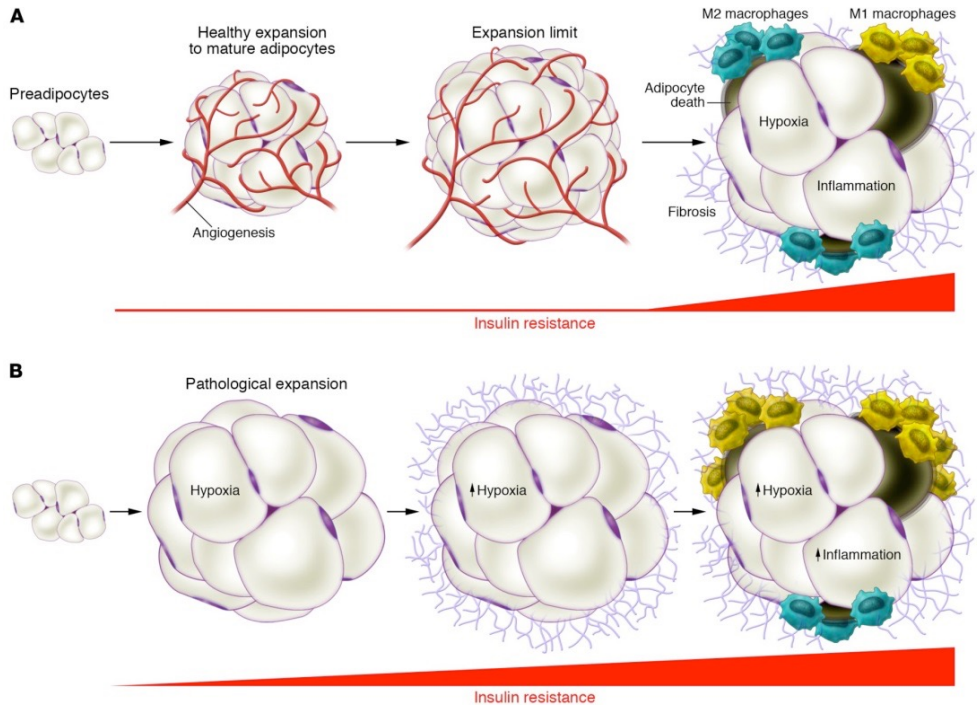

Figure 1.3. Healthy and unhealthy adipose tissue expansion.

(A) The conversion of preadipocytes to mature adipocytes is accompanied with activation of angiogenesis, thereby maintaining sufficient oxygen supply. Continued attempts to store excess nutrient supply as triglycerides above the expansion limit of adipocytes results in the onset of hypoxia and inflammation . Hypoxia occurs in regions of adipose tissue with insufficient oxygen supply. (B) In contrast, unhealthy adipose tissue expansion is accompanied by significant enlargement of adipocytes under conditions of limited angiogenesis and corresponding development of hypoxia. Together with the induction of hypoxia inducing factor 1 (HIF-1 alpha), fibrosis is initiated. Furthermore, inflammation increases as a result of the recruitment of M1 macrophages into adipose tissue. M1 macrophages are a pro-inflammatory phenotype. Conversely, M2 macrophages are anti-inflammatory and have been proposed to be involved in tissue repair. Overall the contribution of macrophages in this adipose tissue, is towards a pro-inflammatory bias, which is strongly associated with insulin resistance. Figure taken from (Sun, Kusminski et al. 2011).

These excess lipids remain in the circulation and are deposited in secondary organs such as the liver and heart resulting in lipotoxicity and cardiac damage (Vigouroux, Caron-Debarle et al. 2011). During obesity and T2DM, these circulating lipids activate the innate immune system and maintain a state of chronic low grade or meta-inflammation within adipose tissue (Creely, McTernan et al. 2007). Taken together, these conditions have negative implications for cellular metabolism (Bastard, Maachi et al. 2006, Hotamisligil 2006, Hotamisligil and Erbay 2008). A reduction in insulin sensitivity and metabolic function are two cornerstones of metabolic syndrome (Virtue and Vidal-Puig 2010). As a condition, Metabolic Syndrome (MetS) is defined as the co-existence of conditions including obesity, insulin resistance and dyslipidemia within patients (Abella, Scotece et al. 2014). Individuals exhibiting Metabolic Syndrome display sustained insulin resistance during fasting and post-prandially (Harte, Varma et al. 2012, Piya, Harte et al. 2013). Finally, additional evidence for the functional link between lipid and IR is, that humans with lipodystrophy due to genetic mutations, also present with insulin resistance (Simha and Garg 2009).

1.1.5. Metabolic flexibility is compromised in obesity.

Cells are programmed to exhibit metabolic flexibility (Mingrone, Manco et al. 2005). In response to substrate availability and cellular demand, cells are capable of switching between lipid or glucose oxidation (Astrup, Buemann et al. 1996, Blaak and Saris 2002). Under homeostatic conditions, glucose oxidation is more commonly used as a cellular substrate**.** The randall hypothesis was proposed to explain the etiology of T2DM during obesity. During obesity and T2DM, the excess circulating free fatty acids (substrates in fatty acid oxidation), considered to originate from the more metab-

olically active abdominal adipose depots, may contribute to the impairment of glycolysis and development of glucose intolerance. One process by which this may occur is the stimulation of gluconeogenesis in hepatocytes (stimulated by free fatty acids and results in the creation of glucose from predominantly pyruvate, glycerol or lactate) further compounding the situation. In an attempt to return these elevated glucose levels to a homeostatic level, the pancreas releases insulin to promote the conversion of the glucose to glycogen. The impairment of glycolysis and continued release of insulin to control glucose levels in the blood, places significant pressures on energy homeostasis regulation. Research has suggested that it is the impairment of carbohydrate metabolism and development of glucose intolerance, orchestrated by these circulating free fatty acids, which are responsible for the pathophysiology of T2DM.

1.2. Energy homeostasis in adipose tissue.

1.2.1. Regulation of energy metabolism in a dipose tissue.

Previously dismissed as nothing but a passive site for excess energy storage (Ahima 2006), the identification that adipokines secreted from a dipose tissue can modulate energy homeostasis, insulin action and whole body metabolic processes including glucose and lipid metabolism (Antuna-Puente, Feve et al. 2008, Abella, Scotece et al. 2014, Knights, Funnell et al. 2014), has brought the role of a dipose tissue as an endocrine organ to the fore. The origin of the term adipokines, was coined to collectively represent the group of hormones generated from adipocytes and the stromal vascular fraction within the adipose tissue (Antuna-Puente, Feve et al. 2008). A multitude of cell types including preadipocytes, macrophages and fibroblasts are contained within the stromal vascular fraction (Kim, Choi et al. 2010, Peinado, Jimenez-Gomez

et al. 2010, Liu, Guo et al. 2014). Collectively, these cell types work in coordination with the adipokines secreted from them, to support the a dipose tissue within energy homeostasis (Lehr, Hartwig et al. 2012, Abella, Scotece et al. 2014).

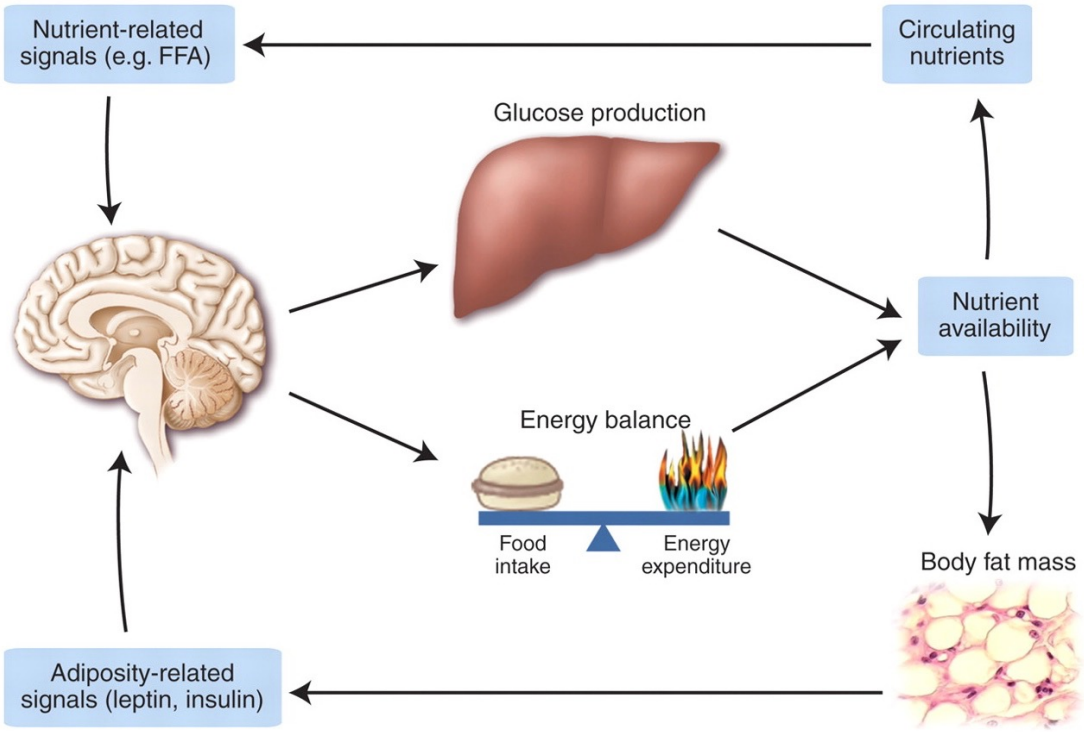

Figure 1.4. Energy homeostasis and hepatic glucose metabolism.

Energy homeostasis is regulated through balancing dietary intake with cellular requirements for energy in the form of ATP. This model displays the different mechanisms involved in coordinating and monitoring availability of nutrients. Signals generated from circulating nutrients or adipose related adipokines e.g. leptin and insulin are transduced to the hypothalamus. As a consequence, changes in energy intake, expenditure and glucose production occur. Under conditions of nutrient excess, glucose production is lowered and nutrients are stored as triglycerides resulting in an increase in body fat mass. Conversely, during starvation, leptin secretion is reduced promoting an enhancement in appetite. Together with a feedback loop from leptin, insulin secretion is lowered reducing storage of essential energy in adipocytes. Figure taken and legend adapted from (Schwartz and Porte 2005).

1.2.2. Role of adipokines in energy homeostasis.

Adipose tissue can respond to both central and peripheral metabolic signals via adipokines (Trayhurn and Wood 2004, Antuna-Puente, Feve et al. 2008). Adipokines can regulate appetite (leptin, 1.2.2.2) as well as energy expenditure (adiponectin,1.2.2.3 thereby extending their role from a cellular level to whole body homeostasis (Dyck 2009). A description of a few critical adipokines and their role within energy homeostasis are given below :

1.2.2.1. TNFα: is a pro-inflammatory cytokine and is primarily secreted from macrophages. Insulin resistance induced through TNFα action, has been proposed to involve dysregulation of fatty acid metabolism together with impairment of insulin signalling (Dyck 2009).

1.2.2.2. Leptin: is a 16kDa non-glycosylated hormone (Kamohara, Burcelin et al. 1997). As a critical regulator of appetite, it works with the central nervous system as a signalling molecule between adipose tissue and the brain. Leptin is secreted from adipocytes and is capable of initiating lipolysis through its stimulatory and feedback activity on the sympathetic nervous system (Kennedy 1953). Furthermore, it is capable of lowering food intake whilst concurrently increasing energy expenditure (Friedman and Halaas 1998). These functions are achieved through signalling to hypothalamic nuclei via neuronal circuits, resulting in the promotion of anorexigenic factors (appetite suppressant) together with the inhibition of the opposing orexigenic (appetite promoting) neuropeptides (Elmquist, Maratos-Flier et al. 1998). In 1994, following

characterisation of the murine obese (ob) gene or human LEP gene, leptin protein was identified as an ob gene product (Zhang, Proenca et al. 1994). Through its appetite suppressing action, leptin is capable of promoting weight loss (Pelleymounter, Cullen et al. 1995). Conversely, during conditions of nutrient deprivation, a key energy sensor AMPK is activated by leptin (Wu, Chao et al. 2013). The detection of high AMP: ATP ratio by AMPK, results in the activation of fatty acid oxidation to enhance shuttling towards oxidative phosphorylation. The ATP generated via oxidative phosphorylation, maintains the capability of mitochondria to meet the energy demands of the cell (Covey, Wideman et al. 2006).

1.2.2.3. Adiponectin: originally identified in 1995 (Scherer, Williams et al. 1995) is secreted in serum and is an insulin sensitising, anti-inflammatory and anti-apoptotic protein (Dridi and Taouis 2009). During obesity and T2DM, adiponectin binds to tthe adiponectin receptor (Hara, Yamauchi et al. 2005). As a result, energy expenditure is reduced resulting in weight gain (Hara, Yamauchi et al. 2005, Tajtakova, Petrasova et al. 2006). Two forms of adiponectin, globular and full-length adiponectin are capable of binding and thereby activating both adiponectin receptors, adipoR1 and adipoR2 (Guillod-Maximin, Roy et al. 2009). Nevertheless, the binding affinity of adipoR1 is greater for the globular compared to the full-length form of adiponectin (Yamauchi, Kamon et al. 2003). Following their activation, a diponectin receptors transduce their signal to a number of signalling messengers including MAPK, PPAR-α and AMPK (Trayhurn and Wood 2004, Iwabu, Yamauchi et al. 2010, Chen, Zhang et al. 2013). Insulin resistance and obesity have been shown to be inversely proportional to plasma adiponectin expression levels (Trayhurn and Wood 2004). Furthermore, observational

studies revealed that the reduction of adiponectin expression was linked to a greater incidence of metabolic syndrome (Kozlowska and Kowalska 2006, Miczke, Szulinska et al. 2006, Shimomura, Maeda et al. 2006, Tajtakova, Petrasova et al. 2006, Mojiminiyi, Abdella et al. 2007). Finally, observation studies have concluded that human adiponectin levels in those with T2DM are greatly reduced compared to their non-diabetic counterparts (Vasseur, Meyre et al. 2006). Administration of adiponectin in mice with obesity and insulin resistance boosted their low basal circulating adiponectin levels and corresponded with an improvement in their insulin sensitivity together with enhanced glucose tolerance (Yamauchi, Kamon et al. 2003).

1.2.3. Energy homeostasis dysregulation in obesity and T2DM.

Obesity is often associated with dysregulated adipokine secretion (Nawrocki, Rajala et al. 2006). In obese and insulin resistant patients, adiponectin is downregulated, whilst leptin is increased (Qi, Takahashi et al. 2004). Mutations in the ob gene are accompanied by insufficient expression of leptin. It is this downregulation of leptin, which is responsible for the 3-fold increase in the weight of ob/ob mice compared to wild type mice (Schafer, Halle et al. 2004). Leptin and insulin signalling are known as the adipo-insular axis and are integral for regulating nutrient and energy balance (Perry and Wang 2012). The exact mechanisms responsible for coordinating both the local and global effects of leptin in promoting insulin sensitivity are unknown and require further characterisation.

1.3. Mitochondrial health and function.

Mitochondrial health is vitally important for cellular viability and function (Magalhaes, Venditti et al. 2014). As the powerhouse of the cell, mitochondria are responsible for liberation of the energetic substrate, ATP via the fatty acid cycle and oxidative phosphorylation (Figure 1.8) (Hafner, Brown et al. 1990).The symbiotic relationship between the mitochondria and nucleus enables nuclear synthesis of the majority of the 1500 mitochondrial proteins (37 are encoded in the mitochondrial genome, 13 of which are required for oxidative phosphorylation) (Anderson, Bankier et al. 1981, Gaston, Tsaousis et al. 2009).These include subunit 6 (mt-ND6) of NADH dehydrogenase (complex I) and subunit 6 (mt-ATP6) of ATP synthase (complex V) (Van Bergen, Blake et al. 2014). Given the critical role of mitochondria to cellular health, the process of nuclear synthesis of mitochondrial proteins may have arisen to minimise the effect of the greater mitochondrial mutation rate, as much as 10-20 times that of the nuclear genome (De Pauw, Demine et al. 2012). Coupled with this, mitochondrial DNA repair enzymes have a low activity status (Linnane, Marzuki et al. 1989, Wang, Lin et al. 2009). Therefore, quality control mechanisms have evolved within the mitochondria in an attempt to overcome some of the limitations of this inefficient DNA repair system. One example of these quality control mechanisms is mitochondrial biogenesis (Attardi and Schatz 1988, Medeiros 2008, Ren, Pulakat et al. 2010, Weckbecker and Herrmann 2013).

1.3.1. Mitochondrial biogenesis.

Mitochondrial biogenesis protects mitochondrial health through the maintenance of mtDNA quality (Scarpulla, Vega et al. 2012). This process is achieved via cycles in-

volving the coalescence of old mitochondria and their subsequent division (Ren, Pulakat et al. 2010). As a result, functional mitochondrial DNA is retained whilst compromised mitochondrial DNA is selectively eliminated (Ren, Pulakat et al. 2010). Mitochondrial DNA synthesis occurs *de novo* during the cell cycle to return mitochondria mtDNA abundance to their homeostatic levels (Sheng and Cai 2012). However, during obesogenic conditions, mitochondrial biogenesis is impaired thereby contributing to mitochondrial dysfunction. Mitochondrial biogenesis is coordinated at a transcriptional level by peroxisome proliferator activated receptor co-activator 1 alpha (PGC1α) (Fernandez-Marcos and Auwerx 2011) and nuclear respiratory factor 1 (NRF-1) (Escriva, Rodriguez-Pena et al. 1999). Together these promote the induction of the catalytic subunit of the mitochondrial DNA polymerase (POLG) and expression of other biogenesis transcription factors i.e. mitochondrial transcription factor A (Tfam) and oxidative phosphorylation (OXPHOS) genes required for mitochondrial replication (Murholm, Dixen et al. 2009, Elachouri, Vidoni et al. 2011). Previous studies have identified that patients who possess mutations in either a mitochondrial or nuclear gene involved in mitochondrial function, exhibit disturbances in their respiratory capacity (Pich, Bach et al. 2005). Thus respiratory or oxidative capacity is a reflection of both mitochondrial biogenesis and mitochondrial morphology regulated via mitochondrial dynamics.

1.3.2. Mitochondrial dysfunction.

Mitochondrial dysfunction is most commonly defined as the inability of mitochondria to produce ATP in response to cellular demand (Bournat and Brown 2010). Nevertheless, this definition can be extended to incorporate changes to mitochondrial biogene-

sis, reduction in fatty acid oxidation or increased production of reactive oxygen species (ROS) (Lowell and Shulman 2005, Zorzano, Liesa et al. 2009).

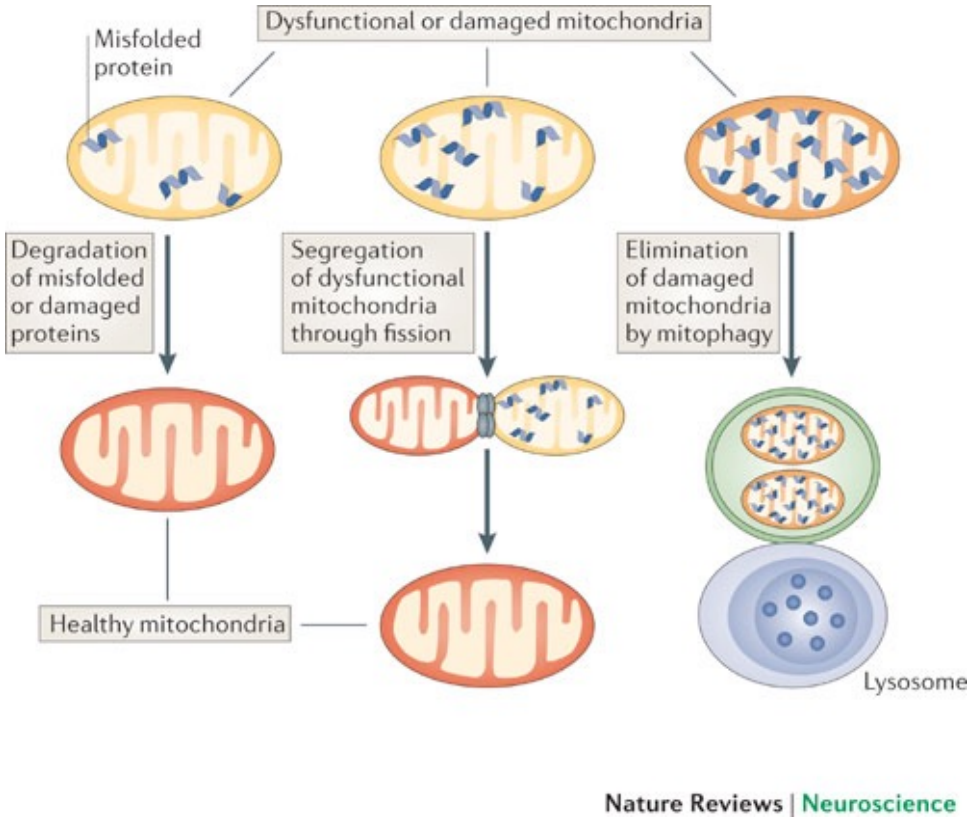

Figure 1.5. Origins of mitochondrial dysfunction.

Mitochondrial quality control involves surveillance and protection strategies to limit mitochondrial damage and ensure mitochondrial integrity. This quality control occurs at the following molecular, organelle and cellular levels. Figure and legend taken from *(Sheng and Cai 2012)*.

Importantly, mitochondrial dysfunction has been proposed to account for the generation of toxic lipid metabolites via the fatty acid cycle and hampering of metabolic fitness, which accompany the stunted adipogenic capacity and Adipose tissue dysfunction (Vankoningsloo, Piens et al. 2005, Liu, Lin et al. 2012). Finally, evidence in favour of the role of mitochondrial dysfunction in those individuals with T2DM is the

co-association of reduced mitochondrial oxidative phosphorylation capacity and insulin resistance in elderly or obese individuals (Petersen, Dufour et al. 2004). Furthermore, mitochondrial dysfunction extends beyond the inability to synthesise sufficient ATP, to processes of mitochondrial DNA abundance and mitochondrial morphology (Okamoto and Shaw 2005, Yu, Robotham et al. 2006). In the skeletal muscle of obese and T2DM, a reduction of mitochondrial copy number together with enhanced mitochondrial fission have been observed (Barthelemy, Ogier de Baulny et al. 2001, Jeng, Yeh et al. 2008). Mitochondrial dynamics, which involves mitochondria fission, is discussed in further detail in section 1.4.2.

1.3.3. Causes of mitochondrial dysfunction.

Despite multiple studies in skeletal muscle implicating a connection between insulin resistance and mitochondrial dysfunction, little data is available in white adipose tissue (WAT), regarding the involvement of mitochondria during conditions of insulin resistance or AT dysfunction.

1.3.4. Mitochondrial dysfunction in adipose tissue.

In humans, insulin resistance has been found to co-exist with a lower mitochondrial oxidative phosphorylation activity (Petersen, Dufour et al. 2004). Nevertheless, whether insulin resistance is a primary or secondary effect of mitochondrial dysfunction is unknown (Shulman 1999, Shulman 2000, Guilherme, Virbasius et al. 2008, Amati, Dube et al. 2011, Koliaki and Roden 2014). In an attempt to address this question, studies performed in skeletal muscle of obese and T2DM subjects found that these cells are often exposed to a high fat load (Sparks, Xie et al. 2005, Catta-Preta,

Martins et al. 2012). Recapitulating this scenario and analysis of mitochondrial dynamics in skeletal muscle biopsies from either morbidly obese (Semple, Crowley et al. 2004), following a high fat feed in humans with an ideal BMI (Richardson, Kashyap et al. 2005, Sparks, Xie et al. 2005) or mice (Rong, Qiu et al. 2007) resulted in the downregulation of the mitochondrial biogenesis gene, PGC1α (Puigserver and Spiegelman 2003, Mitra, Nogee et al. 2012). As mentioned earlier in section 1.3.1, the respiratory capacity of mitochondria is a reflection of both mitochondrial biogenesis and morphology that are regulated via mitochondrial dynamics.

1.4. Mitochondrial dynamics.

In response to changes in their cellular environment, mitochondria are able to alter their morphology and abundance through the balance of "fusion" and "fission" events (Liesa, Palacin et al. 2009). Together with mitophagy, mitochondrial dynamics genes selectively identify and eliminate dysfunctional mitochondria (Twig, Elorza et al. 2008, Twig, Hyde et al. 2008).

1.4.1. Fusion.

Mitochondrial fusion is characterised by two independent events culminating in the coordinated fusion of inner and outer mitochondrial membranes from separate mitochondria to form a single larger mitochondrion (Huang, Galloway et al. 2011). The mitochondrial membrane proteins involved are Opa1 (inner mitochondrial membrane protein) and Mfn1/2 (outer mitochondrial membrane protein).

Opa1: Optic atrophy 1 is a dominant autosomal mutation resulting in atrophy of the optic nerve and often progresses to visual blindness (Figure 1.9) (Eiberg, Kjer et al. 1994, Alexander, Votruba et al. 2000, Olichon, Landes et al. 2007, Song, Chen et al. 2007, Akepati, Muller et al. 2008). The regulation of Opa1 occurs at a post-transcriptional level through alternative splicing (Song, Chen et al. 2007). Splicing at exons 4,4b and 5b can generate a total of 8 mRNA isoforms (Satoh, Hamamoto et al. 2003, Akepati, Muller et al. 2008). Opa1 isoforms that include exon 4 (Opa1 isoform 1, the most abundant in mice and humans) have been shown to influence mitochondrial fusion activity and maintain membrane potential (Akepati, Muller et al. 2008). Following the generation of Opa1 isoforms, proteolytic cleavage represents a secondary level of Opa1 regulation (Satoh, Hamamoto et al. 2003, Duvezin-Caubet, Jagasia et al. 2006, Ishihara, Fujita et al. 2006, Ehses, Raschke et al. 2009). Proteolytic cleavage generates shorter Opa1 isoforms, at the expense of a reduction in the abundance of the longer isoforms (Olichon, Emorine et al. 2002, Ishihara, Fujita et al. 2006, Ehses, Raschke et al. 2009, Quiros, Ramsay et al. 2012). Only these longer isoforms possess the capacity to redress defective mitochondrial fusion in Opa1 knockout cells (Guillery, Malka et al. 2008).

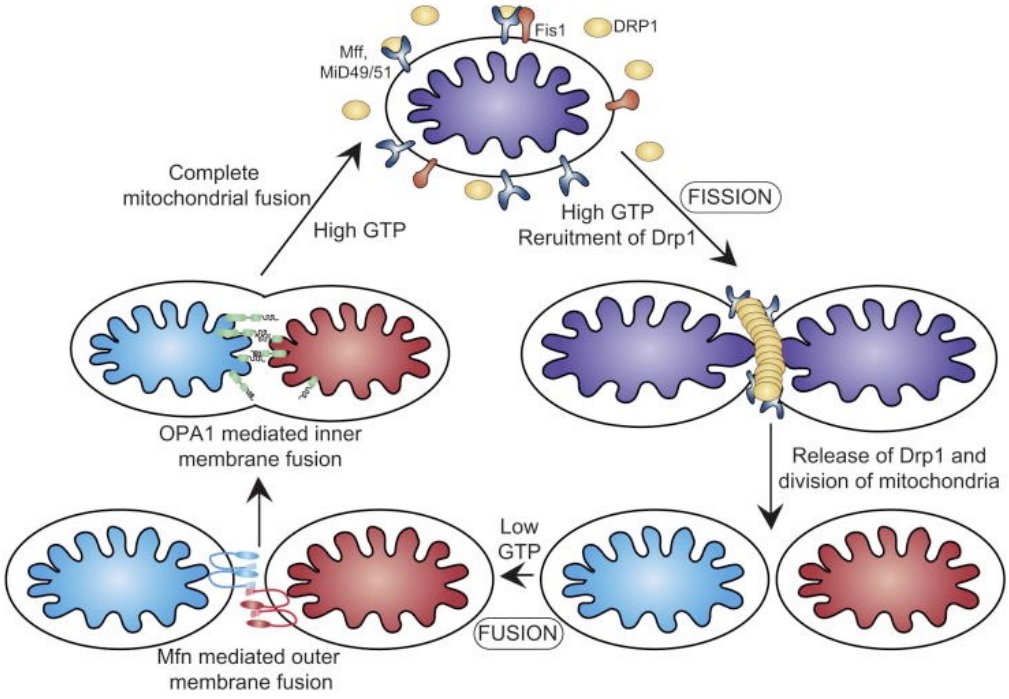

Figure 1.6. Proteins involved in mitochondrial dynamics.

Mitochondrial fission involves the translocation of Drp1 from its cytosolic location to the outer mitochondrial membrane. Fis1 together with the other integral membrane proteins of Mff, MiD49 and MiD51 have been proposed to assist in the recruitment of Drp1 to the outer mitochondrial membrane. Nevertheless, the role and mechanism of these putative Drp1 receptors are still under investigation. Drp1 creates a concentric ring around the mitochondria restricting the mitochondrial tubule and mediating fission to generate two asymmetric daughter mitochondria. Fusion, involves Mfn1/2 and Opa1. Opa1 mediates the tethering of inner mitochondrial fusion whilst Mfn mediate outer mitochondrial fusion. Together these contribute to the coalescence of two mitochondria to a single mitochondrion. This coalescence allows mixing of mitochondrial contents including protein and DNA. Complete mitochondrial fusion is dependent on GTP hydrolysis. Mitochondrial fission factor (Mff), mitochondrial dynamics proteins of 49 and 51kDa (MiD49/51), Guanosine triphosphate (GTP), optic atrophy 1 (Opa1), dynamic related protein (Drp1), mitochondrial fission protein 1 (Fis1), Mfn (mitofusin). Figure taken from (Osellame, Blacker et al. 2012).

Mfn2: Mitofusin 2 is localised within the outer mitochondrial membrane and assists with mitochondrial fusion (Figure 1.9) (Chen, Detmer et al. 2003, Bach, Naon et al. 2005). Mutations within Mfn2 gene cause the autosomal dominant neurodegenerative disease Charcot-Marie-Tooth type 2A (CMT) resulting in weakness and loss of muscle control particularly in the lower extremities e.g. the feet. (Zuchner, Mersiyanova et al. 2004) Knockdown of Mfn2 is associated with lower mitochondrial oxygen consumption together with diminished mitochondrial membrane potential (Pich, Bach et al. 2005). These observations also exist within patients with known Mfn2 mutations within their fibroblasts. Fibroblasts from patients with amino acid substitutions from R364Q or A166T have greater oxygen consumption at rest together with a diminished mitochondrial membrane potential (Loiseau, Chevrollier et al. 2007).

Mfn1: Mitofusin 1 is a human homolog of Mfn2 (Santel, Frank et al. 2003). In keeping with their homologous nature, Mfn1 shares 80% sequence identity with Mfn2 (Detmer and Chan 2007). Likewise, the functional domains of the GTPase, Coiled-coil regions, GTPase effector domain and transmembrane domain are conserved across Mfn1 and 2 (Ishihara, Eura et al. 2004). A localisation sequence located within the carboxy terminus of the protein directs the localisation of the transmembrane GTPase protein to the outer mitochondrial membrane (Santel, Frank et al. 2003). Mitochondrial fusion is initiated through formation of a dimeric anti-parallel coiled-coil structure (Koshiba, Detmer et al. 2004). Formation of this complex, engages the tethering of two mitochondria and signifies that mitochondrial fusion has begun (Koshiba, Detmer et al. 2004). Loss of function mutations in Mfn1 is lethal to developing

embryos, as it results in defects within placenta formation (Chen, McCaffery et al. 2007).

FOXC2: Forkhead transcription factor 2 is capable of inducing mitochondrial fusion (Lidell, Seifert et al. 2011) and is associated with a lean and insulin sensitive phenotype (Cederberg, Gronning et al. 2001). Furthermore, its critical role as a metabolic regulator is evidenced by its ability to transactivate Tfam and initiate mitochondriogenesis resulting in elongated mitochondrial morphology (Bergman, Van Citters et al. 2001). Correlation analyses between FOXC2 and mitochondrial fusion genes (Mfn2, Mfn1 and Opa1) have confirmed a positive association and provide support to suggestions that the regulation of fusion by FOXC2 extends from mice to humans (Lidell, Seifert et al. 2011).

1.4.2. Fission.

Fission involves the segregation of one mitochondrion into two smaller mitochondria (James, Parone et al. 2003). This process is unequal, and is used to segregate the compromised mitochondrial membrane and its components from an otherwise functional organelle (Figure 1.9) (Twig, Elorza et al. 2008, Galloway, Lee et al. 2012, Elgass, Pakay et al. 2013). Where possible, components such as lipids within the mitochondrial membrane are recycled and the remainder of the defective mitochondrial membrane is tagged for degradation by ubiquitylation (Praefcke and McMahon 2004). Similar to the ubiquitylation of misfolded proteins, compromised mitochondria are shuttled via the lysosome pathway towards mitophagy (mitochondrial equivalent of

cellular autophagy) (Twig, Elorza et al. 2008, Twig, Hyde et al. 2008). Mitochondrial fission requires Drp1 and Fis1 proteins.

Drp1: is a key protein required for fission and translocates from the cytosol to the mitochondria with assistance from Fis1 (Figure 1.9) (Smirnova, Shurland et al. 1998). Once localised to the outer mitochondrial membrane, Drp1 punctuate holes within the mitochondria required for initiation and assembly of future sites of fission (Smirnova, Griparic et al. 2001). Importantly, these scission sites are created as a concentric ring within the outer mitochondrial membrane (Taguchi, Ishihara et al. 2007). Together with the scission sites and a GTP hydrolysis reaction, mitochondrial membranes can become severed and physically separated from one another (Liesa, Palacin et al. 2009). Nevertheless, the mitochondrial fission proteins involved in the division of the inner mitochondrial membranes remain unresolved.

Fis1: is a 17kDa protein and functions as the mechanical scissors to finalise and coordinate the creation of two separated mitochondria (Stojanovski, Koutsopoulos et al. 2004). Ubiquitously expressed and dispersed throughout the mitochondrial network and is thought to be the limiting factor for mitochondrial fission (Yoon, Krueger et al. 2003).

1.4.3. Dysregulation of mitochondrial dynamics.

How mitochondrial dynamics become dysregulated is unknown. Understanding the molecular mechanisms that underlie this phenomenon, offers a key opportunity to develop therapeutics or biomarkers for diabetes and insulin resistance. In diabetic mice,

their adipocyte expression, abundance of mtDNA and mitochondrial dynamics proteins is lower than non-diabetic mice (Rong, Qiu et al. 2007). The balance of mitochondrial fusion and fission are key to maintaining mitochondrial health and morphology (Zorzano, Liesa et al. 2009, Liesa and Shirihai 2013). Over-activation of fission or an absence of balanced fusion initiates the fragmentation of mitochondria (Ferrier 2001, James, Parone et al. 2003, Huang, Galloway et al. 2011). Mitochondrial fragmentation results in the generation of smaller and greater numbers of mitochondria. Depending on the duration and severity of the imbalanced fission, the mitochondrial population may become compromised or reduced in abundance through their removal by mitophagy (Jheng, Tsai et al. 2012). Both mitochondrial fragmentation and a reduction in mitochondrial membrane potential must occur before mitochondria are shuttled towards mitophagy (Lee, Jeong et al. 2004). Under conditions of transient or acute cellular stress, mitochondrial fusion can be upregulated to compensate for damage induced within the mitochondria (Huang, Galloway et al. 2011). Investigation of the effect of cellular stress within cultured cells have revealed that mitochondria display the ability to resolve damage such as misfolded mitochondrial proteins or the effects of cellular stress such as production of reactive oxygen species (ROS) (Michel, Wanet et al. 2012). If unresolved, damage induced to cells would require their removal by apoptosis (Ferrier 2001).

1.5. Mitochondrial bioenergetics.

Mitochondrial bioenergetics is a measure of mitochondrial capacity. Measurement of oxidative phosphorylation enables quantification of the rate of ATP synthesis within cells and thereby provides a snapshot of the energetic demands of cells in real time.

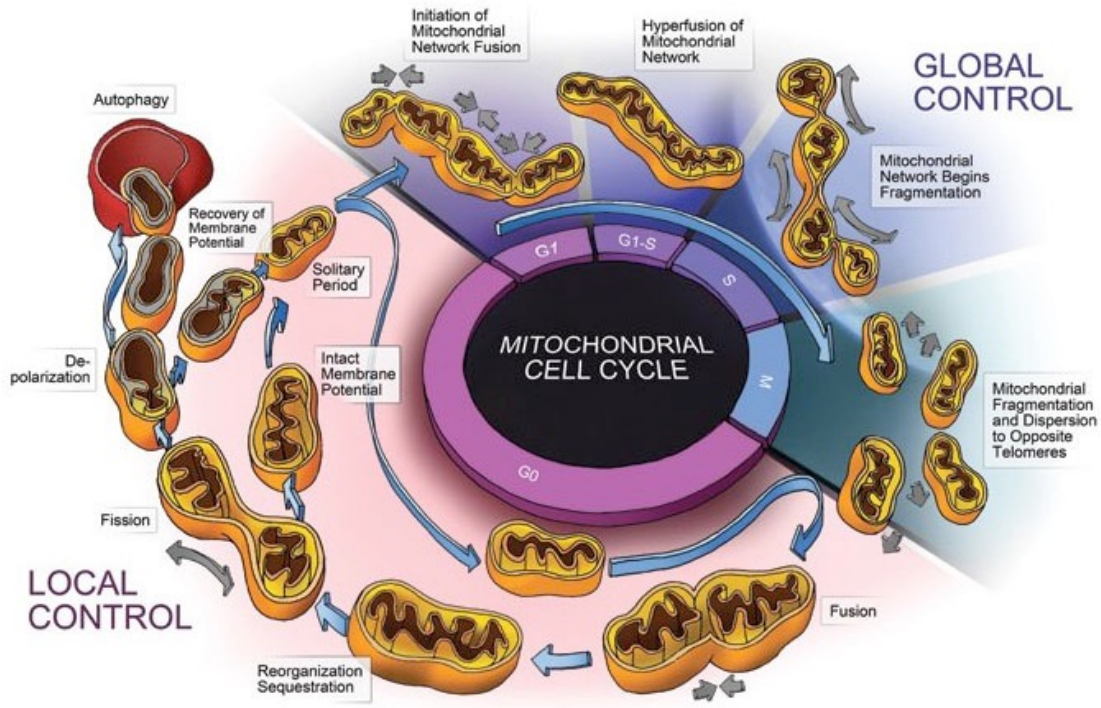

Figure 1.7. Quality control pathway: The life cycle of a mitochondrion and the involvement of mitochondrial dynamics proteins.

Local control is exerted at the level of the G0 phase of the cell cycle (resting phase). During this phase, mitochondrion undergo fusion, fission, depolarisation and autophagic degradation. Global control is governed by the cellular metabolism and thus demand for energy needed to perform cell division and re-organisation of cellular components between cells during metaphase. Examples of these global signal effects on mitochondria include, the presence of hyperfused mitochondrial network (cell growth-synthesis, G1-S phase) or mitochondrial fragementation (cellular synthesis and mitosis, S and M phases). Figure from Ferree,A. and Shirihai,O. Chapter 2. Mitochondrial oxidative phosphorylation: (748). Advances in Experimental Medicine and Biology (2012).

1.5.1. Quantitative measurement of OXPHOS can be performed *in situ.*

Measuring mitochondrial bioenergetics can be performed in situ (Gerencser, Chinopoulos et al. 2012) within a cell or following isolation of the mitochondrial fraction from cells (Hafner, Brown et al. 1990). Recent developments in mitochondrial bioenergetics have enabled in situ measurements of intracellular mitochondria. Despite a slight compromise in precision for in situ analyses, this significantly outweighs the damage and time required to perform bioenergetic analyses on isolated mitochondria (Hafner, Brown et al. 1990). Additional advantages include the physiological relevance of maintaining mitochondria within their cellular environment (Nicholls 2002, Nicholls, Johnson-Cadwell et al. 2007). Mitochondria exhibit inter-organelle contacts with the ER and interact with their cytoplasmic environment.

Maintaining mitochondria within its surrounding environment permits a more realistic recapitulation of its interaction with other organelles and cellular role (Affourtit, Jastroch et al. 2011). The measurement in real time allows determination of the dynamic flux of mitochondrial ATP production in response to energy demand. Mitochondrial dysfunction is most commonly defined as the inability of mitochondria to produce ATP in response to cellular demand (Nicholls 2002). Through parallel measurement of mitochondrial potential and respiration, the effect of chemical, genetic treatment on mitochondrial function together with the target site (within the mitochondrial complexes of the oxidative phosphorylation chain) and distribution of this effect can be more accurately determined (Brand and Nicholls 2011).

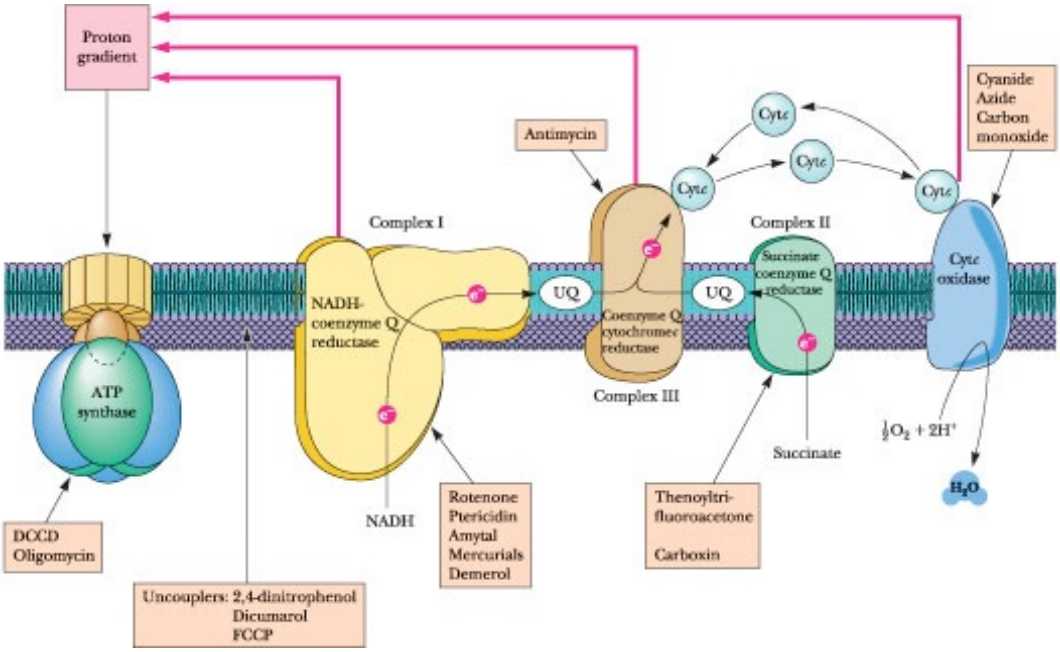

Figure 1.8. The oxidative phosphorylation cycle.

Oxidative phosphorylation cycle involves electron transfer (e-) sequentially through complexes I to V. Accompanying this are a series of redox reactions culminating at the ATP synthase in the generation of ATP (adenosine triphosphate). Complex inhibitors (given in orange boxes) Oligomycin is an ATP synthase inhibitor. Through its inhibition of this mitochondrial membrane bound complex, it is capable of blocking oxidative phosphorylation from proceeding past this point of the electron transport chain. As a consequence, only electrons generated through mitochondrial uncoupling, allow protons to diffuse using UCP1 (uncoupling protein 1) from the outer to inner mitochondrial membrane.

FCCP (carbonyl cyanide-p-trifluoromethoxyphenylhydrazone) is a mitochondrial uncoupling agent, used to increase mitochondrial permeability to protons through depolarisation of the mitochondrial membrane potential. FCCP measures the maximal oxygen consumption rate of cellular mitochondria. Antimycin inhibits complex III of the electron transport chain resulting in leaking of electrons to molecular oxygen resulting in the generation of superoxides. Rotenone inhibits Complex I of the electron transport chain (specifically the NADH dehydrogenase enzyme). The cocktail of antimycin/rotenone quantifies non-mitochondrial respiration rate within the assayed cells.

Maintaining mitochondria within its surrounding environment permits a more realistic recapitulation of its interaction with other organelles and cellular role (Affourtit, Jastroch et al. 2011). The measurement in real time allows determination of the dynamic flux of mitochondrial ATP production in response to energy demand. Mitochondrial dysfunction is most commonly defined as the inability of mitochondria to produce ATP in response to cellular demand (Nicholls 2002). Through parallel measurement of mitochondrial potential and respiration, the effect of chemical, genetic treatment on mitochondrial function together with the target site (within the mitochondrial complexes of the oxidative phosphorylation chain) and distribution of this effect can be more accurately determined (Brand and Nicholls 2011).

1.6. Summary.

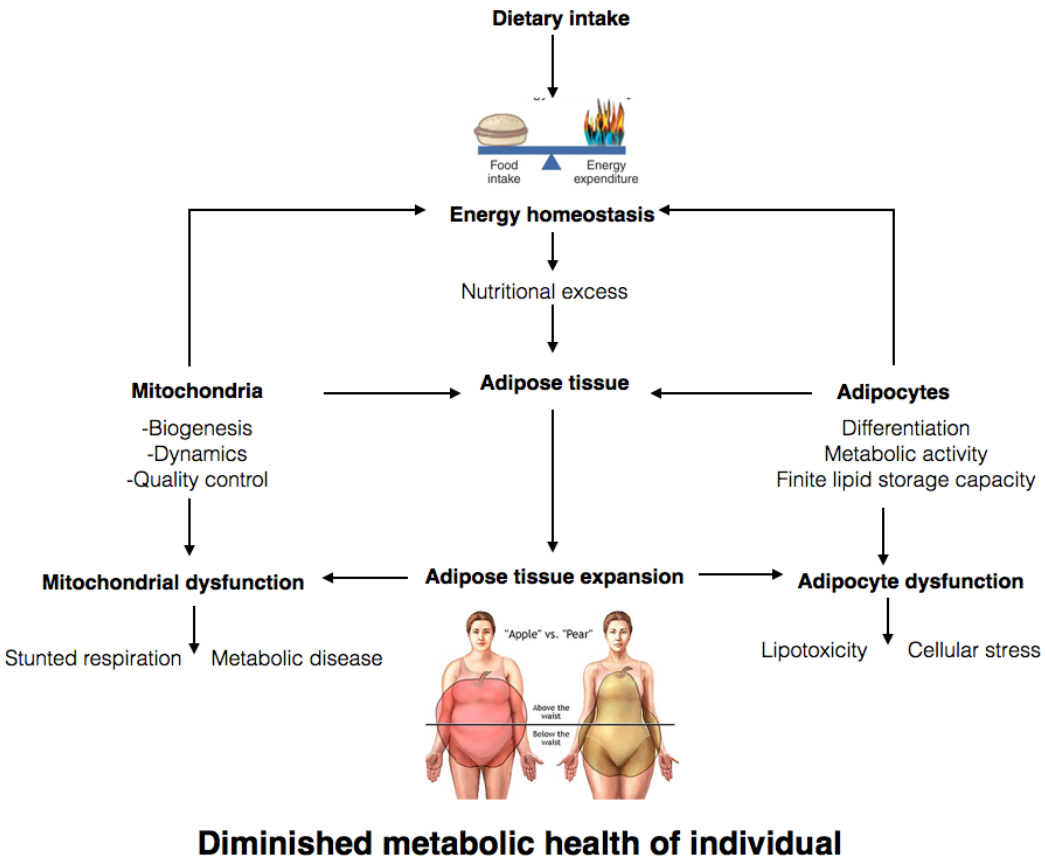

In summary, adiposity and T2DM are often accompanied by mitochondrial dysfunction. Whilst, the role of mitochondrial dynamics in the regulation of mitochondrial abundance have been previously addressed and is known to influence mitochondrial abundance and morphology, its link to the regulation of mitochondrial function in adipocytes remains largely uncharacterised. As the primary energy storage tissue, adipose tissue functions together with mitochondrial dynamics to maintain energy homeostasis. As such, investigating both theconsequences of adiposity on the balance of markers of mitochondrial dynamics together with regulation of this process at a molecular level is of vital importance

and may provide the basis for future research into novel therapeutic interventions for obesity and T2DM.

1.7 Aims and Objectives.

Aim: Assess the regulation of mitochondrial dynamics in adipocytes and adipose tissue.

The four key **objectives** of my thesis were as follows:

1. Define mitochondrial dynamics within human adiposity.
2. Bariatric surgery; implications of the surgical procedure and weight loss on mitochondrial dynamics.
3. To study the regulation of mitochondrial dynamics by signalling pathways in adipocytes.
4. Modelling the interaction between putative p38 beta isoform inhibitors and their effects on mitochondrial morphology and bioenergetics.

Based on previous literature, I wished to test and examine the following hypotheses:

1. Mitochondrial dynamics proteins are differentially expressed in the subcutaneous a dipose tissue of lean, overweight and obese individuals.
2. Mitochondrial dynamics can be redressed through weight loss induced by bariatric surgery in T2DM individuals.
3. p38 positively regulates mitochondrial dynamics and adipocyte differentiation.
4. Modelling of p38 and selection of putative p38 β isoform inhibitors.
5. p38 inhibition diminishes mitochondrial bioenergetics and is accompanied by mitochondrial fragmentation in adipocytes.

Chapter 2:

The role of adiposity in mitochondrial dynamics.

2.1. Introduction.

Obesity is a key contributory factor in the development of insulin resistance. (Fernandez-Sanchez, Madrigal-Santillan et al. 2011) Obesity is defined as an individual whose body mass index is above 30 kg/m^2 (World Health Organisation). The co-existence of insulin resistance and obesity are known significant risk factors for the development of T2DM (Bastard, Maachi et al. 2006, Abdullah, Peeters et al. 2010). During periods of excess nutritional intake, which if continuous would result in obesity, cellular substrates are converted for storage into cells as triglycerides (Scherer 2006). However, the site of fat storage also has metabolic implications for the individual (Sun, Kusminski et al. 2011). In particular, central obesity, characterised by the deposition of fat in the abdominal region (Rosen and Spiegelman 2006) (subcutaneous and visceral adipose tissue), is a greater risk factor for the development of T2DM compared to that posed by peripheral obesity (accumulation of fat around the hips and thighs) (Kraunsoe, Boushel et al. 2010). Mitochondria are indispensable for energy homeostasis (Liesa and Shirihai 2013) (Magalhaes, Venditti et al. 2014) and are responsible for generating the essential cellular substrate, ATP via oxidative phosphorylation (Robertson 2014). Tasked with maintaining energy homeostasis, mitochondria are capable of adapting their abundance and thus capacity to meet the energetic needs of the cell, through mitochondrial biogenesis (Medeiros 2008) and dynamics (Zorzano, Liesa et al. 2009, Picard and Turnbull 2013). Mitochondrial dynamics regulates mitochondrial abundance (Jeng, Yeh et al. 2008), morphology (da Silva, Mariotti et al. 2014) and health through fusion and fission (Okamoto and Shaw 2005, Palaniyandi, Qi et al. 2010). Fusion generates a larger mitochondrion from two smaller mitochondria, through coalescence of mitochondrial membranes and contents (Mouli, Twig et

al. 2009). In contrast, fission generates two smaller mitochondria from a large/fused mitochondrion (Chan 2006). Furthermore, insulin resistance and compromised lipid metabolism have been shown to correlate with a reduction in both mitochondrial copy number (Michel, Wanet et al. 2012) and function (Nunnari and Suomalainen 2012). As a consequence downstream mitochondrial functions such as oxidative phosphorylation are impaired in skeletal muscle as a consequence of insulin resistance (Jheng, Tsai et al. 2012). This is supported by evidence of the diminished oxidative phosphorylation capacity shown in pre- diabetic and age-related insulin resistant subjects (Sparks, Xie et al. 2005, Mustelin, Pietilainen et al. 2008, Fernandez-Sanchez, Madrigal-Santillan et al. 2011). Furthermore, previous findings have indicated that inhibiting mitochondrial fission in the skeletal muscle of mice with genetic or diet-induced obesity, reversed the insulin resistance and development of smaller and fragmented mitochondria normally present in obese mice (Bach, Pich et al. 2003). To date, most studies have focused on characterisation of mitochondrial processes in skeletal muscle, due to its role as the primary site of glucose uptake and utilisation within the body (Dyar, Ciciliot et al. 2014). Recently, adipose tissue has received greater recognition for its role not only in energy storage but its role as an endocrine organ within glucose homeostasis, (Rosen and Spiegelman 2006) involving amongst others, adiponectin (Dridi and Taouis 2009) (see introduction section 1.2.2.3) for a more detailed description). Therefore, adipose tissue is a more representative model in which to investigate mitochondrial dynamics (Tseng, Cypess et al. 2010). In support of this, human fibroblasts from patients with naturally occurring mutation (A166T or R364Q) in the mitochondrial fusion protein, Mfn2, correspond with greater basal oxygen consumption under conditions of unaltered mitochondrial mass and normal

functionality of their oxidative phosphorylation complexes (Loiseau, Chevrollier et al. 2007).

The purpose of this study was to investigate whether mitochondrial dynamics were influenced by adiposity thereby offering a potential explanation for the incidence of mitochondrial dysfunction in obesity.

2.2. Research design and methods.

2.2.1. Selection and description of participants:

A female cohort consisting of lean (Age 38±8yr; BMI: 22.9±0.9 kg/m^2, n = 10), overweight (Age 38±9yr; BMI: 26.8±1.5kg/m^2, n = 10) and obese (Age 42±10yr; BMI: 34.1±2.1kg/m^2, n = 10) subjects participated in our study. Ethical approval was obtained from the local research ethics committee (LREC). Prior to enrolment, all participants provided written informed consent and completed a comprehensive medical evaluation. Detailed medical drug histories were taken and those subjects on medication considered to alter inflammatory status were excluded, including thiazolidinediones. Abdominal subcutaneous adipose tissues (AbSc AT) were collected, flash frozen immediately and stored in -80°c freezers until use. Fasted blood samples were taken prior to surgery and sera were analysed as detailed below.

2.2.2. Analyses of blood samples.

Fasted blood samples were used to assess the metabolic profiles of all participants. The lipid and fasted plasma glucose were determined using routine laboratory methods, undertaken by colleagues in the biochemistry laboratory, at University Hospital Coventry and Warwickshire. In brief, the routine b lood tests included glucose and a

full lipid profile (TGs, HDL-cholesterol and LDL-cholesterol), as noted in Table 1. Insulin measurements were performed by a solid phase enzyme amplified sensitivity multiplex immunoassay (Millipore, UK) and glucose was measured by a glucose oxidase method (YSL 200 STAT plus).

2.2.3. Isolation of mRNA and qPCR.

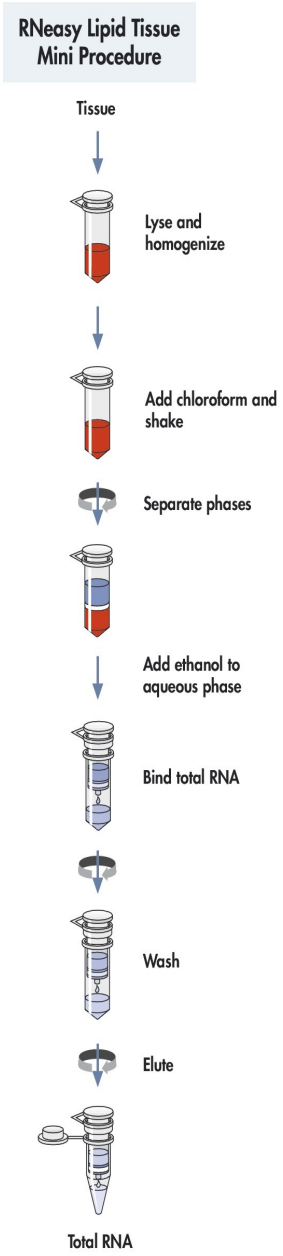

Figure 2.1. RNA extraction: RNeasy lipid tissue kit protocol (Qiagen).

A tissue sample (50mg, 1ml Qiazol) was homogenised (1 min) and incubated at room temperature (RT, 5 mins). Chloroform (200µl) was added to the sample,vigourously shaken (15s) and incubated at RT (3 mins). All flow throughs were discarded. Centrifugation ensured optimal separation of the organic and aqueous phases (12,000g for 15min at 4c). The upper aqueous phase containing RNA was removed and placed in a new tube. A 1:1 equivalent of 70% ethanol was added to aqueous phase and vortexed. The sample was centrifuged (8,000g for 15s at RT), binding the RNA to the column. A series of wash steps remove non specifically bound carbohydrates, fatty acids and proteins (RW1), and guadinine salts (RPE). which would interfere with RT-PCR reactions whilst retaining RNA > 200 bases on the silica column. DNase treatment following elution removed contaminating sources of DNA from the RNA sample.

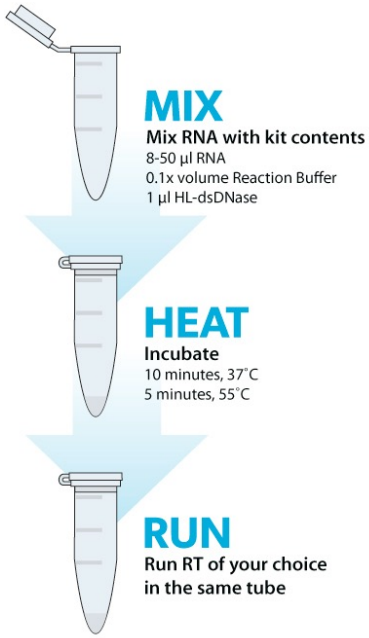

Figure 2.2. DNase treatment: removing sources of DNA contamination from the RNeasy lipid tissue kit eluant (based on Invitrogen DNase protocol).

RNA eluant from RNeasy lipid kit (30µl) was incubated with DNase I reaction buffer (3µl, 10x stock solution), DNase I (3µl, 1U/µl)**.** DNase treatment (Invitrogen) was performed to remove any source of contaminating genomic DNA after elution of genomic material from the RNeasy lipid mini kit (Figure 2.1 following RNA elution and 2.2 for protocol). The reaction mix was incubated (10min at room temperature). Following incubating the DNase I was inactivated through addition of EDTA (1µl of 25mM) and heat treated (55c,5min). Image adapted from http://www.tataa.com/wp-content/uploads/2012/11/Heat-and-Run-Workflow.jpg.

RNA was quantified using the Nanodrop ND-100 Spectrophotometer (Labtech, UK). Ribosafe RNase inhibitor, (1µl) was added after RNA quantification to preserve RNA integrity and minimise RNA degradation and loss of quality upon storage at -80c. The priming premix was prepared on ice. Briefly, 500ng of each RNA sample was reverse transcribed to cDNA (Bioline) using random hexmaers (1µl, 40µM stock), dNTP (1µl,10mM) and DEPC-treated water (up to final volume of priming mix of 10µl). Samples were incubated in these RNase free reaction tubes (70c, 10min) before being chilled on ice (10min). A reaction premix was prepared, with volumes described here given per reaction, 5x RT buffer (4µl), Ribosafe RNase inhibitor (1µl), Bioscript reverse transcriptase (1µl) and diethyl pyrocarbinate (DEPC)-treated water (up to a final reaction premix of 10µl). DEPC is a nonspecific inhibitor of RNases. The reaction premix was added to the priming premix and mixed by pipetting. Samples were incubated as follows; 10min at 25c then 42c, 30 min). The synthesis reaction was terminated by heat inactivation (85c for 5 min). The cDNA sample was chilled on ice for 15min before further use. cDNA samples were amplified using Taqman primers and probes (Applied Biosystems, UK, OPA1; Hs_00323399_m1, Mfn2; Hs_00208382_m1, Fis1; Hs_00211420_m1, Drp1; Hs_00247147_m1, FOXC2; Hs_00270951_s1, CD68; Hs02836816_g1) and universal PCR master mix (Applied Biosystems, UK) in an ABI 7500 thermocycler (Life Technologies).

2.2.4. Quantitative reverse transcription polymerase chain reaction program and gene expression analyses

Gene expressions were determined using quantitative real-time PCR (qRT-PCR) and were normalised to a housekeeping gene (18s, Applied Biosystems). Each sample was measured in triplicate. The expression of each gene was defined as a delta threshold cycle (ΔCt) value (where ΔCt = Ct of gene of interest – Ct of 18S). The data was transformed from ΔCt to 2-ΔΔCt to allow the trend in gene expression to be expressed as relative fold change in arbitrary units (AU) of averaged overweight and obese subjects compared to average mitochondrial dynamics gene expression of lean subjects. Bar charts were selected to represent the mRNA expression of mitochondrial dynamics genes, with error bars indicating the standard error of the mean across the subjects of each BMI category (lean,overweight.obese).

Experimental conditions:

qRT-PCR master mix per reaction:

Taqman gene expression master mix: 12.5µl

Taqman gene expression assay: 1.25µl

House keeping gene: 1.25µl

cDNA: 1µl

Nuclease free water: 9µl

Final volume: 25µl

Thermal cycling conditions:

Hold: 50c , 2 min

Hold: 95c, 10 min

Cycle (40 cycles): 95c, 15s

Cycle: (40 cycles) 60c, 1 min

2.2.5. Protein determination and western blot analysis.

Human adipose tissue was homogenised and resuspended in 1x RIPA lysis buffer (Millipore) containing protease inhibitor (Roche) and phosphatase inhibitor (100µl of 100mM Sodium fluoride and 100µl of 100mM Sodium vanadate, Sigma Aldrich). Protein concentrations were assessed by Biorad assay (detergent compatible protein assay kit, Bio-Rad laboratories, CA) using BSA as a standard (Sigma). Concentrations were quantified using a nanospectrophotometer (Geneflow, UK) A_{595}. 20µg of protein samples were loaded per well. For OPA1 (7.5% sodium dodecyl sulphate poly-acrylamide gel, SDS-PAGE) and Fis1 (12.5%), the percentages of SDS-PAGE gel used are given in brackets . Protein expression of OPA1 (1:1000, anti-rabbit, abcam, ab42364) and MFN2 (1:1000, anti-mouse, abcam, ab56889) were measured using the primary antibodies given in the brackets . Anti-mouse and anti-rabbit (1:1000, cell signalling technology, #7074 and #7076 and anti-mouse (1:10,000, the binding site) secondary antibodies were used to detect primary antibodies (anti-rabbit for Opa1 and anti-mouse for Mfn2 probed westerns) . All antibodies were diluted in 0.2% iBlock. Equal protein loading was confirmed by examining β-actin protein expres-sion. ECL was used to determine chemiluminescence and to visualise protein bands

(GE healthcare, UK). The intensity of each band was determined by densitometry (ImageQuant, Amersham).

2.2.6. Mitochondrial copy number determination.

Total DNA was extracted from paired subcutaneous adipose tissue using DNeasy blood and tissue kit (Figure 2.3) (Qiagen). RNase treatment was performed to prevent co-purification of RNA with genomic DNA. The relative amounts of nuclear and mitochondrial DNA were determined by PCR. DNA was amplified using SYBR green in an ABI 7500 thermocycler (Life technologies). The abundance of each gene was calculated as the ratio between mitochondrial threshold cycle (Ct) value and nuclear threshold cycle. Each sample was measured in duplicate against a mitochondrial (m) / nuclear (n) DNA primer set. The following primer sequences were used: *Cytochrome b forward (mitochondrial), 5′-GCGTCCTTGCCCTATTACTATC-3′, and Cytochrome b reverse, 5′-TATCCGCCATCCCATACATT-3′.* β-*actin forward (nuclear), 5-ACCCACACTGTGCCCATCTAC′-3 and* β-*actin reverse 5′-TCGGTGAGGATCTTCATGAGGTA-3* as previously published (Ferber, Peck et al. 2012). ND1 forward (mitochondrial), *5′-ATGGCCAACCTCCTACTCCT-3′* and ND1 reverse, *5′-GCGGTGATGTAGAGGGTGAT-3′* and BECN1 forward (Nuclear), 5′-*CGAGGCTCAAGTGTTTAGGC*-3′ and BECN1 reverse, 5′-*ATGTACTGGAAACGCCTTGG*-3′ (Hsieh, Weng et al. 2011). Melt curve analyses to confirm the production of a single, primer specific product.

Figure 2.3 DNA extraction: DNeasy Blood and tissue protocol (Qiagen).

Adipose tissue (25mg) was placed in a microcentrifuge tube (1.5ml) containing buffer ATL (180µl). Proteinase K was added (20µl) to the tube and mixed with the ATL and tissue by vortexing. Using a heat block the adipose tissue sample was lysed by incubation (56c, 2hr) and regular vortexing (every 15min). Upon completion of lysis, RNase A (4µl,100mg/ml working stock) was added to the reaction tube, vortexed and incubated (room temperature, 2min). The lysed and RNase free adipose tissue sample was vortexed (15s). Following this, buffer AL (200µλ) and ethanol (96-100% HPLC grade, 200µλ) were added to the reaction tube and the sample was vortexed. The mixture was transferred to a DNeasy mini spin column and centrifuged (6000g, 1min). At each stage the flow through and collection tube were discarded and replaced. The column was washed with buffer AW1 (500µλ) and centrifuged (6000g, 1min). The DNeasy mini spin column was placed in its fresh collection tube and washed a second time to dry the membrane and remove residual ethanol (500µl, buffer AW2, 20000g, 3min). DNA was eluted in a minicentrifuge tube (2ml) using buffer AE (200µl, incubated for 1min at room temperature, centrifuge 6000g for 1min).

2.2.7. Statistical analyses.

Data were examined for normality according to the Shapiro-Wilks criteria (originally published in 1965, this normality test is appropriate for sample sizes of less than 50). Non-normally distributed data were log-transformed prior to statistical analyses. Analyses were performed in SPSS version 21 (IBM) and figures were generated using Numbers for Mac (version 3.2). Analysis of variance (ANOVA) was used to evaluate differences in between the BMI categories (lean, overweight and obese). An unpaired student's t-test was used to compare mRNA expression of mitochondrial dynamics genes in AbSc AT between obese or overweight patients and the lean controls. A *p* value of 0.05 or less was considered statistically significant. All data are presented as means ± S.E.M unless otherwise stated.

2.3. Results.

2.3.1 Effect of adiposity on clinical parameters of the human AbSc AT cohort

Unpaired t-test analyses were performed to identify differences in the clinical parameters between lean versus overweight and lean versus obese. Fasted Glucose levels were significantly higher in obese compared to the lean cohort (Table 1, $p < 0.05$). No differences were noted between the fasted glucose levels of lean and overweight subjects. Total-cholesterol, triglycerides, LDL-cholesterol and HDL-cholesterol were not significantly different between all three cohorts (lean, overweight, obese). Insulin levels were significantly higher in obese compared to lean subjects (Table 1. $p < 0.05$). Glucose and insulin were measured in fasted plasma samples. These clinical parameters are consistent with previous studies (Bastard, Maachi et al. 2006, Neff 2013) and define these sub-

jects as a representative cohort for the investigation of adiposity and mitochondrial dynamics.

	Lean (n=10)	Overweight (n=10)	Obese (n=10)
BMI (kg/m	22.9 ± 0.9	26.8 ± 1.5***	34.1 ± 2.1***
Glucose (mmol/L)	4.8 ± 0.4	4.7 ± 0.5	5.5 ± 0.8*
Cholesterol (mmol/L)	5.4 ± 1.3	5.6 ± 0.4	6.0 ± 1.2
Triglycerides (mmol/L)	1.1 ± 0.6	1.3 ± 0.2	1.5 ± 0.6
LDL (mmol/L)	3.2 ± 0.8	2.8 ± 0.1	4.3 ± 0.9
HDL (mmol/L)	1.9 ± 0.7	2.2 ± 0.7	1.4 ± 0.3
Insulin (mmol/L)	4.7 ± 1.3	4.9 ± 1.8	12.1 ± 7.1*

Table 1. Comparison of the clinical parameters within the cohort.

Data are presented as mean ± SD. ANOVA was used to compare between BMI groups. $p < 0.05$ was considered statistically significant. $p < 0.05$*, $p < 0.01$** and $p < 0.001$***. lean; n = 10, overweight; n = 10 and obese; n = 10. Age was not included as it was not available for all subjects. Glucose (glucose oxidase method) and insulin (enzyme amplified sensitivity multiplex immunoassay) data are from fasted blood samples. Lipid, glucose and insulin profiling were performed by colleagues in the biochemistry lab and previous diabetes research staff at University Hospital Coventry and Warwickshire.

2.3.2. Effect of adiposity on markers of mitochondrial fission.

mRNA expression of genesinvolved in mitochondrial fission; Fis1 and Drp1 were measured by qRT-PCR in AbSc AT. Fis1 expression increased in AbSc AT with BMI (Figure 2.4. lean vs obese: $p = 0.008$). Furthermore, mRNA Drp1 expression with adiposity also significantly increased with BMI (Figure 2.4. lean vs overweight: $p = 0.06$ and lean vs obese; $p = 0.018$). Taken together, markers of mitochondrial fission were higher in obesity.

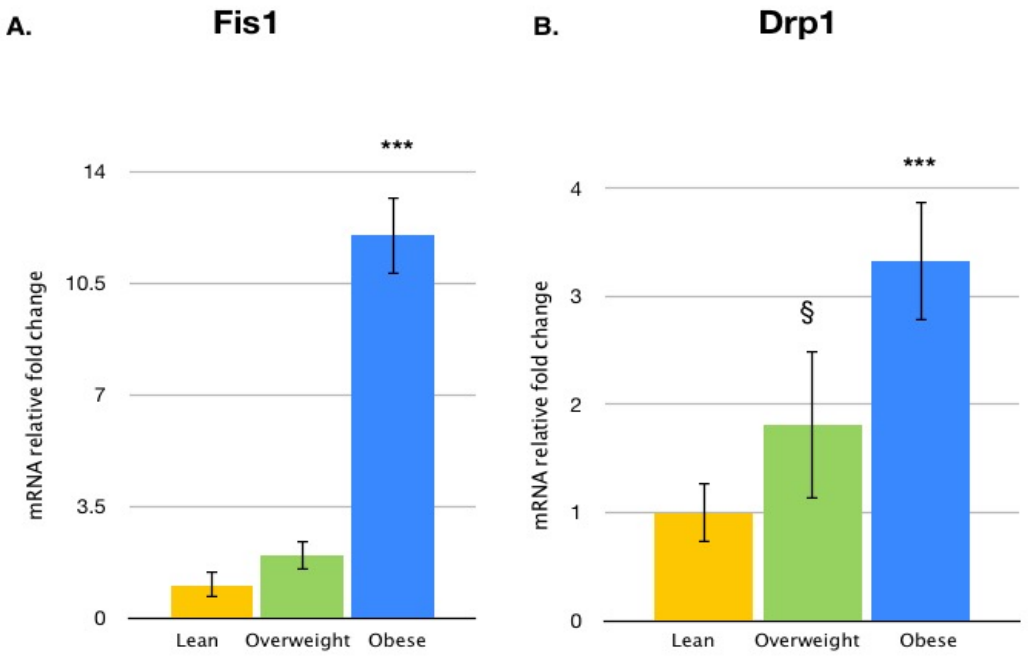

Figure 2.4. Markers of mitochondrial fission increased with adiposity.

mRNA expression of genes involved in mitochondrial fission; A) Fis1 and B) Drp1. All experiments were performed in triplicate. Unpaired t-tests were performed to assess the effect of BMI on either Drp1 or Fis1 expression. $p < 0.05$ was considered statistically significant. $p = 0.06$§ , $p < 0.05$*, $p < 0.01$** and $p < 0.001$***. lean; n = 10, overweight; n = 10 and obese; n = 10. Data are represented as means ± S.E.M.

2.3.3. Effect of adiposity on markers of mitochondrial fusion.

mRNA expression of genes involved in mitochondrial fusion; FOXC2, Mfn2 and Opa1 were measured by qRT-PCR in AbSc AT. Mfn2 and Opa1 increased at both an mRNA and protein expression level whilstthe transcriptional regulator of fusion, FOXC2 expression decreased in mRNA expression with adiposity. Mfn2 increased significantly in expression in obese subjects (Figure 2.5A-B. lean versus obese, mRNA: $p = 0.04$, protein: $p = 0.03$). Furthermore the second mitochondrial fusion gene Opa1 expression was significantly higher in obese compared to lean (Figure 2.5C-D. lean vs obese: mRNA: $p = 0.004$ and protein: $p = 0.001$). Conversly, FOXC2 mRNA expression was significantly lower in obese compared to lean subjects (Figure 2.5E. FOXC2: lean vs obese; $p < 0.001$).

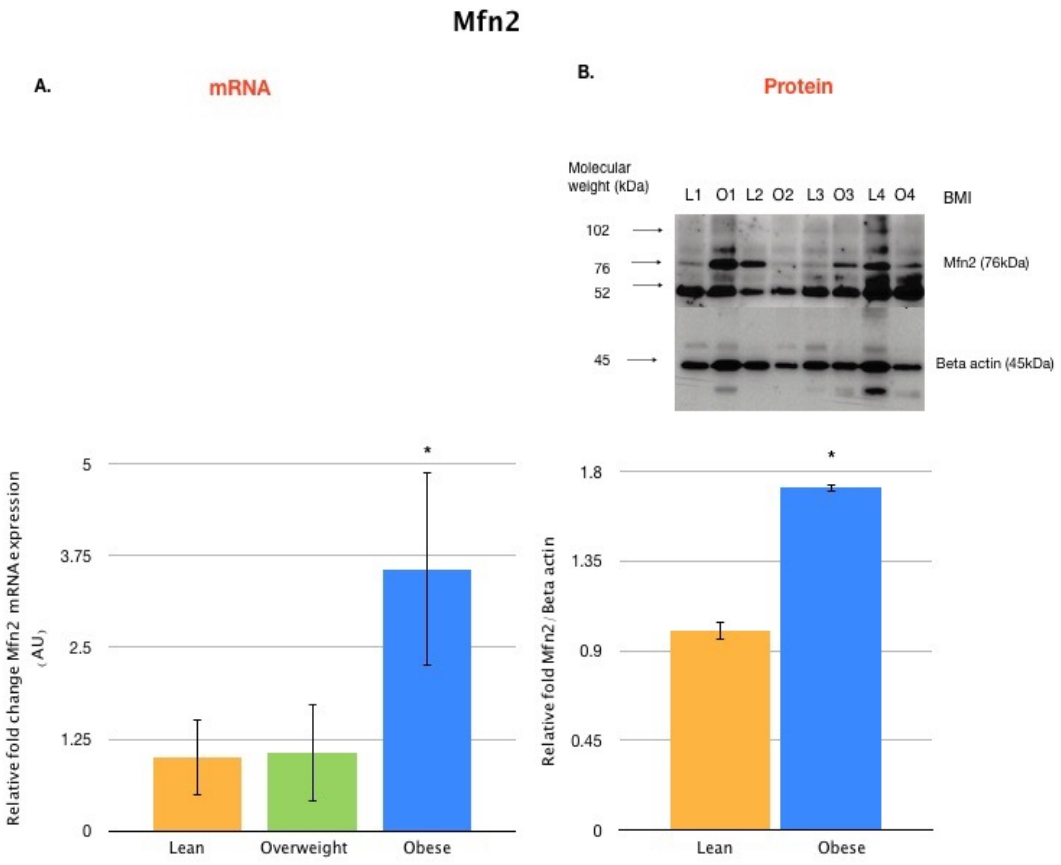

Figure 2.5. Markers of mitochondrial fusion increased with adiposity.

mRNA and protein expression of genes involved in mitochondrial fusion; A-B) Mfn2. All experiments were performed in triplicate. Unpaired t-tests were performed to assess the effect of BMI on Mfn2 expression. $p < 0.05$ was considered statistically significant. $p < 0.05$*. lean; n = 10, overweight; n = 10 and obese; n = 10. L1-L4 represent 4/10 lean subjects. O1-4 represent 4/10 obese subjects. These subjects were selected to highlight that despite differential expression of Mfn2 amongst the 10 patients, collectively a significant increase in Mfn2 protein expression was identified. Data are represented as means ± S.E.M.

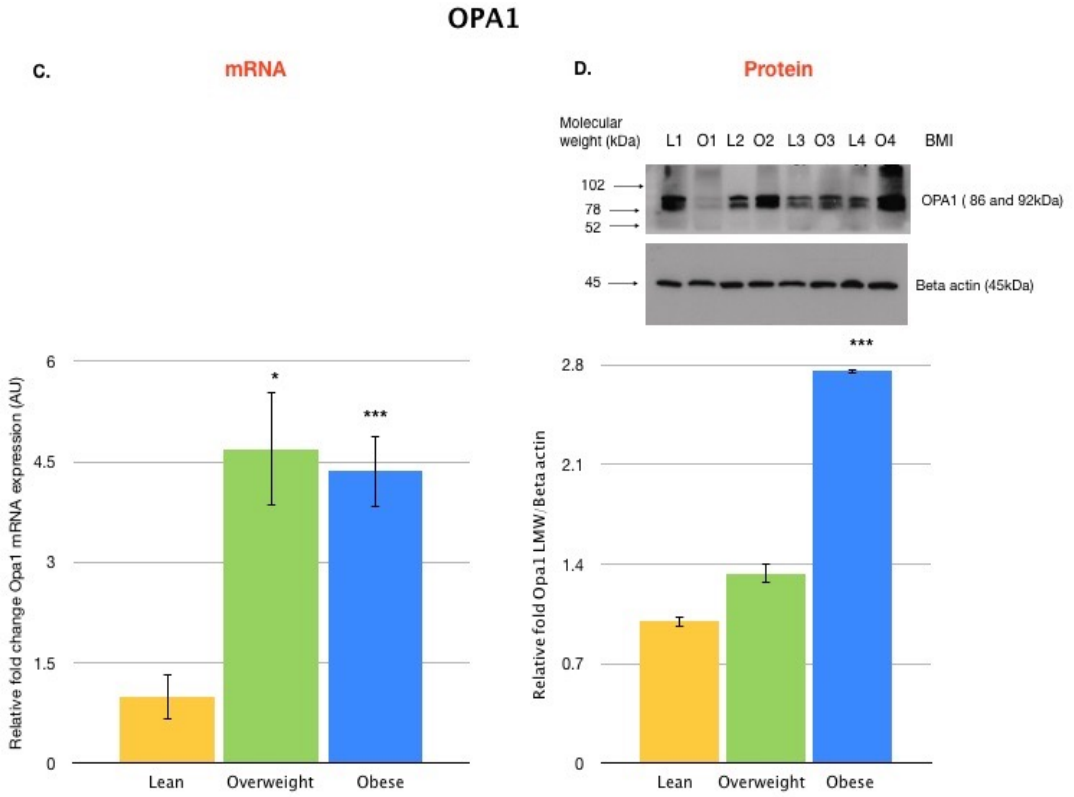

Figure 2.5 continued. Markers of mitochondrial fusion increased with adiposity. mRNA and protein expression of genes involved in mitochondrial fusion; C-D) Opa1.All experiments were performed in triplicate. Unpaired t-tests were performed to assess the effect of BMI on Opa1 expression. $p < 0.05$ was considered statistically significant. $p < 0.05$*, $p < 0.01$** and $p < 0.001$***. lean; n = 10, overweight; n = 10 and obese; n = 10. L1-L4 represent 4/10 lean subjects. O1-4 represent 4/10 obese subjects. These subjects were selected to highlight that despite differential expression of Opa1 amongst the 10 patients, collectively a significant increase in Opa1 protein expression was identified. Data are represented as means ± S.E.M.

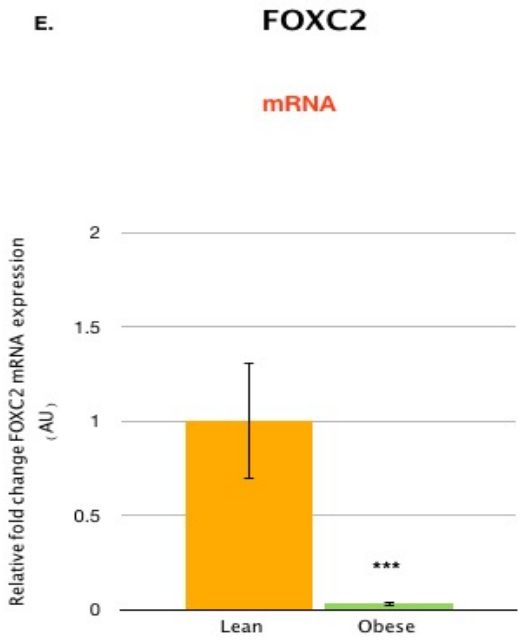

Figure 2.5 continued. Transcriptional regulator of mitochondrial fusion, FOXC2 decreased with adiposity

mRNA expression of genes regulating mitochondrial fusion; FOXC2 (E). All experiments were performed in triplicate. Unpaired t-tests were performed to assess the effect of BMI on FOXC2 expression. $p < 0.05$ was considered statistically significant. $p < 0.05$*, $p < 0.01$** and $p < 0.001$***. lean; n = 10, overweight; n = 10 and obese; n = 10. Data are represented as means ± S.E.M.

2.3.4 Balance of mitochondrial dynamics in adiposity

The balance of mitochondrial fusion and fission genes is essential to the maintenance of mitochondrial number, structure and morphology. Correlation analyses between markers of mitochondrial fusion and fission genes were performed to assess if the regulation of mitochondrial dynamics was altered by adiposity. Parametric analyses of Mfn2 vs Opa1 identified that these genes were positively and significantly associated in lean subjects (Figure 2.6. Mfn2 vs Opa1 mRNA; lean: $R^2 = 0.655$, $p = 0.04$). Conversely, in obese subjects, Mfn2 and Opa1 were no longer significantly positively associated (Figure 2.3. Mfn2 vs Opa1; obese: $R^2 = 0.407$, $p = 0.243$). No significant correlations were noted for the fission genes (Drp1 and Fis1) for either the lean or obese subjects.

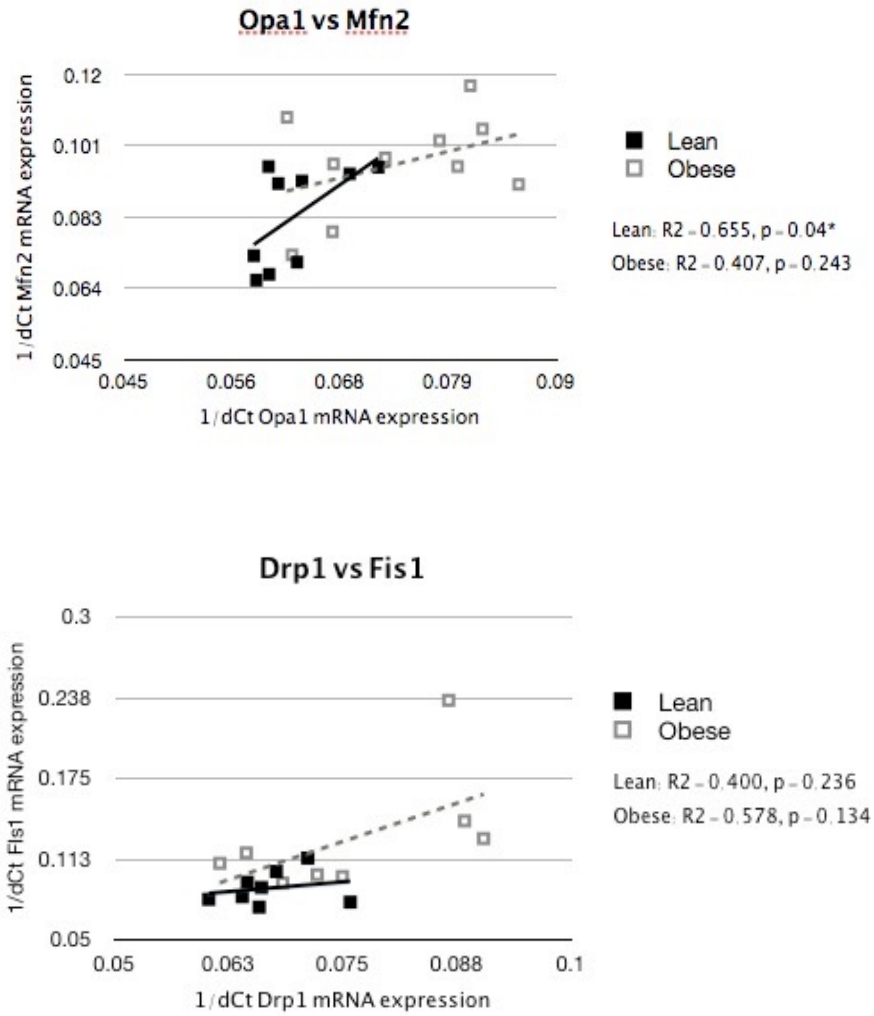

Figure 2.6. Balance of markers of mitochondrial dynamics in adiposity.

Parametric correlation analyses were performed to assess the relationship between the mitochondrial fusion markers, Mfn2 and Opa1 and mitochondrial fission markers, Drp1 and Fis1 and whether these were altered by adiposity. All mRNA expression data are an average of triplicate measurements. $p < 0.05$ was considered statistically significant. $p < 0.05$*, $p < 0.01$** and $p < 0.001$***. lean; n = 10 and obese; n = 10. Data are represented as means ± S.E.M.

2.3.5 Mitochondrial copy number in abdominal subcutaneous adipose tissue (AbSc AT) of lean, overweight and obese cohorts

Total genomic DNA was extracted from all the adipose tissuesamples and abundance of mitochondria specific (Cytochrome B (CytB)) and nucleus specific (β-actin) genes were measured using PCR. Approximate mitochondrial DNA content was calculated as the ratio of mitochondrial gene : nuclear gene. Mitochondrial DNA content did not alter significantly by BMI in our cohort (Figure 2.7, lean vs obese; $p > 0.05$).

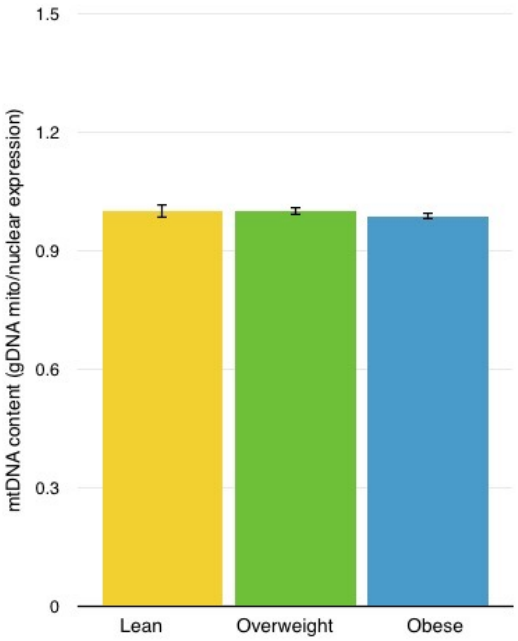

Figure 2.7. Mitochondrial DNA content did not alter significantly with adiposity. Amplification of mitochondrial (CytB) and nuclear genes (Beta actin) were performed by PCR to assess the relative mitochondrial DNA content in abdominal subcutaneous adipose tissue of all patients in our cohort. The relative mitochondrial DNA content was defined as a ratio between mitochondrial gene : nuclear gene expression. All experiments were performed in triplicate. Unpaired t-tests were performed to assess the effect of BMI on mitochondrial abundance. $p < 0.05$ was considered statistically significant. lean; n = 10, overweight; n = 10 and obese; n = 10. All data were non significant. Data are represented as means ± S.E.M.

2.3.6. Correlation analyses between mitochondrial DNA content and mitochondrial dynamics genes.

Parametric correlation analyses were performed to evaluate whether the relationship between mitochondrial DNA content and markers of mitochondrial dynamics was affected by adiposity. This was not the case,as a positive and significant relationship between FOXC2 and mitochondrial abundance in lean subjects (Figure 2.8. FOXC2 vs mito; lean: $R^2 = 0.744$, $p = 0.03$) and a less positive but still significant correlation in obese subjects (Figure 2.8. FOXC2 vs mito; obese: $R^2 = 0.704$, $p = 0.03$).

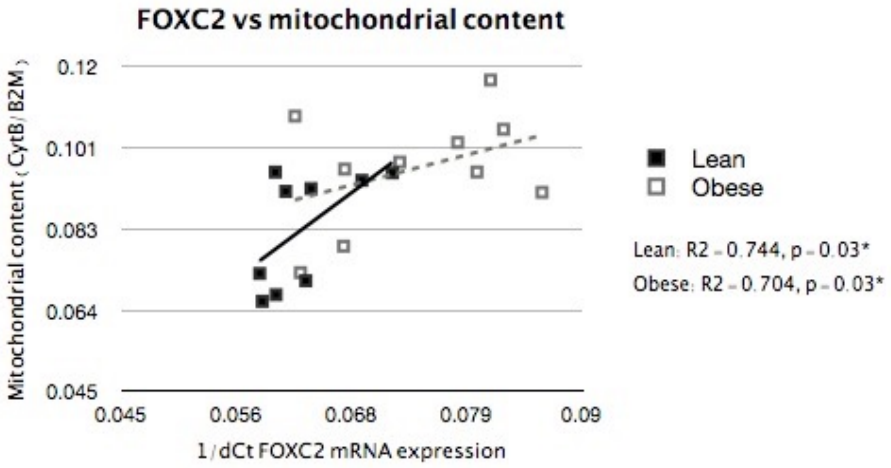

Figure 2.8. Correlation analyses between mitochondrial DNA content and markers of mitochondrial dynamics genes

Parametric correlation analyses were performed to assess the relationship between the mitochondrial DNA content and markers of mitochondrial dynamics gene expression. All mRNA expression data are an average of triplicate measurements. $p < 0.05$ was considered statistically significant. $p < 0.05$*, $p < 0.01$** and $p < 0.001$***. lean; n = 10 and obese; n = 10.

2.4. Discussion.

Previous studies have noted metabolic dysfunction within obesity (Virtue and Vidal-Puig 2010, Picard and Turnbull 2013). With the critical role of mitochondrial dynamics in controlling the abundance and health of mitochondria, any disturbance could result in negative implications for metabolism (Kelley, He et al. 2002, Szewczyk and Wojtczak 2002, Bakkman, Fernstrom et al. 2010). The results of this study demonstrate that markers of mitochondrial dynamics are altered with adiposity in AbSc AT and the expression of genes involved in fusion and fission, with the exception of FOXC2,were more highly expressed in overweight and obese individuals compared to lean individuals.

Mitochondrial dynamics during adiposity was studied by evaluating expression levels of gene markers of fission as well as fusion. This approach offers the ability to explore whether a single or multiple mitochondrial fission genes were altered by adiposity. Our data demonstrates that markers of mitochondrial fission increased with adiposity, as evidenced by the significantly increased expression levels of Fis1 and Drp1 in obese compared to lean controls (Figure 2.4). These data are consistent with previous studies in endothelial cells, which found a higher expression of Fis1 compared to healthy volunteers (Shenouda, Widlansky et al. 2011). Based on our and others observations that markers of mitochondrial fission are increased, it may be expected that mitochondrial DNA content would also increase, in the absence of any changes to mitochondrial fusion. Nevertheless, upon evaluation of the mitochondrial DNA content in our human AbSc AT revealed no significant change in mitochondrial DNA content with adiposity was observed (Figure. 2.7). Considering this result, the lack of significant increase in mitochondrial DNA content as a consequence of enhanced markers of mitochondrial fission is not only unexpected but is also in contradiction with the reduction in mitochondrial DNA con-

tent and size described in the skeletal muscle of obese subjects compared to their lean counterparts (Jheng, Tsai et al. 2012). A number of potential explanations can be offered to support our observations. Firstly, the increase in the expression of markers of mitochondrial fission may be compensated by an equivalent upregulation of expression of the markers of mitochondrial fusion. This possibility was investigated and will be discussed in further detail, later in this discussion. Secondly, others have suggested that a change in mitochondrial abundance may not necessarily indicate the full extent of changes to mitochondrial function (Jeng, Yeh et al. 2008). In light of this, even in the absence of changes to mitochondrial DNA content, the functional capacity of the individual mitochondria in obese individuals may differ from those of lean subjects. Indeed others have shown in islet cells, that knockout of Opa1, a gene involved in mitochondrial fusion did not affect mitochondrial DNA content (Jeng, Yeh et al. 2008, Picard and Turnbull 2013) but that their mitochondria displayed a significant decrease in electron transport chain complex IV and stunting of insulin secretion (Picard and Turnbull 2013).Furthermore, previous studies have highlighted that the presence of compromised mitochondria result in negative metabolic consequences for these individuals (Shenouda, Widlansky et al. 2011) possibly exerted through the induction of mitochondrial fragmentation (Jheng, Tsai et al. 2012). In order to consider the implications of our enhanced expression of markers of mitochondrial fission and consistency of mtDNA content, further studies would be required to assess the metabolic health of mitochondria in our subjects (Bakkman, Fernstrom et al. 2010, Brand and Nicholls 2011, Cabrera, Ziemba et al. 2012).

Returning to gene expression analysis of the opposing arm of mitochondrial dynamics from mitochondrial fission, markers of mitochondrial fusion also increased

with adiposity. In our study, Opa1 and Mfn2 mRNA and proteins expressions were significantly increased in obese compared to lean subjects (Figure 2.5 C and D). Whilst the mechanism for induction of Opa1 expression is unknown, others have shown that ob/ob mice fed with a high fat diet, had a lower Opa1 expression in their islets prior to the development of diabetes (Keller, Choi et al. 2008). In contrast, the increase in Opa1 expression in our AbSc AT study may present an earlier stage than the pre-diabetic status shown in the mice. In line with this study, FOXC2 expression in our AbSc AT samples were significantly diminished in obese subjects compared to lean controls (Figure 2.5E). As a transcriptional regulator of mitochondrial fusion, FOXC2 has been shown to represent a lean and insulin sensitive phenotype (Lidell et al. 2011).

In summary, mRNA and protein expression of markers of mitochondrial dynamics geneswere significantly increased with adiposity. Optimal mitochondrial dynamics requires balanced mitochondrial fusion and fission, in order to prevent the development of mitochondrial dysfunction (Zorzano, Liesa et al. 2009, Zorzano, Liesa et al. 2009, Liesa and Shirihai 2013). The balance of markers of mitochondrial fusion genes was different between lean and obese subjects. Parametric analyses of Mfn2 vs Opa1 identified that these genes were positively and significantly associated in lean subjects (Figure 2.6). However, the significance of the relationship between fusion gene expression was not upheld within the obese cohort. This result may indicate that the balance of mitochondrial dynamics is affected by adiposity and would support the known essential role of optimal mitochondrial dynamics in preventing the development of mitochondrial dysfunction.. The ex vivo treatment of our AbSc AT with palmitate , previously identified to inhibit mitochondrial fusion, would allow manipulation of fusion. Fusion has been character-

ised as selective and an essential pre-requisite for the subsequent intiation of mitochondrial fission, required to detect and remove dysfunctional mitochondrial components by mitophagy (Twig et al. 2008). Through the treatment of palmitate in obese subjects, would allow us to explore if the reduction of mitochondrial fusion was accompanied by changes in mitochondrial fission and how their mitochondria compared metabolically to those of the lean individuals whose fusion was already expressed at a lower level than those of the obese subjects.

The present study extends our understanding of mitochondrial dynamics in adipocytes as an entire system. The observation that markers of mitochondrial dynamics expression are altered in obese AbSc AT offers a potential explanation for the reduction in metabolism and dysregulation of energy homeostasis known to accompany adiposity (Kelley, He et al. 2002, Sparks, Xie et al. 2005).

Bariatric surgery is one of the most successful methods to resolve insulin resistance (Levy, Fried et al. 2007, Buchwald, Estok et al. 2009, Carlsson, Peltonen et al. 2012, Nijhawan, Richards et al. 2013). As a consequence, up to 85% of patients ameliorate their T2DM status following bariatric surgery (Bloomston, Zervos et al. 1997, Scopinaro 2002, Sjostrom 2005, Pories 2008). As a novel extension of this study, markers of mitochondrial dynamics was studied in pre and post bariatric surgery adipose tissue samples together with the effect of weight loss on the regulation of mitochondrial dynamics (Chapter 3).

Chapter 3

Bariatric Surgery:

Effects on markers of mitochondrial fission and fusion expression.

3.1. Introduction.

In Chapter 2, higher adiposity was shown to increase the expression of mitochondrial fission (Drp1 and Fis1) and fusion genes (Mfn2 and Opa1) in overweight and obese AbSc AT (Figures 2.4 and 2.5). Obesity is known to be a prominent risk factor for the development of insulin resistance and T2DM. By 2035, the financial cost of treating diabetes and its associated secondary complications is estimated at £39.8 billion (WHO, 2013). Given the public health burden of T2DM and obesity globally, understanding at a molecular level, the regulation of insulin sensitivity and T2DM, is of vital significance (DeFronzo 2004). Currently, bariatric surgery represents the most effective treatment for long-term resolution of T2DM and control of obesity above that which can be achieved through lifestyle alone e.g. exercising and dieting (Levy, Fried et al. 2007, Cunneen 2008, Pories 2008). Previous studies have identified that weight loss induced following surgery provides beneficial effects within cellular metabolism including resolution of insulin resistance and remission of T2DM (Niskanen, Uusitupa et al. 1996, Guldstrand, Ahren et al. 2003, Villareal, Banks et al. 2008). Weight loss (Ziccardi, Nappo et al. 2002, Gumbs, Modlin et al. 2005) has also been shown to correspond with significant changes in beta cell function and endoplasmic reticulum stress (ER) (Gregor, Yang et al. 2009, Bradley, Conte et al. 2012).

Several studies show that mitochondrial dysfunction is present in metabolic disorders such as insulin resistance and T2DM (Lowell and Shulman 2005, Zorzano, Liesa et al. 2009, Bournat and Brown 2010, Jheng, Tsai et al. 2012). As the regulators of energy metabolism (Rosen and Spiegelman 2006, Liesa and Shirihai 2013), mitochondria and their health are tightly regulated. Mitochondrial dysfunction can result from an imbalance in mitochondrial fusion and fission or an overactivation of mito-

chondrial fission (Figure 1.5) (Lowell and Shulman 2005, Zorzano, Liesa et al. 2009, Jheng, Tsai et al. 2012). Mitochondrial dynamics contributes to the maintenance of mitochondrial abundance and function through the selective sequestering of compromised mitochondria that are shuttled towards mitophagy and thus removed from the mitochondrial population (Figure 1.7) (Twig, Hyde et al. 2008). Without balanced mitochondrial dynamics, compromised mitochondria would accumulate. The presence of imbalanced mitochondrial dynamics within these individuals could provide an explanation for diminished metabolic health of cells, which often accompanies T2DM (Mouli, Twig et al. 2009).

Despite the critical role of the mitochondria within cellular metabolism, the regulation and balancing of mitochondrial dynamics in adipose tissue remain poorly characterised. Without mitochondrial dynamics, cells would continually accumulate damaged mitochondria, which if allowed to persist, would compromise cellular metabolism and survival (Lowell and Shulman 2005, Michel, Wanet et al. 2012). To date, most research has focused on investigation of insulin resistance and mitochondrial dynamics within skeletal muscle. Therefore, the aim of this study was to address whether mitochondrial dynamics were imbalanced in our T2DM cohort and if the type of surgical procedure or weight loss induced after surgery could influence mitochondrial dynamics in AbSc AT.

3.2. Materials and Methods.

3.2.1 Selection and description of participants:

29 female Caucasian patients who were scheduled to undergo Bariatric Surgery (Gastric banding, (GB), n = 8; 54 ± 11 years old, Sleeve Gastronectomy (SG) like gastric plication surgery (n = 13; 55 ± 6 years old) or Biliopancreatic diversion (BPD), n = 8; 52 ± 3 years old) procedures at ISCARE Clinic Centre in the Czech Republic participated in this study under ethical approval. Prior to enrolment, all participants provided written informed consent and completed a comprehensive medical evaluation. All patients had a BMI > 35 kg/m^2 and T2DM. Samples of abdominal subcutaneous adipose tissues (AbSc AT) were taken at time of surgery and 6 months after surgery. These samples were collected as a surgical biopsy. The post surgical sample was taken at 6 months after surgery as the weight loss for patients across all surgical procedures was estimated from previous studies to correspond to a around 20% weight loss. A follow-up is planned by our collaborators to collect a further AbSc AT biopsy from each patient, by the same surgical method, 1 year after their bariatric surgery.

All groups were matched for age (54 ± 7 years), BMI (Pre 41.9 ± 6) and duration of diabetes. Aspirin and medications for diabetes were discontinued, under medical supervision, 3 days before each proposed study test.

3.2.2. Body composition and basal metabolic variables.

Body fat compositions were measured pre-operatively and 6 months after surgery by dual energy x-ray absorptiometry (DEXA) using a whole body Hologic QDR 2000 scanner (Hologic Europe, Vilvoorde, Belgium).

3.2.3. Surgical procedures.

For the current study we used adipose tissue from three different types of bariatric surgical procedure. They are explained as follows:

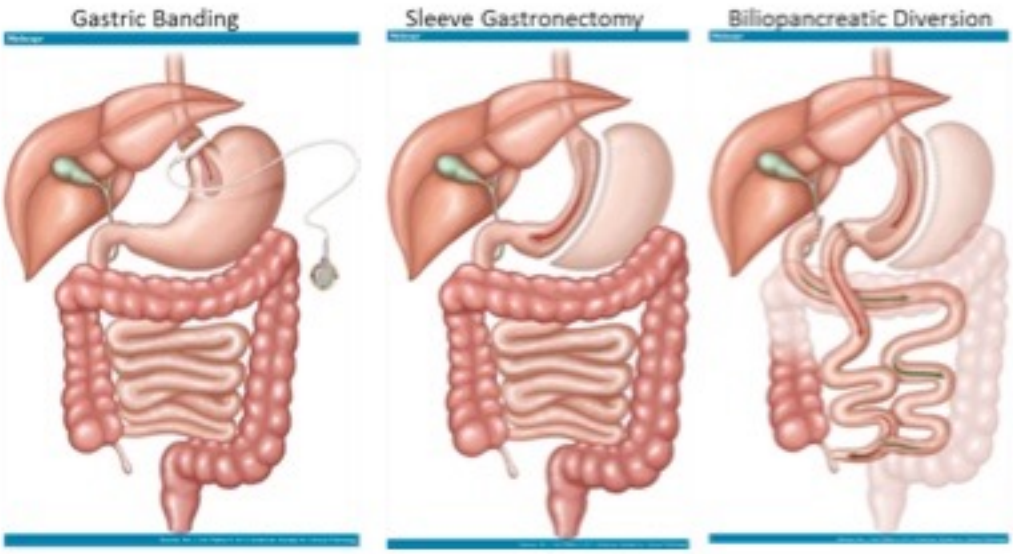

Figure 3.1. Types of bariatric surgery:**Gastric Banding (GB), Sleeve Gastronectomy (SG) and Biliopancreatic Diversion (BPD).** Clinical observations have highlighted that the more extensive structural remodelling of the gastrointestinal tract during bariatric surgery, the more significant the correlation with diabetes resolution. Images taken from (Neff 2013). BPD > SG > Band for post surgical remission of T2DM.

GB, or laproscopic adjustable gastric banding (LAGB) involves placement of a silicone band immediately below the gastro-oesophageal junction at the upper part of the stomach (Dixon, Straznicky et al. 2012). This results in physical division of the upper and lower part of the stomach. Restriction of the opening between the two parts of the stomach using the silicone band can influence hunger and satiety (Burton and Brown 2011). The size of the opening can be altered post operatively (Cherian, Tentzeris et al. 2010). Adjusting the band appears to promote reduction in food consumption by lowering feelings of hunger. The advantages of the procedure are its reversibility and adjustability, maintenance of normal digestive processes and absorption of nutrients and vitamins (Schouten, Wiryasaputra et al. 2010). The disadvantages are the greater lag time between surgical procedure and initial weight loss. Lower proportions of patients lose 50% of their excess body weight compared to other bariatric procedures and issues with band adjustment/positioning (Aarts, Dogan et al. 2014).

Sleeve Gastronectomy (SG) procedure, 75% of the stomach's capacity is removed, reducing the amount of food that can be consumed. Whilst stomach function is virtually unchanged, remodelling involves resection of the greater curvature of the stomach at 4cm proximal to the pylorus (Skrekas, Antiochos et al. 2011, Neff 2013). The advantages of this procedure include the rapid, significant and sustained weight loss of more than 50% based on 3-5+ year follow up data (Himpens, Dobbeleir et al. 2010) and improved satiety, reduction in hunger and appetite via changes in the secretion of gut hormomes (accessed on 17.6.14: http://asmbs.org/obesity-and-surgery-learning-center/bariatric-surgery-procedures/#sleeve). Nevertheless, like all surgical procedures, SG presents a number of disadvan-

tages including the irreversible nature of the procedure and possibility of long-term vitamin deficiencies (Pech, Meyer et al. 2012).

Biliopancreatic diversion (BPD) involves extensive remodeling of the stomach and bypassing of the small intestine (Ferrannini, Rosenbaum et al. 2014). A small pouch is created which is attached to the colon bypassing the small intestine. Unlike SG and GB, this diversion results in a significant decrease in the absorption of nutrients, calories and fat-soluble vitamins (Levy, Fried et al. 2007, Tice, Karliner et al. 2008). This procedure is considered to resolve T2DM most effectively (Buchwald, Estok et al. 2009). Further advantages include up to 70% excess weight loss 5 years after surgery and up to 70% lower absorption of dietary fat ((Dolan, Hatzifotis et al. 2004) accessed 17.6.14:http://asmbs.org/obesity-and-surgery-learning-center/bariatric-surgery-procedures/#sleeve). Given the complicated nature of the BPD procedure, post-surgical disadvantages may include greater propensity for vitamin, mineral and protein deficiencies and longer post-surgical recuperation (Topart, Becouarn et al. 2014).

3.2.4. Analyses of blood samples and adipose tissue.

Fasted serum and plasma samples were used to assess the metabolic, hormonal and inflammatory profiles of all participants (e.g. glucose, cholesterol, triglycerides, HDL, HbA1c, insulin). Fasted glucose and insulin (Roche, Modular Analytics E170, Mannheim, Germany) measurements undertaken by our Czech collaborators allowed calculation of Homeostasis Model Assessment indices (HOMA-insulin resistance) (Matthews, Hosker et al. 1985).

HOMA-IR was calculated as follows: [HOMA-IR= Fasted Insulin (μU/l) x Fasted glucose (mmol/l))/22.5]. LDL Cholesterol was calculated using the Friedewald formula (Friedewald, Levy et al. 1972).

Adipose tissue samples were flash frozen in liquid nitrogen, immediately after collection, and then placed directly at -80°c freezer for storage until use, to ensure minimal damage or degradation.

3.2.5. Isolation of mRNA and qPCR.

See adiposity chapter 2, section 2.2.3 for description

3.2.6. Protein determination and western blot analysis.

See adiposity chapter 2, section 2.2.5 for description

3.2.7. Mitochondrial copy number determination.

See adiposity chapter 2, section 2.2.6 for description

3.2.8 Statistical analyses.

Data were examined for normality according to the Shapiro-Wilks criteria. Non-normally distributed data were log-transformed prior to statistical analyses. Analyses were performed in SPSS version 21 (IBM) and figures were generated using Numbers (Mac version 3.2). Analysis of variance (ANOVA) was used to evaluate differences in weight loss induced changes between the 3 surgical procedures (GB, SG and BPD). A paired student's t test was used to compare mRNA and protein expression of mito-

chondrial dynamics markers in AbSc AT before and after weight loss. A *P* value of 0.05 or less was considered statistically significant. All data are presented as means ± S.E.M unless otherwise stated. Power analysis revealed that 29 samples were sufficient to determine a statistically significant difference in mitochondrial copy number that may arise due to Bariatric Surgery. The sample size calculation was done using G*Power version 3.1.9 (Dusseldorf, Germany). An assay, the details of which are provided in*: Mitochondrial copy number determination* section 2.2.6 generated mitochondrial copy numbers from 29 samples with a power of 0.84 and an $\alpha = 0.16$ given $R = 0.41$.

3.3. Results.

3.3.1. Clinical parameters following bariatric surgery.

On average, subjects lost 25% of their initial body weight 6 months after bariatric surgery (GB, BPD and SG; Table 2, $p < 0.01$). Bariatric surgery resulted in an average percentage excess BMI loss across subjects of 33% ± 13 ($p < 0.05$, Table 2). Across all surgical procedures, values of insulin sensitivity determined through homeostatic model assessment of insulin resistance (HOMA-IR) were more than halved from 11.90±8.63 to 5.11±2.95 ($p < 0.01$, Table 2). HbA1c levels decreased significantly post-surgery from 5.6±0.94 to 4.5± 0.82 ($p < 0.01$, Table 2). Furthermore, fasted levels of plasma markers of glucose homeostasis were markedly improved following surgery (glucose (9.26±2.48 to 7.22±1.65 mmol/L) and insulin (28.8±18.57 to 16.28±9.01 μU/ml), both $p < 0.01$, Table 2).

	LAGB		GP		BPD		All Surgery types	
Timepoint	Pre	Post	Pre	Post	Pre	Post	Pre	Post
♀	8		13		8		29	
Age (Y)	54 ± 11		55 ± 6		52 ± 3		54 ± 7	
BMI (kg/m^2)	41.9 ± 7.26	37.26 ± 7.8	40.03 ±5.45	35.7 ± 4.36	44.7 ± 4.9	37.3 ± 4.59	41.9 ± 6.01	36.6 ± 5.45
Glucose (mmol/L)	9.60 ± 2.72	7.10 ± 1.70	9.09 ± 2.19	7.29 ± 1.69	9.17 ± 2.91	7.21 ± 1.71	9.26 ± 2.48	7.22 ± 1.65
Insulin (μU/ml)	26.7 ± 7.73	15.7 ± 5.93	26.4 ± 20.5	16.29 ± 11.34	34.68±23.3	16.93 ±8.27	28.8 ±18.57	16.28 ± 9.01
HOMA-IR	11.33 ±4.38	5.26 ± 3.0	11.12±9.63	5.06 ± 3.23	13.69±19.7	5.03 ± 2.77	11.90 ±8.63	5.11 ± 2.95
Cholesterol (mmol/L)	4.83 ± 0.88	4.35 ± 0.68	4.98 ± 0.74	4.83 ± 0.84	5.20 ± 1.13	3.90 ± 0.98	5.00 ± 0.88	4.43 ± 0.90
Triglycerides (mmol/L)	1.72 ± 0.78	1.19 ± 0.50	2.10 ± 1.43	1.45 ± 0.73	1.62 ± 0.72	1.66 ± 0.70	1.86 ± 1.09	1.44 ± 0.67
LDL (mmol/L)	2.99 ± 0.80	2.72 ± 0.60	2.87 ± 0.77	2.87 ± 0.62	3.46 ± 1.14	2.37 ± 0.73	3.09 ± 0.91	2.67 ± 0.67
HDL (mmol/L)	1.05 ± 0.28	1.08 ± 0.28	1.14 ± 0.35	1.17 ± 0.32	1.00 ± 0.22	0.76 ± 0.12	1.08 ± 0.30	1.03 ± 0.31
HbA1C	5.34 ± 0.99	4.6 ± 0.68	5.73 ± 1.04	4.83 ±1.03	5.74 ± 0.85	4.14 ± 0.42	5.6 ± 0.94	4.5 ± 0.82

Table 2. Comparison of clinical parameters pre and post surgery.

Data are presented as mean ± SD. * = $p < 0.05$ and ** = $p < 0.01$. Fasted glucose and insulin values are shown. HOMA-IR was calculated as follows: [HOMA-IR = fasted insulin (U/l) * faster glucose (mmol/l))/22.5]. Percentage excess BMI loss = (pre operative BMI - current BMI/pre operative-25) * 100).

3.3.2. Influence of the different surgical procedures on clinical parameters following bariatric surgery.

Stratification of subjects based on their surgical procedure revealed distinct differences in their post-surgical clinical and mitochondrial gene expressions (Table 2). BPD patients saw the greatest number of biochemical parameters significantly improve following surgery including glucose, insulin, HbA1c and percentage excess BMI loss. Whilst BPD provided the most consistent improvement in clinical parameters following surgery, no single surgical procedure could account for all the significant reductions in clinical parameters observed following bariatric surgery. Taken together, weight loss rather than the type of surgical procedure provides a more comprehensive explanation for the changes observed in clinical parameters in abdominal subcutaneous adipose tissue (AbSc AT) 6 months after surgery.

3.3.3. mRNA expression of the mitochondrial fission markers, Fis1 and Drp1 before and after bariatric surgery

Fis1 and Drp1 play important roles in mitochondrial fission. After 6 months, following weight loss accompanying bariatric surgery, mRNA expressions of Drp1 and Fis1 were significantly reduced when all patients were included in the analysis irrespective of the surgical procedure (Figure 3.2 A and B. pre vs post, $p < 0.05$). Upon stratification of the data by surgical procedure, all the surgeries showed a trend towards reduced expression but only patients undergoing GB surgery displayed a significant decrease in Fis1 mRNA expression (Figure 3.3A. GB; $p = 0.02$), while Drp1 was consistently and significantly downregulated across all surgical procedures (Figure 3.2A. overall pre vs post-surgery; $p < 0.04$, Figure 3.3A. GB; $p = 0.02$, 3.3B. SG; $p = 0.04$ and 3.3C. BPD; $p = 0.03$). These data lend support to the observation that although the surgical procedure may influence the outcome of mitochondrial fission marker expression , weight loss may be the biggest factor involved in this process. Figure 3.4 shows the mRNA expressions of Drp1 and Fis1 for each patient pre and post bariatric surgery.

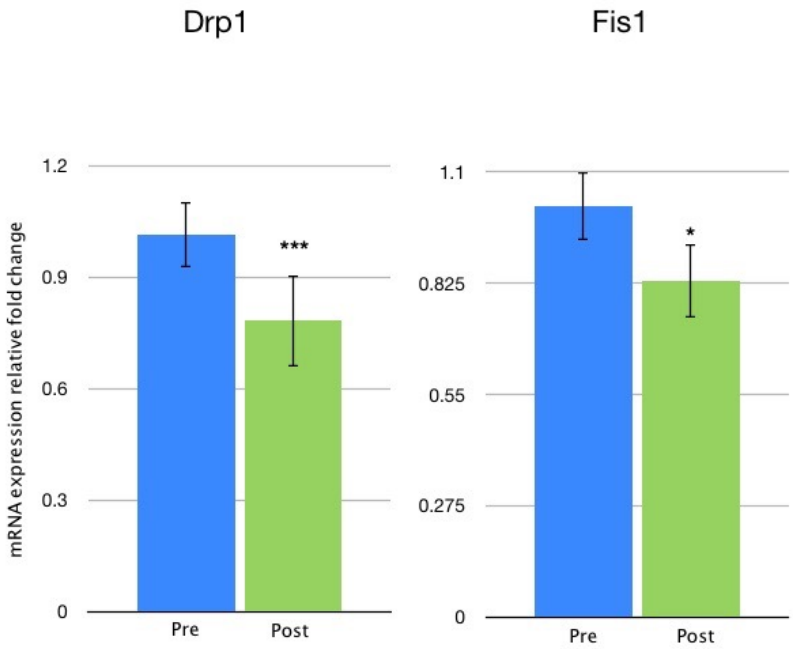

Figure 3.2. Markers of mitochondrial fission, Drp1 and Fis1 decrease significantly after bariatric surgery.

mRNA expression of genes involved in mitochondrial fission; A) Drp1 and B) Fis1. All experiments were performed in triplicate. Paired t-tests were performed at an individual subject level between mRNA expression values of either Drp1 or Fis1 in their pre and post surgical sample (n = 29 pre, n = 29 post). $p < 0.05$ was considered statistically significant. $p < 0.05$*, $p < 0.01$** and $p < 0.001$***. p values were compared to before surgery mRNA expression level. Data are represented as means ± S.E.M.

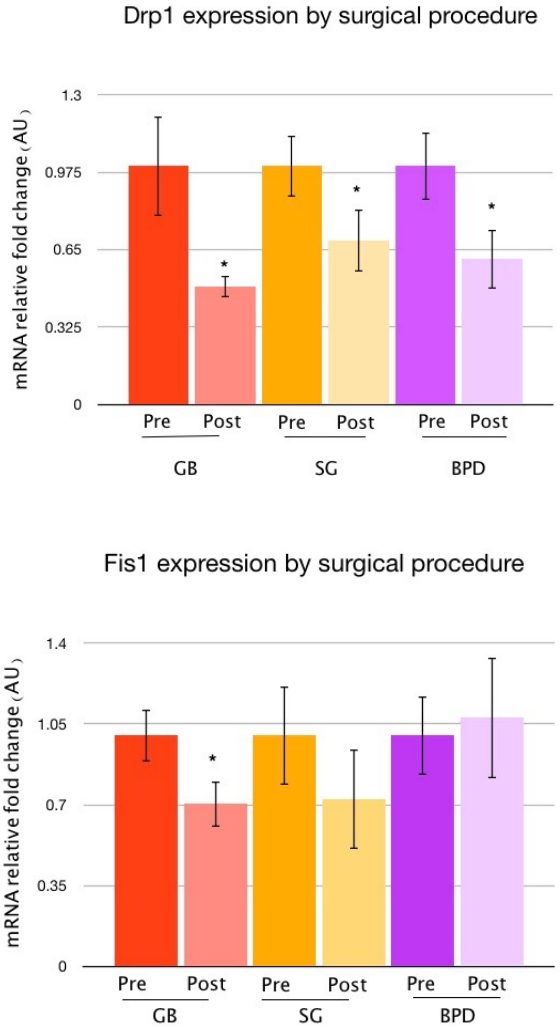

Figure 3.3. mRNA expression of the markers of mitochondrial fission, Drp1 and Fis1 stratified by surgical procedure.

mRNA expression of genes involved in mitochondrial fission; Gastric Banding (GB), Sleeve Gastronectomy (SG) and Biliopancreatic diversion (BPD). All experiments were performed in triplicate. Paired t-tests were performed at an individual subject level between mRNA expression values in their pre and post surgical sample (n = 29 pre, n = 29 post). $p < 0.05$ was considered statistically significant. $p < 0.05$*, $p < 0.01$** and $p < 0.001$***. p values were compared to before surgery mRNA expression level.

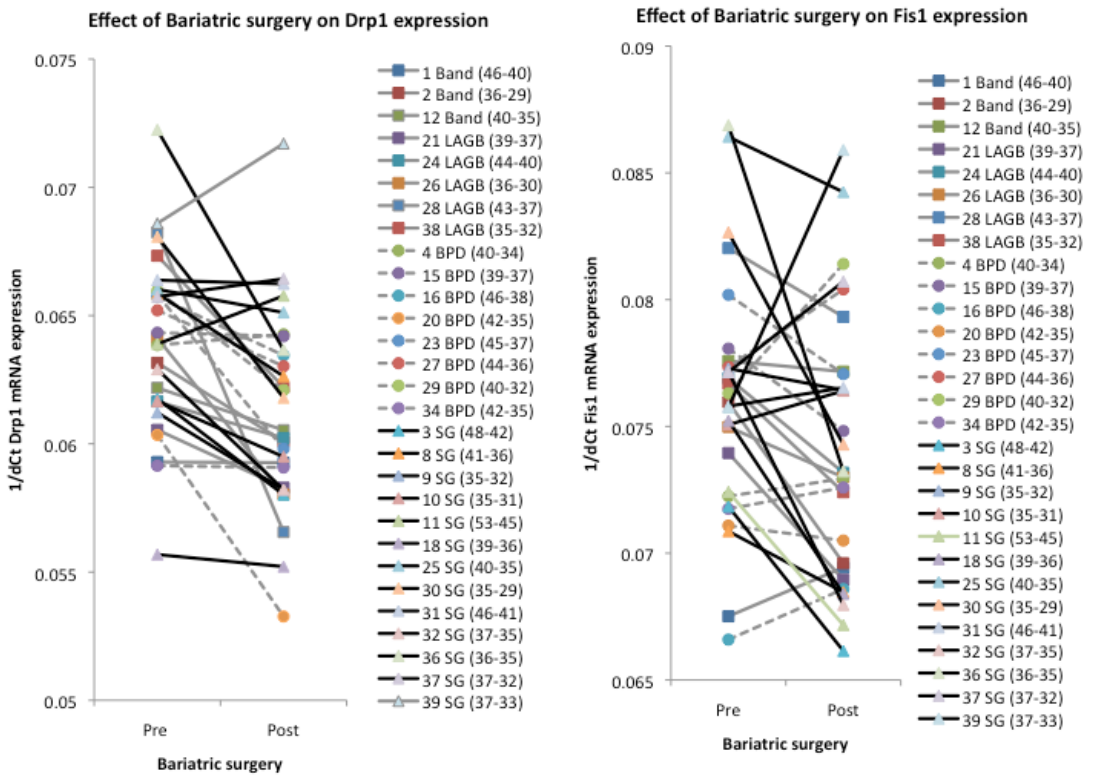

Figure 3.4. Individual patient Drp1 and Fis1 mRNA expressions pre and post bariatric surgery.

mRNA expression of genes regulating mitochondrial fission; A) Drp1 and B) Fis1. All experiments were performed in triplicate. Data for each individual patient is shown as 1/dCt expression. Patient number is given as numerical value before notation of surgical procedure. Patients undergoing the same surgical procedure have their 1/dCt mRNA expression colour coded as follows: grey (Gastric banding, LAGB and band), black (Sleeve gastronectomy, SG) and dashed (Biliopancreatic diversion, BPD). Paired t-tests were performed at an individual subject level between mRNA expression values of either Drp1 or Fis1 in their pre and post surgical sample (n = 29 pre, n = 29 post). $p < 0.05$ was considered statistically significant. $p < 0.05$*, $p < 0.01$** and $p < 0.001$***. p values were compared to before surgery mRNA expression level.

3.3.4. mRNA and protein expression of the mitochondrial fusion markers, Mfn2 and Opa1 before and after bariatric surgery

Mfn2 and Opa1 play an important role in the regulation of mitochondrial fusion. Therefore, their expression was evaluated next to understand the complete regulation of mitochondrial dynamics in adipose tissue. Both Mfn2 mRNA, protein and Opa1 mRNA revealed a significant overall reduction in expression following bariatric surgery (Figure 3.5A. $p = 0.004$ and B. protein; $p = 0.03$). Opa1 protein expression did not alter significantly post-surgery (Figure 3.5D.). Upon stratification of the data by surgical procedure, only patients undergoing SG displayed a significant decrease in Mfn2 (Fig. 3.6A) mRNA expression, despite a general trend across all patients towards a reduction in fusion expression regardless of the surgical procedure. These data lend support to the observation that although the surgical procedure may influence the outcome of mitochondrial fission marker expression , weight loss may be the biggest factor involved in this process. Figure 3.7 shows the mRNA expressions of Mfn2 and Opa1 for each patient pre and post bariatric surgery.

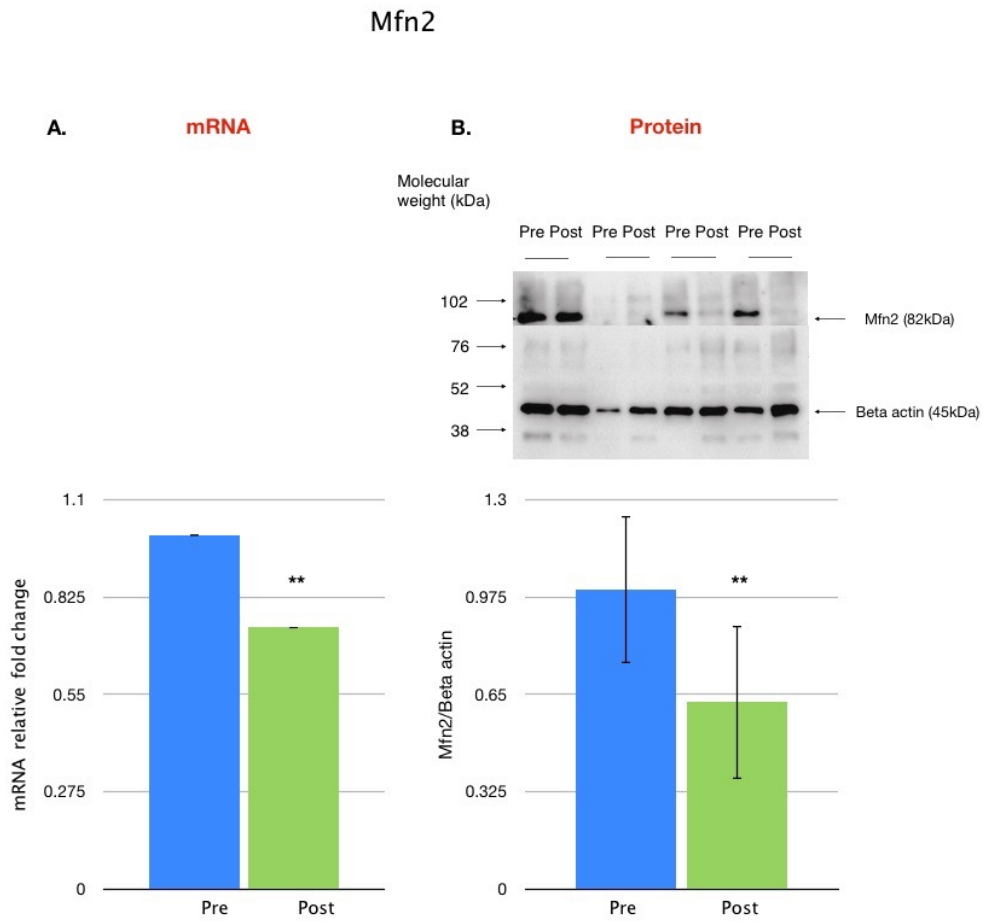

Figure 3.5. Mfn2, a marker of mitochondrial fusion decreases in mRNA and protein expression after bariatric surgery.

Expression of Mfn2 gene involved inmitochondrial fusion; A) mRNA and B) protein. All experiments were performed in triplicate. Paired t-tests were performed at an individual subject level between mRNA expression values of Mfn2 in their pre and post surgical sample (n = 29 pre, n = 29 post). $p < 0.05$ was considered statistically significant. $p < 0.05$*, $p < 0.01$** and $p < 0.001$***. p values were compared to before surgery mRNA expression level. Data are represented as means ± S.E.M.

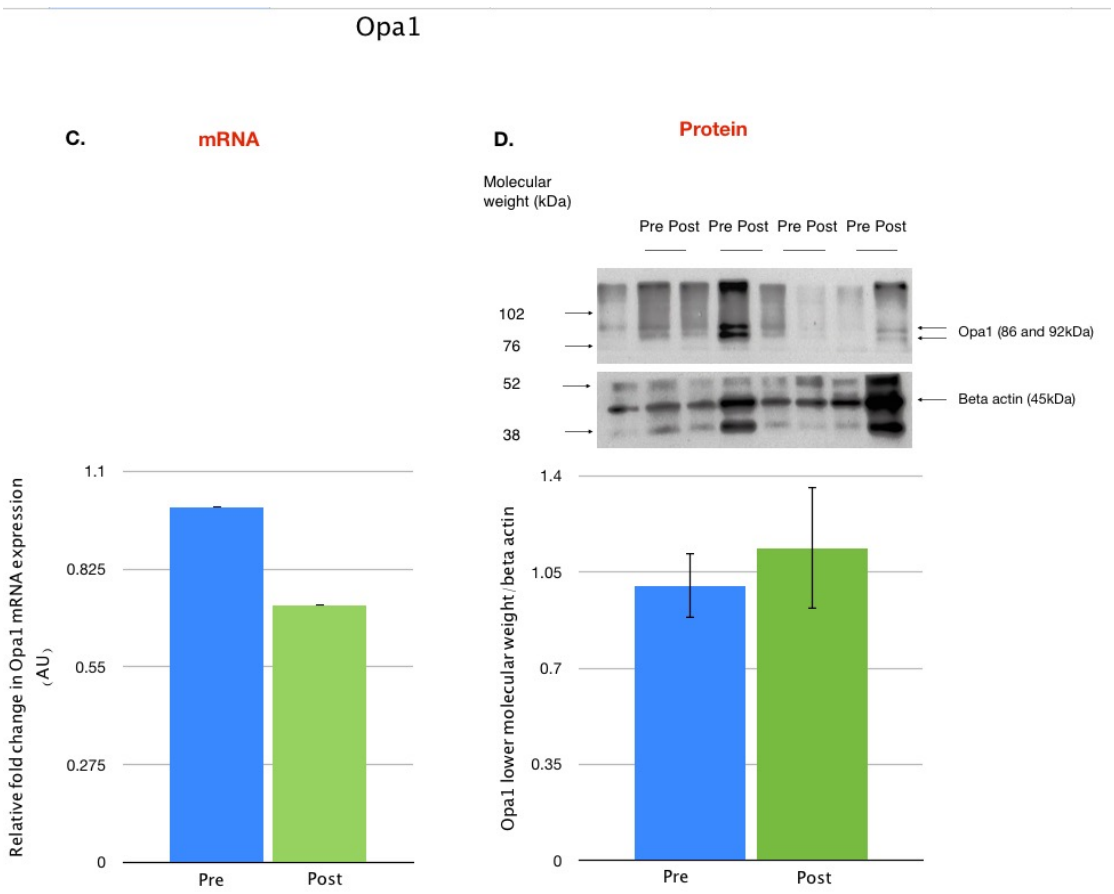

Figure 3.5 continued. Opa1, a marker of mitochondrial fusion decreases in mRNA and protein expression after bariatric surgery .

Expression of Opa1 gene involved in mitochondrial fusion; C) mRNA and D) protein. All experiments were performed in triplicate. Paired t-tests were performed at an individual subject level between mRNA expression values of Opa1 in their pre and post surgical sample (n = 29 pre, n = 29 post). $p < 0.05$ was considered statistically significant. $p < 0.05$*, $p < 0.01$** and $p < 0.001$***. p values were compared to before surgery mRNA expression level. Data are represented as means ± S.E.M.

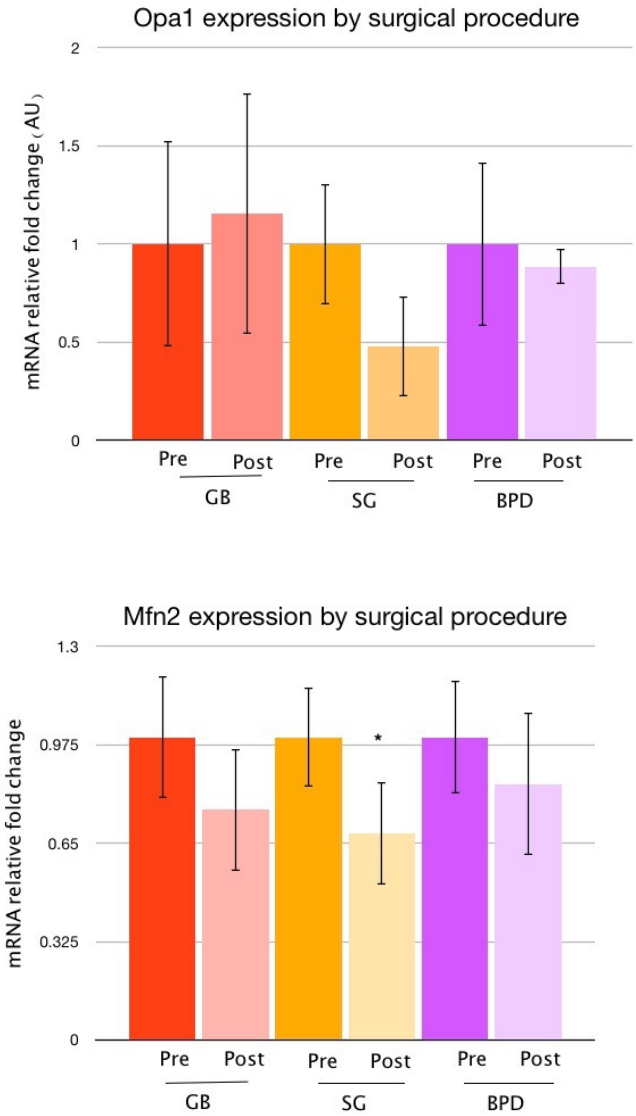

Figure 3.6. mRNA expression of the markers of mitochondrial fusion, Opa1 and Mfn2, stratified by surgical procedure.

mRNA expression of genes regulating mitochondrial fission; Gastric Banding (GB), Sleeve Gastronectomy (SG) and Biliopancreatic diversion (BPD). All experiments were performed in triplicate. Paired t-tests were performed at an individual subject level between mRNA expression values in their pre and post surgical sample (n = 29 pre, n = 29 post). $p < 0.05$ was considered statistically significant. $p < 0.05$*, $p < 0.01$** and $p < 0.001$***. p values were compared to before surgery mRNA expression level.

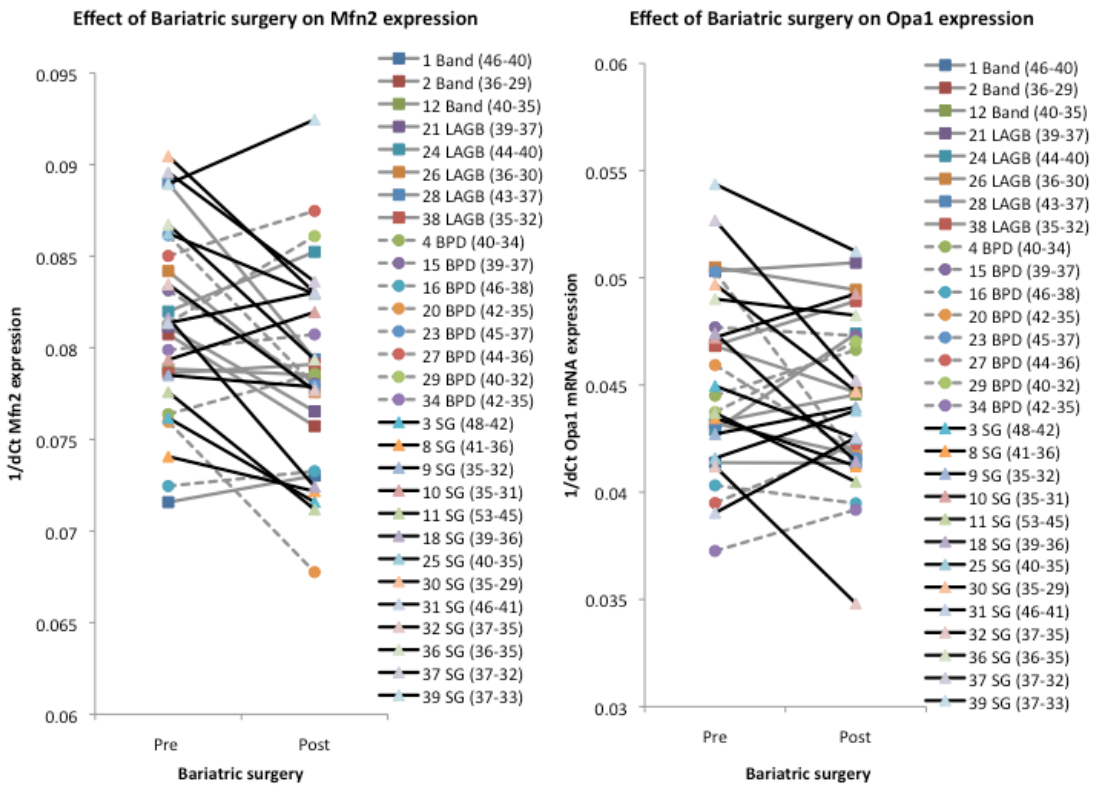

Figure 3.7. Individual patient Mfn2 and Opa1 mRNA expressions pre and post bariatric surgery .

mRNA expression of genes regulating mitochondrial fission; A) Mfn2 and B) Opa1. All experiments were performed in triplicate. Data for each individual patient is shown as 1/dCt expression. Patient number is given as numerical value before notation of surgical procedure. Patients undergoing the same surgical procedure have their 1/dCt mRNA expression colour coded as follows: grey (Gastric banding, LAGB and band), black (Sleeve gastronectomy, SG) and dashed (Biliopancreatic diversion, BPD). Paired t-tests were performed at an individual subject level between mRNA expression values of either Drp1 or Fis1 in their pre and post surgical sample (n = 29 pre, n = 29 post). $p < 0.05$ was considered statistically significant. $p < 0.05$*, $p < 0.01$** and $p < 0.001$***. p values were compared to before surgery mRNA expression level.

3.3.5. Effect of bariatric surgery on mitochondrial DNA content.

Mitochondrial DNA content in both assay methods (CytB/beta actin and ND1/ BECN1) increased significantly after surgery (Figure 3.8; $p < 0.001$). Therefore, weight loss may bring about changes in mitochondrial abundance through redressing the balance of mitochondrial dynamics. Fisher r-to-z transformation was performed to assess if there were any significant differences between the correlations obtained for the two-mitochondrial DNA expression assay methods. Evaluation of the correlation coefficients revealed a non-significant z-score of -0.5 and $p = 0.6$. Therefore, the correlations in both assays did not differ significantly from one another (Figure 3.8). Figure 3.9. shows the mitochondrial DNA content in AbSc AT before and after bariatric surgery according to surgical procedure.

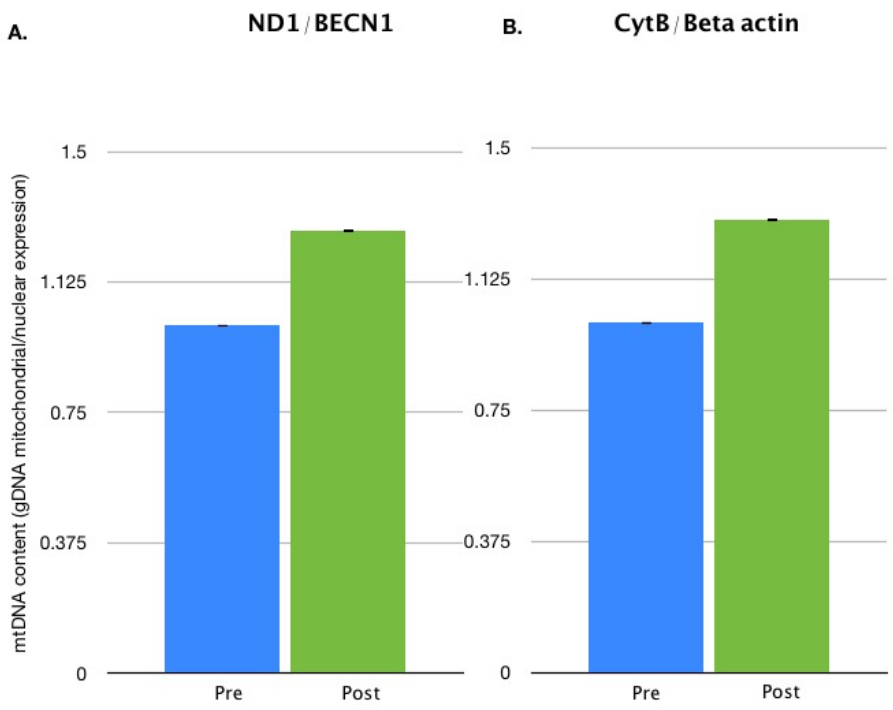

Figure 3.8. Mitochondrial DNA content before and following bariatric surgery. Genomic DNA (gDNA) was isolated from AbSc AT taken before and after bariatric surgery (n = 29). Mitochondrial DNA content was defined as the relative mitochondrial/nuclear DNA expression: A) ND1/BECN1 pre vs post, B) CytB/Beta actin pre vs post. Data are represented as means ± S.E.M. Paired t-tests were performed on an individual level between isolated genomic DNA from pre and post bariatric surgery. $p < 0.05$*, $p < 0.01$** and $p < 0.001$***. p values were compared to mitochondrial DNA content before surgery.

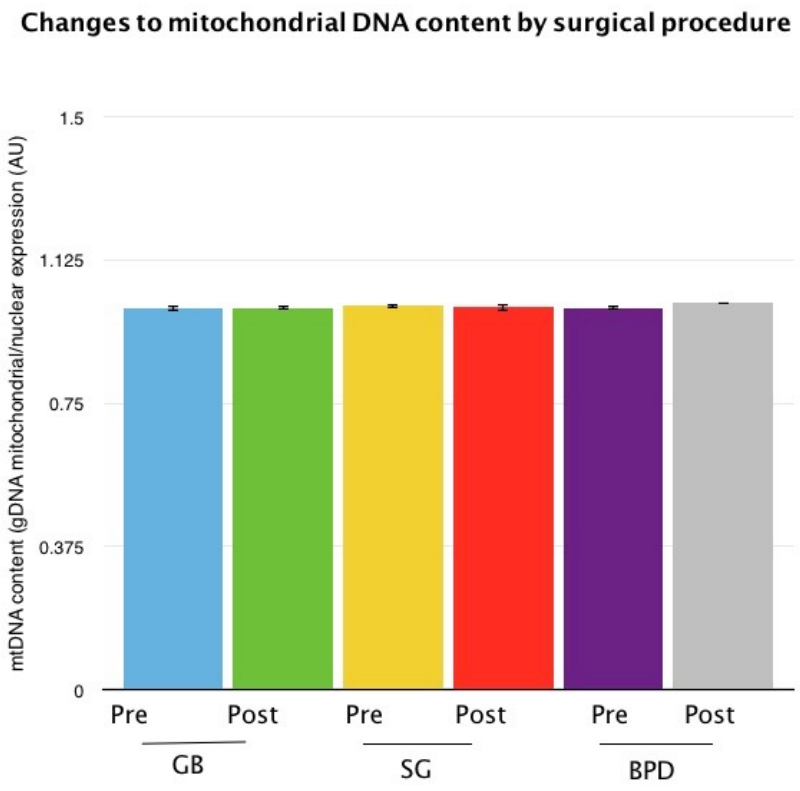

Figure. 3.9. Changes to mitochondrial DNA content by surgical procedure

Genomic DNA (gDNA) was isolated from AbSc AT taken before and after bariatric surgery. Mitochondrial DNA content was defined as the relative mitochondrial/ nuclear DNA expression using the ND1/BECN1 assay. pre vs post for gastric banding (GB) (n = 8), pre vs post for sleeve gastronectomy (SG) (n = 13) and pre vs post for biliopancreatic diversion (BPD) (n = 8). Data are represented as means ± S.E.M. Paired t-tests were performed on an individual level between isolated genomic DNA from pre and post bariatric surgery. p values were compared to mitochondrial DNA content before surgery. All data were non significant.

3.3.7. Glucose correlates with markers of mitochondrial dynamics.

After weight loss, expression of the markers of mitochondrial dynamics Drp1, Opa1 and Mfn2 became positively and significantly correlated with plasma glucose levels (Figure 3.10. A. Drp1; pre: R^2 = -0.165, p = 0.393, post: R^2 = 0.394, p = 0.035, B. Mfn2; pre: R^2 = 0.045, p = 0.816, post: R^2 = 0.499, p = 0.015, and C. Opa1; pre: R^2 = 0.052, p = 0.788, post: R^2 = 0.462, p = 0.012). The correlation coefficients by Fisher r-to-z transformation, used to determine if there is a statistically significant difference between two correlations revealed that all mitochondrial dynamics markers with the exception of Fis1 were significantly altered after bariatric surgery (Figure 3.10A. Glucose vs Drp1 z-score = 2.1, p = 0.03, 3.10C. Glucose vs Mfn2 z-score = -1.81, p = 0.07 and 3.10D. Glucose vs Opa1 z-score = -1.61, p = 0.1).

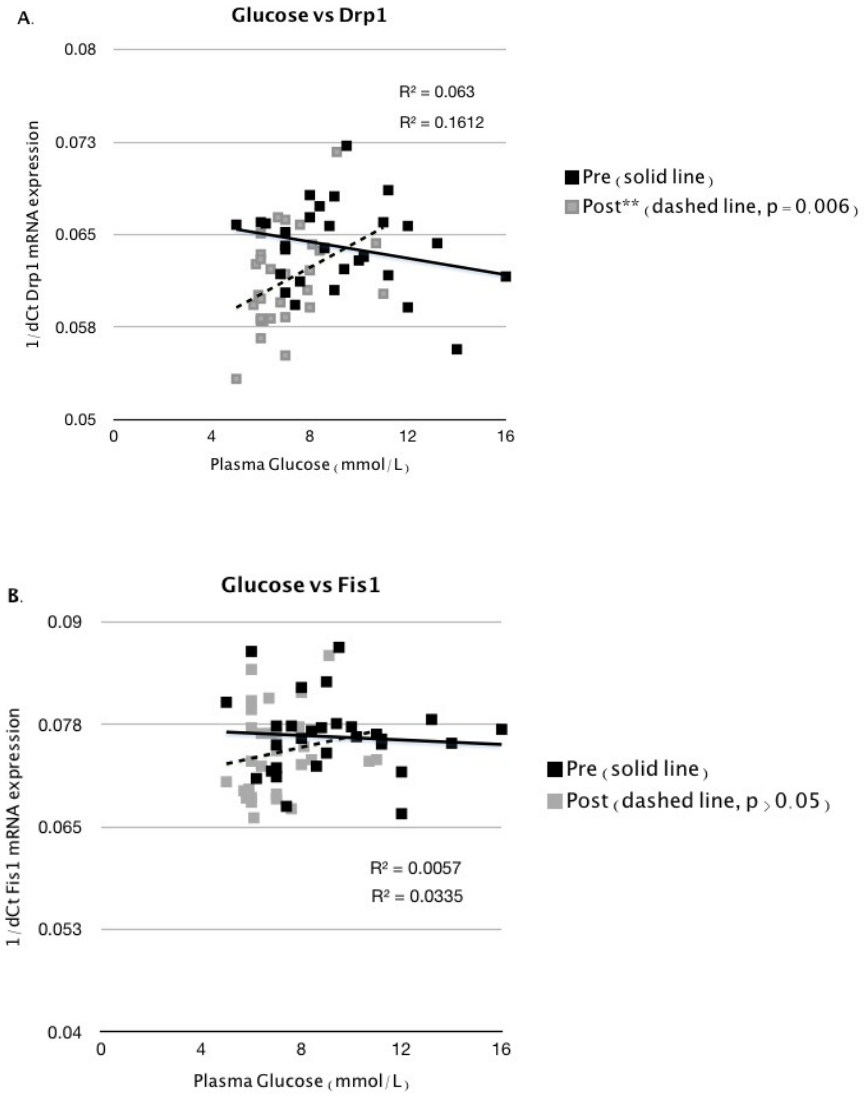

Figure 3.10. Glucose correlates with mRNA expression of the mitochondrial fission gene Drp1 expression.

Parametric correlation analyses were performed to evaluate the relationship between fasting glucose levels and mitochondrial dynamics gene expression (n = 29). All mRNA expression data are an average of triplicate measurements. $p < 0.05$ was considered statistically significant. $p < 0.05$*, $p < 0.01$** and $p < 0.001$***.

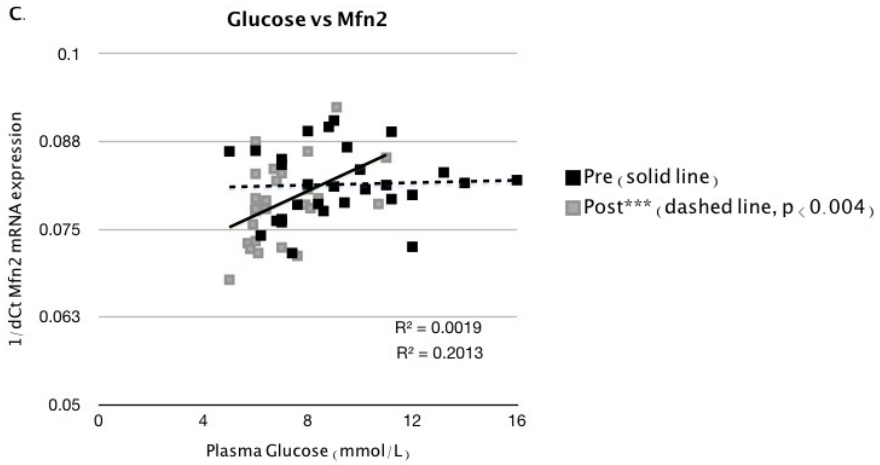

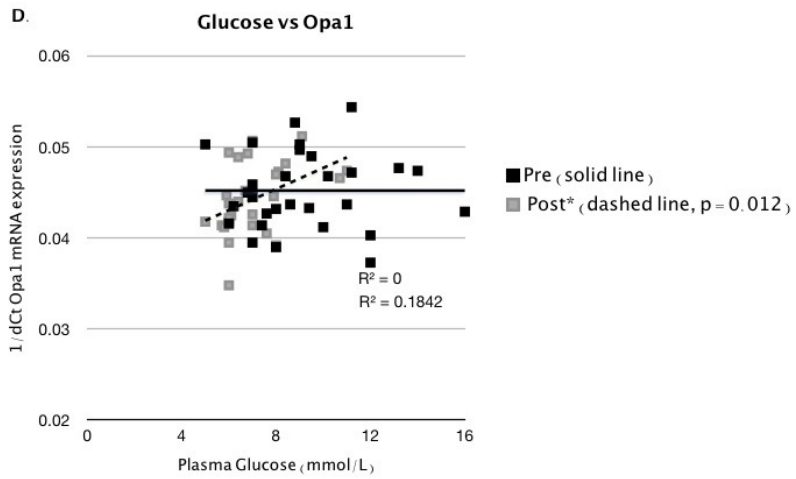

Figure 3.10. continued. Glucose correlates with mRNA expression of the mitochondrial fusion genes Mfn2 and Opa1.

Parametric correlation analyses were performed to evaluate the relationship between fasting glucose levels and mitochondrial dynamics gene expression (n = 29). All mRNA expression data are an average of triplicate measurements. $p < 0.05$ was considered statistically significant. $p < 0.05$*, $p < 0.01$** and $p < 0.001$***.

3.3.8. Macrophage markers and bariatric surgery.

CD68 was used to characterise macrophage expression in AbSc AT (Figure 3.11. CD68 vs BMI). Following bariatric surgery, no statistically significant change in macrophage gene expression was identified (Figure 3.12. mRNA, $p = 0.11$). In support of the hypothesis that changes in mitochondrial dynamics occurs independently of macrophages the expression of CD68 did not correlate with mRNA and protein expression of mitochondrial dynamics genes (Mfn2, Opa1, Fis1 and Drp1). These data demonstrate that macrophage infiltration into AbSc AT was not responsible for changes observed in mitochondrial dynamics.

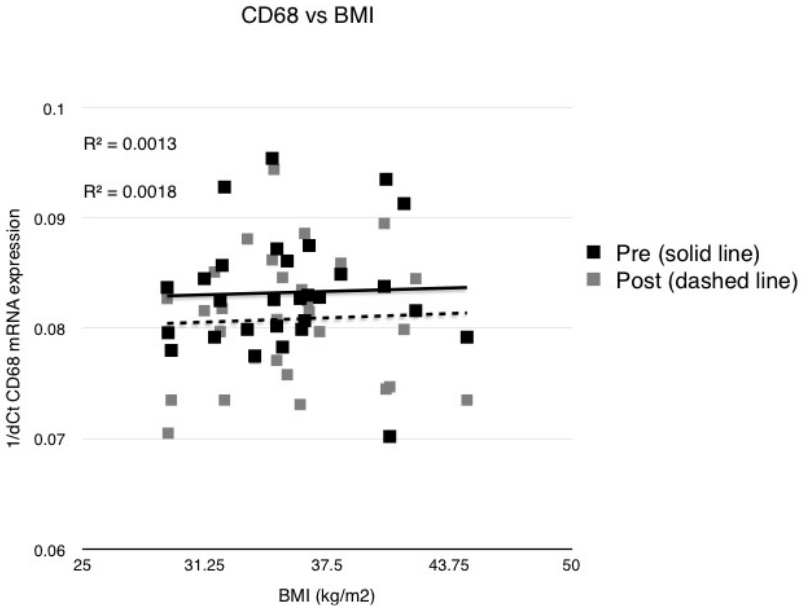

Figure 3.11. CD68 versus BMI.

CD68 was used to characterise macrophage expression in abdominal subcutaneous adipose tissue. Values for 1/dCt are an average of triplicate measurements of each sample. n = 29 pre, n = 29 post.

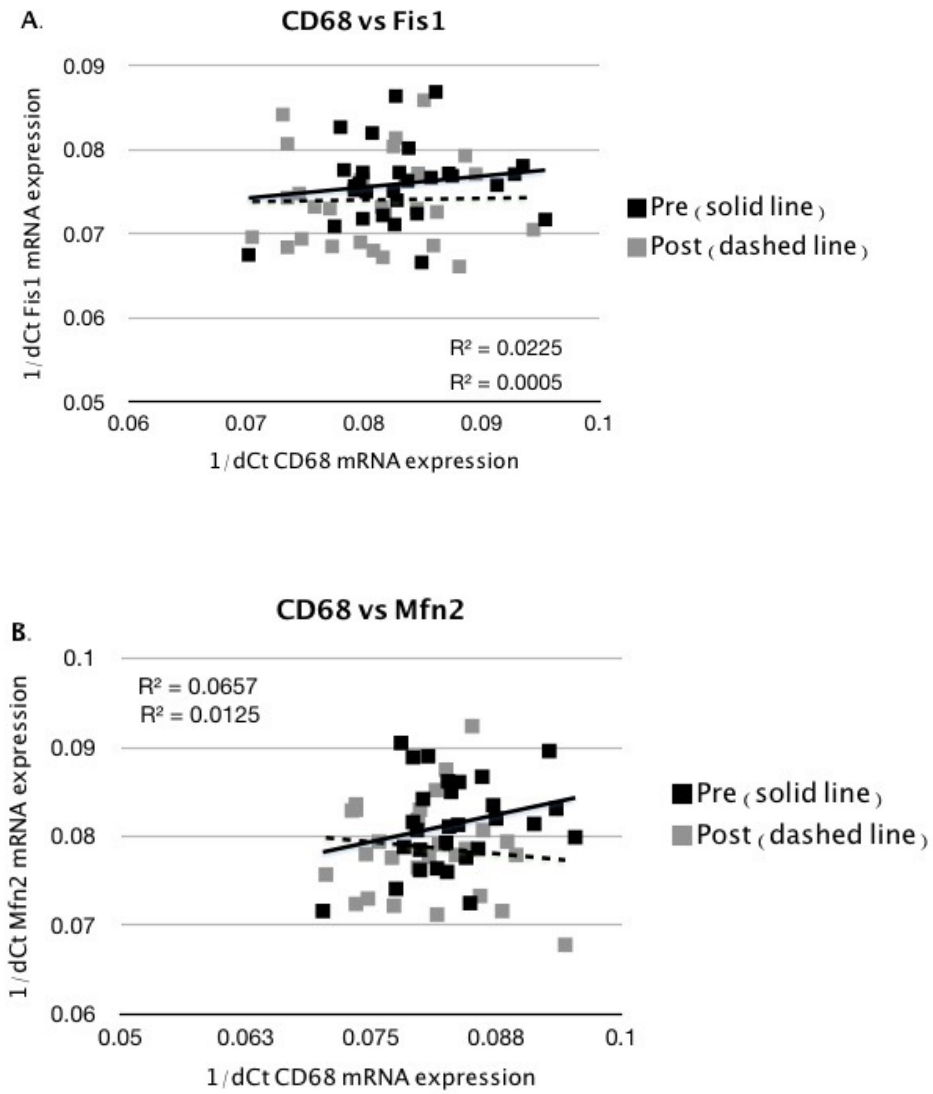

Figure 3.12. Macrophage markers and bariatric surgery.

CD68 was used to characterise macrophage expression in AbSc A.T. Values for 1/dCt are an average of triplicate measurements of each sample. n = 29 pre, n = 29 post. All data were non significant.

3.4. Discussion.

This study sought to examine and evaluate the effects of weight loss induced by bariatric surgery on mitochondrial dynamics within AbSc AT of T2DM subjects. The results of this study demonstrate that weight loss accompanying bariatric surgery can positively influence the expression of markers of mitochondrial dynamics genes.

Consistent with previous clinical studies BMI, HOMA-IR and plasma glucose markedly improved following bariatric surgery (Levy, Fried et al. 2007, Aarts, Dogan et al. 2014). Previous reports involving skeletal muscle biopsies taken before and after surgery, highlight that the rates of diabetes remission and return to normal glycaemic control vary according to the surgical procedure (Buchwald, Estok et al. 2009). In an attempt to address, whether the nature of the surgical procedure or weight loss could alter the expression of markers of mitochondrial dynamic gene in this study, we firstly examined the clinical parameters before and after surgery. The entire cohort represented three different types of elective bariatric surgery, Gastric banding (GB, Sleeve gastronectomy (SG) and Biliopancreatic diversion (BPD). The degree of surgical remodelling has often been hypothesised to be responsible for the differences in weight loss and diabetes remission (Pournaras, Osborne et al. 2010). In this study, subjects across all surgery types lost an average of 33±13 % of their excess weight 6 months after surgery (Table 2). However, amongst the clinical parameters measured (HbA1c, BMI, glucose, insulin, HOMA-IR, triglycerides and cholesterol), no single surgical procedure could account for the significant reductions observed (Table 2). Therefore, we concluded that weight loss rather than the surgical procedure might be responsible for the post-surgery improvements.

Considering weight loss and diabetes remission by surgical procedure, BPD corresponded with the greatest excess BMI loss 6 months after surgery (Table 2).In the context of the hypothesis that BPD, which involves the greatest degree of surgical remodelling should experience greater improvements in diabetes remission, it would be expected that the HOMA-IR score should be most significantly decreased. Indeed, despite the pre bariatric HOMA-IR score of BPD patients of appoximately 13 compared to 11 for GB and SG patients, the post bariatric surgery for the BPD patients were lower than those of the other two surgical procedures (HOMA-IR: 5.03 compared to 5.26 (GB) and 5.06 (SG)). These data lend support to the hypothesis that the greater the surgical remodelling the greater the rate of diabetes remission. One potential explanation for this physiological improvement, is the reduction in lipid absorption, which mainly occurs in the large intestine that is largely bypassed due to the BPD remodelling surgery. As a consequence, these lipids do not reach the circulation is such greater concentrations and minimise the activation of hepatic gluconeogenesis and secretion of pancreatic insulin, that have been proposed in the Randall hypothesis to contribute to the disruption of glycolysis and glucose homeostasis (section 1.1.5). Further investigation of the impact of weight loss on mitochondrial dynamics required analysis of mRNA expression.

Fission involves the segregation of one mitochondrion into two smaller mitochondria and involves proteins, Drp1 and Fis1 (Ferrier 2001). Drp1 translocates from the cytosol to the mitochondria with assistance of Fis1 (Smirnova, Griparic et al. 2001, Lee, Jeong et al. 2004) (Figure 1.5). Once localised to the outer mitochondrial membrane, Drp1 punctuate holes within the mitochondria required for the initiation and assembly of future sites of fission. Fis1 are the mechanical scissors that finalise

and coordinate the creation of two smaller separated mitochondria (James, Parone et al. 2003, Stojanovski, Koutsopoulos et al. 2004). Expression analyses of markers of mitochondrial fission, Drp1 and Fis1, revealed a significant reduction in mRNA expression after surgery (Figures 3.2-3.4). This is a critical post surgical improvement, as evidence of the negative effects of over-activation of fission have been presented both in human and mouse studies including a significantly higher expression of Fis1 in endothelial cells of T2DM individuals compared to healthy control subjects (Shenouda, Widlansky et al. 2011). Furthermore, the enhancement of Fis1 expression in these endothelial cells resulted in mitochondrial fragmentation (Shenouda, Widlansky et al. 2011). Unlike control subjects, mitochondria of T2DM subjects are known to be smaller and punctuate (Shenouda, Widlansky et al. 2011). These findings together with the use of diet induced or genetic mouse induction models of obesity (Jheng, Tsai et al. 2012), demonstrate a possible link between increased markers of mitochondrial fission and insulin resistance. The opposing arm of mitochondrial dynamics, mitochondrial fusion, allows mixing of mitochondrial contents including metabolites, protein and DNA across the mitochondrial population (Twig, Hyde et al. 2008) and involves the proteins, Mfn2 (Chen, Detmer et al. 2003, Bach, Naon et al. 2005) and Opa1 (Akepati, Muller et al. 2008) (Figure 1.5). Following its initiation, mitochondrial fusion promotes the formation of multimeric Mfn2 complexes, which enable physical tethering of outer mitochondrial membranes between surrounding mitochondria (Olichon, Emorine et al. 2002). Opa1 performs a similar functional role within the inner mitochondrial membrane to promote and enable fusion to progress (Cipolat, Martins de Brito et al. 2004, Olichon, Landes et al. 2007). Expression analysis of mi-

tochondrial fusion genes highlighted a significant decrease in Mfn2 and Opa1 mRNA levels following bariatric surgery (Figures 3.5-3.7).

Thus far, the data clearly shows an overall alteration in the expression of markers of mitochondrial dynamics. In particular, markers of mitochondrial fission expression diminished following surgery as judged by the significant reductions in Fis1 and Drp1 mRNA expression induced after weight loss (Figures 3.2-3.4). Therefore, in order to better understand the implications of this for cellular metabolism, mitochondrial DNA content in AbSc AT of pre and post bariatric samples was undertaken (Figure 3.8-3.9). Power analysis revealed that the sample size of this study is sufficient to determine a statistically significant difference in mitochondrial DNA expression that may arise after bariatric surgery. Analyses of mitochondrial DNA expression by two previously published methods (Hsieh, Weng et al. 2011, Ferber, Peck et al. 2012), revealed no significant difference in mitochondrial DNA content before and after bariatric surgery(Figure 3.8). Furthermore, both assays exhibited no significant differences in their correlation coefficients for determination of the mitochondrial DNA content in AbSc A.T before and following bariatric surgery (Figure 3.9). The lack of change in mitochondrial DNA content is likely to have arisen due to the equivalent proportional increase in mitochondrial fusion and fission gene expression. Nevertheless, this result generates only half the picture of the implications of changes in markers of mitochondrial dynamics gene expression, as the metabolic activity of the individual mitochondria may be profoundly changed even in the absence of changes to mitochondrial DNA content. Therefore, in order to provide a more complete picture of the effects of bariatric surgery on markers of mitochondrial dynamics it may be necessary to perform bioenergetic assay profiling of pre and post bariatric

samples across the entire cohort (n = 29 patients, paired pre and post samples). Given the improved expression of the mitochondrial dynamics markers and lack of change in mitochondrial DNA content after bariatric surgery, we sought to identify if glucose could explain in part at least, the improvements in the expression of mitochondrial dynamics markers. Debate still exists as to the effect of bariatric surgery on insulin sensitivity when non-diabetic and diabetic patients are compared (Garcia-Fuentes, Garcia-Almeida et al. 2006, Lin, Davis et al. 2009, Pournaras, Osborne et al. 2010, Dixon, Straznicky et al. 2012). Firstly, comparisons of the pre and post-surgery fasted glucose levels were completed. Fasted glucose decreased significantly following surgery. Secondly, correlation analyses were undertaken to compare the relationship between markers of mitochondrial dynamics gene expression and glucose. Drp1, Opa1 and Mfn2 became positively and significantly correlated with plasma glucose following bariatric surgery (Figure 3.11A-C). Taken together, the positive correlation between glucose and Drp1, Opa1 and Mfn2 after surgery identifies that glucose metabolism and mitochondrial dynamics may be under similar regulatory control.

Finally, the presence of macrophages in AbSc AT of pre and post bariatric samples was assessed to investigate the role of macrophage infiltration as a potential mechanism for overall improvement in expression of the markers of mitochondrial dynamics. In adipose tissue, macrophage infiltration has been shown to occur in obese individuals and those with T2DM status (Weisberg, McCann et al. 2003, Curat, Miranville et al. 2004). CD68 (marker of macrophage) mRNA expression did not decrease in a significant manner following weight loss induced through surgery (Figure 3.11.). In support of the hypothesis that, changes in mitochondrial dynamics occurs

independently of macrophages, the expression of CD68 did not correlate with mRNA expression of the mitochondrial dynamics genes (Figure 3.12 A-B.Fis1 and, Mfn2).

In conclusion, the results from this study demonstrate that the expression of markers of mitochondrial fusion and fission in AbSc AT of T2DM individuals is mainly altered by weight loss.Taken together, the redressing of markers of mitochondrial dynamics gene expression reflects a possible mechanism through which mitochondrial dysfunction could be resolved following weight loss induced by bariatric surgery.

The observation that markers of mitochondrial fission are more highly expressed in overweight and obese AbSc AT offers a potential explanation for the reduction in metabolism known to accompany adiposity (Robertson 2014). Nevertheless, the upstream signaling pathways and genes that regulate mitochondrial dynamics remain unknown. As a stress kinase, p38 has been previously reported to be upregulated under conditions of cellular stress. Given this context and evidence of the involvement of p38 in adipocyte maturation (Engelman, Lisanti et al. 1998, Engelman, Berg et al. 1999) and mitochondrial dynamics genes in triglyceride accumulation (Kita, Nishida et al. 2009), lead us to speculate that p38 may be involved in regulating mitochondrial dynamics. Assessment of the mechanisms of p38 action and its influence on mitochondrial dynamics are the subject of the next chapter.

Chapter 4:

The role of p38 in mitochondrial dynamics.

4.1. Introduction.

4.1.1 p38.

As a signal transduction mediator, p38 is involved in mediating a wide range of cellular processes including inflammation, the cell cycle, death, differentiation and senescence in response to extracellular stimuli (Zarubin,T. and Han,J. 2005). p38 belongs to one of the four main groups of mitogen activated protein kinases (MAPKs); 1: extracellular singal regulated kinases (ERK) , 2: c-jun stress activated kinases (JNK), 3: ERK/big MAP kinase 1 (BMK1) and 4: p38 MAPK (Rouse J, Cohen P and Trigon S, et al.1994)

Originally isolated following inflammatory stimulation via lipopolysaccharide (LPS), p38 alpha was isolated as a 38kDa tyrosine phosphorylated protein. The Threonine (Thr) - Glycine (Gly) - Tyrosine (Tyr) (abbreviated to TGY) dual phosphorylation motif is a key characteristic of p38 kinases (Han,J et al .1994).

p38 activation may occur in response to extracellular stress (e.g. inflammatory cytokine release (TNF or IL-1, UV light or heat) or growth factor secretion (e.g those contained in foetal bovine serum used during cell culture, FBS) (Lee, JC. et al.1994). Additional influences include the cell type such as 3T3-L1 adipocytes whose p38 is activated upon treatment with insulin. To date, the majority of research has worked on characterisation of the alpha and beta isoforms whose expression is most ubiquitous.

Evidence of the biological consequences of p38 activation, which are transduced through either MKK6 or MKK3 upon complexing of p38 with ATP and MK2, its cellular substrate, include a regulatory role in the proliferation and differentiation or immune system cells and as a regulator of oxidation (Sweeney, G et al. 1999). Furthermore, p38 plays an important role in control of senescence and tunour suppres-

sion. Namely, that activation of MKK6 and MKK3 following enhancement of p38 activity promote the development of a senescent phenotype (Cuenda, A. et al. 1997). Conversely, under conditions where p38 activation is diminished including tumours, due to their ability to modulate p38 MAPK signalling, lead to the promotion of tumorigenic conditions and subsequent induction of further tumour growth (Mahtani, KR. et al. 2001). Whilst knowledge of the involvement of p38 in signalling with the mitochondrial proteins such as Bax and Bad (Bcl2 family member, pro-apoptotic proteins), and BCL-xL (anti-apoptotic protein and Bcl2), which assist in the regulation of apoptosis, little is known about the involvement of p38 in other mitochondrial processes such as mitochondrial dynamics.

4.1.2. Mitochondrial biogenesis, dynamics and effect of p38 on these processes

The most important roles of mitochondria are to produce energy for the cell in the form of ATP through respiration, and to regulate cellular metabolism (Nunnari and Suomalainen 2012, Robertson 2014). Mitochondrial biogenesis (Attardi and Schatz 1988), dynamics (Zorzano, Liesa et al. 2009) and bioenergetics are critical in coordinating not only cellular abundance of mitochondria but also ensuring optimal mitochondrial function and health. With these mechanisms at their disposal, mitochondria are responsible for maintaining energy homeostasis.

Mitochondrial biogenesis assists energy homeostasis through the maintenance of mitochondrial abundance thereby compensating for the normal mitochondrial turnover (Menzies and Hood 2012). Creation of new mitochondria occurs during the cell cycle by de novo synthesis and division of pre-existing mitochondria (Posakony, England et al. 1977). Peroxisome proliferator-activated receptor-gamma coactivator α

(PGC-1α) and Mitochondrial transcription factor A (Tfam) are key regulators of mitochondrial biogenesis (Prigione and Adjaye 2010). During conditions of nutrient depletion, the accompanying increase in the AMP/ATP ratio detected by two energy sensors, Sirtuin 1 (SIRT1) and AMP-activated protein kinase (AMPK), triggers initiation of a downstream signalling cascade, resulting in the activation of PGC-1α and liberation of energy stored within triglycerides located predominantly within adipose tissue (Puigserver, Rhee et al. 2001). Functional studies of mitochondrial biogenesis have proposed that p38 is capable of phosphorylation and activation of PGC-1α (Puigserver, Rhee et al. 2001). Treatment of C2C12 myocytes, a skeletal muscle cell line with the p38α and β isoform inhibitor, SB203580, resulted in inhibition of stimulated PGC-1α promoter activity (Akimoto, Pohnert et al. 2005).

4.1.3. p38 and adipogenesis

Furthermore, p38 is known to regulate adipogenesis (Engelman, Lisanti et al. 1998). Adipocytes have been most extensively employed to investigate cell differentiation. Previous studies have highlighted that cellular differentiation regulated through p38 is accompanied by an increase in the expression of mitochondrial biogenesis genes (Ducluzeau, Priou et al. 2011). During cellular differentiation, terminally differentiated adipocytes are more metabolically active compared to their preadipocyte precursors (Ducluzeau, Priou et al. 2011). In conjunction with their enhanced lipid storage capacity, mitochondria within adipocytes require extensive remodelling (Kita, Nishida et al. 2009) involving mitochondrial dynamics and biogenesis to support the greater metabolic requirements of adipocytes (De Pauw, Demine et

al. 2012). In coordination with mitochondrial biogenesis, mitochondrial function, health and abundance are regulated by mitochondrial dynamics.

4.1.4. Mitochondrial dynamics and potential role of p38. Mitochondrial dynamics (Liesa, Palacin et al. 2009, Zorzano, Liesa et al. 2009, Shenouda, Widlansky et al. 2011, Liesa and Shirihai 2013) involves the opposing processes of fusion (coalescence of two mitochondria to form a larger mitochondrion) and fission (division of mitochondria to form two smaller mitochondria). Through dynamic remodelling of mitochondria, the abundance (through mitochondrial dynamics and biogenesis (Ren, Pulakat et al. 2010)) and optimal health of the mitochondrial population (through selective mitophagy of compromised mitochondria) are maintained. The GTPase proteins (Hoppins, Lackner et al. 2007), Mfn2 and Opa1 are involved within mitochondrial fusion (Legros, Lombes et al. 2002), whilst Drp1 and Fis1 participate in mitochondrial fission (Dikov and Reichert 2011, Elgass, Pakay et al. 2013). Central to this study is exploration of mitochondrial morphology (Okamoto and Shaw 2005) and whether p38 is capable of exerting influence on the balance of mitochondrial dynamics (Zorzano, Liesa et al. 2009). A number of key lines of evidence from observational studies have led us to propose a role for p38 within mitochondrial dynamics of adipocytes. In addition to the insulin resistance that accompanies T2DM, patients often exhibit a reduction in mitochondrial metabolism (Gerencser, Chinopoulos et al. 2012) and expression of mitochondrial biogenesis genes (Mustelin, Pietilainen et al. 2008). Cellular differentiation, which is regulated through p38, is known to enhance mitochondrial biogenesis suggesting that p38 may also be affected in patients with diminished mitochondrial metabolism. Firstly, mtDNA copy number (Shay, Pierce et al.

1990, Jeng, Yeh et al. 2008) in diabetic subjects is lower as compared to their Lean counterparts. This reduction in abundance has been linked with diminished mitochondrial oxidative phosphorylation capacity (Brand and Nicholls 2011, Saada 2014) of up to 40% (Petersen, Dufour et al. 2004) and ATP synthesis. Secondly, PGC-1α of morbidly obese AbSc AT (Semple, Crowley et al. 2004), which regulates mitochondrial biogenesis (Rong, Qiu et al. 2007) is reduced by 3-fold compared to healthy controls. Finally, mitochondrial dysfunction (Michel, Wanet et al. 2012) observed in skeletal muscle of Obese and T2DM patients, is associated with a significant reduction of mitochondrial area (Kelley, He et al. 2002) and respiration in adipose tissue (Kraunsoe, Boushel et al. 2010).

In summary, this study sought to address whether p38 was involved in the regulation of mitochondrial dynamics and bioenergetics in adipocytes.

4.2. Methods.

4.2.1. Cell culture of 3T3-L1 (Category II HEPA filtered cell culture hood);

4.2.1.1 Preadipocytes for markers of mitochondrial dynamics gene expression assays

3T3-L1 preadipocytes were seeded at $1x10^6$/2ml in a 6 well plate (6WP) and incubated at 37C, 5% CO2. Media was replaced every 48 hours (2ml per well). After 2 days, 3T3-L1 preadipocytes reached confluency (100%). Any protein or RNA samples were harvested for further expression analyses. Individual protein samples (per well) were harvested by removing culture media, washing the monolayer twice with cold PBS, addition of RIPA lysis buffer (250µl), shaking incubation on ice, scraping

and storage in eppendorfs (2 ml) at -20C until required. RNA samples were harvested by removing culture media, washing the monolayer twice with cold PBS, addition of Qiazol (250µl), shaking incubation on ice, scraping and storage in eppendorfs (2 ml) at -20C until required. RNA was extracted using RNeasy kit (Qiagen, see 2.1).

4.2.1.2. Optimisation of seeding density and culture conditions for mitochondrial bioenergetics assay:

This decision was taken to optimise the mitochondrial bioenergetics assay prior to the evaluation of any mitochondrial stress reagents or drug treatments. The optimal basal oxygen consumption rate, in the absence of any treatments is < 400pmol/min/mg. Therefore, the cell seeding density which corresponded most closely to this optimal oxygen consumption rate was selected for future mitochondrial bioenergetics assays.

Assay protocol:

Day before the assay:

Cell seeding: 3T3-L1 fibroblast cells (preadipocytes) were seeded at 3 densities in the morning; 1 x 10^4, 2 x $10^4$and 3x10^4/well (100ul, 37C pre warmed 10% FBS DMEM-F12) in an mitochondrial bioenergetics specific seahorse bioscience 24 well plate (24WP) cell culture plate and incubated (5% CO 2 and 37C). After 4 hours, the cells had adhered to the culture plate, and the volume of media was increased to 250ul (37C pre warmed 10% FBS DMEM-F12) before returing the 24WP to the incubator overight.

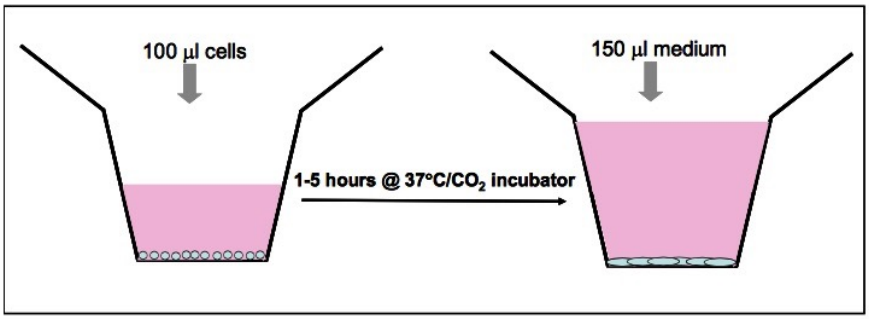

Figure 4.1. Seeding of 3T3-L1 preadipocytes. 3T3-L1 fibroblast cells (preadipocytes) were seeded at 3 densities; 1 x 10^4, 2 x $10^4$and 3x10^4/well (pre warmed 10% FBS DMEM-F12) seahorse bioscience 24 well plate (24WP) cell culture plate and incubated (5% carbon dioxide and 37C). After 4 hours, media (150ul) was added (37C pre warmed 10% FBS DMEM-F12) before returing the 24WP to the incubator overight.

Equilibration of the seahorse assay cartridge containing the fluorescent probes:

Hydrate all wells of the seahorse assay cartridge with provided equilibration buffer (1ml/well). Incubate at 37C in the seahorse carbon dioxide free incubator overnight.

Preparation of running assay media (1L, final concentrations are given below):

8.3g/L DMEM* base powder

1.85g/L sodium chloride

1mM sodium pyruvate

30mM alpha-D- glucose

MilliQ water up to 1L

*DMEM (Sigma D3050, no L-glutamine, glucose, phenol red, sodium pyruvate or sodium bicarbonate supplements).

No buffering capacity, essential requirement for running media for use in the bioenergetics assay. Pre warm to 37c in a 5% C02 incubator using a 25ml (T25) vented culture flask. Transfer an aliquot of the 1L solution (50ml per assay) into a conical flask. Using a pH meter, stirrer plate and magnetic stirrer bar, carefully titrate dropwise using a pasteur pipette either hydrochloric acid (HCl, ImM stock,if solution too alkaline) or sodium hydroxide (NaOH 1mM stock, if solution too acidic) until the running assay media is at pH to 7.4. Sterile filter the solution in the cell culture hood by passing the solution through a 0.2um filter attached to a 50ml syringe into a fresh and sterile T25 flask. Store the solution in the fridge for use in the assay the following day.

Day of the assay:

Remove the stress reagents and any drug treatments from -20C to allow these to thaw.The seahorse 24WP containing the pre-seeded 3T3-L1 preadipocytes was examined for cellular adherence. The media (200ul of the 250ul 10% FBS DMEM-F12) was removed and the cells were washed twice with seahorse running assay media (serum free, 1ml per wash and discarded). The cells in the assay plate were examined under the light microscope, both before removal of the growth media and after replacement with the seahorse running media change.

No disturbance of the cell monolayer was identified. Plating the 3T3-L1, 16 hours prior to the assay, resulted in an 80% confluent cellular monolayer on the day of the assay, as determined by examination under the light microscope. Once the cells were washed using the seahorse running media, a final addition of running media was added and the cells were incubated in a CO2 free, 37C incubator (provided by Sea-

horse bioscience) for 1 hour. During this time, all the stress reagents and drug treatments were prepared.

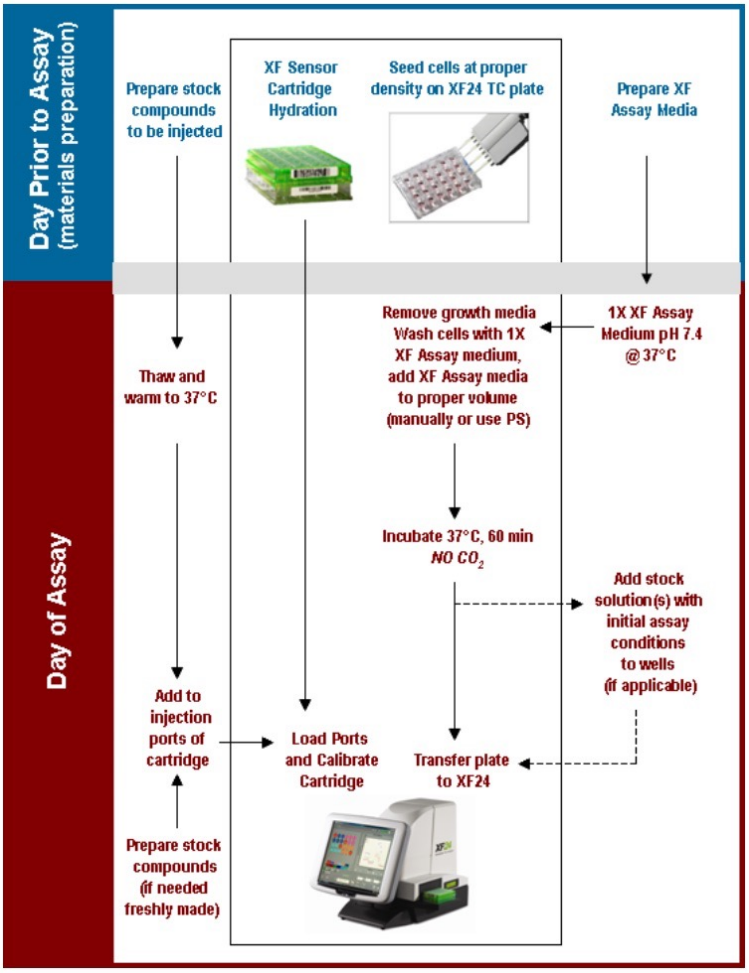

Figure 4.2. Flow chart of mitochondrial bioenergetics assay protocol.

The stock compounds include mitochondrial stress reagents (oligomycin, FCCP, antimycin, rotenone) and any drug treatments (e.g. SB203580, p38 inhibitor). XF sensor cartridge contains the fluorescent probes which measure oxygen and pH. The hydration solution is provided by Seahorse bioscience. XF24 TC is the tissue culture plate in which cells are seeded into and the plate on which the sensor cartridge sits when the assay is performed. The XF assay media is an unbuffered, serum and phenol free basic DMEM that has been supplemented with sodium chloride, sodium pyruvate and d-glucose (see 4.2.1.2 for exact concentrations). XF24 is the instrument which the mitochondrial bioenergetics assay is performed at 37C.

4.2.1.3.. Optimisation of treatment conditions of 3T3-L1 preadipocytes with mitochondrial inhibitors and uncouplers:

Mitochondrial stress reagents were purchased from sigma aldrich: Oligomycin (75351), FCCP (carbonyl cyanide-p-trifluoromethoxyphenylhydrazone, C2920), Antimycin and Rotenone (A8674 and R8875).

Mitochondrial stress test reagents and drug treatment preparation: The mitochondrial stress test reagents were assessed individually within 3T3-L1 preadipocytes seeded at 2 x 10^4/well. Oligomycin was assayed at 0.25, 0.5, 0.75 and 1 µM (final concentration in well, 1ml of 2.5, 5.0, 7.5 and 10µM working stocks were prepared in running media). Oligomycin is an ATP synthase inhibitor. Through its inhibition of this mitochondrial membrane bound complex, it is capable of blocking oxidative phosphorylation from proceeding past this point of the electron transport chain. As a consequence, only electrons generated through mitochondrial uncoupling, allow protons to diffuse using uncoupling protein (UCP1) from the outer to inner mitochondrial membrane. Therefore, oxygen consumption-rate changes following oligomycin administration were used to semi-quantitatively measure ATP production and proton leak. FCCP (carbonyl cyanide-p-trifluoromethoxyphenylhydrazone) was assayed at 0.25, 0.5, 0.75 and 1 µM (final concentration in well, 1ml of 2.5, 5.0, 7.5 and 10µM working stocks were prepared in running media). FCCP is a mitochondrial uncoupling agent, used to increase mitochondrial permeability to protons through depolarisation of the mitochondrial membrane potential. FCCP measures the maximal oxygen consumption rate of cellular mitochondria. FCCP concentration should be tightly titrated, as treatment of cells with supra-concentrations of this compound is known to initiate

apoptosis. Antimycin/Rotenone were assayed at 0.25, 0.5, 0.75 and 1µM (final concentration of each in well, 1ml of 2.5, 5.0, 7.5 and 10µM working stocks were prepared in running media).Antimycin inhibits complex III of the electron transport chain resulting in leaking of electrons to molecular oxygen resulting in the generation of superoxides. Rotenone inhibits Complex I of the electron transport chain (specifically the NADH dehydrogenase enzyme). The cocktail of antimycin/rotenone quantifies non-mitochondrial respiration rate within the assayed cells.

Loading the seahorse cartridge with drug treatments and/or stress reagents:

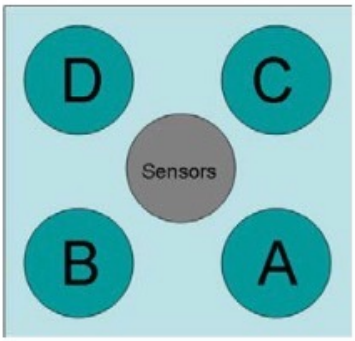

Figure 4.3. Loading pattern for use of mitochondrial stress reagent or drug treatment in mitochondrial bioenergetics assay. The contents of the ports are released alphabetically throughout the bioenergetics assay and should be loaded as follows A: Oligomycin or drug treatment (SB203580) (75ul), B: FCCP (carbonyl cyanide-p-trifluoromethoxyphenylhydrazone, 75ul), C: Antimycin/Rotenone cocktail (75ul).All ports included as part of the assay protocol should be occupied. For the untreated wells, i.e. those not receiving either a mitochondrial stress reagent or drug treatment, running media solution should be placed (75ul) in these relevant ports. In the case of the standard stress reagent assay i.e. oligomycin, FCCP and then antimycin-rotenone, the port D can remain unoccupied and excluded from the bioenergetics assay protocol. However, in the case where a drug treatment is preadministered in port A before the commencement of the mitochondrial stress assay (Oligomycin, FCCP, antimycin/Rotenone), all ports A-D will be required.

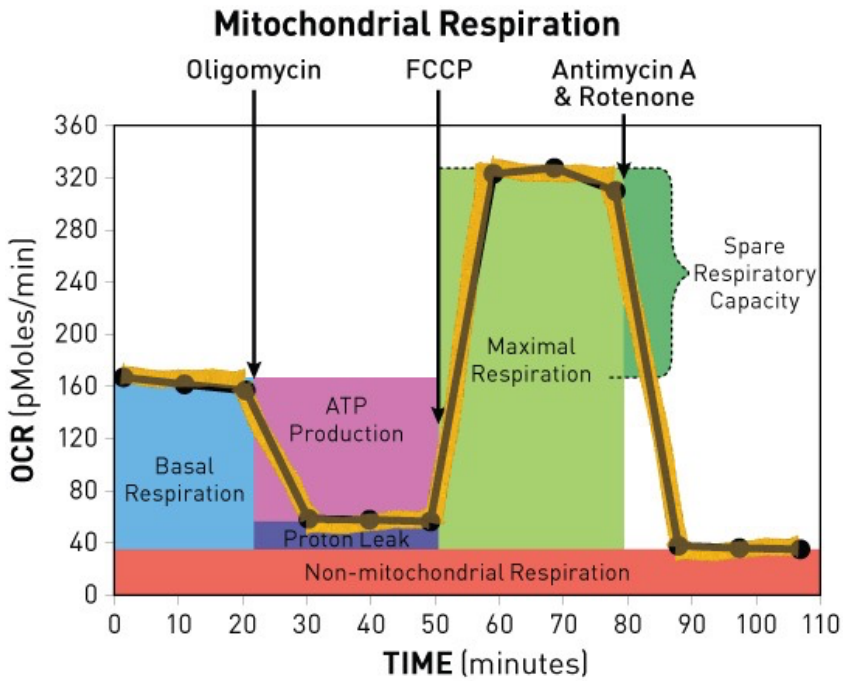

Figure 4.4. Mitochondrial stress test bioenergetic profile.

Oligomycin is an ATP synthase inhibitor and is used to semi-qunatitatively measure ATP production and proton leak. FCCP (carbonyl cyanide-p-trifluoromethoxyphenylhydrazone) measures the maximal oxygen consumption rate of cellular mitochondria. OCR denotes oxygen consumption rate.The cocktail of antimycin/rotenone quantifies non-mitochondrial respiration rate within the assayed cells.

Calculation of mitochondrial bioenergetics:

Oxygen consumption rate (OCR) data for each well was normalised per mg/protein for chemical treatment. The spare respiratory capacity and coupling efficiencies were calculated from the oxygen consumption values according to the following formulae:

Spare respiratory capacity = (FCCP/ Basal respiration OCR)*100

Coupling efficiency = 1 – (Oligomycin/Basal respiration OCR)

4.2.2.1. Differentiation of 3T3-L1 preadipocytes (fibroblasts) to adipocytes:

Differentiation protocol:

3T3-L1 preadipocytes were seeded at 2x104/2ml in 6WP in growth media and incubated at 37C, 5% CO2. Media was replaced every 48 hours (2ml per well). After 3 days, 3T3-L1 preadipocytes reached confluency (100%).The next day, the media was changed from growth media (Day 0) to differentiation media (prewarmed to 37C, 2 washes with phosphate buffered saline (PBS) at 37C, to remove residual growth media). After 48 hours (Day 2), cells were washed twice with PBS and placed in nutrition media (Days 4-6) for 48 hours. Finally for the final days of 3T3-L1 differentiation the cells were returned to growth media (Day 6-8). Differentiation protocol was completed on day 8. Any protein or RNA samples were harvested for further expression analyses. Individual protein samples (per well) were harvested by removing culture media, washing the monolayer twice with cold PBS, addition of RIPA lysis buffer (250µl), shaking incubation on ice, scraping and storage in eppendorfs (2 ml) at -20C until required. RNA samples were harvested by removing culture media, washing the monolayer twice with cold PBS, addition of Qiazol (250µl), shaking incubation on ice, scraping and storage in eppendorfs (2 ml) at -20C until required. RNA was extracted using RNeasy kit (Qiagen, see 2.1).

Growth media (GM):

DMEM F12 supplemented with 10% foetal bovine serum (FBS), penicillin (100 U/ml), streptomycin (100 µg/ml) and L-glutamine (10mM).

Differentiation media (DM, final concentrations, Promocell supplement mix)

DMEM F12 supplemented with 10% foetal bovine serum (FBS), IBMX 44µg/ml), insulin (0.5µg/ml, human recombinant), dexamethasone (400ng/ml), d-Biotin (8 µg/ml), L-thyroxine (9ng/ml) and Ciglitazone (3µg/ml).

Nutrition media (NM, Promocell supplement mix)

DMEM F12 supplemented with 10% foetal bovine serum (FBS), insulin (0.5µg/ml, human recombinant), dexamethasone (400ng/ml), d-Biotin (8 µg/ml).

RIPA lysis buffer (1x RIPA lysis buffer (Millipore) containing protease inhibitor (Roche) and phosphatase inhibitor (100µl of 100mM Sodium fluoride and 100µl of 100mM Sodium vanadate, Sigma Aldrich),

4.2.2. Cytotoxicity of SB203580.

4.2.2.1. Principles of the MTT assay: A tetrazolium salt, 3-(4,5-dimethylthiazol-2-yl)-2,5-diphenyltetrazolium bromide (MTT) is used in a colorimetric assay to assess the affect of a compound on cell viability. Respiring cells promote the conversion of the tetrazolium dye MTT into an insoluble formazan through an enzyme based catalysis involving NAD(P)H-dependent oxidoreductase. The conversion from MTT to formazan is accompanied by a colour change from yellow to purple. Cellular respiration is quantified by absorbance at 570nm, with purple indicating greater cellular respiration.

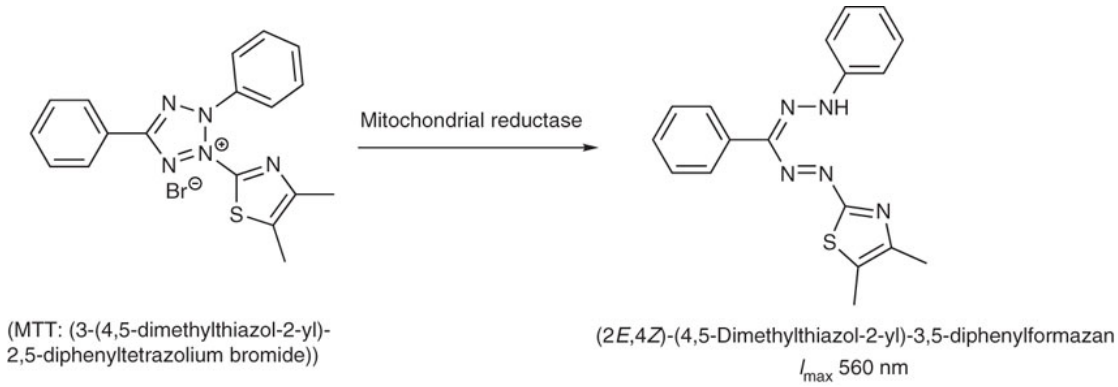

Figure 4.5. MTT assay

The conversion from MTT to formazan is accompanied by a colour change from yellow to purple. Cellular respiration is quantified by absorbance at 570nm, with purple indicating greater cellular respiration. Figure from Ebada et al. Nature protocols 3. 1820-1831 (2008).

This assay is performed to quantify the minimum concentration of a compound that cells can be exposed to, in order to elicit the compound's functional role whilst preserving the respiration of most of the cultured cells. The assay was performed according to the manufacturer's protocol (Sigma Aldrich, M2128). Briefly the assay was performed as follows;

4.2.2.2 Assay protocol: 2 days prior to the MTT assay, 3T3-L1 preadipocytes were plated into a 6 well plate at a density of 1 x 10^5/ml. Once confluent, the media was removed and the cells were washed twice with PBS. Media was replaced with 0.2% BSA DMEM-F12 (2ml/well, no antibiotics). Cells were serum starved 3 hours before the assay. The working stock of MTT was 5mg/ml. (M2128, Sigma Aldrich) Control cells were treated with equivalent volumes of DMSO to that used to treat cells with SB203580 compound. Following incubation of the 3T3-L1 at 37°c and 5% CO_2 for 0,

30 minutes, 1hr and 2 hours, cells were washed twice with PBS. MTT (20µg/well) was added to the wells and 3T3-L1 were incubated in the dark (due to the light sensitive nature of MTT) for a further 4 hours at 37°c and 5% CO_2. Cells were washed twice more with PBS and the formazan crystals were eluted in 2ml DMSO: Isopropanol (1:1 ratio).

4.2.2.3. Calculation of cytotoxicity: Absorbance was read at 570 nm. Background absorbance at 690 nm was subtracted from this reading. MTT incubated in the absence of cells was used to assess non-specific binding of dye to plastic which may influence the absorbance readings. Cytotoxicity was determined as the difference in absorbance between control and SB203580 treated cells and was expressed as a percentage. Each value for cytotoxicity is an average of 8 measurements.

4.2.3. Gene expression analyses of adipocyte differentiation.

PPAR-γ (Mm01184322_m1) gene expression along with Oil red O lipid staining was used to determine the differentiation status of 3T3-L1 cells through normal differentiation and p38 inhibitor treatment.

4.2.4. Manipulation of p38 expression and mitochondrial bioenergetics.

The XF24 Seahorse Bioanalyser was used to assay the effect of p38 on mitochondrial bioenergetics (see sections 4.2.1.2 to 4.2.1.3 for assay protocol and cell culture conditions). Mitochondrial bioenergetics with p38 inhibition by SB203580 treatment was assessed in 3T3-L1 preadipocyte cells. Protein quantification was performed using

Biorad protein assay (500-006, Biorad) and BSA as a standard (2mg/ml). The protein concentration given for each well is an average from triplicate measurements.

4.2.5. Mitochondrial DNA content of 3T3-L1 preadipocytes.

Total DNA was extracted from 3T3-L1 preadipocytes using DNeasy kit (Qiagen) according to the manufacturer's protocol (see Figure 2.3 for DNA extraction protocol). RNase treatment was performed to prevent co-purification of RNA with genomic DNA. DNA quantification was performed using Nanodrop spectrophotometer The relative amounts of nuclear and mitochondrial DNA were determined by qPCR using 20ng of isolated genomic DNA as a template. DNA was amplified using SYBR green in an ABI 7500 thermocycler (Life technologies) The abundance of each gene was defined as a ratio between mitochondrial threshold cycle (Ct) value and nuclear threshold cycle. Each sample was measured in duplicate against a mitochondrial (m)/ nuclear (n) DNA primer set. The following primer sequences were used: COXII; Forward 5'-AATTGCTCTCCCCTCTCTACG-3 and reverse 5'-GTAGCTTCAGTATCATTGGTGC-3', RIP140 Forward 5'-CGGCCTCGAAGGCGTGG-3' and reverse 5'-AAACGCACGTCAGTATCGTC-3', ND2 and Beta-2-microglobulin as previously published in (Murholm, Dixen et al. 2009) and (Wai, Ao et al. 2010) respectively. These primer sets were more appropriate than the CytB/Beta actin used in the human adipose tissue mitochondrial DNA expression analyses as their primer efficiency and melt curve analyses produced a single PCR product.

4.2.6. Transfection of 3T3-L1.

Plasmids transfected: pCDNA3.0-GFP (Ampicillin resistant, provided by Dr. Jürgen Muller, University of Warwick) and MKK6 overexpression (mitogen activated protein kinase kinase 6, human MKK6 (Glu) Addgene plasmid 13518; provided by Roger Davis from the Addgene repository; details of the molecular cloning and construction of these plasmid expression vectors are published in their paper (Raingeaud, Whitmarsh et al. 1996)). MKK6(Glu) is the replacment of Ser207 and Thr211 from the wildtype MKK6 with Glu. MKK6 or MAP2K6 (mitogen-activated protein kinase kinase 6) is a member of the dual specificity protein kinase family, which functions as a mitogen-activated protein (MAP) kinase kinase. MKK6 phosphorylates and activates p38 MAP kinase and is an essential component of p38 MAP kinase mediated signal transduction pathway**.** Constitutive over-expression of MKK6 activates p38 kinase activity. Therefore, this construct was used to activate p38.

3T3-L1 preadipocytes were seeded at a density $1.25x10^5$/ml in 6 well plates and maintained in 10% FBS (antibiotic free, 2mM L-glutamine, 5% CO_2 and 37°c). Cells were transfected at 70% confluency with 5µg plasmid (2.5µg each plasmid, where cells were co-transfected with GFP) and Lipofectamine 2000 (Invitrogen) using manufacturer's protocol. Briefly, plasmid DNA and Lipofectamine complexes were incubated to allow complex formation (1:2 ratio Plasmid DNA: Lipofectamine, 45 minutes room temperature incubation in Optimem reduced serum media).

Media in 3T3-L1 was replaced 4 hours after transfection with fresh 10% growth media (FBS, antibiotic free). Cells were harvested 48 hours post transfection. Mitochondrial fusion and fission gene expressions were analysed by qRT-PCR as described in methods section of the bariatric chapter 2.2.3 and 2.2.4 .

4.2.7.1. Mitochondrial morphology: Effects of p38 inhibition by SB203580.

3T3-L1 were seeded at a density $1.25x10^5$/ml in glass bottomed petri dishes (35mm collagen coated, γ-irradiated, glass bottomed petri dishes, Matex corporation) and maintained in 10% FBS (antibiotic free, 2mM L-glutamine, 5% CO_2 and 37°c). Cells were washed twice with 0.2% BSA DMEM to remove residual serum and allowed to recover for an hour (5% CO_2 and 37°c) prior to treatment or mitochondrial labelling.

Image acquisition: Labelling of mitochondria was performed using Mitotracker Red (250nM, 30 minutes). Images were captured as a time-lapse series on Leiss 63x lens. 10 fields were selected per petri dish and mitochondrial morphology was assessed by field images taken across 3 petri dishes.

Image processing: Within ImageJ, images were processed through sharpening; the location of edges feature and the image was despeckled. A binary image generated automatically from the original image using the analyse particle macro provided a semi quantitative determination of mitochondrial size and morphology using the area measurement of neighbouring pixel (μm^2) and test data set of manually defined, by human inspection, mitochondrial morphologies. For each of the 6 mitochondrial sub-types, Peng et al wrote an algorithm to define its distinct morphological features, thereby allowing future automatic characterisation of different mitochondrial subtypes from a confocal microscopy image. Prior to each treatment, 10 fields were captured for DMSO treated 3T3-L1. Following addition of SB203580, 3T3-L1 were incubated

for 15 minutes prior to time-lapse acquisitions. Unpaired t tests were performed to assess statistical significance of p38 inhibition.

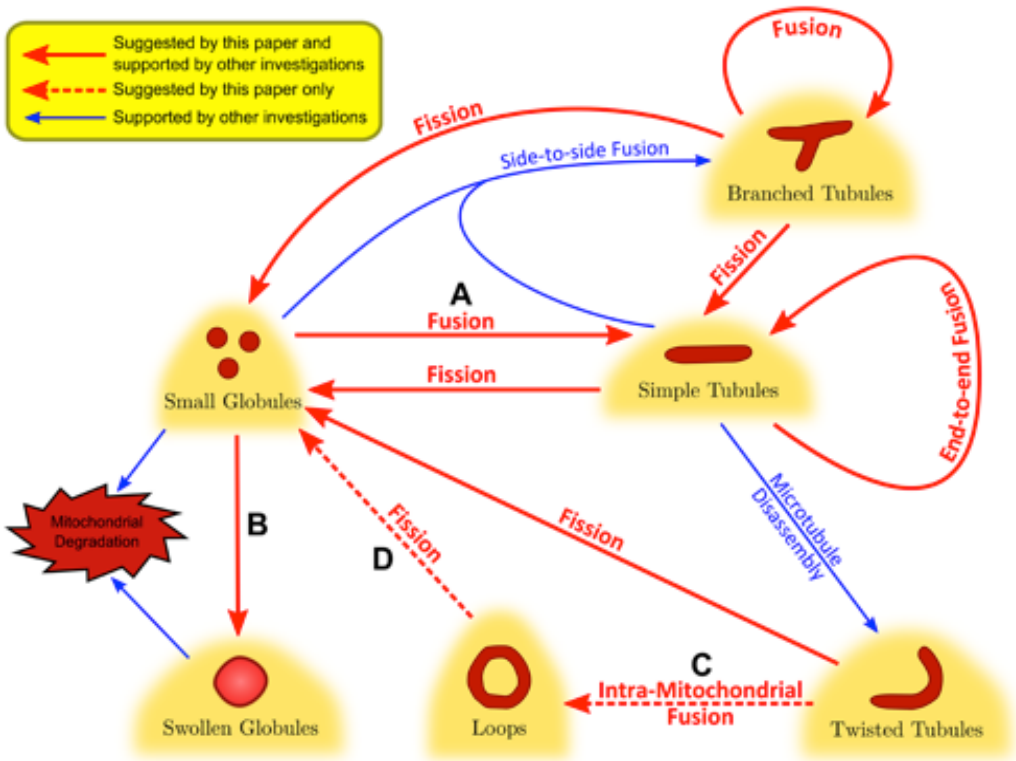

Figure 4.6. Proposed model for the generation of mitochondrial morphological subtypes.

Small globules generated during mitosis through end-to-end fusion become tubules following cell division (A). Nevertheless, not all of these small globules progress to form simple tubules at the end of cell division (B). In the event of insufficient genome copies within mitochondria they may be shuttled towards mitophagy to remove these from the population owing to their lower mitochondrial proofreading and subsequent accumulation of mutations (C). Twisted tubules may be generated through microtubule disassembly of tubules or through intra-mitochondrial fusion of twisted tubules to form loops. Through enhanced mitochondrial recruitment of Drp1, small globules may be generated from division of tubules (D). Figure from and legend based on (Peng, Lin et al. 2011).

4.2.7.2. Image analysis of mitochondrial morphology in 3T3-L1 by time-lapse confocal microscopy.

Mitochondrial morphology was assessed and quantified using image processing software. Within ImageJ (NIH), the time-lapse video was separated into a series of stepwise stills. At each given position of the image, the individual intensity of all pixels was measured across the entire viewing field. A binary image of mitochondria was generated for each time frame through image processing within ImageJ. Using the "Analyse particles" Macro, the total number of mitochondria, average mitochondrial size and total mitochondria area were quantified. To address the question of mitochondrial motility, a sequentially subtraction protocol and median filter were used across the entire timeframe. Each of these images was subjected to quantification of pixel intensities. Any change in pixel intensity, above or below maximum pixel intensity was recorded for that time point and given a value from 0 to 1. 0 corresponded to no movement, whilst 1 indicated movement of the mitochondria outside the bounds of that pixel. To facilitate multiple comparisons of time frames and different cell treatments (DMSO or SB203580 treated), the index of motility was normalised to account for the total mitochondrial area and averaged over the first minute of imaging.

Meanwhile, detailed morphological analysis required additional classification and image processing. The original images were segmented in MicroP. This program written in Matlab and kindly donated to by Dr. J.Y Peng *et al (Peng, Lin et al. 2011)*, enabled automatic classification of mitochondria into one of six subtypes; small globules, large globules, straight tubules, twisted tubules, loops and branched tubules. The subtypes were colour coded from the segmented image file to generate a new object clas-

sification image. The colours assigned were; blue: small globules, yellow: large/ swollen globules, green: straight tubules, orange: twisted tubules, purple: twisted tubules and red: loops. The relative abundance of each subtype was expressed as a percentage of the total mitochondrial population. Morphological analyses were used to determine if p38 inhibition resulted in any acute changes to mitochondrial morphology.

4.3. Results.

4.3.1. p38 and differentiation.

4.3.1.1. Triglyceride accumulates through adipocyte differentiation.

Triglyceride accumulation was semi quantitatively assessed by Oil red O staining. Lipid accumulation in the mature adipocytes (D4 onwards) was significantly higher compared to the preadipocytes of D0 (Figure 4.7. D4 vs D0; 2.4±0.3 fold, $p = 0.005$, D6 vs D0; 1.7±0.4 fold $p = 0.0002$ and D8 vs D0; 2.3±0.6 fold, $p = 0.02$).

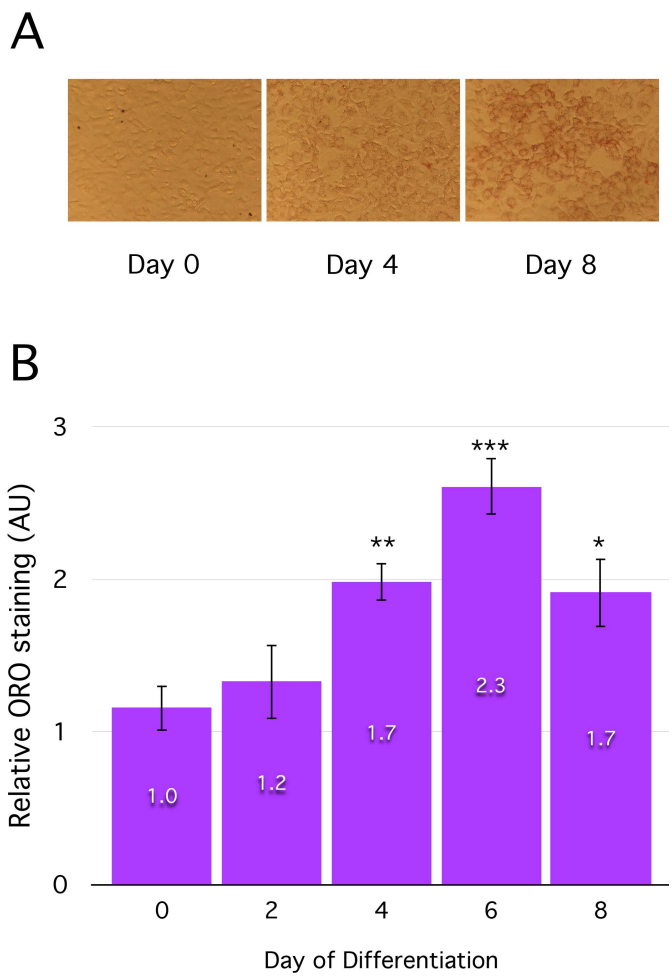

Figure 4.7. Triglyceride accumulates with adipocyte differentiation.

Adipocyte differentiation (3T3-L1) is accompanied by an increase in triglyceride accumulation. Images of Oil Red O (ORO) stained 3T3-L1 were taken at 20x magnification (A). Red indicates lipid accumulation. ORO absorbance values were measured at A_{595nm} to semi quantitatively determine triglyceride accumulation (B). Unpaired t-tests were performed to assess the statistical significance of changes in ORO staining relative to Day 0 (n = 3 per day). Statistical significance was defined as a $p < 0.05$*. $p < 0.05$*, $p < 0.01$** and $p < 0.001$***. AU denotes arbitrary units, as the data is expressed as fold change in ORO staining relative to day 0. Data are given as mean ± S.E.M.

4.3.1.2 Effect of p38 inhibition through 3T3-L1 differentiation

SB203580 was utilised to inhibit p38 throughout differentiation from preadipocytes to fully differentiated 3T3-L1 (Day 0 (D0) being the day differentiation was initiated and when preadipocytes were 100% confluent adipocytes up to day 8 (D8).

mRNA expression of PPAR-γ, a regulator of adipocyte differentiation, was used to characterise the effect of p38 inhibition on adipocyte maturation. On D2-D6, PPAR-γ expression was significantly lower in p38-inhibited cells compared to DMSO treated controls (Figure 4.8. D2; 0.83±0.01 relative fold, $p = 0.01$ and D4 0.27±0.07 relative fold; $p = 0.01$).

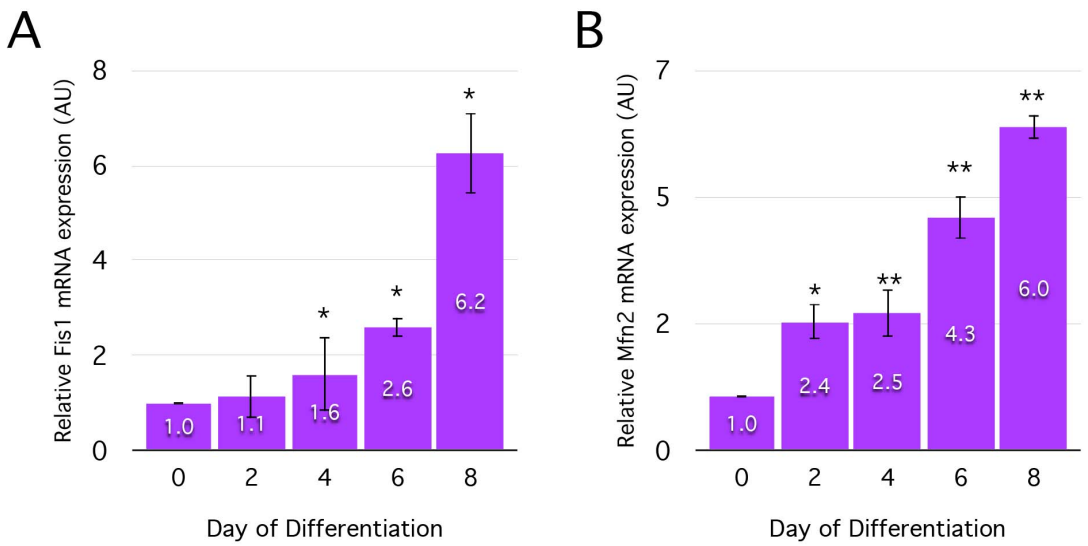

Figure 4.8. Effect of p38 inhibition through 3T3 differentiation.

mRNA expression of PPAR-γ involved in mitochondrial differentiation was analysed and compared against a DMSO control in chronically p38 inhibited 3T3s. Media containing 10μM SB203580 (SB) was changed every 24 throughout differentiation (day 0-8). All experiments were performed in triplicate. Unpaired t-tests were performed to assess the statistical significance of changes in gene expression of 3T3 differentiation relative to day 0. Statistical significance was defined as a $p < 0.05$*. $p < 0.05$*, $p < 0.01$** and $p < 0.001$***. AU denotes arbitrary units, as the data is expressed as fold change in PPAR-γ mRNA expression relative to day 0. Data are given as mean ± S.E.M.

4.3.1.3 Mitochondrial dynamics throughout adipocyte differentiation

Fis1 mRNA expression increased significantly and steadily from D2, peaking at D8 through 3T3-L1 differentiation (Figure 4.9; D8 vs D0; 6.2±1 fold, $p < 0.001$). Mfn2 mRNA expression also steadily and significantly increased up to D8 as differentiation progressed (Figure 4.9. (D4 vs D0; 2.5±0.3 relative fold, $p = 0.002$, D6 vs D0; 6.0±0.3 fold, $p = 0.003$).

In summary, markers of mitochondrial fusion and fission gene expression are dynamic in nature and consistent with previous reports (Ducluzeau, Priou et al. 2011), with their expressions peaking at the later stages of 3T3-L1 differentiation.

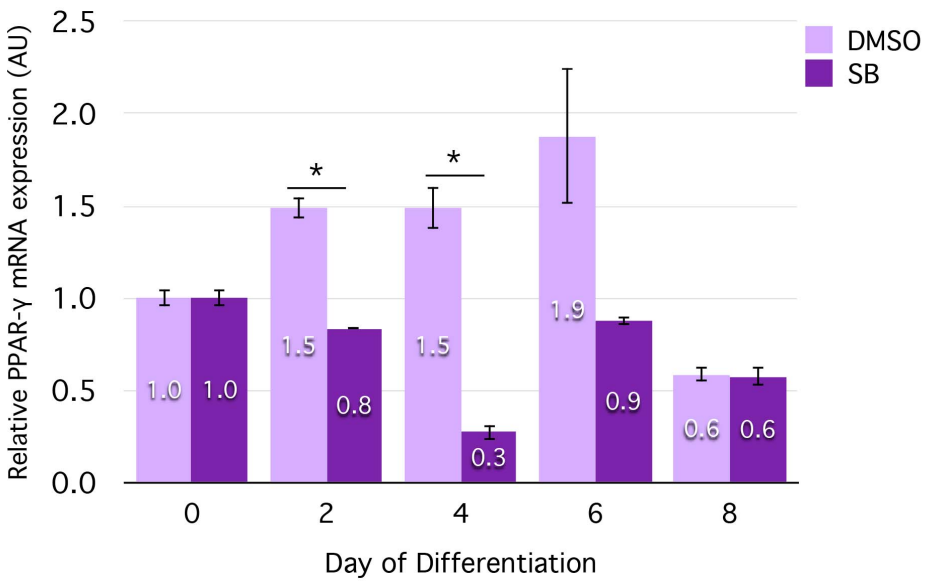

Figure 4.9. Markers of mitochondrial dynamics expression through adipocyte differentiation.

mRNA expression of markers of mitochondrial fission: Fis1 (A) and fusion: Mfn2 (B) were measured throughout 3T3-L1 differentiation. All experiments were performed in triplicate.Unpaired t-tests were performed to assess the statistical significance of changes in mitochondrial gene expression relative to day 0. Statistical significance was defined as a $p < 0.05$* and $p < 0.01$**. $p < 0.05$*. AU denotes arbitrary units, as the data is expressed as fold change in mRNA expression relative to day 0. Data are given as mean ± S.E.M.

4.3.2. Effect of p38 inhibition on mitochondrial dynamics and abundance.

4.3.2.1. Timecourse optimisation for p38 inhibition.

Serum starved 3T3-L1 preadipocytes were treated for up to 4 hours with either DMSO or SB203580. SB203580, a p38 inhibitor was reconstituted in DMSO. An equivalent volume of DMSO was included in the control treated 3T3-L1. Protein expressions of phospho-p38, total p38 and beta actin were quantified. Phospho-p38 inhibition (p-p38) was most significantly decreased after 1 hour (Figure 4.10. SB203580 1hr vs DMSO control, ~ 2 fold reduction, $p < 0.0001$). Furthermore, inhibition of p-p38 expression was sustained up to 2 hours after treatment (Figure 4.10. SB203580 2hr vs DMSO control, 0.3 fold lower expression, $p = 0.02$). After 4 hours of SB203580 treatment, no significant change in p-p38 expression compared to DMSO treated 3T3-L1 was noted.

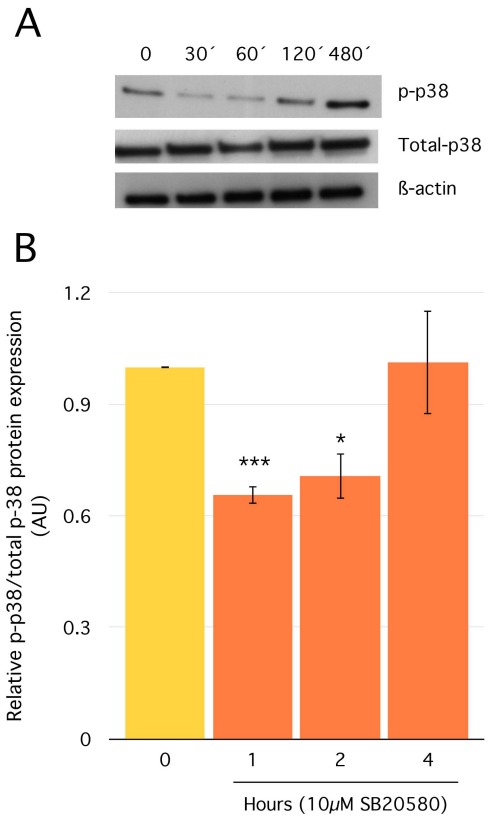

Figure 4.10. Timecourse of p38 inhibition.

3T3-L1 preadipocytes were used to optimise the cell culture conditions for chemical inhibition of p38 by SB203580 (Calbiochem). Protein samples were collected at 0, 30, 60 and 120 minutes after SB incubation (n = 3, serum starved). Controls were treated with an equivalent volume of DMSO. Unpaired t-test analyses were used to determine the statistical significance of p38 inhibition by SB203580 in 3T3-L1 relative to DMSO treated controls. Statistical significance was defined as a $p < 0.05$* and $p < 0.001$***. AU denotes arbitrary units, as the data is expressed as fold change in phospho (p-p38) expression relative to DMSO treatment at timepoint 0. Data are given as a mean ± S.E.M.

4.3.2.2. Cytotoxicity assessment of the p38 inhibitor, SB203580.

The effect of both p38 inhibitor concentration and treatment timecourse were evaluated in 3T3-L1 preadipocytes. At each timepoint, a new DMSO control was included. Statistical analysis using an unpaired t-test and assuming non equal variance, revealed no significant reduction in cell respiration as assessed by the MTT assay, after 4 hours and across a concentration range of 2.5 to SB15μM were used (Figure 4.11; DMSO control; 100±12%, SB2.5μM; 107±19% $p < 0.25$, SB5μM; 109±18% $p < 0.23$, SB10μM; 106±26%, $p<0.40$ and SB15μM; 122±36% $p < 0.35$).

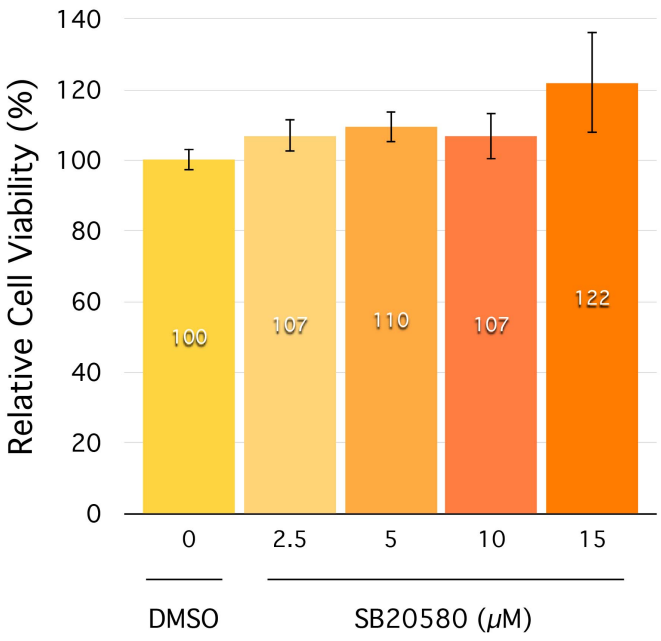

Figure 4.11. Cytotoxicity of the p38 inhibitor, SB203580.

3T3-L1 preadipocytes were used to define the cytotoxicity of SB203580 (Calbiochem). Confluent 3T3 preadipocytes were serum starved for 3 hours before being treated with 10μM of SB203580 for 2 hours (n = 8). Controls were treated with an equivalent volume of DMSO (n = 8). Cytotoxicity was expressed as a percentage of the ratio of SB203580 treated absorbance/control absorbance * 100. Unpaired t-test analyses were used to determine the statistical significance of any cytotoxic effects of SB203580 on 3T3-L1. $p < 0.05$* was considered statistically significant. Data are given as a mean ± S.E.M.

4.3.2.3. Effect of p38 inhibition by SB203580 on markers of mitochondrial fission.

Acute p38 inhibition by SB203580 was carried out 3T3-L1 preadipocytes and total protein collected every 30 minutes up to 2 hours. Statistical analysis revealed a significant reduction in Fis1 protein expression up to 2 hours after treatment (Figure 4.12. 30 minutes of SB203580 vs DMSO control; 0.69± 0.01 fold, $p < 0.001$, 60 minutes of SB203580 vs DMSO control; 0.64 ± 0.02 fold, $p < 0.001$ and 120 minutes of SB203580 vs DMSO control; 0.49 ± 0.009 fold), $p < 0.001$).

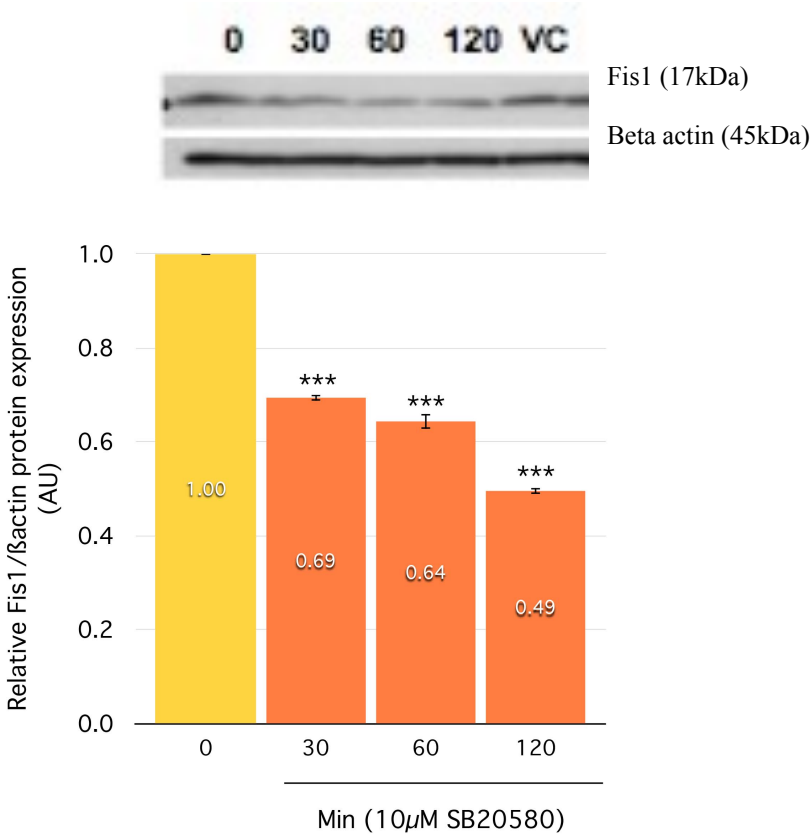

Figure 4.12. Fis1 protein expression decreases significantly following p38 inhibition.

3T3-L1 preadipocytes were seeded at 2 x 10^4/well and grown until confluent (5% CO_2, 37^0c). Cells were treated with either SB203580 (10µM) or DMSO (control) for up to 2 hours. 20µg of protein was loaded per well. Beta actin was used as a loading control. n = 3 per treatment. Unpaired t-test analyses were carried out to determine the effect of p38 inhibition on Fis1 expression. Statistical significance was confirmed if $p < 0.05$*. $p < 0.001$***. VC denotes DMSO 2hr vehicle control. AU denotes arbitrary units, as the data is expressed as fold change in Fis1 protein expression relative to DMSO treatment at timepoint 0. Data are given as a mean ± S.E.M.

4.3.2.4 Effect of p38 inhibition by SB203580 on markers of mitochondrial fusion.

Mfn2 protein expression was statistically decreased by SB203580 treatment (Figure 4.13; SB30′; 1.2±0.08 fold $p = 0.09$ and SB60′; 1.6±0.75 fold $p = 0.4$). In summary, acute p38 inhibition by SB203580 significantly decreased Mfn2 expression.

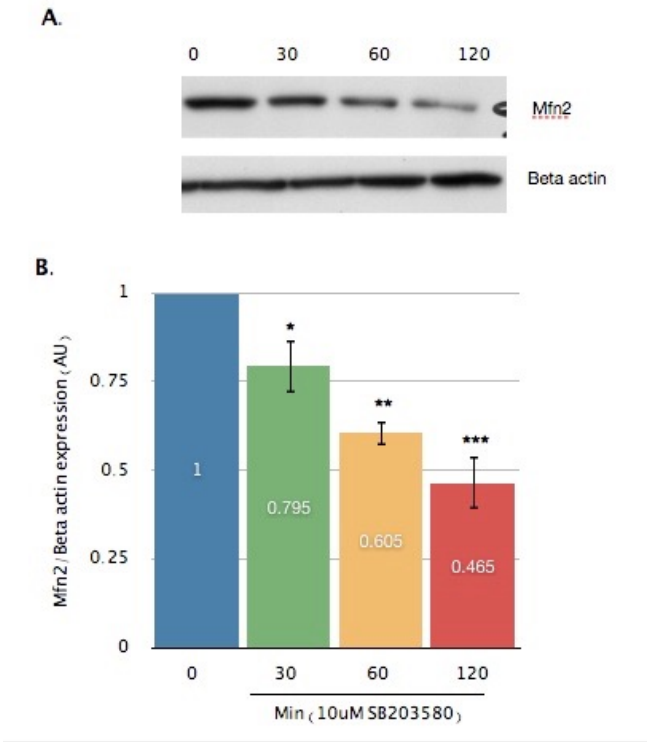

Figure 4.13. Mfn2 protein expression decreases significantly following p38 inhibition.

3T3-L1 preadipocytes were seeded at 2 x 10^4/well and grown until confluent (5% CO_2, 37^0c). Cells were treated with either SB203580 (10µM) or DMSO (control cells only) for up to 2 hours. 20µg of protein was loaded per well. Beta actin was used as a loading control (A). n = 3 per treatment. Unpaired t-test analyses were carried out to determine the effect of p38 inhibition on Mfn2 expression (B)..Statistical significance was confirmed if $p < 0.05$*, $p < 0.01$** and $p < 0.001$***. VC denotes DMSO 2hr vehicle control. AU denotes arbitrary units, as the data is expressed as fold change in Mfn2 protein expression relative to DMSO treatment at timepoint 0. Data are given as a mean ± S.E.M.

4.3.2.5. Effect of p38 inhibition on mitochondrial copy number.

Mitochondrial copy number was assessed in p38-inhibited 3T3-L1 preadipocytes by two genomic DNA methods. The results expressed as a ratio between mitochondrial and nuclear genomic DNA indicated no statistically significant change in mitochondrial DNA content as a result of p38 inhibition which was expected because this is only acute treatment and by 2 hours the number of mitochondrial DNA content starts declining (Figure 4.14. ND1/B2M; 120′ SB203580, 1.0±0.01 relative to control, $p < 0.09$ and COXII/RIP140; 120′ SB203580, 0.92±0.05, $p < 0.09$).

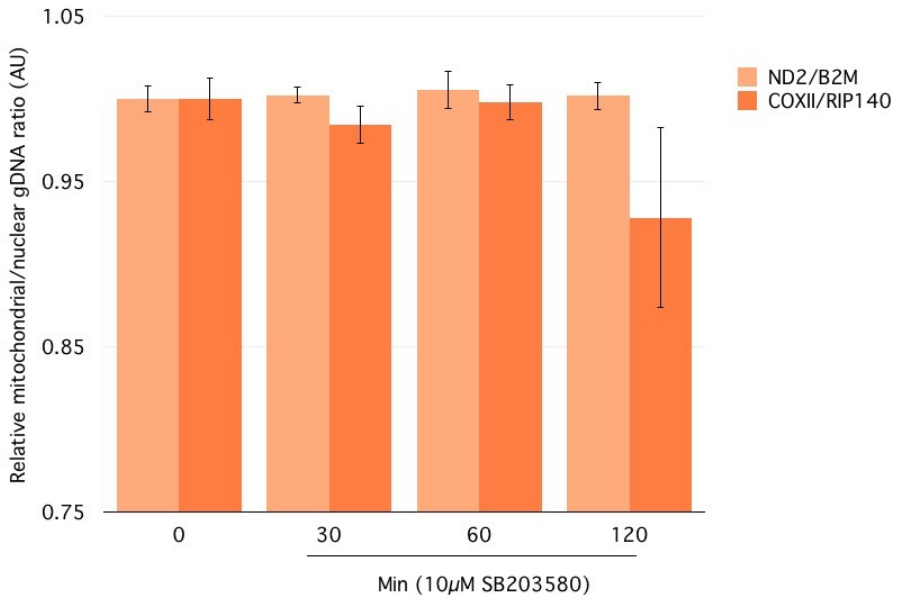

Figure 4.14. Mitochondrial DNA content remained unchanged following p38 inhibition.

3T3-L1 preadipocytes were treated with SB (10μM) or DMSO (control cells) for up to 2 hours. Mitochondrial DNA content was assessed by two primer sets (expressed as mitochondrial/nuclear primer sets; ND2/B2M and COXII/RIP140). Each treatment was assayed three times for each primer set. The data presented here, represent the average of these triplicate readings; all data were non significant.AU denotes arbitrary units, as the data is expressed as relative mitochondrial/nuclear gDNA ratio at time-point 0 min. Data are given as a mean ± S.E.M.

4.3.3. Effect of p38 inhibition on mitochondrial bioenergetics.

4.3.3.1 Optimisation of Seahorse mitochondrial bioenergetics assay; cell density, culturing conditions, concentration of stress test reagents.

Preadipocytes were seeded at 4 densities; 1 x 10^4, 2 x 10^4, 1x10^5 and 1x10^6/well. The optimal seeding density was 2 x 10^4, as evidenced by a single monolayer and average oxygen consumption rate (OCR) values of 276±79 pmol/0_2/min. The optimal stress test reagent concentrations, as defined by the changes in OCR were Oligomycin 1µM, FCCP 0.5µM and antimycin/rotenone 1µM. All future seahorse mitochondrial bio-energetics assays were treated with these optimised stress test concentrations. Un-treated cells were included to assess the basal OCR throughout the seahorse assay (Figure 4.14).

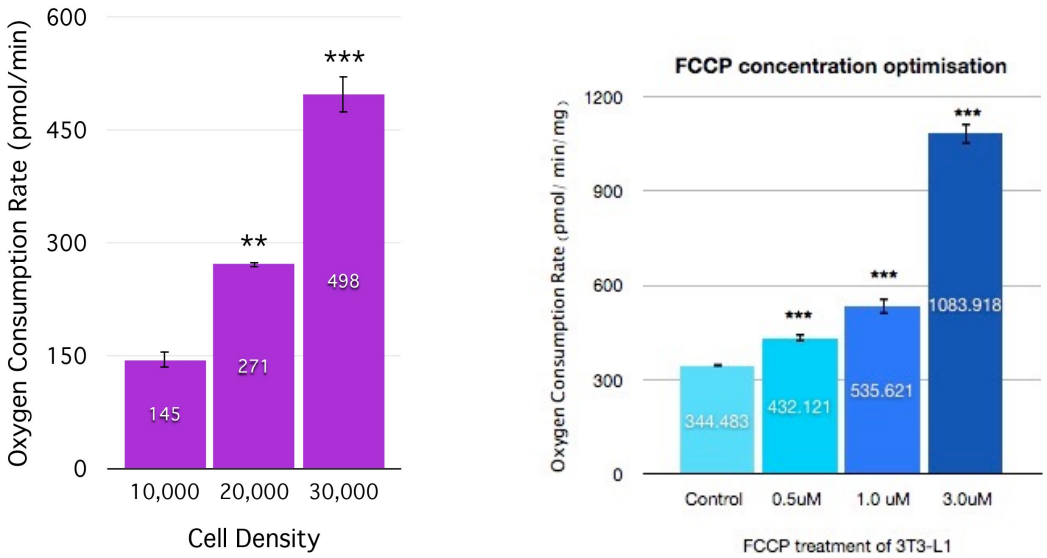

Figure 4.15. Optimisation of seahorse mitochondrial bioenergetics assay; cell density, culturing conditions, concentration of stress test reagents.

Oxygen consumption rates (OCR) of 3T3-L1 preadipocytes, given as the standard output measurement from the mitochondrial bioenergetics assay were normalised per mg of protein. This was acheived through cell lysis with RIPA lysis buffer, scraping of the monolayer of each well individually and performing of a BioRad protein assay. Using a bovine serum albumin stock (BSA, 2mg/ml) a standard curve of BSA concentration against absorbance (A595nm, at 0.25mg/ml increments). Based on the absorbance values of each cell lysate, the BSA standard curve was used to determine the protein concentration of each well. As a result, the OCR rates together with the known protein concentrations were used to normalise all the OCR data to per mg. 3T3-L1 adipocytes were used to assess basal mitochondrial respiratory rate. Statistical significance was confirmed if $p < 0.05$*, $p < 0.01$** and $p < 0.001$***. Unpaired t tests were used to assess for statistical significance.

4.3.3.2. p38 inhibition and mitochondrial bioenergetics.

p38 was inhibited by the previously characterised p38 inhibitor, SB203580.The spare respiratory capacity (SRC) of 3T3-L1 preadipocytes decreased in a dose-dependent manner, within the concentration range of 0-15µM SB203580. The SRC of the adipocytes was significantly decreased between the SB203580 concentrations 7.5 to 15µM (Figure 4.15. SB 7.5µM; SRC, 191±5 % vs 242±7% ctrl $p < 0.01$, SB 10µM; SRC 145±34% vs ctrl 242±7%, $p < 0.02$ and SB 15µM; SRC 117±52% vs 236±7% ctrl, $p < 0.024$). The coupling efficiency was significantly decreased in adipocytes treated with 10µM of the p38 inhibitor compared to control cells. (Figure 4.15. C.E; SB 10µM 81±0.009% vs 86±0.004% ctrl, $p<0.02$, SB 15µM 80±0.05% vs 86±0.004% ctrl, $p < 0.08$).

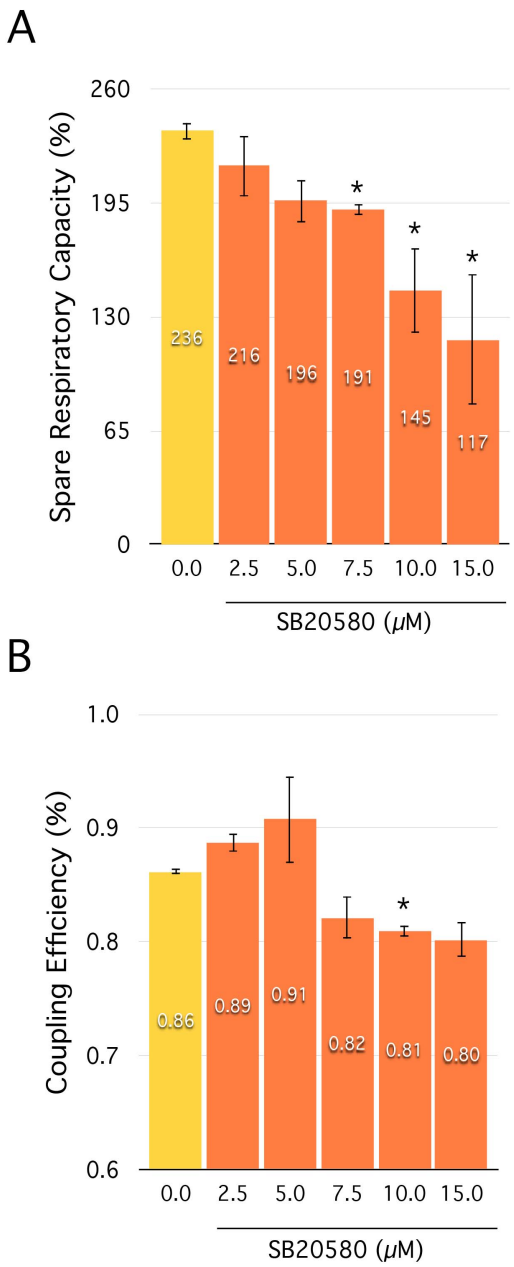

Figure 4.16. Inhibition of p38 reduces mitochondrial efficiency.

3T3-L1 preadipocyte spare respiratory capacity is calculated by maximal oxygen consumption (FCCP)/basal respiration. Coupling efficiency (C.E), is calculated by 1 – (Oligomycin or SB 10μM treated)/(Basal respiration). n = 5 per treatment. Using a bovine serum albumin stock (BSA, 2mg/ml) a standard curve of BSA concentration against absorbance (A595nm, at 0.25mg/ml increments). Based on the absorbance values of each cell lysate, the BSA standard curve was used to determine the protein concentration of each well. As a result, the OCR rates together with the known protein concentrations were used to normalise all the OCR data to per mg. Statistical significance was confirmed if $p < 0.05$*. Unpaired t tests were used to assess for statistical significance.

4.3.3.3. Optimisation of MKK6(Glu) transfection in 3T3-L1.

MKK6 or MAP2K6 (mitogen-activated protein kinase kinase 6) is a member of the dual specificity protein kinase family, which functions as a mitogen-activated protein (MAP) kinase kinase. MKK6 phosphorylates and activates p38 MAP kinase and is an essential component of p38 MAP kinase mediated signal transduction pathway**.** Constitutive over-expression of MKK6 activates p38 kinase activity. Therefore, this construct was used to activate p38. Transfection of 3T3-L1 preadipocytes with either 1.0µg or 2.5µg of pCDNA3-GFP and pCDNA3-Flag MKK6(Glu) overexpression plasmid resulted in a statistically significant increase in Mfn2 mRNA expression of 2.9±0.10 and 3.9±0.12 fold respectively compared to GFP control plasmid alone (Figure 4.16. 1.0µg GFP/MKK6; $p < 0.01$ and 2.5µg GFP/MKK6; $p < 0.05$). Plasmid pCDNA3-Flag MKK6 (Glu) which contains insert MKK6 (Glu) was constructed in Dr. Roger Davis's lab and was obtained from Addgene (Raingeaud, Whitmarsh et al. 1996).

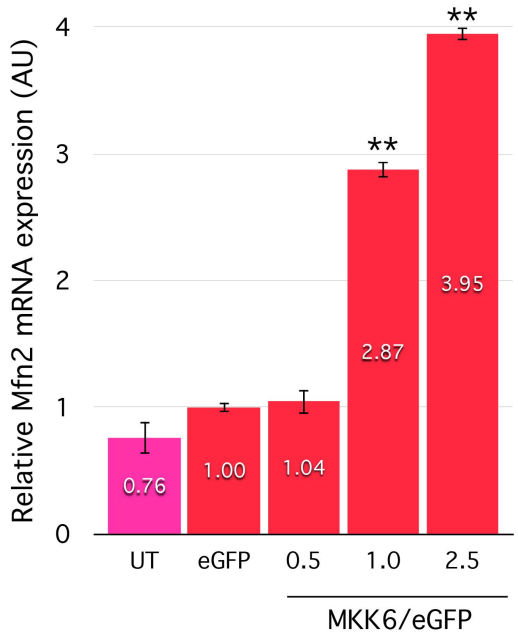

Figure 4.17. Optimisation of MKK6 (Glu) transfection in 3T3-L1 preadipocytes.

MKK6 or MAP2K6 (mitogen-activated protein kinase kinase 6) is a member of the dual specificity protein kinase family, which functions as a mitogen-activated protein (MAP) kinase kinase. MKK6 phosphorylates and activates p38 MAP kinase and is an essential component of p38 MAP kinase mediated signal transduction pathway**.** Constitutive over-expression of MKK6 activates p38 kinase activity. Lipofectamine 2000: plasmid DNA complex ratios 2:1 was used for transfection. 3T3-L1 preadipocytes were transiently co-transfected in serum free MEM with MKK6(Glu)/eGFP with 0.5, 1.0 or 2.5µg of plasmid. Control plasmid's contained the eGFP vector alone. After 4 hours the transfection cocktail was removed and replaced with 10% growth media. Cells were harvested 48 hours after transfection. Each plasmid condition was examined in 5 assays. AU denotes arbitrary units, as the data is expressed as relative Mfn2 mRNA expression in eGFP control plasmid. UT denotes untransfected and eGFP (green fluorescent protein, control plasmid). MKK6 (Glu) constitutvely activates p38. Data are given as a mean ± S.E.M.Statistical significance was confirmed if $p < 0.05$*. $p < 0.01$**. Unpaired t tests were used to assess for statistical significance.

4.3.3.4. Effect of p38 activation by MKK6 (Glu), on markers of mitochondrial fission and fusion.

mRNA expression of Fis1 increased following MKK6 (Glu) transfection (Figure 4.18. 2.5µg MKK6; Fis1 1.7±0.13 fold increase, $p = 0.02$). MKK6 (Glu) transfection significantly enhanced Mfn2 expression (Figure 4.18. 2.5µg MKK6; 3.9±0.24 fold increase, $p < 0.01$).

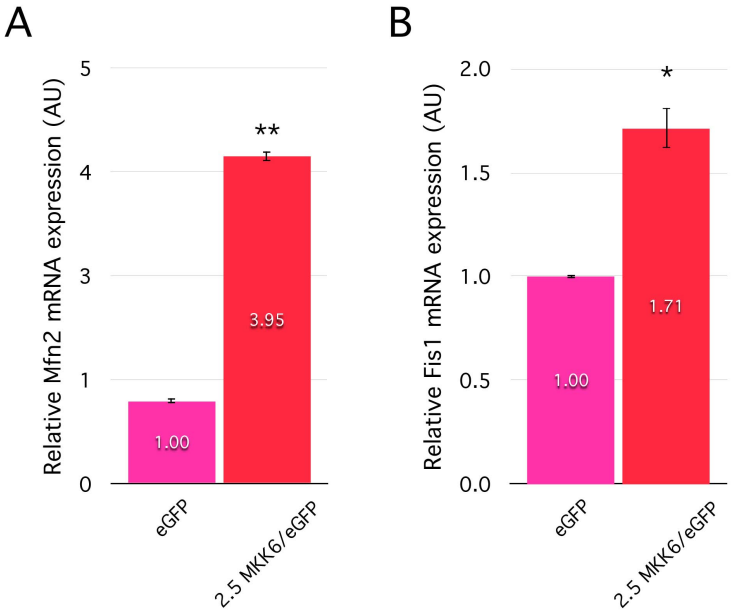

Figure 4.18.Transfection of MKK6 (Glu) into 3T3-L1 preadipocytes enhances mRNA expression of mitochondrial fusion (A) and fission (B) markers

MKK6 or MAP2K6 (mitogen-activated protein kinase kinase 6) is a member of the dual specificity protein kinase family, which functions as a mitogen-activated protein (MAP) kinase kinase. MKK6 phosphorylates and activates p38 MAP kinase and is an essential component of p38 MAP kinase mediated signal transduction pathway**.** Constitutive over-expression of MKK6 activates p38 kinase activity. 3T3-L1 preadipocytes were transiently transfected with 2µg MKK6 (Glu)/eGFP or pCDNA3.1 eGFP plasmid. The effect of genetic overexpression of MKK6, on markers of mitochondrial fission Fis1 and fusion Mfn2 were assessed by mRNA expression. 6 samples of MKK6 (Glu), 6 samples of eGFP (control plasmid) and 6 samples of untransfected controls (UT) were collected. AU denotes arbitrary units, as the data is expressed as relative Mfn2/Fis1 mRNA expression in eGFP control plasmids. Data are given as a mean ± S.E.M. Statistical significance was confirmed if $p < 0.05$*. $p < 0.01$**. Unpaired t tests were used to assess for statistical significance.

4.3.3.5. Effect of acute p38 inhibition on mitochondrial size and abundance.

The average size of mitochondria significantly reduced in p38 inhibited cells compared to DMSO control treated cells (Figure 4.18. SB203580 treated vs Ctrl; $38\mu m^2 \pm 7$ vs $76\mu m^2 \pm 23$, $p < 0.04$, n = 3 plates/average of 3 image fields per plate).

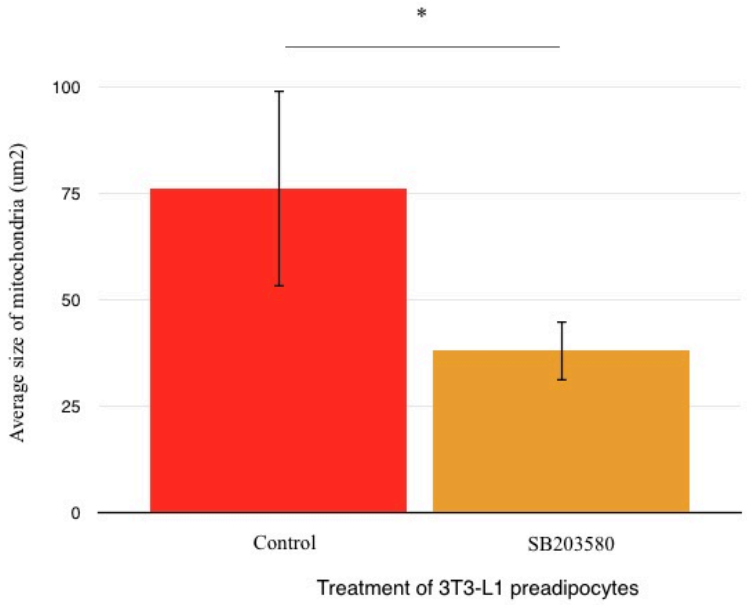

Figure 4.19. Effect of acute p38 inhibition on mitochondrial size and abundance. 3T3-L1 preadipocytes were treated with SB (10µM) or DMSO (control cells) for 20 minutes. The average size of mitochondria was assessed in fixed 3T3-L1 cells using the analyse particles macro to identify edges of mitochondria amongst MitoRed labelled mitochondria in a 2D confocal microscopy image. The data presented here, represent the average of 10 fields of view from 3 petri dishes. Data are given as a mean ± S.E.M. Statistical significance is indicated where unpaired t-test analyses value are $p < 0.05$*.

4.3.3.6. Effect of acute p38 inhibition on mitochondrial morphology.

The abundance of the 6 mitochondrial subtypes (small globule, large globule, straight tubule, twisted tubule, loops and branched tubules) were affected by p38 inhibition. In particular, analysis of the time-lapse live microscopy videos revealed a significant reduction in the abundance of small globules in p38 inhibited 3T3-L1 preadipocytes compared to DMSO control counterparts (Table 3. Small globules; average of 87% control time lapse images compared to 54% in SB203580 treated preadipocytes, $p < 0.05$). Whilst a marginal increase was noted in the straight tubule population after p38 inhibition, this relationship was non-significant (Table 3. Control; 7.3 vs 12 p38 inhibited, $p < 0.05$). The population of twisted tubules remained unchanged by p38 inhibition. Perhaps the most striking changes in mitochondrial morphology were the extensive enhancement of branched tubules (Table 3. branches tubules; control vs p38 inhibited, 4% vs 28%, $p < 0.05$) and the appearance of a loop population in p38 inhibited cells undetected within the control 3T3-L1 mitochondrial population (Table 3. SB203580 treated; Loops, 5% vs undetected in control cells). Considering these live confocal imaging data in the context of the model proposed for the generation of mitochondrial subtypes (Figure 4.6), control cells appear to be in a mitochondrial fission dominant phenotype whilst SB203580 cells were in a mitochondrial fusion dominant phenotype.

Treatment	Percentage of 3T3 preadipocytes with mitochondrial morphology (%)					
	Small globules	Swollen globules	Straight tubules	Twisted tubules	Loops	Branched tubules
Control-TL-1	84±1.3	-	9.5±1.4	1±0.3	-	5.5±1.3
Control-TL-2	85.2±1.7	-	9.3±1.2	0.6±0.3	-	4.8±0.8
Control-TL-4	89.2±3.3	-	5.8±1.5	0.3±0.3	-	4.8±2.2

Treatment	Percentage of 3T3 preadipocytes with mitochondrial morphology (%)					
	Small globules	Swollen globules	Straight tubules	Twisted tubules	Loops	Branched tubules
Ctrl-TL	91±1.7	-	5.9±1.1	0.3±0.2	-	2.5±0.6
SB5'-TL	42±6.2	-	14.3±3.1	1.5±0.9	3.4±2.2	37.4±5.7
SB20'-TL	65±6.5	-	9.8±3.3	1±1.2	1.6±3.8	18.6±6

Table 3. Effect of p38 inhibition on the composition of mitochondrial subtypes in 3T3-L1.

The percentages represent an average of 10 image fields per petri dish. The numbers in the treatment description correspond to the petri dish from which the data was generated. Details of the processes involved in generating the different mitochondrial subtypes are given in figure 4.1. TL denotes stills taken from time lapse from live confocal microscopy imaging of mitochondria.SB20' denotes treatment of 3T3-L1 for 20 minutes with SB203580. Statistical significance was confirmed if $p < 0.05$*. $p < 0.01$**. Unpaired t tests were used to assess for statistical significance.

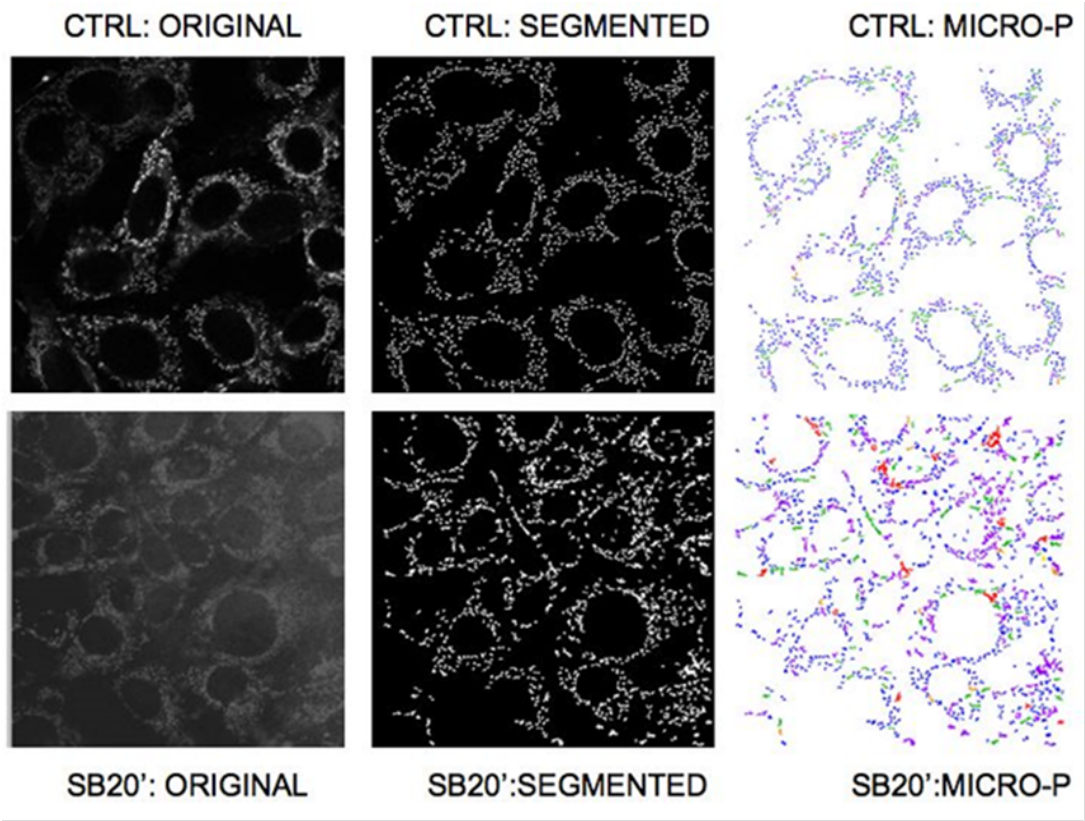

Figure 4.20. Effect of p38 inhibition on mitochondrial morphology subtypes. Automated analysis of changes in mitochondrial size and abundance using the analyse particles and micro-P macro in Matlab. Micro-P macro was kindly provided by J.Peng and colleagues for use in mitochondrial subtype anaylsis. 6 petri confocal glass bottomed dishes per condition (3 for live imaging) were cultured for imaging of control or 20 minutes SB203580 treated 3T3 preadipocytes. Both live and fixed cells were assessed. Fixed and live cells were considered separately for analysis. Values for mitochondrial size and abundance are representative of an average across 3 petri dishes ± S.D. The subtypes were colour coded as; blue: small globules, yellow: large/swollen globules, green: straight tubules, orange: twisted tubules, purple: twisted tubules and red: loops.

4.4. Discussion.

Recent data from studies conducted in skeletal muscle have demonstrated a link between obesity and mitochondrial dynamics (Huang, Eriksson et al. 1999, Kelley, He et al. 2002, Russell, Foletta et al. 2014). Whilst mitochondrial dynamics have been more extensively characterised in skeletal muscle, studies in adipose tissue are limited. In recent years, the central role of adipose tissue in controlling energy metabolism and the significant impact of balancing energy homeostasis (Rosen and Spiegelman 2006) on mitochondrial function has become better understood. Mitochondrial function is regulated through biogenesis and morphology. Regulation of mitochondrial morphology is orchestrated by mitochondrial dynamics (Okamoto and Shaw 2005, Huang, Galloway et al. 2011). A clear connection between mitochondrial dynamics and health is demonstrated by the observation that mammalian cells devoid of mitochondrial fusion display stunted growth rates and diminished respiratory capacity (Legros, Lombes et al. 2002, Huang, Galloway et al. 2011). Furthermore, chemical inhibitors of mitochondrial fission, Mdivi, an inhibitor of mitochondrial fission,has been shown to attenuate phosphorylation of p38 within the skeletal muscle of ob/ob mice (Jheng, Tsai et al. 2012). Together these observations provide preliminary evidence, to support further exploration of the potential role of p38 in regulating mitochondrial dynamics.

The results of the present study identified strongly suggest that p38 is involved in mitochondrial dynamics. A robust and well-defined model system, 3T3-L1, a murine preadipocyte cell line was used (Todaro and Green 1963) due to its well-characterised heterogeneous phenotype together with its flexibility to inhibit or activate differentation and assess its effect on metabolic function. Furthermore, the

breadth of previous studies involving investigation of adipocyte differentation and inhibitor studies allows for comparison, contrast and extension of our studies with those previously published. The mitogen activated protein kinase gene (MAPK), p38 has been implicated in the accumulation of triglyceride in differentiating adipocytes (Kita, Nishida et al. 2009) and is an essential gene required for adipogenesis (Engelman, Berg et al. 1999).

Gene expression analyses of p38 (Figure 4.7) and markers of mitochondrial dynamics (Fis1 and Mfn2, Figure 4.9) throughout 3T3-L1 differentiation were consistent with those previously reported (Ducluzeau, Priou et al. 2011). Phospho-p38 is known to rapidly decrease from its peak in the early stages of differentiation to barely detectable levels at the terminal stages of differentiation (Engelman, Lisanti et al. 1998). Moreover, analysis of mitochondrial dynamics gene expression was consistent with Ducluzeau et al who concluded that adipocyte differentiation corresponded with an increase in expression of Mfn2 and Fis1 genes. Markers of mitochondrial fusion, Mfn2 (Bach, Naon et al. 2005) and fission, Fis1 (James, Parone et al. 2003, Lee, Jeong et al. 2004, Stojanovski, Koutsopoulos et al. 2004) have been documented to assist mitochondrial remodelling during cellular differentiation (Kita, Nishida et al. 2009). Collectively, these observations provide evidence for a novel functional link between p38 and the coordination of mitochondrial dynamics. PPAR-γ, is highly expressed within adipose tissue (Medina-Gomez, Gray et al. 2007, Lodhi, Yin et al. 2012).Given its established role in adipocyte differentiation (Siersbaek, Nielsen et al. 2010), inhibition of p38, which prevents adipogenesis, would be predicted to correspond with a significant reduction of PPAR-γ mRNA expression . As expected, PPAR-γ expression was significantly lower in 3T3-L1 treated with SB203580

throughout differentiation (Figure 4.8). Thus, as a result of failure of 3T3-L1 to differentiate, lipid accumulation was significantly stunted and cells maintained a more fibroblastic phenotype (Faust, Schmitt et al. 2012).

SB203580, a p38α and β isoform inhibitor was assayed to assess the duration of p-p38 inhibition together with its cytotoxicity in 3T3-L1 preadipocytes (Badger, Bradbeer et al. 1996). p-p38 expression was significantly decreased in our 3T3-L1 preadipocytes, after incubating for 30 minutes to an hour with SB203580 (10μM, Figure 4.10). This was accompanied by no significant reduction in mitochondrial DNA content(Figure 4.11). However, markers of mitochondrial fission and fusion,Fis1 and Mfn2 respectively, decreased significantly in protein expression following this acute p38 inhibition (Figures 4.12 and 4.13). Given the inability of mitochondria to swiftly reverse mutations and DNA damage induced by chemical (e.g. drug compounds) or environmental factors (UV or stress induced damage), mitochondrial health is frequently challenged, and mitochondria are required to detect and remove damaged mitochondria (Mercer, Neph et al. 2011). Mitochondrial bioenergetics is instrumental in maintaining a mitochondrion's role as the energy provider for cells (Tseng, Cypess et al. 2010). In order to address whether mitochondrial bioenergetics was reduced following p38 inhibition, the spare respiratory capacities and coupling efficiencies of 3T3-L1 preadipocytes treated with or without SB203580 were compared. Considering the significant reduction in Fis1 expression in p38 inhibited 3T3-L1 preadipocytes, it would be anticipated that mitochondrial bioenergetics may be negatively affected. Respiration together with parallel measurements of membrane potential offers extensive quantitative data, functional perspectives and may identify the site of p38 action and downstream effects of mitochondrial dysfunction (Zhuang,

Demirs et al. 2000, Brand and Nicholls 2011). Spare respiratory capacity significantly decreased in a dose-dependent manner with SB203580 (Figure 4.15). In conjunction, 3T3-L1 preadipocytes treated with SB203580 at 10μM experienced a significant reduction in their mitochondrial coupling efficiency (Figure 4.15). Taken together, whilst no change in mitochondrial DNA content was observed, mitochondria were respiring closer to their maximum oxygen consumption rate. Consistent respiration close to the SRC of the mitochondria would generate additional mitochondrial stress and increase the likelihood of mitochondrial damage. One example of mitochondrial damage is oxidative stress, where greater levels of reactive oxygen species (ROS) are generated through formation of radical molecules (e.g. superoxide anion, single ion form of oxygen and is produced in the electron transport chain) above those which can be neutralised through anti-oxidants (e.g. superoxide dismutase, catalyse the breakdown of the superoxide anion into oxygen and hydrogen peroxide) (Lodo et al, 2010).

Finally, MKK6 overexpression vector (MKK6 (Glu) (Raingeaud, Whitmarsh et al. 1996, Enslen, Raingeaud et al. 1998, Remy, Risco et al. 2010)) was transfected into 3T3-L1 preadipocytes (Figure 4.16). Preadipocytes were selected, as the transfection efficiency is greater than that of differentiated adipocytes. This transfection study complemented the pharmacological inhibition of p38α and β by SB203580. MKK6, as a constitutive activator of p38, is sufficient to stimulate differentiation without the requirement for differentiating factors, insulin, dexamethasone and 1-methyl-3-(2-methylpropyl)-7H-purine-2,6-dione (IBMX) and has been confirmed by other researchers to enhance p38 activity. As a novel extension of this work, I characterised the effect of MKK6 on the expression of markers of mitochondrial dynamics. Mfn2

mRNA expression quadrupled in MKK6(Glu) transfected preadipocytes, whilst Fis1 expression doubled (Figure 4.17). Mitochondrial fusion has been shown to be critical in the control of the mitochondrial life cycle,as selective fusion is a pre-requisite for subsequent cycles of fission (Twig et al, 2008). As such the greater enhancement of markers of mitochondrial fusion may represent an additional quality control mechanism to prime the mitochondria that a larger population of mitochondria will be cycling through a cell and ensure that an enhancement in the expression of mitochondrial dynamics genes and metabolism does not occur at the expense of mitochondrial quality.Exactly how this is acheived is unclear at present, but cross-talk signalling between the nucleus and mitochondria may play a role.

Finally, the effect of p38 on mitochondrial morphology was assessed through live confocal microscopy of 3T3-L1 preadipocytes with and without p38 inhibition by SB203580. Following p38 inhibition, the average size of mitochondria significantly reduced compared to DMSO controls (Figure 4.18). Furthermore, the morphological subtypes were altered by p38 inhibition. 20 minutes of p38 inhibition was sufficient not only to lower the abundance of small globules but also to increase the number of straight tubules and generate previously unseen loops (Table 3). Based on the model proposed by Peng et al (Figure 4.6) the appearance of mitochondrial loops together with the reduction of small globules and increase in straight tubules may signify tha t p38 inhibition shifts the balance of mitochondrial dynamics towards a fusion dominant phenotype. A fusion dominant phenotype would like translate into a less metabolically active mitochondrial population, as over time mutations which occur naturally throughout the mitochondrial life cycle, would not be repaired as swiftly as those undergoing regular mitochondrial fission. As p38 inhibition was shown to reduce mito-

chondrial size, the snapshot images captured by time lapse confocal microscopy may represent a timepoint within mitochondrial dynamics, immediately prior to mitochondrial fission identified by the analyse particles ImageJ analysis.

In conclusion, our present findings strongly suggest that p38 regulates mitochondrial dynamics. Further studies involving assessment of the rate of mitochondrial dynamics and bioenergetics in MKK6 transfected 3T3-L1 and human preadipocyte models will be required to provide additional support to our work.

Chapter 5:

Selection and assessment of p38 α and β isoform selective inhibitors on mitochondrial bioenergetics.

5.1. Introduction.

5.1.1. MAPK family.

Mitogen activated protein kinases (MAPK) have been preserved throughout evolution. The abundance of these MAPKs from yeast to mammals reflects their significant role within cells. One of the best characterised of the 14 human MAPKs is p38 (Lee, Kumar et al. 2000, Cohen 2002, Metz, Johnson et al. 2011).

5.1.2 Role of p38 MAPK pathway.

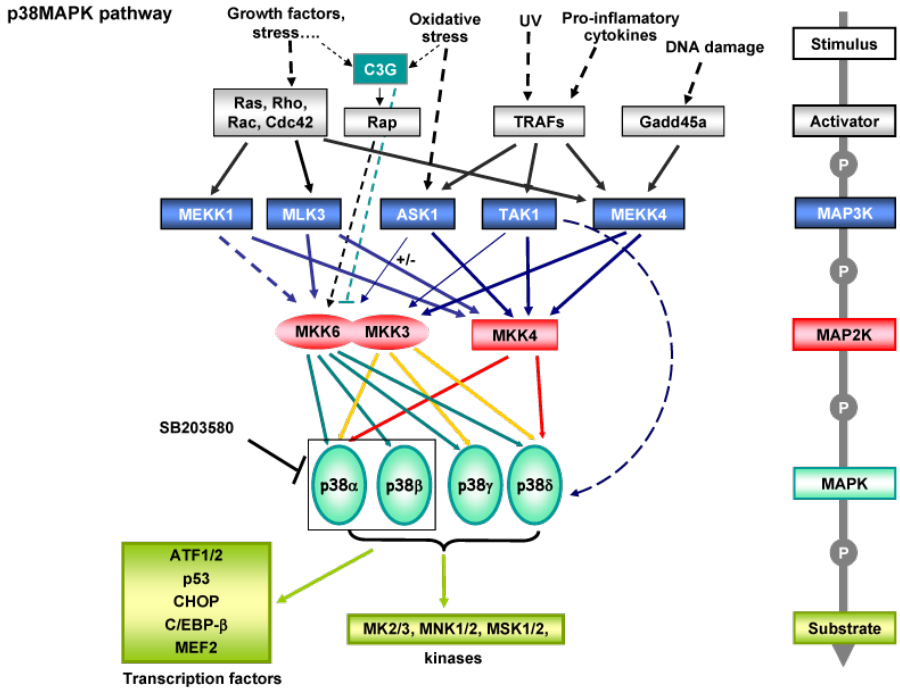

Figure 5.1. Roles of the p38 MAPK pathway.

A variety of stimuli, mainly stress stimuli, activate p38 MAPK through complex kinase cascades including a MAP3K that phosphorylates a MAP2K that, in turn, phosphorylates p38 MAPK. Cellular intermediates, like GTPases, receptor adapter proteins or cell cycle checkpoint proteins, among others, transmit the stimulus to the ki-

nase cascades. Once activated, the different p38 MAPK either phosphorylates cytoplasmic targets or translocate into the nucleus leading to the regulation of transcription factors involved in cellular responses. MKK6 is the major activator of all p38 MAPK isoforms, while MKK3 and MKK4 are more specific and can only activate some isoforms. Legend and figure originally created by Almudena Porras and Carmen Guerrero.http://atlasgeneticsoncology.org/Deep/MAPK14-p38ainCancerID20089.html.

5.1.3. p38 isoforms and abundance.

Four p38 isoforms have been identified within mammalian cells. The structural similarity and tissue specificity distinguish between these isoforms (Lee, Kumar et al. 2000). Whilst, α and β isoforms are ubiquitously expressed, δ and γ are selectively expressed in only a few tissue types (Risco and Cuenda 2012). p38γ is found mainly in skeletal muscle and δ predominates in testes, pancreas and small intestine (Cuadrado and Nebreda 2010). Furthermore, p38α and p38β, which share similar tissue localisation, are 75% homologous (Badrinarayan and Sastry 2011). In contrast, p38γ and p38δ are more restricted in their tissue localisations and share 57% and 63% homology to p38α (Enslen, Raingeaud et al. 1998, Enslen, Brancho et al. 2000).

```
Human p38α    ------------------------------------MSQERP-TFYRQELN-----KTIWEV
Mouse p38α    ------------------------------------MSQERP-TFYRQELN-----KTIWEV 2
Human p38β    ------------------------------------MSGPRA-GFYRQELN-----KTVWEV 20
Human p38δ    ------------------------------------MSLIRKKGFYKQDVN-----KTAWEL 21
Human MK2     MLSNSQGQSPPVPFPAPAPPPQPPTPALPHPPAQPPPPPPQQFPQFHVKSGLQIKKNAII 60
                                                   .       * : .::     *.   :
                                        ATP
Human p38α    PERYQNLSPVGSGAYGSVCAAFDTKTGLRVAVKKLSRPFQSIIHAKRTYRELRLLKHMKH 80
Mouse p38α    PERYQNLSPVGSGAYGSVCAAFDTKTGHRVAVKKLSRPFQSIIHAKRTYRELRLLKHMKH 80
Human p38β    PQRLQGLRPVGSGAYGSVCSAYDARLRQKVAVKKLSRPFQSLIHARRTYRELRLLKHLKH 80
Human p38δ    PKTYVSPTHVGSGAYGSVCSAIDKRSGEKVAIKKLSRPFQSEIFAKRAYRELLLLKHMQH 81
Human MK2     DDYKVTSQVLGLGINGKVLQIFNKRTQEKFALKMLQDCPKARREVELHWRAS------QC 114
                .       :* *  *.*    : :   :.*:* *.   ::   ..  :*        :

Human p38α
Mouse p38α    ENVIGLLDVFTPARSLEEFNDVYLVTHLMGADLNNIVKC--QKLTDDHVQFLIYQILRGL 138
Human p38β    ENVIGLLDVFTPARSLEEFNDVYLVTHLMGADLNNIVKC--QKLTDDHVQFLIYQILRGL 138
Human p38δ    ENVIGLLDVFTPATSIEDFSEVYLVTTLMGADLNNIVKC--QALSDEHVQFLVYQLLRGL 138
Human MK2     ENVIGLLDVFTPASSLRNFYDFYLVMPFMQTDLQKIMG---MEFSEEKIQYLVYQMLKGL 138
              PHIVRIVDVYENLYAGRKCLLIVMECLDGGELFSRIQDRGDQAFTEREASEIMKSIGEAI 174
               ::: ::**:    : ..   . :        :..*       ::: . . :: .: ..:
                                          DFG          TXY
Human p38α
Mouse p38α    KYIHSADIIHRDLKPSNLAVN---EDCELKILDFGLARHTD--DEMTGYVATRWYRAPEI 193
Human p38β    KYIHSADIIHRDLKPSNLAVN---EDCELKILDFGLARHTD--DEMTGYVATRWYRAPEI 193
Human p38δ    KYIHSAGIIHRDLKPSNVAVN---EDCELRILDFGLARQAD--EEMTGYVATRWYRAPEI 193
Human MK2     KYIHSAGVVHRDLKPGNLAVN---EDCELKILDFGLARHAD--AEMTGYVVTRWYRAPEV 193
              QYLHSINIAHRDVKPENLLYTSKRPNAILKLTDFGFAKETTSHNSLTTPCYTPYYVAPEV 234
              :*:** .: ***:** *:  .    :. *:: ***:*:.:    .  *   * :* ***:

Human p38α    MLNWMHYNQTVDIWSVGCIMAELLTGRTLFPGTDHIDQLKLILRLVGTPGAELLKKISSE 253
Mouse p38α    MLNWMHYNQTVDIWSVGCIMAELLTGRTLFPGTDHIDQLKLILRLVGTPGAELLKKISSE 253
Human p38β    MLNWMHYNQTVDIWSVGCIMAELLQGKALFPGSDYIDQLKRIMEVVGTPSPEVLAKISSE 253
Human p38δ    ILSWMHYNQTVDIWSVGCIMAEMLTGKTLFKGKDYLDQLTQILKVTGVPGTEFVQKLNDK 253
Human MK2     LG-PEKYDKSCDMWSLGVIMYILLCGYPPFYSNHGLAISPGMKTRIRMGQYEFPNPEWSE 293
              :    :*::: *:**:* **  :* * . * ... :     :          *.     .:

Human p38α    SARNYIQSLTQMPKMNFANVFIGANPLAVDLLEKMLVLDSDKRITAAQALAHAYFAQYHD 313
Mouse p38α    SARNYIQSLAQMPKMNFANVFIGANPLAVDLLEKMLVLDSDKRITAAQALAHAYFAQYHD 313
Human p38β    HARTYIQSLPPMPQKDLSSIFRGANPLAIDLLGRMLVLDSDQRVSAAEALAHAYFSQYHD 313
Human p38δ    AAKSYIQSLPQTPRKDFTQLFPRASPQAADLLEKMLELDVDKRLTAAQALTHPFFEPFRD 313
Human MK2     VSEEVKMLIRNLLKTEPTQRMT-----ITEFMNHPWIMQSTKVPQTPLHTSRVLKEDKER 348
                :.     :    : : :. :         ::: :   ::  :   :.   ::      .

Human p38α
Mouse p38α    PDDEPVAD-PYDQSFESRDLLIDEWKSLTYDEVISFVPP----PLDQEEMES 360
Human p38β    PDDEPVAD-PYDQSFESRDLLIDEWKSLTYDEVISFVPP----PLDQEEMES 360
Human p38δ    PEDEPEAE-PYDESVEAKERTLEEWKELTYQEVLSFKPPEPPKPPGSLEIEQ 364
Human MK2     PEEETEAQQPFDDSLEHEKLTVDEWKQHIYKEIVNFSPIARKDSRRRSGMKL 365
```

Domain: Kinase, ATP, DFG, TXY, Mutations;

Symbols: "*" identical; "." semi-conserved; ":" conserved substitutions;

Amino acids: Small (small+ hydrophobic (aromatic -Y): AVFPMILW; Acidic: DE; Basic – H: RK; Hydroxyl + sulfhydryl + amine + G: STYHCNGQ

Figure 5.2. Sequence homology of p38 isoforms.

Multiple sequence alignment of amino acid sequence of p38 isoforms. Abbreviations of amino acids are as follows: A: alanine, D: aspartic acid, E: glutamic acid, F: phenylalanine, G: glycine, H: histidine, I: isoleucine, K: lysine, L: leucine, M: methionine, N: asparagine, P: proline, Q: glutamine, R: arginine, S: serine, T: threonine, V: valine, W: tryptophan, Y: tyrosine. DFG motif are the key amino acid residues contained with the p38 activation loop. ATP is the location of the ATP binding pocket. TXY are the conserved threonine and tyrosine kinase residues responsible for the activity of the MAPK. Uniprot preference numbers: human p38α (Q16539), mouse p38α (P47811), human p38β (Q15759), human p38δ (O15264) and human MK2 (P49137).

5.1.4 Structural features and activation of MAPK's.

p38 has two domains, ATP binding site (catalytic site) and a docking domain. p38 kinase activation occurs at the C-terminal activation loop (Wang, Canagarajah et al. 1998). Located within this activation loop are two phosphorylation sites, Tyr^{182} and Thr^{180} (Lee, Kumar et al. 2000). Following activation of p38 the docking motif coordinates interaction with substrates of p38. Occurring outside the p38 ATP active site, this motif is most commonly referred to as DEJL or "D motifs" (Akella, Min et al. 2010). The p38α substrate MK2, and phosphatases have been shown to interact with DEJL motifs (Akella, Min et al. 2010).

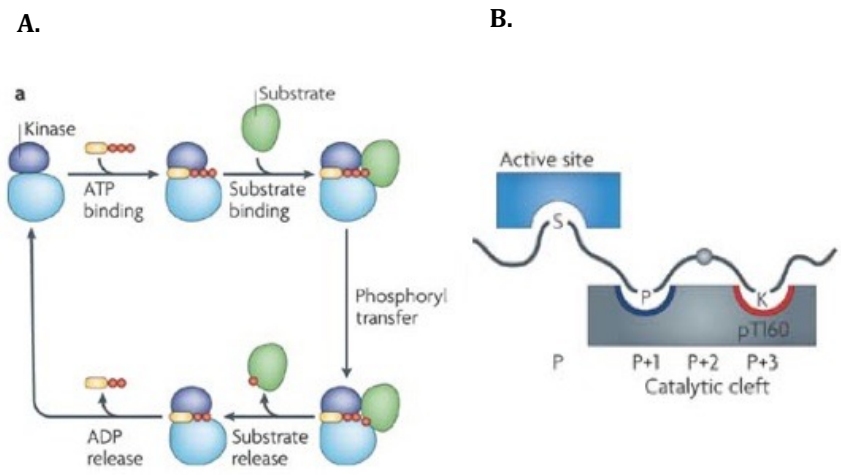

Figure 5.3. Structural specificity, substrates and mechanism of action of p38 receptor isoforms. A) The basic catalytic cycle for substrate phosphorylation by a kinase. Starting top left, ATP binds to the active site of the kinase. This is followed by binding of the substrate to the active site. Once bound, the γ-phosphate of ATP (red) is transferred to a Ser, Thr or Tyr residue of the substrate. After phosphorylation, the substrate is released from the kinase. The last step shown is the release of ADP from the active site. B) p38 consists of a catalytic cleft and an active site, which binds ATP. p38 activity requires dual phosphorylation at the threonine residue 180 (pT180, not T160 which is a typo in figure) and tyrosine 182 residue. Figure and legend taken from (Ubersax and Ferrell 2007).

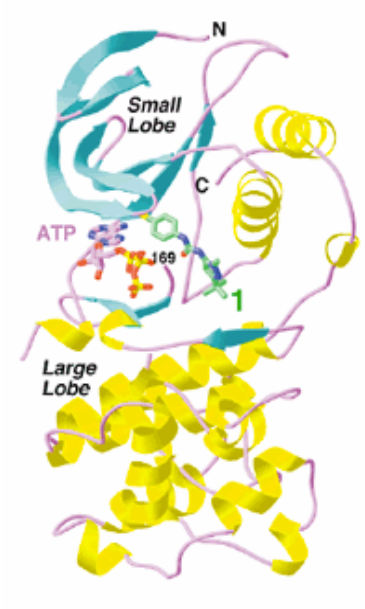

Figure 5.4. Crystal structure of the human p38α MAPK.

Crystal structure of p38α MAPK presented at 2.5 Å resolution. The ATP molecule in its binding site is depicted in purple. The green molecule (1) is an ATP competitive p38 inhibitor. Beta strands are shown in blue, α-helices in yellow and the connecting loops in purple. The small lobe . Figure taken from (Pargellis, Tong et al. 2002).

5.1.5. Regulation of p38 activation.

Through site directed mutagenesis studies of human p38α, Thr^{180} was found to be necessary for catalysis whilst Tyr^{182} may be required for substrate recognition (Lisnock, Tebben et al. 1998). Furthermore, human p38 kinase activity was 10-20 fold higher in dual phosphorylated p38α compared to singly phosphorylated p38 at Thr^{180} alone (Whitmarsh and Davis 1999, Weston, Lambright et al. 2002). In addition to the phosphorylation status of p38, the nature of activation signal also influences the duration of activation (Mansour, Resing et al. 1994). Under normal homeostatic condi-

tions, p38 MAPK activation levels are low (Brancho, Tanaka et al. 2003). In response to changes in the extracellular environment, e.g. LPS stimulation, p38 MAPK pathway is transiently activated (Han, Lee et al. 1994). Given the role of p38 MAPK activity, in cell proliferation, it is vital that p38 is only activated where necessary (Sharma, He et al. 2003, Faust, Schmitt et al. 2012). The level of p38 activation is tightly and finely controlled by a series of negative feedback mechanisms and serine and threonine phosphatases (Dickinson and Keyse 2006). Multiple phosphatases are capable of acting on a single kinase (Saxena and Mustelin 2000, Risco and Cuenda 2012).

5.1.5.1. Dissecting the role of key amino acids in p38 catalytic activity and substrate binding.

Crystal structures between p38α and its substrates have shown that they interact primarily within the hydrophobic docking groove (Jiang, Li et al. 1997, Kumar, McDonnell et al. 1997, Cohen and Knebel 2006). This observation has been complemented by crystallographic determination of p38 and a p38 α/β inhibitor SB203580 (Eyers, Craxton et al. 1998, Davies, Reddy et al. 2000).

*5.1.5.2 SB203580: Binding mode within p38*α **MAPK**

SB203580 has a central imidazole core connected to three rings (Wang, Canagarajah et al. 1998) forming a shape similar to a propeller. The pyridine ring of SB203580, overlaps part of the ATP binding within p38α (Tong, Pav et al. 1997). Both the adenine ring of ATP and the pyridine ring of SB203580 occupy the same site within the ATP binding pocket. SB203580 elicits its ATP competitive action by steric hindrance

by preventing the adenine ring of ATP from accessing the ATP binding site (Gum, McLaughlin et al. 1998). Through this conformation, a hydrogen bond is created between the amide of Met^{109} in p38α and the nitrogen of pyridine ring of SB203580 (Tong, Pav et al. 1997).This interaction is analogous to the hydrogen bond between adenine of ATP and amide of Met^{109} in p38α.

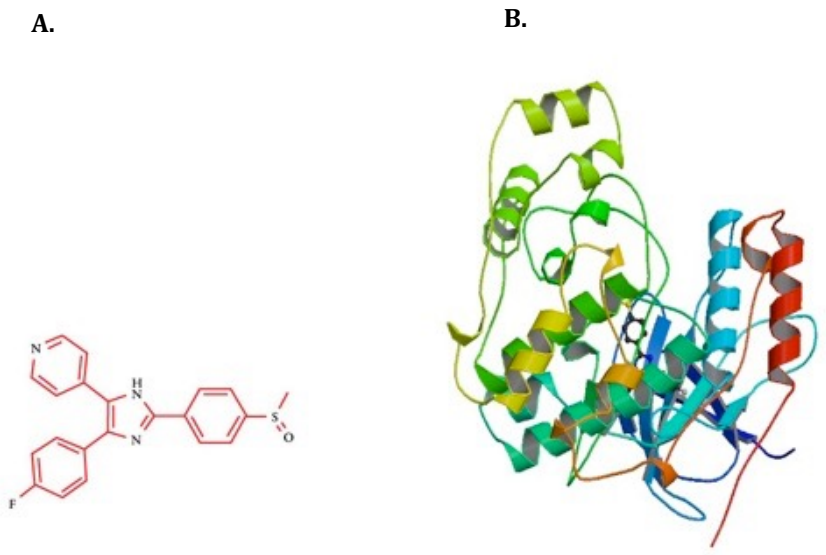

Figure 5.5. p38α inhibitor, SB203580 molecule alone (A) and complexed within the p38α crystal structure (B). SB203580 is a p38α and β inhibitor shown here in 2D (A) and as a ribbon representation, in complex with the human p38α (B) (PDB: 1a9u). 2D structure depicted was taken from cell signalling technology website (URL; http://www.cellsignal.com/product/productDetail.jsp?productId=5633)

Only a small portion of SB203580 interacts directly with amino acids present in the ATP binding site (Wilson, McCaffrey et al. 1997). Adjacent to the ATP binding site, a small hydrophobic groove is created by the presence of Thr^{106} residue on a small side

chain. The 4-fluorophenyl ring of SB binds within this groove (Tong, Pav et al. 1997). In spite of, SB203580′s ATP competitive inhibitor activity, the most significant interaction of this compound occurs between this Thr^{106} of p38α and SB (Wilson, McCaffrey et al. 1997). Site directed mutagenesis to a more hydrophobic and bulkier amino acid side chain at position 106, created a p38α MAPK insensitive to SB203580 (Eyers, Craxton et al. 1998).

5.1.6 DFG in vs. out inhibitors.

5.1.6.1 Design of p38 inhibitors: DFG-in versus DFG-out inhibitors.

The key structural differences between p38 isoforms exist at the ATP binding pocket. In p38α and β,these isoforms share the same three residues (Thr106, His107, Leu108). In the more distant homologs p38δ or γ however, these amino acids are different (Met106, Pro107 and Phe108). Site directed mutagenesis studies in yeast and bacteria, have shown that a single change from Met^{106} to Thr^{106} in isoforms p38δ or γ is sufficient to confer sensitivity to SB203580 (Eyers, Craxton et al. 1998, Gum, McLaughlin et al. 1998). Another key structural difference between the more closely related p38α and β is located within the hydrophobic binding pocket (Cohen 2002). The relative orientation of the N- and C- terminals in p38β results in a smaller hydrophobic binding pocket for substrates. The effect of mutating residue 106 in wild type p38α was assessed by enzyme based kinase assays (Davies, Reddy et al. 2000). Substitution of Thr for Glutamine (Gln) increased the Km for ATP by 17 fold relative to the wild type enzyme (Kumar, Jiang et al. 1999, Lee, Kumar et al. 2000). Glutamine is a more hydrophilic and larger amino acid than Threonine. Furthermore, the small

size and hydrophobic nature of the native pocket, would have been expected to reduce the ATP binding affinity in the resulting p38α mutant (Ross, Armstrong et al. 2002).

The first generation of p38 inhibitors were optimised as competitive ATP inhibitors. As many kinases have an ATP binding site, undesirable off target/non-selective effects against other kinases can result from ATP competitive inhibitors. In an attempt to overcome this issue, three key residues located in the activation loop of p38α (D, Aspartic acid, F, Phenylalanine and G, Glycine) became the target motif for a new class of p38 inhibitors e.g BIRB-796 (Pargellis, Tong et al. 2002). In an unbound state, the DFG motif assumes a 'DFG-in' conformation.

5.1.6.2. Solution state NMR spectroscopy

Magnetic properties of spin exist in the isotopes (1H and 13C) due to additional neutrons compared to protons, which are balanced in the cases of 2H and 12C (classified in the periodic table). The principle of NMR, is that in the presence of a magentic field, isotopes with additional neutrons (1H and 13C) absorb electromagnetic radiation at a defined frequency for that isotope (Slichter,C.P. 1990). Furthermore, the strength of the magnetic field can alter the intensity of the signal at this frequency. Those nuclei which orientate in the opposing direction to the applied magnetic field are of a higher energy state than those which align with the magnetic field (Grant,D.M and Harris,R.K. 1996).

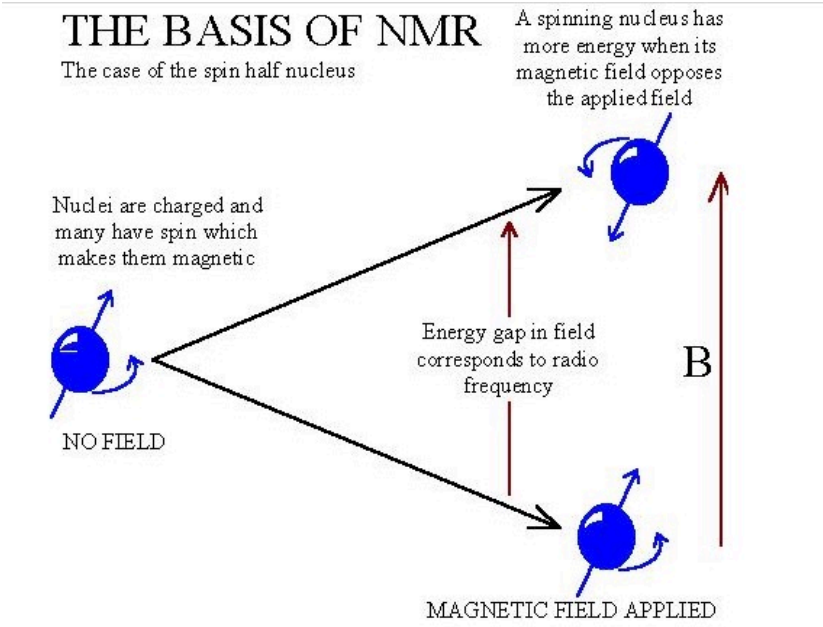

Figure 5.6. Principles of Nuclear Magnetic Resonance.

Figure taken from http://chem.ch.huji.ac.il/nmr/whatisnmr/whatisnmr.html. Upon absorption of the electromagnetic radiation, the sample is excited using a radio frequency pulse. Electrons within each nuclei, create a local magnetic field to shield the protons from the externally applied magnetic field. The shielding effects due to the movement of protons has been extensively characterised and are used to provide structural information about a compound. Once the magnetic field is removed, the absorbed electromagnetic radiation (resonance) is released (http://www2.chemistry.msu.edu/faculty/reusch/VirtTxtJml/Spectrpy/nmr/nmr1.htm). The degradation of this absorbed electromagnetic radiation corresponds to a return in the energetic status of the nuclei to ground state and the spin state of the individual nuclei are balanced and neutral. The interconnection of atomic nuclei and application of a magnetic field allows a distinctive spectra similiar to a 'molecular fingerprint' to be

generated. Therefore, this spectra enables the identity of chemical substances to be confirmed. In the case of ligand binding to p38α, solution state NMR revealed that the DFG motif shifts to a 'DFG-out' conformation (Vogtherr, Saxena et al. 2006).

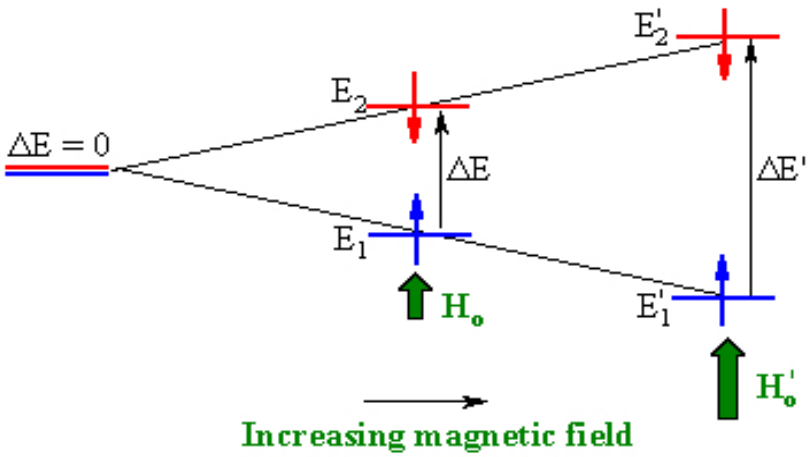

Figure 5.7. Energy profile of nuclei in NMR.

H in green indicates the direction of the externally applied magnetic field. E indicates the energy status of each atomic nuclei spin state. In the ground state,, shown on the left, with no magnetic field applied, the difference in energy is zero. Upon application of an magnetic field, those atomic nuclei in red, are orientated in the opposing direction to the applied magnetic field. Therefore these excited nuclei have a higher energetic profile than the ground state. Conversely, those nuclei whose spin is orientated in the same direction as the applied field, have a lower energy profile in their excited state. The greater the strength of the magnetic field applied, the greater the energy difference between the aligned and non aligned spins of the nuclei (http://www2.chemistry.msu.edu/faculty/reusch/VirtTxtJml/Spectrpy/nmr/nmr1.htm).

Solution state NMR revealed that following ligand binding to p38α, the DFG motif shifts to a 'DFG-out' conformation (Vogtherr, Saxena et al. 2006).

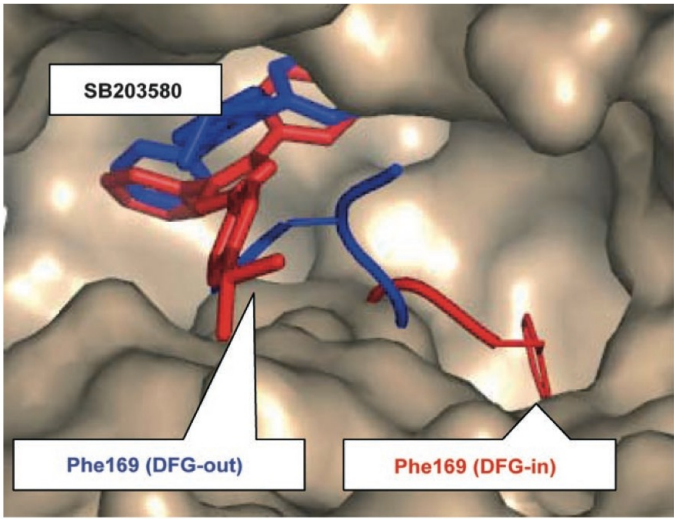

Figure 5.8. Conformational difference in binding mode between DFG-in vs DFG-out inhibitors.

Crystal structure of p38 complexed with BIRB-796 (2.1 Å resolution; R_{factor}= 0.241; R_{free}=0.279, DFG-out inhibitor). DFG (is an abbreviation denoting the amino acids, asparatic acid (D), phenylalanine (F) and glycine (G)). SB203580, a DFG-in inhibitor, is presented within the binding pocket as a reference. Shown is a molecular-surface representation of p38 with the main chain of the DFG motif highlighted in red (DFG-in conformation) and blue (DFG-out conformation). Phe 169 and BIRB-796 are shown as stick representations and are color coded in red (DFG-in) and blue (DFG-out). In the DFG-in form, the side chain of Phe 169 resides in a hydrophobic pocket, whereas it points outwards in the DFG-out form. They observed approximate occupancies of 50 % for the DFG-in and DFG-out conformations in the ensemble average of the crystal. Figure and legend taken from (Vogtherr, Saxena et al. 2006).

5.1.6.3. Substrate binding to p38α

p38 substrate binding occurs at the DFG motif within the activation loop of p38α. Three conformational modes of p38α exist: inactive unbound to ATP (ligand), phosphorylated (Tyr[182] and Thr[180]) but not activated and fully activated p38α-ATP-MK2 (White, Pargellis et al. 2007). Structural differences at the activation loop accompany the distinct DFG modes between unbound-p38 and AMP-PNP-p38α kinase (non hydrolysable ATP analogue). Ligand binding was shown to correspond to the conversion of the activation loop from DFG-in to DFG-out conformation.

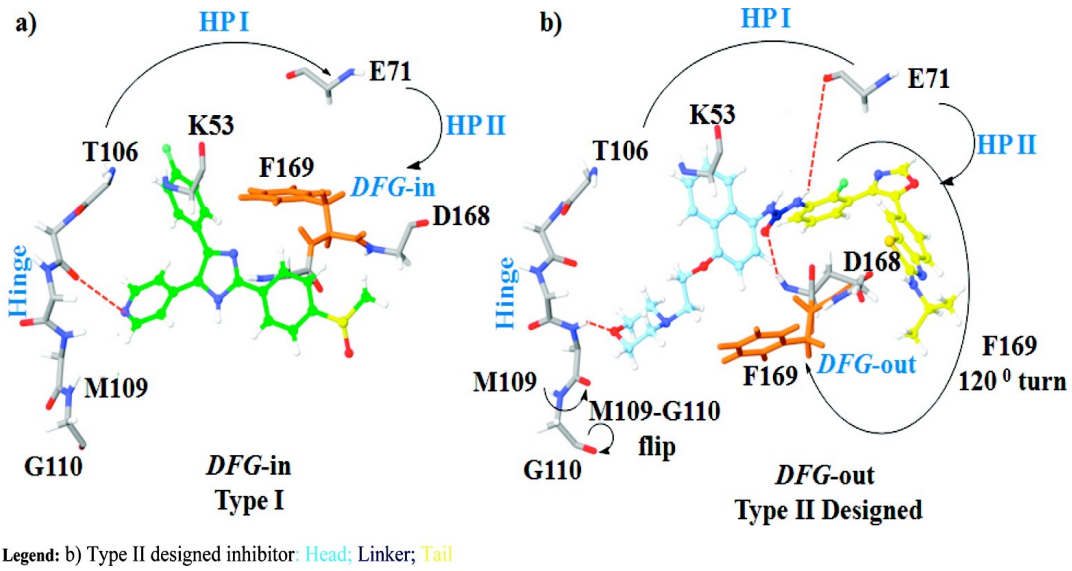

Figure 5.10. Binding modes of two different types of p38 MAPK inhibitors,

Type I, ATP site binders (a) and (b) Type II, DFG-out inhibitors. Compounds which belong to group (a) involve activation of the ATP site inhibitor with the hinge region; the F169 in the DFG-in conformation blocks the hydrophobic pockets (termed HPI and HPII in the figure above). In contrast (b) the designed type II inhibitor comfortably occupies the larger area of the active site created by the 120^0 turn of F169 leading to the transition into a DFG-out conformation and opening of the hydrophobic back pockets, HPI and II. A small M109-G110 flip is also observed. The designed type II p38 MAP kinase inhibitor interacts with the hinge region (head), DFG-loop (linker), and hydrophobic pocket (tail). Green compound is SB203580 . Figure and legend taken from (Badrinarayan and Sastry 2011).

5.1.6.4. BIRB-796: DFG-out p38 inhibitor.

Due to the action of BIRB-796, interconversion of DFG-out back to DFG-in is prevented (Moffett, Konteatis et al. 2011). Solution NMR analysis of BIRB-796 action on p38α revealed the presence of an NMR signal corresponding to Phe^{169} (Vogtherr, Saxena et al. 2006). This Phe^{169} residue is usually located within a hydrophobic pocket, in a site proximal to the ATP binding site (Vogtherr, Saxena et al. 2006). Furthermore, this residue only becomes accessible when the activation loop is in DFG-out conformation (Badrinarayan and Sastry 2011). BIRB-796, can block both p38 activity and activation. DFG-in binders such as SB203580 do not interfere with p38 activation and formation of DFG loop does not affect their binding (Kumar, Jiang et al. 1999).

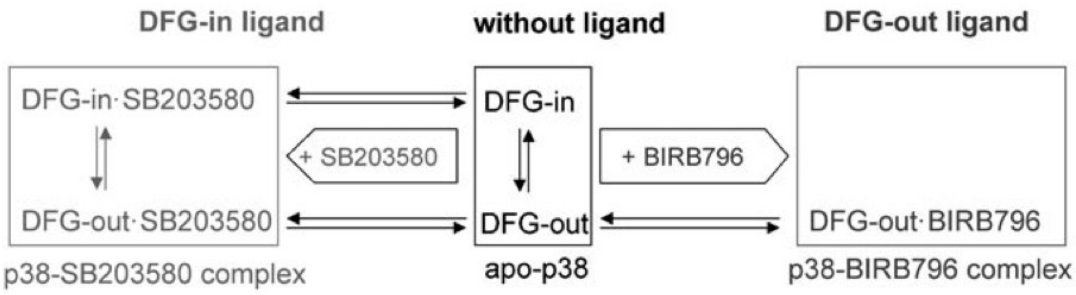

Figure 5.11. Kinetic scheme for the conformational exchange of the DFG motif.

In the apo protein (unbound ligand state), the DFG-in and DFG-out forms are in slow (kHz) conformational exchange. Ligand BIRB-796 binds to the DFG-out conformation and freezes the conformational equilibrium in a defined state. Ligands such as SB203580 leave the DFG equilibrium unaffected. Figure and legend taken from (Vogtherr, Saxena et al. 2006).

Solution state NMR enabled determination of the equilibrium constants for DFG interconversion (Vogtherr, Saxena et al. 2006).Investigation of the rates of DFG-in and DFG-out binding kinetics revealed that DFG-in inhibitors e.g SB203580 were mainly a diffusion controlled (Vogtherr, Saxena et al. 2006). The 2-fold lower magnitude observed for DFG-out inhibitors of similar molecular size, suggested an alternative mechanism of action (Vogtherr, Saxena et al. 2006). Kinetic analysis of BIRB-796 revealed a half-life of dissociation for p38 MAPK of 23 hours. The molecular basis for the enhanced affinity and association of BIRB-796 with p38 kinase resides in its morpholino substituent. Structural analysis of hydrogen bonding interactions between this BIRB-796 and an amide at position 109 of MAPK's main chain has been proposed to stabilise this interaction (Vogtherr, Saxena et al. 2006).

5.2 Drug design.

Drug design is concerned with the development of orally active, efficacious, bioavailable, safe and compounds which can be easily formulated into a drug. Bioavailability, safety (non-toxic) and formulation ease are together what we might call 'drug-like properties'. The challenge of drug design is to find molecules that bind to and affect the target protein while maintaining good drug-like properties. At the early stages of drug design, screening large compound libraries for drugability is prohibitively expensive and time consuming. Therefore, Lipinski's rules are one of the simple means of assessing the physical properties of compounds.

5.2.1. Lipinski's rule of 5 (Lipinski 1997):

Compounds fulfilling the rule-of-5 criteria have a greater chance of being an orally bioavailable drug. Details of the rule of five criteria are given below:

- A compound's molecular weight is less than 500 g/mol.
- The compound's lipophilicity, expressed as a quantity known as log*P* (the logarithm of the partition coefficient between water and 1-octanol), is less than 5.
- The number of groups in the molecule that can donate hydrogen atoms to hydrogen bonds (usually the sum of hydroxyl and amine groups in a drug molecule) is less than 5.
- The number of groups that can accept hydrogen atoms to form hydrogen bonds (estimated by the sum of oxygen and nitrogen atoms) is less than 10.

Identifying new compounds or 'hits' requires numerous drug design methodologies. Effective application of quantitative structure activity relationship (QSAR) requires a continuous and smooth functional relationship to exist between numerical descriptors and a property e.g. inhibitory activity against p38 (Walker, Jaworska et al. 2003, Fliri, Loging et al. 2009). Within large datasets, these requirements may not be upheld. In order to circumvent situations where a smooth functional relationship may not exist between numerical descriptors and a desired chemical property e.g. kinase inhibitory activity, compounds may be subdivided either by clustering by chemical structure or creation of a smaller dataset of compounds with a common and similar mechanism of activity (Gillet, Willett et al. 2003). Therefore, through the introduction of multiple smaller datasets from a single larger dataset, may allow

outliers, that were non-homogeneous with the rest of the larger dataset to be usefully incorporated and included as part of the overall QSAR analysis. In the context of p38 kinase inhibitors, the advantages and the limitations of each approach will be discussed.

5.2.2. Toxicology and bioavailability considerations in drug design.

Compounds identified through modelling should be evaluated for their proposed toxicology and drugability. Toxicology can be estimated based on the functional groups contained within compounds and previous drug design projects (Metz, Johnson et al. 2011). These can predict the potential route of ADME (Absorption, Distribution, Metabolism and Excretion) (Butina, Segall et al. 2002).

In order to improve the drugability of the compounds, chemical subgroups with a lower hydrophobic character were substituted in place of the napthyl and tolyl rings previously included within the drug-like compound (Moffett, Konteatis et al. 2011). Evaluation of previously published inhibitors, SB203580 and BIRB-796 was initially undertaken using fragment based drug design (Jiang, Li et al. 1997, Moffett, Konteatis et al. 2011). This involved selecting either thiophene urea and pyrazole urea as the core chemical scaffolds. The side chains are constructed around the central core producing a novel putative p38 inhibitor. Newly created putative p38 inhibitors are computationally assessed for their binding affinity to its drug target, the p38α. Throughout this process, the abundance and strength of the molecular docking interactions are considered between the substrate and the new drug candidate.

A number of key principles underlie drug design and assessment of their potential drug like activity.

5.2.3. Selection of compounds with putative inhibitory activity against p38.

5.2.3.1. Descriptor selection.

Descriptors were selected to enable a large database of compounds to be evaluated and identify compounds with drug-like activity. When presented with this scenario, descriptors offer the capability to cluster compounds according, for example, by their two-dimensional (2D) or three dimensional (3D) features (Bissantz, Kuhn et al. 2010). Careful selection of descriptors is essential for accurate and meaningful analysis of large datasets. Principle component analysis is used to capture those descriptors exhibiting the greatest variance within the dataset (Cohen 2002). However, most variation across the dataset does not always imply the most important descriptors (Macias, Mia et al. 2005, Gong, Cai et al. 2013, Li and Colosi 2013). Selection of the most appropriate descriptor is one that can distinguish between compounds that mimic or oppose vital biological and chemical interactions within ATP-p38 kinase interaction.

Two key challenges to successful inhibitor design are those of specificity and affinity for their target kinase. High sequence homology between the estimated 500 human kinases, commonly results in undesirable off target effects (Fabian, Biggs et al. 2005). In an attempt to address this, screening for a compound's kinase activity against representatives of the different kinase subfamilies is vital (Enslen, Brancho et al. 2000,

Gill, Frederickson et al. 2005). Screening an entire commercial database of up to a million compounds is impractical. Compound clustering and selection of those with proposed inhibitory activity against p38 creates a more manageable panel of potential inhibitors to screen via *in vitro* kinase assays. Compounds can be clustered based on structural or chemical similarity (Sheridan and Kearsley 2002, Raghavendra and Maggiora 2007, Sheridan 2007, Gong, Cai et al. 2013). The outcome of cluster analysis is influenced by information content and user defined parameters e.g. descriptor selection (Macias, Mia et al. 2005, Li and Colosi 2013).

5.2.3.2. Structural similarity.

Structural similarity of compounds can be clustered based on their 2D or 3D characteristics. A major drawback of cluster analyses based on a 3D structural similarity, are the level of complexity that must be encapsulated by descriptors (Liu, Chen et al. 2010). This includes, not only those feature descriptors required to define the 2D structure (the presence or absence of chemical groups) but also, the relative arrangement of these structural groups with respect to each other and the environment in which they reside (Fliri, Loging et al. 2009). In addition, within 3D, compounds exhibit spatial flexibility (Gong, Cai et al. 2013). Therefore, in order to provide a suitable evaluation of a compound, multiple conformations of a single compound should be included into the dataset prior to this drug's subsequent evaluation by structural clustering. As such, the orders of magnitude of feature descriptors required above that of 2D structural definition generate a larger number of clusters each containing fewer compounds compared to 2D analysis (Bissantz, Kuhn et al. 2010). In essence, the computational expense and time required to produce and subsequently evaluate these

compounds during the virtual screening of compounds with its target receptor does not necessarily translate into a greater selection of 'hits' to compensate for the additional information provided by the 3D over the 2D structure. On balance, 2D offers a simple but effective method to define the structural information of individual compounds within a large drug database. Three key elements that define a structure at a molecular level are configuration, conformation and constitution (Nikolova and Jaworska, 2003). In 2D analysis, all chemical groups present in compounds can be incorporated within a molecular fingerprint. A molecular fingerprint consists of a binary sequence of 1's and 0's indicating the presence or absence of different chemical substructures. Typically these molecular fingerprints are over a 1000 digits in length (Swamidass and Baldi 2007). This molecular fingerprint represents the constitutional assignment of a molecule's structure (Swamidass and Baldi 2007). Despite its obvious simplicity, defining a compound by the absence or presence of molecular substructures is computationally inexpensive. Therefore, it is an attractive initial approach for assessing a compound collections' diversity. The topological descriptors that define a molecules' constitution include, degree of connectivity of an individual atom to others within the molecule, pharmacophore points, number of individual atoms, bonds or rings (Lisnock, Tebben et al. 1998, Bissantz, Kuhn et al. 2010). The structural key generated for each molecule can be clustered by various methods including Ward's, Jarvis-Patrick, K-means, sphere exclusion or scaffold directed clustering.

5.3. Compound clustering.

5.3.1. Scaffold directed clustering.

The nature of the bond and atom linkage between the different substructures within a molecule is lost following fingerprint generation (Chuaqui, Deng et al. 2005). Due to the use of a single descriptor to capture the 2D features of a compound, it is not possible to reform the structure from a fingerprint (Xue, Godden et al. 2000). The topological descriptor value may not be unique between molecules (Xue, Godden et al. 2000). Despite the different nature of two compounds it may help to identify key functional groups required for p38 kinase inhibitor-p38 kinase interaction.

In 3D, the features of a molecule's structure can be defined by configuration and conformation (Nikolova and Jaworska, 2003). Configuration describes how atoms are linked to one another and the bond angles resulting from their arrangement (Nikolova and Jaworska, 2003). Finally, conformation is the spatial arrangement in 3D, of atoms from a molecule,which is most thermodynamically favourable i.e. lowest energy state (Nikolova and Jaworska, 2003).

5.3.2 Sphere exclusion clustering.

Often within drug discovery, the ability to rapidly organise compounds into sets of clusters containing similar compounds is extremely useful when working with large datasets. One method by which this can be achieved is sphere exclusion clustering. This method enables broad sampling. Initially, a single compound is selected as the 'seed' compound for a cluster (Bacha et al, 2007, Daylight Fingerprint Chemical Information systems). The remaining compounds within the compound library which

display chemical similarity are incorporated into this cluster. Any 'hermit', whose chemical identity differs from the rest of the dataset, remains separate from the generated cluster. Once all those compounds which match the chemical similarity of the initial cluster have been included within this cluster, a new initial 'cluster centre' compound is selected. With the exception of the compounds clustered in this first cluster, all remaining compounds are included and the process is repeated. This continues iteratively until all compounds have either been clustered or are termed 'hermits' i.e they do not successfully cluster with any of the generated cluster groups.

5.3.3. Compound library design.

An application of structure based drug design is the creation of a compound collection library. All compounds share a common scaffold core. A compound's activity against a target kinase is assumed to derive from the nature of the functional groups surrounding its scaffold core (Friesner, Banks et al. 2004, Badrinarayan and Sastry 2011). The hallmarks of molecular fingerprinting are encompassed in their ability to define the structural similarity between pharmacophore groups (Swamidass and Baldi 2007). Defined as the neighbourhood principle, it assumes that those compounds with similar structural characteristics defined by their descriptors will exhibit similarity in their activity (Nikolova and Jaworska, 2003). Furthermore, data assumption distributions underpin the use of structural features classification and measures of relative similarity between structures. The limitations, errors and potential bias introduced by these data assumptions should be considered carefully for their impact of compounds resulting descriptor based similarity analysis.

5.3.4. Molecular docking of drug-like compounds into target receptor.

Co-crystallisation of compound and kinase are required to confirm the binding mode (Badger, Bradbeer et al. 1996, Gum, McLaughlin et al. 1998, Pargellis, Tong et al. 2002). Furthermore, key amino acid interactions made between compound and kinase responsible for eliciting its function can be visualised. If the key residues within the kinase have already been characterised e.g. p38 kinase, Thr106 and Met109 in p38α kinase, co-crystallisation of a new compound confirms if this binding mode is maintained (Bellon, Fitzgibbon et al. 1999, Walker, Jaworska et al. 2003).

5.3.5. Assessing drug-like compounds in the context of p38.

SB203580 was utilised throughout the course of this thesis to assess the effects of p38 mediated regulation of mitochondrial dynamics. The model system for investigation of p38 regulation was the cell line 3T3L-1 adipocytes. The focus of this chapter is the selection of putative p38 inhibitors from the AZ compound collection. Computational modelling and assessment of the mitochondrial bioenergetics in the presence of these putative p38β inhibitors would lend additional evidence in support of the hypothesis that p38 is involved in the regulation of mitochondrial dynamics.

5.4. Methods.

5.4.1. X-ray crystallography structures of human and mouse p38 isoforms (α and β).

Crystal structures of p38 isoform (α and β) receptors were obtained from the protein database (PDB). 1KV2 (human p38 alpha, BIRB-796 co-crystallised, (Pargellis, Tong et al. 2002)), 1A9U (human p38 alpha, co-crystallised with SB203580, (Wang,

Canagarajah et al. 1998)), 3GP0 (p38 beta human with nitotinib,(Filippakopoulos , Malet, Coutard et al. 2009), 3GC8 (p38 beta human with dihydroquinazoline, (Patel, Cameron et al. 2009)), 2EWA (p38 alpha mouse co-crystallised with SB203580, (Vogtherr, Saxena et al. 2006)) and 2OZA (p38 alpha mouse and human MK2, (White, Pargellis et al. 2007)).

5.4.2. Hierarchical clustering of AZ p38 inhibitor actives compound database (Wards clustering).

An AstraZeneca FOYFI method (in-house developed software) was utilised to define the structural keys for 3259 compounds (Blomberg N 2009). These structural keys; created in a method similar to daylight fingerprinting which allows the presence or absence of predefined substructures and descriptors to be represented in a binary code. 1 refers to the presence and 0 to the absence of a defined substructure or descriptor feature. within each compound. 3259 compounds were clustered using Wards clustering. This clustering was based on chemical similarity of the compounds' substructures and descriptors. Tanimoto similarity e.g between two molecules A and B is calculated as the number of 1 bits (presence, using binary) divided by the sum number of 1 bits in (a) and (b) minus those 1 bits which they share in common (c). Importantly, even if the result of this calculation is a value of 1, the molecules may not be identical but simply share similar substructures across their entire molecular structure. This methodology is most commonly used with binary fingerprints (i.e. the presence, 1 or absence of a substructure, 0).

$$\text{Similarity } (A,B) = c / a + b - c$$

Conversely, the tanimoto distance is used to identify dissimilarity between a pair of molecules. Therefore, using this rationale, the shared absence of a substructure across a pair of molecules is taken to reflect a similarity between these two molecules. The range of distance values are 0 or positive. Importantly, smaller molecules often display less tanimoto similarity. This is taken into account during the calculation of tanimoto distance as:

$$\text{Distance}(A,B) = d / a + b - d$$

number of substructures shared between the two molecules (d) divided by the sum number of substructures in (a) and (b) minus (d).

The tanimoto distance defined for the hierarchical clustering was 0.3. A tanimoto distance of 0.3 is equivalent to a tanimoto similarity of 0.7 (Tanimoto Similarity = 1 – tanimoto distance).

5.4.3. Selection of compounds from the AZ database: Two-dimensional clustering of putative p38 inhibitors based on their activity and chemical similarity (sphere exclusion).

Two-dimensional clustering was performed across the entire AZ compound collection (Figure 5.9). The compounds were clustered separately by activity (activity across multiple kinases) or structure. The results were analysed together, to identify 'hot-spots' where clusters of compounds with similar structures and activities were located. For molecular docking studies, compound clusters from the larger AZ compound collection were selected if their co-cluster contained at least 5 compounds. Furthermore, the inhibition of a given compound against p38 needed to be a minimum of 50%. 296

compounds met this criterion and were docked into 6 available p38 crystal structures respectively (1KV2, 1A9U, 3GPO, 3GC8, 2EWA and 2OZA). These 6 p38 structures represent both human and mouse p38 isoforms α (human; 1KV2 and 1a9u, mouse; 2EWA. 2OZA) and β (human; 3GP0 and 3GC8) identified to date. Therefore, through assessment of both apo and drug-bound ligands with the p38 enabled predictions of the binding modes and key amino acid, H-bond and other short distance interactions e.g van der Waals between a drug compound and p38, required to inhibit further p38 phosphorylation .

5.4.4. Docking interactions between p38 isoforms and inhibitors.

Crystal structures available from PDB were prepared in Schrodinger Maestro (a commercial computational modelling suite, only accessible at AZ not at Warwick due to licensing costs)using the protein preparation wizard. 296 compounds from the hierarchical clustering were docked into the p38 isoforms (α and β). Ligand docking following energy minimisation was performed using Glide 2.5. A maximium of 10,000 conformations, an RMSD of 0.25Å and standard docking protocol were applied to all 296 ligands. Explicit waters were included in the ATP binding site. Glide docking scores were normalised using the following equation: New score = (original glide score – mean glide score) -10. This enabled the glide scores defined to approximate a similar area of scoring space across all receptors. Strain correction terms were applied to the output glide docking score.

Input conformations were the same across all 6 p38 proteins tested. All ligand pose scores (calculated from energy of binding, electrostatic or covalent bonding interactions between the ligand and the protein) were mean-centred (to minimise the

lenth of the axis for the ligand pose scores, and limit the effect of any significant outliers) to allow cross-comparison between different input proteins.

5.4.5. Selection of putative p38 isoform selective inhibitors.

To assess the selectivity of a compound for a particular isoform of p38, the glide scores for that compound were assessed as follows:

Selectivity of a compound for p38 alpha = best p38 alpha / mean (best alpha, best p38 beta, best p38 delta, best p38 gamma).

5.4.6. MTT Cytotoxicity assay.

2 days prior to the MTT assay, 3T3 preadipocytes were plated into a 6 well plate at a density of 1 x 10^5/ml. Preadipocytes rather than differentiated adipocytes were used as the expression of phospho-p38 which we are trying to inhibit through treatment with AZ_0002 (putative p38 beta inhibitor) is more highly expressed in preadipocytes than adipocytes). Once confluent, the media was removed and the cells were washed twice with PBS. Media was replaced with 0.2% BSA DMEM (2ml/well, no antibiotics, sodium pyruvate supplemented). The cells were serum starved 3 hours before the assay. The working stock of Thiazolyl Blue Tetrazolium Bromide (MTT, M2128, Sigma Aldrich) was 5mg/ml dissolved in water. Control cells were treated with equivalent volumes of DMSO to those used to solubilise the AZ compound. Following incubation of the 3T3 preadipocytes at 37°c and 5% CO_2 for 0, 30 minutes or 3 hours, cells were washed twice with PBS. MTT (20µl of 5mg/ml stock; final concentration is 25µM/well) was added to the wells and 3T3 cells were incubated for a further 4 hours

at 37°c and 5% CO_2. Cells were washed twice more with PBS and the formazan crystals were eluted in 2ml DMSO: Isopropanol (1:1 ratio). Absorbance was read at 570 nm. Background absorbance at 690 nm was subtracted from this reading. MTT incubated at 37°c and 5% CO_2 in the absence of cells was used to assess non-specific binding of dye to plastic which may influence the absorbance readings. Cytotoxicity was determined as the difference in absorbance between control and AZ treated cells and was expressed as a percentage. Each value for cytotoxicity is an average of triplicate measurements.

5.4.7. Serial dilution of AZ_p38 compounds.

A working stock of 10mM was made for compound, AZ_0002 (putative p38β inhibitor). This compound was compared against a reference compound, SB203580 10μM (IC_{50}, 0.02μM, against p38α and β). The AZ compound was serially diluted to a final concentration/well of 2.22 – 0.0001μM (in DMSO) and assayed in duplicate. SB203580 was assayed alongside the AZ compound at a concentration of 10μM.

5.4.8. Mitochondrial bioenergetics assay.

3T3-L1 preadipocytes were seeded at 20,000/100μl per well into XF24 microplate. Preadipocytes were selected, as the basal phospho-p38 (p-p38) expression was significantly high compared to differnetiated adipocytes but also, we sought to identify if p38 inhibition (following AZ_0002, putative p38 beta inhibitor) translated into any significant functional effect on mitochondria oxidative capacity. Once adhered, the 3T3′s were incubated in a final volume of 250μl growth media. Cells were grown overnight at 37^0c, 5% CO_2 in 10% FBS (Biosera, South American origin): DMEM/

F12 (11039_054), 5ml Penicillin/Steptomycin (15140-122, 10,000 Units/ml Pencillin, 10,000 µg/ml Streptomycin), 2mM L-glutamine (25030-081). Cell culture reagents were purchased from Invitrogen.

Mitochondrial stress reagents were purchased from Sigma Aldrich and prepared to a final concentration/well as follows: Oligomycin (1µM 75351), FCCP (0.5µM,C2920), Antimycin and Rotenone (1µM cocktail of both compounds, A8674 and R8875). SB203580 (10µM, Cell signalling technology), AZ_0002 (0.1 µM, 0.01µM and 0.005µM), concentrations given in brackets are final stock concentrations assayed per well (see section 4.2.1.3, for detailed assay protocol and inhibitory activities of the stress reagents in oxidative phosphorylation). The final concentration that 3T3 preadipocytes were treated with was 10 fold lower than the final stock concentration (0.01, 0.001 and 0.0005µM respectively. The compound was provided by AstraZeneca, Alderley Edge, Cheshire). The XF24 Seahorse Bioanalyser was used to assay the effect of the predicted p38β isoform inhibitor on mitochondrial bioenergetics.

5.4.9. Mitochondrial copy number determination (mtDNA/nDNA ratio).

Total DNA was extracted from 20,000 3T3-L1 using DNeasy kit (Qiagen) following treatment for 0, 30 minutes, 3 hours with AZ putative isoform inhibitor (see Figure 2.3). Control cells were treated with DMSO at equivalent volume to inhibitor treated cells. 3T3 preadipocytes were treated with the highest concentration of AZ_p38β_inhibitor (0.1 µM) used in the mitochondrial bioenergetics assay. The relative amounts of nuclear (Beta 2 microglobulin, B2M or receptor-interacting protein 140; RIP140) and mitochondrial DNA (NADH-ubiquinone oxidoreductase chain 2; ND2 or Cy-

cloxygenase II; COXII) were determined by qPCR with previously published primer sequences (Murholm, Dixen et al. 2009, Wai, Ao et al. 2010). The two primer sets (ND2/B2M and COXII/RIP140) were purchased from Invitrogen. COXII forward; 5′-AATTGCTCTCCCCTCTCTACG-3′, COXII reverse; 5′-GTAGCTTCAGTATCATTGGTGC-3′, RIP140 forward; 5′-CGGCCTCGAAGGCGTGG-3′, RIP140 reverse; 5′-AAACGCACGTCAGTATCGTC-3′, ND2 forward; 5′-AGGGATCCCACTGCACATAG-3′, ND2 reverse; 5′-TGAGGGATGGGTTGTAAGGA-3′, B2M forward; 5′-TGTCAGATATGTCCTTCAGCAAGG-3′ and B2M reverse; 5′-TGCTTAACTCTGCAGGCGTATG-3′.

5.5. Results:

5.5.1. Hierarchical clustering analyses of known p38 active's within the AZ compound collection.

Cluster analysis based on chemical similarity of core scaffold structures within the AstraZeneca compound collection generated 16 clusters (Figures 5.12). 38 clusters were generated when the AZ compound collection was clustered based on their kinase activity profile (Figures 5.12).

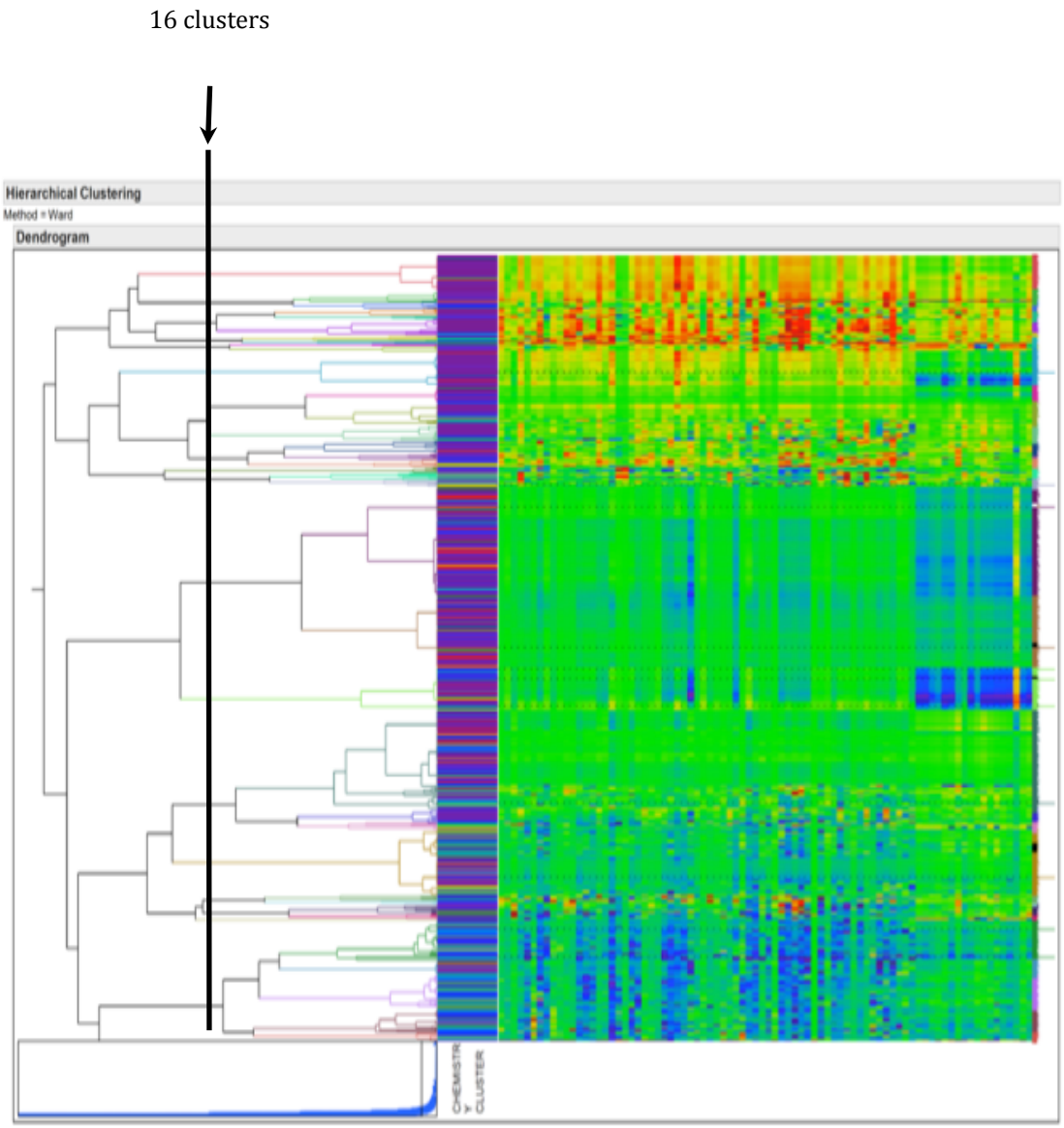

Figure 5.12. Hierarchical clustering analyses of known p38 inhibitor compounds within the AZ collection. Chemical similarity of the core scaffold structures within AstraZeneca's compound collection generated 16 clusters. 38 clusters were generated based on clustering compounds based on their kinase inhibition profile. The activity of these kinase inhibitors within the compound collection were available across a panel of 69 kinases including p38. Together with a tanimoto distance of 0.3, 38 clusters were generated.

5.5.2. Clustering based on p38 kinase activity from known database

1069 compounds of the 3259 had full activity data against the entire 81 kinase assays including p38α (performed by colleages at AstraZeneca, AZ). These compounds were utilised as a training set for 2190 compounds which had some missing activity data. The chemical similarity of these compounds to the training set enabled missing data on kinase inhibition to be approximated through imputation. 3259 resulting kinase inhibition profiles were generated as a result of this imputation work (Figure 5.10). For molecular docking studies, compound clusters from the larger AZ compound collection were selected if their co-cluster contained at least 5 compounds. Furthermore, for a compound to be considered for further exploration as a potential p38 inhibitor, the compound needed to reduce p38 kinase activity by at least 50%, as determined by the kinase inhibition assay (section 5.2.8). 296 compounds met this criterion and were docked into the 6 p38 protein structures respectively (1KV2, 1A9U, 3GPO, 3GC8, 2EWA and 2OZA).

38 clusters (inhibitory activity of compound)

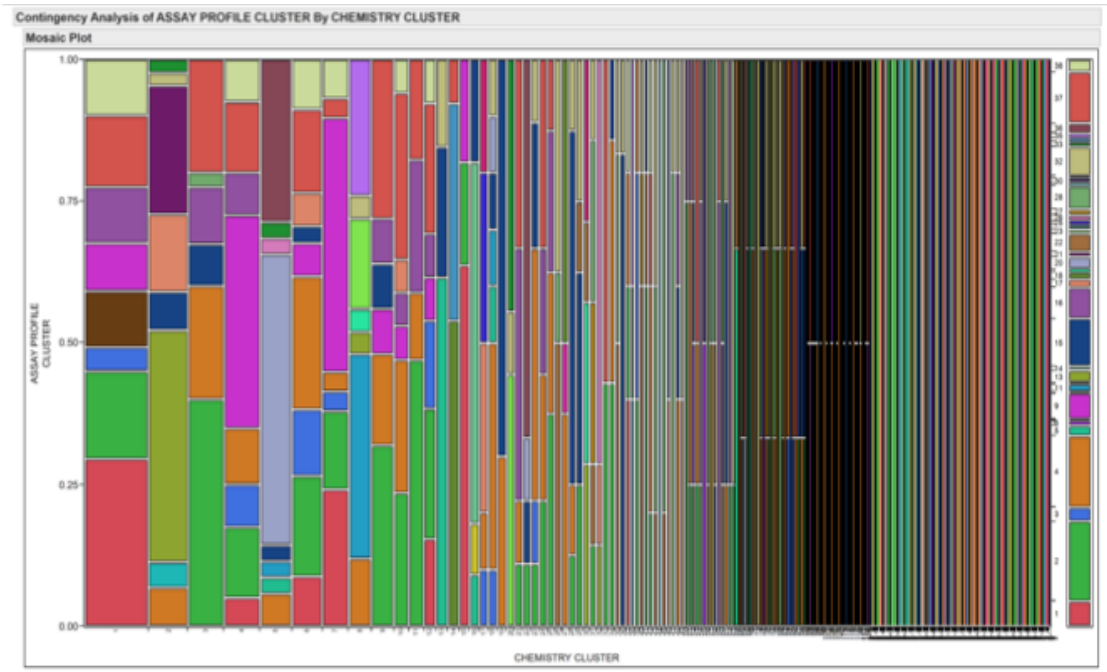

Figure 5.13. Two-dimensional clustering of compounds based on their chemical and kinase activity profile. Identification of compounds, which are present in the same chemical and activity cluster, were used to refine clustering of the compounds. The clusters selected for further investigation were required to contain at least 5 compounds and have an inhibit the p38 kinase activity by at least 50%. From the initial 4299 compounds, 296 were identified for further investigation.

5.5.4 Isoform selectivity of AZ p38 inhibitors.

AZ0002 was selected as a putative p38β selective inhibitor based on its isoform selectivity profile (Table 4). Glide docking scores of the putative p38β inhibitory compound revealed a mean centred score of -8.54 for 3GPO (p38β) and -10.14 for 2EWA (p38α). Comparison of the glide docking scores of this compound with other isoforms revealed lower scores of -5.25 and -4.95 for the p38γ (1CM8) and δ (3COI) respectively. Analysis of the relative isoform specificity score of the AZ_0002 compound was defined as 100% for p38β compared to 67 and 69% for p38γ and p38α respectively.

Compound	p38α selectivity	p38β selectivity	p38γ selectivity	p38δ selectivity	Selection
AZ_0004	1.31	0.77	0.76	0.56	alpha
AZ_0005	1.21	0.79	0.83	0.46	alpha
AZ_0006	1.33	0.75	0.75	0.48	alpha
AZ_0007	1.47	0.61	0.68	0.36	alpha
AZ_0008	1.41	0.71	0.63	0.41	alpha
AZ_0009	0.75	1.2	0.83	0.41	beta
AZ_0010	0.83	1.2	0.81	0.52	beta
AZ_0011	0.79	1.25	0.8	0.5	beta
AZ_0012	0.74	1.3	0.77	0.42	beta
AZ_0002	0.83	1.2	0.8	0.47	beta

Table 4. p38 isoform selectivity of AZ compounds.
To assess the selectivity of a compound for a particular isoform, the glide scores for that compound were assessed as follows: Selectivity of a compound for p38 alpha = best p38 alpha / mean (best alpha, best p38 beta, best p38 delta, best p38 gamma).

Compound	Proposed p38 isoform inhibitor	IC_{50} (μM)
AZ_p38β	beta	0.01
SB203580 (10uM)	alpha and beta	0.02

Table 5. p38 kinase inhibition assay (performed by colleages at AstraZeneca).
AZ_p38 beta was known as AZ_0002 in our studies. The kinase inhibition assay was used to determine the IC_{50} for the AZ_p38 compounds.

5.5.5. Effect of AZ_0002 on mitochondrial DNA content.

Assessment of mitochondrial DNA content by two different mtDNA/nDNA assays (ND2/B2M and COXII/RIP140, Figure 5.11) concluded that treatment of preadipocytes with up to 0.1µM of AZ_0002 for 3 hours did not result in a statistically significant change in mitochondrial DNA content, probably due to limited exposure.

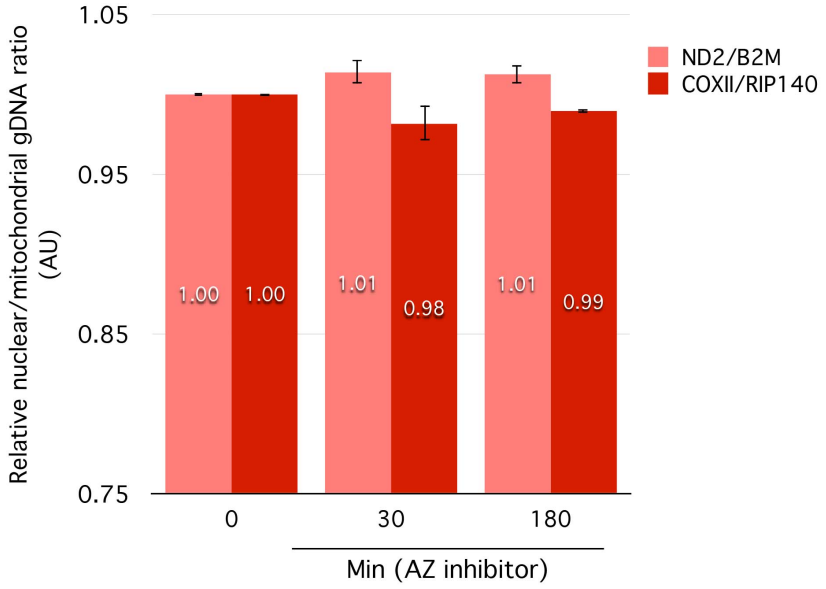

Figure 5.14. Treatment of 3T3-L1 preadipocytes with the putative p38β inhibitor, AZ_ 0002, resulted in no significant change in mitochondrial DNA content.

3T3-L1 were treated with AZ_0002 (10μM) or DMSO (control cells) for up to 3 hours. Mitochondrial DNA content was assessed by two primer sets (ND2/B2M and COXII/RIP140). Each treatment was assayed three times for each primer set. The data presented here, represent the average of these triplicate readings. All data were non significant.

5.5.6. Effect of AZ_0002 on mitochondrial bioenergetics of 3T3-L1 preadipocytes.

Spare respiratory capacity of 3T3-L1 preadipocytes is reduced following acute treatment with putative inhibitor of p38β, AZ_0002. The relative impairment of the spare respiratory capacity with AZ_0002 was equivalent to that achieved by 10μM of SB203580 (Figure 5.15. $p < 0.05$). Furthermore, the coupling efficiencies of mitochondria were significantly decreased following treatment of preadipocytes with either 10μM of SB203580 or AZ_0002 (putative p38β inhibitor) at 0.01μM (Figure 5.15. $p < 0.05$). Intriguingly, the level of statistical significance was greater in SB relative to DMSO controls compared to AZ_002 (putative p38β inhibitor) treated at 0.01μM (Figure 5.15. $p < 0.05$).

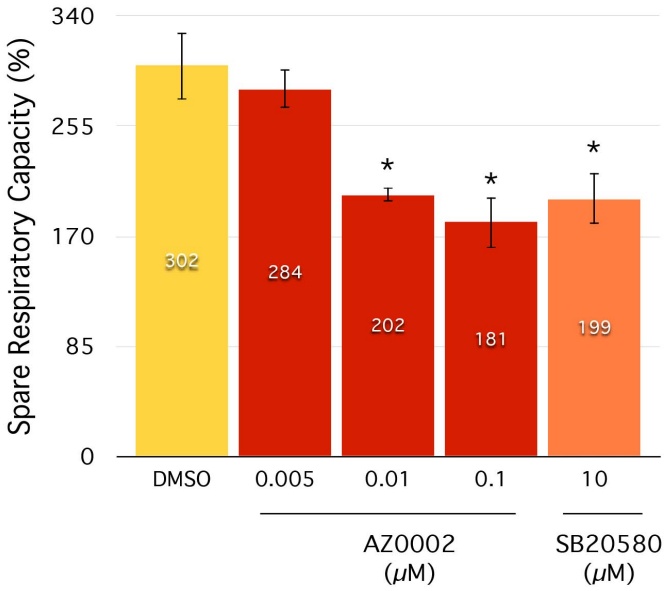

Figure 5.15. Spare respiratory capacities of the 3T3-L1 preadipocytes were markedly diminished in the presence of the putative p38β inhibitor, AZ_0002.

20,000 cells were seeded into an XF24 Seahorse cell culture plate and grown overnight at 37^0c, 5% $C0_2$. Following 30 minutes of pretreatment with an AZ_0002, mitochondrial bioenergetics were assessed using mitochondrial stress reagents (1μM Oligomycin, 0.5μM FCCP, 1μM Antimycin/Rotenone). Spare respiratory capacity presented above, is calculated by division of basal respiration from maximal oxygen consumption (FCCP uncoupled respiration). Oxygen consumption rates per well were normalised per mg of protein (O_2/min/mg). Concentrations of AZ_p38 inhibitor chosen were selected based on their IC_{50} in the p38 kinase activity assay (p38α 0.01μM).

5.6. Discussion.

Hierarchical cluster analysis was utilised as a methodology to select putative isoform selective compounds. Initially we sought to investigate the difference in the number of clusters that would be generated if chemical similarity or kinase activity were used to define the AstraZeneca (AZ) compound collection. A sub-group of 3259 compounds previously identified by AZ to have potential inhibitory activity against kinases including p38 were utilised within initial cluster analyses (Figure 5.12). Clustering of compounds based on their chemical similarity generated 16 clusters whilst inhibitory activity profile against a range of kinases including p38 clustering of the core scaffold structures produced 38 clusters (Figure 5.13).

Co-clustering of the AZ compounds by inhibitory activity against a panel of kinases and chemical similarity enabled us to reduce the likelihood of false positives. Furthermore, the overlapping of clusters in this manner assisted us in selecting compounds with a greater probability of p38 inhibitory activity. Within the sub-group of 3259, a panel of 110 kinase assays had been performed to identify kinase activity profile of these compounds. However, as inhibition data was not available across all compounds, the decision was taken to exclude given kinase inhibition assays (28/110 assays) rather than compounds. This rationale was selected as we did not want to compromise chemical diversity within the compound collection. 1069 compounds contained full kinase inhibition profiling across the 82 assays. These compounds were used as a training set and multivariate analysis was performed on these compounds. Following this analysis, the missing data pattern within the panel of 3259 compounds was identified and missing data was imputed.

Clusters selected for further investigation were required to contain at least 5 compounds and have an inhibitory action against kinases of greater than 50%. 296 compounds met these eligibility criteria. The scaffold substructures contained within these 296 compounds were identified. Once identified, the core scaffold structures that exemplified these known AZ actives were used to identify new compounds within the larger AZ compound database. Furthermore, Scifinder was used to search published compounds containing similar scaffold structures. Substructure searching enabled any previous biological knowledge of these scaffold cores within diabetes, inflammation and ER stress to be evaluated. Molecular docking was undertaken to postulate the nature and selectivity by which these compounds and predict how they may interact with the MAPK receptors, p38α and β. Following modelling of the putative amino acid interactions between the p38β and AZ_0002 inhibitor, we sought to investigate whether mitochondrial bioenergetics could be affected by this compound. In previous studies with SB203580 we identified that p38 inhibition resulted in a reduction in spare respiratory capacity of 3T3-L1 preadipocytes (Chapter 4). The extensive characterisation of amino acid interactions between p38α or β and SB revealed the essential amino acid interactions required for its inhibitory kinase action. Thr^{106} located within a small side chain in a small hydrophobic groove adjacent to the ATP binding site, is the critical amino acid interaction required between SB and p38α in order for it elicit its inhibitory activity. Spare respiratory capacity diminished following incubation of 3T3-L1 preadipocytes with the AZ_0002, p38β inhibitor (Figure 5.15). Whilst, mitochondrial copy number was slightly reduced following 30 minutes of acute treatment with p38 inhibitor AZ_0002, it did not decline to a statistically significant degree as a more chronic treatment was probably required (Figure 5.14).

Spare respiratory capacity (SRC) is calculated by comparison of the oxygen consumption rate (OCR) in an uncoupled versus a closed normal oxidative phosphorylation. As the addition of FCCP, a mitochondrial uncoupler occurs after the 30 minutes, any changes observed in SRC were not due to changes in mitochondrial biogenesis. Furthermore, the dose dependent nature of the decline in SRC supports the view that changes in SRC are due to the effects of the addition of the compound and not other factors such as cell death (performed by AstraZeneca, data not shown). The concentrations selected reflected a range around the predetermined IC_{50}. For assessment of the effect of our AZ_0002, putative p38β inhibitor compound, final concentrations of 0.1, 0.01 (IC_{50} of the compound) and 0.005μM on mitochondrial bioenergetics of 3T3-L1 preadipocytes were assayed.

In conclusion our study has highlighted that p38 can regulate mitochondrial function. Site directed mutagenesis studies would be required to complement and support the amino acid interactions modelled between p38 (β) and p38 β inhibitor.

Chapter 6:

Overall discussion and conclusions

6.0. Discussion.

The aim of this thesis was to understand the role of mitochondrial dynamics in obesity associated type 2 diabetes. To study this we used human adipose tissue from lean, overweight and obese individuals and observed that mitochondrial dynamics was dysregulated in adipose tissue of obese subjects compared to lean. To further understand the effect of obesity we used pre and post bariatric surgery samples where the effect of weight loss and surgical procedure were studied in the regulation of mitochondrial dynamics. The ultimate aim was to study how this important system is regulated in adipose tissue. Our preliminary study showed that p38 MAPK pathway may have an important role in the regulation of mitochondrial dynamics, and therefore, the effect of this pathway on the regulation of mitochondrial fission and fusion was investigated using the 3T3-L1 murine cell line.

6.1. Is mitochondrial dynamics differentially regulated in the subcutaneous adipose tissue of lean, overweight and obese individuals?

Chapter 2 describes the study of mitochondrial fusion and fission in human AbSc AT of lean, overweight and obese subjects.

Adipose tissue plays an important role in the regulation of energy homeostasis and was used for the investigation of mitochondrial dynamics. It also acts as an endocrine organ and depot for dietary nutritional excess, storing triglycerides within adipocytes until they are required by the cell. The regulation of mitochondrial dynamics was studied by evaluating expression levels of markers of mitochondrial fission as well as fusion. This approach offers the ability to explore whether a single or multiple mitochondrial fission marker genes were altered by adiposity. Our data demonstrates that markers

of mitochondrial fission increased with adiposity, as evidenced by the significantly increased expression levels of Fis1 in obese compared to lean controls (Figure 2.4).Considering the opposing arm of mitochondrial dynamics next, markers of mitochondrial fusion genes (Opa1 and Mfn2) were significantly and positively correlated in AbSc AT of lean subjects (Figure 2.6). Conversely, in obese individuals no significant correlation was present (Figure 2.6). This suggests a dysregulation of mitochondrial dynamics in obese, as a consequence mitochondrial health may be compromised leading to a reduction of mitochondrial bioenergetics.

Our results clearly support previous studies, which indicate that markers of mitochondrial dynamics are affected by adiposity and support the known essential role of optimal mitochondrial dynamics in preventing the development of mitochondrial dysfunction. Mitochondrial dynamics adapts to nutritional conditions working to maintain mitochondrial health (Twig, Hyde et al. 2008). Conditions of nutritional excess are joined with fragmented mitochondria (Otera, Wang et al. 2010). A limitation of our study which would require future investigation is the assessment of the bioenergetic capacity and characterisation of the mitochondrial capacity and morphology in adipose tissue from each individual to see how closely our mitochondrial dynamics expression analyses reflect mitochondrial function.

In summary, Chapter 2 concluded that markers of mitochondrial dynamics genes in human AbSc AT were differentially expressed in lean, overweight and obese individuals. Adiposity was accompanied by an increase in expression of the mitochondrial fission (Fis1 and Drp1) and fusion (Opa1 and Mfn2) gene expression markers in AbSc AT.

6.2. Is mitochondrial dynamics affected by weight loss or Bariatric Surgery in T2DM individuals?

Chapter 3 investigated mitochondrial dynamics within morbidly obese T2DM subjects before and after undergoing elective bariatric surgery.

Mitochondrial dysfunction is known to commonly afflict those with T2DM and other metabolic disease such as cardiovascular disease (Sjostrom, Lindroos et al. 2004, Ren, Pulakat et al. 2010). A key line of evidence for this hypothesis is that individuals with cardiac function mutations also present with compromised mitochondria and mutations within proteins controlling mitochondrial dynamics (Jung, Martins et al. 2008, Murray, Cole et al. 2008, Doenst, Pytel et al. 2010).

Following the conclusion that mitochondrial dynamics was influenced by adiposity, we investigated whether weight loss would have a positive effect on mitochondrial dynamics. To study this, adipose tissue was used from pre and post bariatric surgery from patients who had significant weight loss 6 months post-surgery.

Despite, indirect evidence of mitochondrial dysfunction, insulin resistance and adiposity, it is still unclear how these processes are connected at a molecular level. Bariatric surgery is one of the most successful methods to resolve insulin resistance (Levy, Fried et al. 2007, Buchwald, Estok et al. 2009, Carlsson, Peltonen et al. 2012, Nijhawan, Richards et al. 2013). Clinical observations have highlighted that the more extensive structural remodelling of the gastrointestinal tract during bariatric surgery, the more significant the correlation with diabetes resolution (Neff 2013). If a single surgical procedure can offer weight loss, diabetes remission and the redressing of mitochondrial dynamics and thus enhance the metabolic activity often lost during obesity, this would offer patients a distinct advantage as well as a clinical argument to-

wards performing this surgical procedure over others available or providing medical care to manage the diabetes and obesity conditions.

Initial investigation of mitochondrial dynamics in subcutaneous adipose tissue before and after bariatric surgery revealed that biliopancreatic diversion (BPD) surgeryhad the greatest number of improvements in clinical parameters and differences in mitochondrial dynamics observed in the post-surgical AbSc AT samples. Consistent with previous studies, it was concluded that weight loss was most likely to be responsible for an individual's remission of T2DM and other clinical improvements (Table 2.) (Hotamisligil 2007, Bradley, Conte et al. 2012) (Figures 3.6 and 3.7). Other studies have concluded that 20% weight loss is necessary to result in a demonstrable improvement in the skeletal muscle insulin sensitivity of extremely obese people (Campos, Rabl et al. 2010, Lima, Pareja et al. 2010, Bradley, Conte et al. 2012). In agreement with this, at 6 months after surgery all our patients had lost at least 20% of their pre-operative weight (Table 2). Thus far, our data clearly shows an overall reduction in the expression of markers of mitochondrial fission and fusion (Figures 3.2 and 3.5).

Similar to the adiposity study, a limitation of our study which would require future investigation is the assessment of the bioenergetic capacity and characterisation of the mitochondrial capacity and morphology in adipose tissue from each individual to see how closely our mitochondrial dynamics expression analyses reflect mitochondrial function.

In summary, this study provides a novel contribution to current knowledge within the field of diabetes and bariatric surgery. This study highlights that the redressing on markers of mitochondrial dynamics expression in AbSc AT reflects a pos-

sible mechanism through which mitochondrial dysfunction can be corrected following weight loss surgery.

6.3. *Does p38 regulate mitochondrial dynamics?*

Chapter 4 characterised the expression profile of the phospho-p38 and mitochondrial dynamics genes during the differentiation of adipocytes. Phospho-p38 is known to rapidly decrease from its peak in the early stages of differentiation to barely detectable levels at the terminal stages (Engelman, Lisanti et al. 1998). Phospho-p38 expression was modulated in 3T3-L1 by chemical inhibition SB203580 or activation by transfection of an MKK6 overexpression using MKK6(Glu), to determine its impact on mitochondrial dynamics.

In recent years, the central role of adipose tissue in controlling energy metabolism and the significant impact of balancing energy homeostasis (Rosen and Spiegelman 2006) on mitochondrial function has become better understood. Mitochondrial function is regulated through biogenesis and morphology. Regulation of mitochondrial morphology is orchestrated by mitochondrial dynamics (Okamoto and Shaw 2005, Huang, Galloway et al. 2011). A clear connection between mitochondrial dynamics and health is demonstrated by the observation that mammalian cells devoid of mitochondrial fusion display stunted growth rates and diminished respiratory capacity (Legros, Lombes et al. 2002, Huang, Galloway et al. 2011).

SB203580, a p38α and β isoform inhibitor was assayed to assess the duration of p-p38 inhibition together with its cytotoxicity in 3T3-L1 preadipocytes (Badger, Bradbeer et al. 1996). p-p38 expression was significantly decreased in our 3T3-L1 preadipocytes, after incubating for 30 minutes to an hour with SB203580 (10μM,

Figure 4.10). This was accompanied by no significant reduction in mitochondrial DNA content (Figure 4.11). However, markers of mitochondrial fission and fusion, Fis1 and Mfn2 respectively, decreased significantly in protein expression following this acute p38 inhibition (Figures 4.12 and 4.13). Our present findings strongly suggest a novel regulation of mitochondrial dynamics by p38. Inhibition of p38 resulted in diminished mitochondrial bioenergetic capacity and thus a reduction in mitochondrial efficiency. A limitation of this study is the lack of qunatification of the change in the rate of mitochondrial dynamics following p38 inhibition.In order to acheive quantitative values for mitochondrial dynamics requires pin point laser activation of a single green fluorescent mitochondria within stably transfected cells. The majority of work in these quantitative experiments thus far has been performed in freshly isolated mouse (from sacrificied mice) or human adipocytes (needle biopsies) using a 2D-scanning laser confocal microscope currently unavailable within our department. The activation plane and specificity of the laser activation of a single GFP labelled mitochondria is beyond the capabilities of our confocal microscope.Therefore, in order to perform these experiments requires the development of a collaboration, which was not possible in our case due to insufficient time (the dynamics experiments were optimised and successful performed only a few weeks before the end of my experimental work) but could be arranged for future projects.Further studies involving assessment of the rate of mitochondrial dynamics and bioenergetics in MKK6 transfected 3T3-L1 and human preadipocyte models will be required to provide additional support to our work.

6.4. Modelling and selection of putative p38 α and β isoform inhibitors.

p38 is known to interact with the putative inhibitors via 3 key amino acid interactions; Thr180, Tyr182 and Met109 (Adams, Boehm et al. 2001). Of the 3259 compounds clustered by chemical similarity of the compounds substructures, descriptors or activity, 296 compounds initially met similar criteria to SB203580. The scaffold substructures contained within these 296 compounds were identified. Once identified, the core scaffold structures that exemplified these known AZ actives were used to identify new compounds within the larger AZ compound database. Molecular docking was undertaken to postulate the nature and selectivity by which these compounds and predict how they may interact with the MAPK receptors, p38α and β. Following modelling of the putative amino acid interactions between the p38β and AZ_0002 inhibitor, we sought to investigate whether mitochondrial bioenergetics could be affected by this compound.

In conclusion our study has highlighted that p38 can regulate mitochondrial function, as treatment of 3T3-L1 preadipocytes resulted in a significantly diminished spare respiratory capacity compared to DMSO treated controls. Whilst the increase is oxygen consumption rate in mitochondria occured following treatment with the p38 inhibitor, looks promising if the duration of this enhancement could be selecively and acutely activated, translation of this compound as an anti-obesity drug is unlikely. One of the main factors that would prevent its transition into future drug development is the risk of increasing cancer through manipulation of p38 signalling. Therefore, these studies were performed to evaluate the regulation of mitochondrial dynamics and the signal transduction processes that accompany it. An additional limitation of our study is that only one exemplar of putative p38 beta inhibitors was assayed within

the mitochondrial bioenergetics assay. Given additional time, would have permitted the remaining 9 from the top 10 selected compounds to be individually assayed. Site directed mutagenesis studies would be required to complement and support the amino acid interactions modelled between p38 (β) and p38 β inhibitor.

6.5. Conclusions.

This thesis sought to expand our knowledge and understanding of the actions of p38 on mitochondrial dynamics in adipose tissue. The current studies have highlighted that markers of mitochondrial dynamics are upregulated in adiposity. Furthermore, assessment of the impact of bariatric surgery in morbidly obese T2DM subjects concluded that weight loss rather than the surgical procedure alone resulted in a reduction in the expression of mitochondrial fusion and fission markers. Together, the results presented in this thesis support previous reports that mitochondrial dynamics are critical to adapt and maintain metabolic health required to meet the energetic demands of the cells in which they reside. Our results extend our understanding of mitochondrial dynamics in adiposity through the novel finding that p38 is involved in the positive regulation of mitochondrial dynamics in adipocytes.

6.6. Future work.

The current studies have highlighted that markers of mitochondrial dynamics are down regulated with adiposity and are positively regulated by p38 within 3T3-L1 preadipocytes. Given additional time for this project, I would have liked to investigate the following concepts in more detail:

- Confocal microscopy of mitochondrial dynamics in transfected with the constitutively active MKK6(Glu) vector in preadipocytes
- Culturing of human adipocytes and p38 inhibition through genetic and pharmacological mechanisms
- Effect of p38 on quality control mechanisms; feedback responses between PQC and mitochondrial dynamics
- Investigate the mechanisms of cross-talk between ER and mitochondrial dynamics and how p38 inhibition impacts upon these.

Bibliography

(1994). "UK Prospective Diabetes Study. XII: Differences between Asian, Afro-Caribbean and white Caucasian type 2 diabetic patients at diagnosis of diabetes. UK Prospective Diabetes Study Group." Diabet Med **11**(7): 670-677.

Aanen, D. K., J. N. Spelbrink and M. Beekman (2014). "What cost mitochondria? The maintenance of functional mitochondrial DNA within and across generations." Philos Trans R Soc Lond B Biol Sci **369**(1646): 20130438.

Abdullah, A., A. Peeters, M. de Courten and J. Stoelwinder (2010). "The magnitude of association between overweight and obesity and the risk of diabetes: a meta-analysis of prospective cohort studies." Diabetes Res Clin Pract **89**(3): 309-319.

Abella, V., M. Scotece, J. Conde, V. Lopez, V. Lazzaro, J. Pino, J. J. Gomez-Reino and O. Gualillo (2014). "Adipokines, metabolic syndrome and rheumatic diseases." J Immunol Res **2014**: 343746.

Adachi, T., T. Toishi, H. Wu, T. Kamiya and H. Hara (2009). "Expression of extracellular superoxide dismutase during adipose differentiation in 3T3-L1 cells." Redox Rep **14**(1): 34-40.

Adams, J. L., J. C. Boehm, T. F. Gallagher, S. Kassis, E. F. Webb, R. Hall, M. Sorenson, R. Garigipati, D. E. Griswold and J. C. Lee (2001). "Pyrimidinylimidazole inhibitors of p38: cyclic N-1 imidazole substituents enhance p38 kinase inhibition and oral activity." Bioorg Med Chem Lett **11**(21): 2867-2870.

Adams, J. L., J. C. Boehm, S. Kassis, P. D. Gorycki, E. F. Webb, R. Hall, M. Sorenson, J. C. Lee, A. Ayrton, D. E. Griswold and T. F. Gallagher (1998). "Pyrimidinylimidazole inhibitors of CSBP/p38 kinase demonstrating decreased inhibition of hepatic cytochrome P450 enzymes." Bioorg Med Chem Lett **8**(22): 3111-3116.

Affourtit, C., M. Jastroch and M. D. Brand (2011). "Uncoupling protein-2 attenuates glucose-stimulated insulin secretion in INS-1E insulinoma cells by lowering mitochondrial reactive oxygen species." Free Radic Biol Med **50**(5): 609-616.

Ahima, R. S. (2006). "Adipose tissue as an endocrine organ." Obesity (Silver Spring) **14 Suppl 5**: 242S-249S.

Ahirwar, A. K., A. Jain, B. Goswami, M. K. Bhatnagar and J. Bhatacharjee (2014). "Imbalance between protective (adiponectin) and prothrombotic (Plasminogen Activator Inhibitor-1) adipokines in metabolic syndrome." Diabetes Metab Syndr.

Akella, R., X. Min, Q. Wu, K. H. Gardner and E. J. Goldsmith (2010). "The third conformation of p38alpha MAP kinase observed in phosphorylated p38alpha and in solution." Structure **18**(12): 1571-1578.

Akepati, V. R., E. C. Muller, A. Otto, H. M. Strauss, M. Portwich and C. Alexander (2008). "Characterization of OPA1 isoforms isolated from mouse tissues." J Neurochem **106**(1): 372-383.

Akimoto, T., S. C. Pohnert, P. Li, M. Zhang, C. Gumbs, P. B. Rosenberg, R. S. Williams and Z. Yan (2005). "Exercise stimulates Pgc-1alpha transcription in skeletal muscle through activation of the p38 MAPK pathway." J Biol Chem **280**(20): 19587-19593.

Al Rawi, S., S. Louvet-Vallee, A. Djeddi, M. Sachse, E. Culetto, C. Hajjar, L. Boyd, R. Legouis and V. Galy (2011). "Postfertilization autophagy of sperm organelles prevents paternal mitochondrial DNA transmission." Science **334**(6059): 1144-1147.

Alexander, C., M. Votruba, U. E. Pesch, D. L. Thiselton, S. Mayer, A. Moore, M. Rodriguez, U. Kellner, B. Leo-Kottler, G. Auburger, S. S. Bhattacharya and B. Wissinger (2000). "OPA1, encoding a dynamin-related GTPase, is mutated in autosomal dominant optic atrophy linked to chromosome 3q28." Nat Genet **26**(2): 211-215.

Alfadda, A. A. (2014). "Circulating Adipokines in Healthy versus Unhealthy Overweight and Obese Subjects." Int J Endocrinol **2014**: 170434.

Alhusaini, S., K. Lois, K. McGee, P. McTernan, S. Kumar and G. Tripathi (2009). "Endoplasmic stress is induced by lipopolysaccharides and high glucose and is alleviated by salicylates in cultured primary human adipocytes." Diabetologia **52**: 110.

Ali, O., D. Cerjak, J. W. Kent, Jr., R. James, J. Blangero and Y. Zhang (2014). "Obesity, central adiposity and cardiometabolic risk factors in children and adolescents: a family-based study." Pediatr Obes **9**(3): e58-62.

Amati, F., J. J. Dube, E. Alvarez-Carnero, M. M. Edreira, P. Chomentowski, P. M. Coen, G. E. Switzer, P. E. Bickel, M. Stefanovic-Racic, F. G. Toledo and B. H. Goodpaster (2011). "Skeletal muscle triglycerides, diacylglycerols, and ceramides in insulin resistance: another paradox in endurance-trained athletes?" Diabetes **60**(10): 2588-2597.

Anderson, S., A. T. Bankier, B. G. Barrell, M. H. de Bruijn, A. R. Coulson, J. Drouin, I. C. Eperon, D. P. Nierlich, B. A. Roe, F. Sanger, P. H. Schreier, A. J. Smith, R. Staden and I. G. Young (1981). "Sequence and organization of the human mitochondrial genome." Nature **290**(5806): 457-465.

Antuna-Puente, B., B. Feve, S. Fellahi and J. P. Bastard (2008). "Adipokines: the missing link between insulin resistance and obesity." Diabetes Metab **34**(1): 2-11.

Aquilano, K., P. Vigilanza, S. Baldelli, B. Pagliei, G. Rotilio and M. R. Ciriolo (2010). "Peroxisome proliferator-activated receptor gamma co-activator 1alpha (PGC-1alpha) and sirtuin 1 (SIRT1) reside in mitochondria: possible direct function in mitochondrial biogenesis." J Biol Chem **285**(28): 21590-21599.

Arimura, S., J. Yamamoto, G. P. Aida, M. Nakazono and N. Tsutsumi (2004). "Frequent fusion and fission of plant mitochondria with unequal nucleoid distribution." Proc Natl Acad Sci U S A **101**(20): 7805-7808.

Arnoult, D., A. Grodet, Y. J. Lee, J. Estaquier and C. Blackstone (2005). "Release of OPA1 during apoptosis participates in the rapid and complete release of cytochrome c and subsequent mitochondrial fragmentation." J Biol Chem **280**(42): 35742-35750.

Astrup, A., B. Buemann, S. Toubro and A. Raben (1996). "Defects in substrate oxidation involved in the predisposition to obesity." Proc Nutr Soc **55**(3): 817-828.

Attardi, G. and G. Schatz (1988). "Biogenesis of mitochondria." Annu Rev Cell Biol **4**: 289-333.

Au-Yong, I. T., N. Thorn, R. Ganatra, A. C. Perkins and M. E. Symonds (2009). "Brown adipose tissue and seasonal variation in humans." Diabetes **58**(11): 2583-2587.

Baan, B., H. van Dam, G. C. van der Zon, J. A. Maassen and D. M. Ouwens (2006). "The role of c-Jun N-terminal kinase, p38, and extracellular signal-regulated kinase in insulin-induced Thr69 and Thr71 phosphorylation of activating transcription factor 2." Mol Endocrinol **20**(8): 1786-1795.

Bach, D., D. Naon, S. Pich, F. X. Soriano, N. Vega, J. Rieusset, M. Laville, C. Guillet, Y. Boirie, H. Wallberg-Henriksson, M. Manco, M. Calvani, M. Castagneto, M. Palacin, G. Mingrone, J. R. Zierath, H. Vidal and A. Zorzano (2005). "Expression of Mfn2, the Charcot-Marie-Tooth neuropathy type 2A gene, in human skeletal muscle: effects of type 2 diabetes, obesity, weight loss, and the regulatory role of tumor necrosis factor alpha and interleukin-6." Diabetes **54**(9): 2685-2693.

Bach, D., S. Pich, F. X. Soriano, N. Vega, B. Baumgartner, J. Oriola, J. R. Daugaard, J. Lloberas, M. Camps, J. R. Zierath, R. Rabasa-Lhoret, H. Wallberg-Henriksson, M.

Laville, M. Palacin, H. Vidal, F. Rivera, M. Brand and A. Zorzano (2003). "Mitofusin-2 determines mitochondrial network architecture and mitochondrial metabolism. A novel regulatory mechanism altered in obesity." J Biol Chem **278**(19): 17190-17197.

Badger, A. M., J. N. Bradbeer, B. Votta, J. C. Lee, J. L. Adams and D. E. Griswold (1996). "Pharmacological profile of SB 203580, a selective inhibitor of cytokine suppressive binding protein/p38 kinase, in animal models of arthritis, bone resorption, endotoxin shock and immune function." J Pharmacol Exp Ther **279**(3): 1453-1461.

Badrinarayan, P. and G. N. Sastry (2011). "Sequence, structure, and active site analyses of p38 MAP kinase: exploiting DFG-out conformation as a strategy to design new type II leads." J Chem Inf Model **51**(1): 115-129.

Bai, Y., R. M. Shakeley and G. Attardi (2000). "Tight control of respiration by NADH dehydrogenase ND5 subunit gene expression in mouse mitochondria." Mol Cell Biol **20**(3): 805-815.

Bakkman, L., M. Fernstrom, P. Loogna, O. Rooyackers, L. Brandt and Y. T. Lagerros (2010). "Reduced respiratory capacity in muscle mitochondria of obese subjects." Obes Facts **3**(6): 371-375.

Bao, S., D. A. Jacobson, M. Wohltmann, A. Bohrer, W. Jin, L. H. Philipson and J. Turk (2008). "Glucose homeostasis, insulin secretion, and islet phospholipids in mice that overexpress iPLA2beta in pancreatic beta-cells and in iPLA2beta-null mice." Am J Physiol Endocrinol Metab **294**(2): E217-229.

Barone, F. C., E. A. Irving, A. M. Ray, J. C. Lee, S. Kassis, S. Kumar, A. M. Badger, J. J. Legos, J. A. Erhardt, E. H. Ohlstein, A. J. Hunter, D. C. Harrison, K. Philpott, B. R. Smith, J. L. Adams and A. A. Parsons (2001). "Inhibition of p38 mitogen-activated protein kinase provides neuroprotection in cerebral focal ischemia." Med Res Rev **21**(2): 129-145.

Barros, L. F., M. Young, J. Saklatvala and S. A. Baldwin (1997). "Evidence of two mechanisms for the activation of the glucose transporter GLUT1 by anisomycin: p38(MAP kinase) activation and protein synthesis inhibition in mammalian cells." J Physiol **504 (Pt 3)**: 517-525.

Barthelemy, C., H. Ogier de Baulny, J. Diaz, M. A. Cheval, P. Frachon, N. Romero, F. Goutieres, M. Fardeau and A. Lombes (2001). "Late-onset mitochondrial DNA depletion: DNA copy number, multiple deletions, and compensation." Ann Neurol **49**(5): 607-617.

Bastard, J. P., M. Maachi, C. Lagathu, M. J. Kim, M. Caron, H. Vidal, J. Capeau and B. Feve (2006). "Recent advances in the relationship between obesity, inflammation, and insulin resistance." European Cytokine Network **17**(1): 4-12.

Bellon, S., M. J. Fitzgibbon, T. Fox, H. M. Hsiao and K. P. Wilson (1999). "The structure of phosphorylated p38gamma is monomeric and reveals a conserved activation-loop conformation." Structure **7**(9): 1057-1065.

Bissantz, C., B. Kuhn and M. Stahl (2010). "A medicinal chemist's guide to molecular interactions." J Med Chem **53**(14): 5061-5084.

Bjorklund, P., A. Laurenius, E. Een, T. Olbers, H. Lonroth and L. Fandriks (2010). "Is the Roux limb a determinant for meal size after gastric bypass surgery?" Obes Surg **20**(10): 1408-1414.

Blaak, E. E. and W. H. Saris (2002). "Substrate oxidation, obesity and exercise training." Best Pract Res Clin Endocrinol Metab **16**(4): 667-678.

Blomberg N, C. D., Kenny PW, Kolmodin K. (2009). "Design of compound libraries for fragment screening." J Comput Aided Mol Des **23**: 513–525.

Bloomston, M., E. E. Zervos, M. A. Camps, S. E. Goode and A. S. Rosemurgy (1997). "Outcome following bariatric surgery in super versus morbidly obese patients: does weight matter?" Obes Surg **7**(5): 414-419.

Bluher, M. (2014). "Adipokines - removing road blocks to obesity and diabetes therapy." Mol Metab **3**(3): 230-240.

Bogacka, I., B. Ukropcova, M. McNeil, J. M. Gimble and S. R. Smith (2005). "Structural and functional consequences of mitochondrial biogenesis in human adipocytes in vitro." J Clin Endocrinol Metab **90**(12): 6650-6656.

Bogacka, I., H. Xie, G. A. Bray and S. R. Smith (2005). "Pioglitazone induces mitochondrial biogenesis in human subcutaneous adipose tissue in vivo." Diabetes **54**(5): 1392-1399.

Borson-Chazot, F., C. Harthe, F. Teboul, F. Labrousse, C. Gaume, L. Guadagnino, B. Claustrat, F. Berthezene and P. Moulin (1999). "Occurrence of hyperhomocysteinemia 1 year after gastroplasty for severe obesity." J Clin Endocrinol Metab **84**(2): 541-545.

Bost, F., M. Aouadi, L. Caron and B. Binetruy (2005). "The role of MAPKs in adipocyte differentiation and obesity." Biochimie **87**(1): 51-56.

Bournat, J. C. and C. W. Brown (2010). "Mitochondrial dysfunction in obesity." Curr Opin Endocrinol Diabetes Obes **17**(5): 446-452.

Bourne, H. R., D. A. Sanders and F. McCormick (1990). "The GTPase superfamily: a conserved switch for diverse cell functions." Nature **348**(6297): 125-132.

Bourne, H. R., D. A. Sanders and F. McCormick (1991). "The GTPase superfamily: conserved structure and molecular mechanism." Nature **349**(6305): 117-127.

Bradley, D., C. Conte, B. Mittendorfer, J. C. Eagon, J. E. Varela, E. Fabbrini, A. Gastaldelli, K. T. Chambers, X. Su, A. Okunade, B. W. Patterson and S. Klein (2012). "Gastric bypass and banding equally improve insulin sensitivity and beta cell function." J Clin Invest **122**(12): 4667-4674.

Brancho, D., N. Tanaka, A. Jaeschke, J. J. Ventura, N. Kelkar, Y. Tanaka, M. Kyuuma, T. Takeshita, R. A. Flavell and R. J. Davis (2003). "Mechanism of p38 MAP kinase activation in vivo." Genes Dev **17**(16): 1969-1978.

Brand, M. D. and D. G. Nicholls (2011). "Assessing mitochondrial dysfunction in cells." Biochem J **435**(2): 297-312.

Brasaemle, D. L. (2007). "The perilipin family of structural lipid droplet proteins: stabilization of lipid droplets and control of lipolysis." Journal of Lipid Research **48**: 2547-2559.

Bray, N. (2014). "Metabolic disorders: Pumping up muscle mitochondria." Nat Rev Drug Discov **13**(7): 496.

Brunmair, B., K. Staniek, F. Gras, N. Scharf, A. Althaym, R. Clara, M. Roden, E. Gnaiger, H. Nohl, W. Waldhausl and C. Furnsinn (2004). "Thiazolidinediones, like metformin, inhibit respiratory complex I: a common mechanism contributing to their antidiabetic actions?" Diabetes **53**(4): 1052-1059.

Buchwald, H., R. Estok, K. Fahrbach, D. Banel, M. D. Jensen, W. J. Pories, J. P. Bantle and I. Sledge (2009). "Weight and type 2 diabetes after bariatric surgery: systematic review and meta-analysis." Am J Med **122**(3): 248-256 e245.

Butina, D., M. D. Segall and K. Frankcombe (2002). "Predicting ADME properties in silico: methods and models." Drug Discov Today **7**(11): S83-88.

Cabrera, J. A., E. A. Ziemba, R. Colbert, L. B. Anderson, W. Sluiter, D. J. Duncker, T. A. Butterick, J. Sikora, H. B. Ward, R. F. Kelly and E. O. McFalls (2012). "Altered expression of mitochondrial electron transport chain proteins and improved myocardial energetic state during late ischemic preconditioning." Am J Physiol Heart Circ Physiol **302**(10): H1974-1982.

Cai, D. (2013). "Central mechanisms of obesity and related metabolic diseases." Rev Endocr Metab Disord **14**(4): 309-310.

Cao, L., H. Shitara, T. Horii, Y. Nagao, H. Imai, K. Abe, T. Hara, J. Hayashi and H. Yonekawa (2007). "The mitochondrial bottleneck occurs without reduction of mtDNA content in female mouse germ cells." Nat Genet **39**(3): 386-390.

Carlson, C. J., S. Koterski, R. J. Sciotti, G. B. Poccard and C. M. Rondinone (2003). "Enhanced basal activation of mitogen-activated protein kinases in adipocytes from type 2 diabetes: potential role of p38 in the downregulation of GLUT4 expression." Diabetes **52**(3): 634-641.

Carlsson, L. M., M. Peltonen, S. Ahlin, A. Anveden, C. Bouchard, B. Carlsson, P. Jacobson, H. Lonroth, C. Maglio, I. Naslund, C. Pirazzi, S. Romeo, K. Sjoholm, E. Sjostrom, H. Wedel, P. A. Svensson and L. Sjostrom (2012). "Bariatric surgery and prevention of type 2 diabetes in Swedish obese subjects." N Engl J Med **367**(8): 695-704.

Catta-Preta, M., M. A. Martins, T. M. Cunha Brunini, A. C. Mendes-Ribeiro, C. A. Mandarim-de-Lacerda and M. B. Aguila (2012). "Modulation of cytokines, resistin, and distribution of adipose tissue in C57BL/6 mice by different high-fat diets." Nutrition **28**(2): 212-219.

Cederberg, A., L. M. Gronning, B. Ahren, K. Tasken, P. Carlsson and S. Enerback (2001). "FOXC2 is a winged helix gene that counteracts obesity, hypertriglyceridemia, and diet-induced insulin resistance." Cell **106**(5): 563-573.

Chan, D. C. (2006). "Mitochondria: dynamic organelles in disease, aging, and development." Cell **125**(7): 1241-1252.

Chandel, N. S. (2014). "Mitochondria as signaling organelles." BMC Biol **12**: 34.

Chen, H., A. Chomyn and D. C. Chan (2005). "Disruption of fusion results in mitochondrial heterogeneity and dysfunction." J Biol Chem **280**(28): 26185-26192.

Chen, H., S. A. Detmer, A. J. Ewald, E. E. Griffin, S. E. Fraser and D. C. Chan (2003). "Mitofusins Mfn1 and Mfn2 coordinately regulate mitochondrial fusion and are essential for embryonic development." J Cell Biol **160**(2): 189-200.

Chen, H., L. Zhang, X. Li, X. Li, G. Sun, X. Yuan, L. Lei, J. Liu, L. Yin, Q. Deng, J. Wang, Z. Liu, W. Yang, Z. Wang, H. Zhang and G. Liu (2013). "Adiponectin activates the AMPK signaling pathway to regulate lipid metabolism in bovine hepatocytes." J Steroid Biochem Mol Biol **138**: 445-454.

Chen, Q., E. J. Vazquez, S. Moghaddas, C. L. Hoppel and E. J. Lesnefsky (2003). "Production of reactive oxygen species by mitochondria: central role of complex III." J Biol Chem **278**(38): 36027-36031.

Chen, W., Q. Yang and R. G. Roeder (2009). "Dynamic interactions and cooperative functions of PGC-1alpha and MED1 in TRalpha-mediated activation of the brown-fat-specific UCP-1 gene." Mol Cell **35**(6): 755-768.

Chen, W. T. and A. S. Lee (2011). "Measurement and Modification of the Expression Level of the Chaperone Protein and Signaling Regulator GRP78/BiP in Mammalian Cells." Methods Enzymol **490**: 217-233.

Christian, M. and M. G. Parker (2010). "The engineering of brown fat." J Mol Cell Biol **2**(1): 23-25.

Chung, S., P. P. Dzeja, R. S. Faustino, C. Perez-Terzic, A. Behfar and A. Terzic (2007). "Mitochondrial oxidative metabolism is required for the cardiac differentiation of stem cells." Nat Clin Pract Cardiovasc Med **4 Suppl 1**: S60-67.

Cipolat, S., O. Martins de Brito, B. Dal Zilio and L. Scorrano (2004). "OPA1 requires mitofusin 1 to promote mitochondrial fusion." Proc Natl Acad Sci U S A **101**(45): 15927-15932.

Cleveland-Donovan, K., L. A. Maile, W. G. Tsiaras, T. Tchkonia, J. L. Kirkland and C. M. Boney (2010). "IGF-I activation of the AKT pathway is impaired in visceral but

not subcutaneous preadipocytes from obese subjects." Endocrinology **151**(8): 3752-3763.

Cohen, P. (2002). "Protein kinases--the major drug targets of the twenty-first century?" Nat Rev Drug Discov **1**(4): 309-315.

Cohen, P. and A. Knebel (2006). "KESTREL: a powerful method for identifying the physiological substrates of protein kinases." Biochem J **393**(Pt 1): 1-6.

Covey, S. D., R. D. Wideman, C. McDonald, S. Unniappan, F. Huynh, A. Asadi, M. Speck, T. Webber, S. C. Chua and T. J. Kieffer (2006). "The pancreatic beta cell is a key site for mediating the effects of leptin on glucose homeostasis." Cell Metab **4**(4): 291-302.

Creely, S. J., P. G. McTernan, C. M. Kusminski, M. Fisher f, N. F. Da Silva, M. Khanolkar, M. Evans, A. L. Harte and S. Kumar (2007). "Lipopolysaccharide activates an innate immune system response in human adipose tissue in obesity and type 2 diabetes." Am J Physiol Endocrinol Metab **292**(3): E740-747.

Cristancho, A. G. and M. A. Lazar (2011). "Forming functional fat: a growing understanding of adipocyte differentiation." Nat Rev Mol Cell Biol **12**(11): 722-734.

Crunkhorn, S., F. Dearie, C. Mantzoros, H. Gami, W. S. da Silva, D. Espinoza, R. Faucette, K. Barry, A. C. Bianco and M. E. Patti (2007). "Peroxisome proliferator activator receptor gamma coactivator-1 expression is reduced in obesity: potential pathogenic role of saturated fatty acids and p38 mitogen-activated protein kinase activation." J Biol Chem **282**(21): 15439-15450.

Cuadrado, A. and A. R. Nebreda (2010). "Mechanisms and functions of p38 MAPK signalling." Biochem J **429**(3): 403-417.

Cunneen, S. A. (2008). "Review of meta-analytic comparisons of bariatric surgery with a focus on laparoscopic adjustable gastric banding." Surg Obes Relat Dis **4**(3 Suppl): S47-55.

Curat, C. A., A. Miranville, C. Sengenes, M. Diehl, C. Tonus, R. Busse and A. Bouloumie (2004). "From blood monocytes to adipose tissue-resident macrophages: induction of diapedesis by human mature adipocytes." Diabetes **53**(5): 1285-1292.

Curat, C. A., V. Wegner, C. Sengenes, A. Miranville, C. Tonus, R. Busse and A. Bouloumie (2006). "Macrophages in human visceral adipose tissue: increased accumulation in obesity and a source of resistin and visfatin." Diabetologia **49**(4): 744-747.

da Silva, A. F., F. R. Mariotti, V. Maximo and S. Campello (2014). "Mitochondria dynamism: of shape, transport and cell migration." Cell Mol Life Sci **71**(12): 2313-2324.

Davies, S. P., H. Reddy, M. Caivano and P. Cohen (2000). "Specificity and mechanism of action of some commonly used protein kinase inhibitors." Biochem J **351**(Pt 1): 95-105.

Davis, K. E., M. Moldes and S. R. Farmer (2004). "The forkhead transcription factor FoxC2 inhibits white adipocyte differentiation." J Biol Chem **279**(41): 42453-42461.

De Pauw, A., S. Demine, S. Tejerina, M. Dieu, E. Delaive, A. Kel, P. Renard, M. Raes and T. Arnould (2012). "Mild mitochondrial uncoupling does not affect mitochondrial biogenesis but downregulates pyruvate carboxylase in adipocytes: role for triglyceride content reduction." Am J Physiol Endocrinol Metab **302**(9): E1123-1141.

DeFronzo, R. A. (2004). "Pathogenesis of type 2 diabetes mellitus." Med Clin North Am **88**(4): 787-835, ix.

Deitel, M., K. Gawdat and J. Melissas (2007). "Reporting weight loss 2007." Obes Surg **17**(5): 565-568.

Dela, F. (2010). "Error in Figure - the Journal of Physiology J Physiol 588.12 (2010) pp 2023 - 2032 "Mitochondrial respiration in subcutaneous and visceral adipose tissue from patients with morbid obesity"." J Physiol.

Delettre, C., G. Lenaers, J. M. Griffoin, N. Gigarel, C. Lorenzo, P. Belenguer, L. Pelloquin, J. Grosgeorge, C. Turc-Carel, E. Perret, C. Astarie-Dequeker, L. Lasquellec, B. Arnaud, B. Ducommun, J. Kaplan and C. P. Hamel (2000). "Nuclear gene OPA1, encoding a mitochondrial dynamin-related protein, is mutated in dominant optic atrophy." Nat Genet **26**(2): 207-210.

Dickinson, R. J. and S. M. Keyse (2006). "Diverse physiological functions for dual-specificity MAP kinase phosphatases." J Cell Sci **119**(Pt 22): 4607-4615.

Dikov, D. and J. Bereiter-Hahn (2013). "Inner membrane dynamics in mitochondria." J Struct Biol.

Dikov, D. and A. S. Reichert (2011). "How to split up: lessons from mitochondria." EMBO J **30**(14): 2751-2753.

Dixon, J. B., N. E. Straznicky, E. A. Lambert, M. P. Schlaich and G. W. Lambert (2012). "Laparoscopic adjustable gastric banding and other devices for the management of obesity." Circulation **126**(6): 774-785.

Doenst, T., G. Pytel, A. Schrepper, P. Amorim, G. Farber, Y. Shingu, F. W. Mohr and M. Schwarzer (2010). "Decreased rates of substrate oxidation ex vivo predict the onset of heart failure and contractile dysfunction in rats with pressure overload." Cardiovasc Res **86**(3): 461-470.

Dolan, K., M. Hatzifotis, L. Newbury, N. Lowe and G. Fielding (2004). "A clinical and nutritional comparison of biliopancreatic diversion with and without duodenal switch." Ann Surg **240**(1): 51-56.

Dong, C., R. J. Davis and R. A. Flavell (2002). "MAP kinases in the immune response." Annu Rev Immunol **20**: 55-72.

Dridi, S. and M. Taouis (2009). "Adiponectin and energy homeostasis: consensus and controversy." J Nutr Biochem **20**(11): 831-839.

Duarte, A., A. F. Castillo, E. J. Podesta and C. Poderoso (2014). "Mitochondrial Fusion and ERK Activity Regulate Steroidogenic Acute Regulatory Protein Localization in Mitochondria." PLoS One **9**(6): e100387.

Ducluzeau, P. H., M. Priou, M. Weitheimer, M. Flamment, L. Duluc, F. Iacobazi, R. Soleti, G. Simard, A. Durand, J. Rieusset, R. Andriantsitohaina and Y. Malthiery (2011). "Dynamic regulation of mitochondrial network and oxidative functions during 3T3-L1 fat cell differentiation." J Physiol Biochem **67**(3): 285-296.

Duvezin-Caubet, S., R. Jagasia, J. Wagener, S. Hofmann, A. Trifunovic, A. Hansson, A. Chomyn, M. F. Bauer, G. Attardi, N. G. Larsson, W. Neupert and A. S. Reichert (2006). "Proteolytic processing of OPA1 links mitochondrial dysfunction to alterations in mitochondrial morphology." J Biol Chem **281**(49): 37972-37979.

Dyar, K. A., S. Ciciliot, L. E. Wright, R. S. Bienso, G. M. Tagliazucchi, V. R. Patel, M. Forcato, M. I. Paz, A. Gudiksen, F. Solagna, M. Albiero, I. Moretti, K. L. Eckel-Mahan, P. Baldi, P. Sassone-Corsi, R. Rizzuto, S. Bicciato, H. Pilegaard, B. Blaauw and S. Schiaffino (2014). "Muscle insulin sensitivity and glucose metabolism are controlled by the intrinsic muscle clock." Mol Metab **3**(1): 29-41.

Dyck, D. J. (2009). "Adipokines as regulators of muscle metabolism and insulin sensitivity." Appl Physiol Nutr Metab **34**(3): 396-402.

Ehses, S., I. Raschke, G. Mancuso, A. Bernacchia, S. Geimer, D. Tondera, J. C. Martinou, B. Westermann, E. I. Rugarli and T. Langer (2009). "Regulation of OPA1 processing and mitochondrial fusion by m-AAA protease isoenzymes and OMA1." J Cell Biol **187**(7): 1023-1036.

Eiberg, H., B. Kjer, P. Kjer and T. Rosenberg (1994). "Dominant optic atrophy (OPA1) mapped to chromosome 3q region. I. Linkage analysis." Hum Mol Genet **3**(6): 977-980.

Elachouri, G., S. Vidoni, C. Zanna, A. Pattyn, H. Boukhaddaoui, K. Gaget, P. Yu-Wai-Man, G. Gasparre, E. Sarzi, C. Delettre, A. Olichon, D. Loiseau, P. Reynier, P. F. Chinnery, A. Rotig, V. Carelli, C. P. Hamel, M. Rugolo and G. Lenaers (2011). "OPA1 links human mitochondrial genome maintenance to mtDNA replication and distribution." Genome Res **21**(1): 12-20.

Elgass, K., J. Pakay, M. T. Ryan and C. S. Palmer (2013). "Recent advances into the understanding of mitochondrial fission." Biochim Biophys Acta **1833**(1): 150-161.

Elmquist, J. K., E. Maratos-Flier, C. B. Saper and J. S. Flier (1998). "Unraveling the central nervous system pathways underlying responses to leptin." Nat Neurosci **1**(6): 445-450.

Emanuelli, B., D. Eberle, R. Suzuki and C. R. Kahn (2008). "Overexpression of the dual-specificity phosphatase MKP-4/DUSP-9 protects against stress-induced insulin resistance." Proc Natl Acad Sci U S A **105**(9): 3545-3550.

Enerbäck, S. (2010). "Brown adipose tissue in humans." Int J Obes (Lond) **34 Suppl 1**: S43-46.

Engelman, J. A., A. H. Berg, R. Y. Lewis, A. Lin, M. P. Lisanti and P. E. Scherer (1999). "Constitutively active mitogen-activated protein kinase kinase 6 (MKK6) or salicylate induces spontaneous 3T3-L1 adipogenesis." J Biol Chem **274**(50): 35630-35638.

Engelman, J. A., M. P. Lisanti and P. E. Scherer (1998). "Specific inhibitors of p38 mitogen-activated protein kinase block 3T3-L1 adipogenesis." J Biol Chem **273**(48): 32111-32120.

Enslen, H., D. M. Brancho and R. J. Davis (2000). "Molecular determinants that mediate selective activation of p38 MAP kinase isoforms." EMBO J **19**(6): 1301-1311.

Enslen, H., J. Raingeaud and R. J. Davis (1998). "Selective activation of p38 mitogen-activated protein (MAP) kinase isoforms by the MAP kinase kinases MKK3 and MKK6." J Biol Chem **273**(3): 1741-1748.

Eri, R. D., R. J. Adams, T. V. Tran, H. Tong, I. Das, D. K. Roche, I. Oancea, C. W. Png, P. L. Jeffery, G. L. Radford-Smith, M. C. Cook, T. H. Florin and M. A. McGuckin (2010). "An intestinal epithelial defect conferring ER stress results in inflammation involving both innate and adaptive immunity." Mucosal Immunol.

Escriva, H., A. Rodriguez-Pena and C. G. Vallejo (1999). "Expression of mitochondrial genes and of the transcription factors involved in the biogenesis of mitochondria Tfam, NRF-1 and NRF-2, in rat liver, testis and brain." Biochimie **81**(10): 965-971.

Eyers, P. A., M. Craxton, N. Morrice, P. Cohen and M. Goedert (1998). "Conversion of SB 203580-insensitive MAP kinase family members to drug-sensitive forms by a single amino-acid substitution." Chem Biol **5**(6): 321-328.

Fabian, M. A., W. H. Biggs, 3rd, D. K. Treiber, C. E. Atteridge, M. D. Azimioara, M. G. Benedetti, T. A. Carter, P. Ciceri, P. T. Edeen, M. Floyd, J. M. Ford, M. Galvin, J. L. Gerlach, R. M. Grotzfeld, S. Herrgard, D. E. Insko, M. A. Insko, A. G. Lai, J. M. Lelias, S. A. Mehta, Z. V. Milanov, A. M. Velasco, L. M. Wodicka, H. K. Patel, P. P. Zarrinkar and D. J. Lockhart (2005). "A small molecule-kinase interaction map for clinical kinase inhibitors." Nat Biotechnol **23**(3): 329-336.

Farzadfar, F., M. M. Finucane, G. Danaei, P. M. Pelizzari, M. J. Cowan, C. J. Paciorek, G. M. Singh, J. K. Lin, G. A. Stevens, L. M. Riley, M. Ezzati and G. Global Burden of Metabolic Risk Factors of Chronic Diseases Collaborating (2011). "National, regional, and global trends in serum total cholesterol since 1980: systematic analysis of health examination surveys and epidemiological studies with 321 country-years and 3.0 million participants." Lancet **377**(9765): 578-586.

Faust, D., C. Schmitt, F. Oesch, B. Oesch-Bartlomowicz, I. Schreck, C. Weiss and C. Dietrich (2012). "Differential p38-dependent signalling in response to cellular stress and mitogenic stimulation in fibroblasts." Cell Commun Signal **10**: 6.

Ferber, E. C., B. Peck, O. Delpuech, G. P. Bell, P. East and A. Schulze (2012). "FOXO3a regulates reactive oxygen metabolism by inhibiting mitochondrial gene expression." Cell Death Differ **19**(6): 968-979.

Fernandez-Marcos, P. J. and J. Auwerx (2011). "Regulation of PGC-1alpha, a nodal regulator of mitochondrial biogenesis." Am J Clin Nutr **93**(4): 884S-890.

Fernandez-Sanchez, A., E. Madrigal-Santillan, M. Bautista, J. Esquivel-Soto, A. Morales-Gonzalez, C. Esquivel-Chirino, I. Durante-Montiel, G. Sanchez-Rivera, C. Valadez-Vega and J. A. Morales-Gonzalez (2011). "Inflammation, oxidative stress, and obesity." Int J Mol Sci **12**(5): 3117-3132.

Ferrier, V. (2001). "Mitochondrial fission in life and death." Nat Cell Biol **3**(12): E269.

Filippakopoulos, P., Barr, A., Fedorov, O., Keates, T., Soundararajan, M., Elkins, J., Salah, E., Burgess-Brown, N., Ugochukwu, E., Pike, A.C.W., Muniz, J., Roos, A., Chaikuad, A., von Delft, F., Arrowsmith, C.H., Edwards, A.M., Weigelt, J., Bountra, C., Knapp, S., Structural Genomics Consortium "Crystal Structure of Human Mitogen Activated Protein Kinase 11 (p38 beta) in complex with Nilotinib." unpublished; accessed PDB record in July 2014.

Fliri, A. F., W. T. Loging and R. A. Volkmann (2009). "Drug effects viewed from a signal transduction network perspective." J Med Chem **52**(24): 8038-8046.

Friedewald, W. T., R. I. Levy and D. S. Fredrickson (1972). "Estimation of the concentration of low-density lipoprotein cholesterol in plasma, without use of the preparative ultracentrifuge." Clin Chem **18**(6): 499-502.

Friedman, J. M. and J. L. Halaas (1998). "Leptin and the regulation of body weight in mammals." Nature **395**(6704): 763-770.

Friesner, R. A., J. L. Banks, R. B. Murphy, T. A. Halgren, J. J. Klicic, D. T. Mainz, M. P. Repasky, E. H. Knoll, M. Shelley, J. K. Perry, D. E. Shaw, P. Francis and P. S. Shenkin (2004). "Glide: a new approach for rapid, accurate docking and scoring. 1. Method and assessment of docking accuracy." J Med Chem **47**(7): 1739-1749.

Fritz, T., L. Niederreiter, T. Adolph, R. S. Blumberg and A. Kaser (2011). "Crohn's disease: NOD2, autophagy and ER stress converge." Gut.

Fu, S., L. Yang, P. Li, O. Hofmann, L. Dicker, W. Hide, X. Lin, S. M. Watkins, A. R. Ivanov and G. S. Hotamisligil (2011). "Aberrant lipid metabolism disrupts calcium homeostasis causing liver endoplasmic reticulum stress in obesity." Nature **473**(7348): 528-531.

Fuchs, S. Y., I. Tappin and Z. Ronai (2000). "Stability of the ATF2 transcription factor is regulated by phosphorylation and dephosphorylation." J Biol Chem **275**(17): 12560-12564.

Gallagher, T. F., G. L. Seibel, S. Kassis, J. T. Laydon, M. J. Blumenthal, J. C. Lee, D. Lee, J. C. Boehm, S. M. Fier-Thompson, J. W. Abt, M. E. Soreson, J. M. Smietana, R. F. Hall, R. S. Garigipati, P. E. Bender, K. F. Erhard, A. J. Krog, G. A. Hofmann, P. L. Sheldrake, P. C. McDonnell, S. Kumar, P. R. Young and J. L. Adams (1997). "Regulation of stress-induced cytokine production by pyridinylimidazoles; inhibition of CSBP kinase." Bioorg Med Chem **5**(1): 49-64.

Galloway, C. A., H. Lee, S. Nejjar, B. S. Jhun, T. Yu, W. Hsu and Y. Yoon (2012). "Transgenic control of mitochondrial fission induces mitochondrial uncoupling and relieves diabetic oxidative stress." Diabetes **61**(8): 2093-2104.

Gandre-Babbe, S. and A. M. van der Bliek (2008). "The novel tail-anchored membrane protein Mff controls mitochondrial and peroxisomal fission in mammalian cells." Mol Biol Cell **19**(6): 2402-2412.

Gao, A. W. and R. H. Houtkooper (2014). "Mitochondrial fission: firing up mitochondria in brown adipose tissue." EMBO J **33**(5): 401-402.

Gao, C. L., G. L. Liu, S. Liu, X. H. Chen, C. B. Ji, C. M. Zhang, Z. K. Xia and X. R. Guo (2011). "Overexpression of PGC-1beta improves insulin sensitivity and mitochondrial function in 3T3-L1 adipocytes." Mol Cell Biochem **353**(1-2): 215-223.

Garcia-Fuentes, E., J. M. Garcia-Almeida, J. Garcia-Arnes, J. Rivas-Marin, J. L. Gallego-Perales, B. Gonzalez-Jimenez, I. Cardona, S. Garcia-Serrano, M. J. Garriga, M. Gonzalo, M. S. de Adana and F. Soriguer (2006). "Morbidly obese individuals with impaired fasting glucose have a specific pattern of insulin secretion and sensitivity: effect of weight loss after bariatric surgery." Obes Surg **16**(9): 1179-1188.

Garcia-Roves, P., J. M. Huss, D. H. Han, C. R. Hancock, E. Iglesias-Gutierrez, M. Chen and J. O. Holloszy (2007). "Raising plasma fatty acid concentration induces increased biogenesis of mitochondria in skeletal muscle." Proc Natl Acad Sci U S A **104**(25): 10709-10713.

Gastaldi, G., A. Russell, A. Golay, J. P. Giacobino, F. Habicht, V. Barthassat, P. Muzzin and E. Bobbioni-Harsch (2007). "Upregulation of peroxisome proliferator-activated receptor gamma coactivator gene (PGC1A) during weight loss is related to insulin sensitivity but not to energy expenditure." Diabetologia **50**(11): 2348-2355.

Gaston, D., A. D. Tsaousis and A. J. Roger (2009). "Predicting proteomes of mitochondria and related organelles from genomic and expressed sequence tag data." Methods Enzymol **457**: 21-47.

Geary, K., L. A. Knaub, I. E. Schauer, A. C. Keller, P. A. Watson, M. W. Miller, C. V. Garat, K. J. Nadeau, M. Cree-Green, S. Pugazhenthi, J. G. Regensteiner, D. J. Klemm and J. E. Reusch (2014). "Targeting mitochondria to restore failed adaptation to exercise in diabetes." Biochem Soc Trans **42**(2): 231-238.

Genoux, A., V. Pons, C. Radojkovic, F. Roux-Dalvai, G. Combes, C. Rolland, N. Malet, B. Monsarrat, F. Lopez, J. B. Ruidavets, B. Perret and L. O. Martinez (2011). "Mitochondrial inhibitory factor 1 (IF1) is present in human serum and is positively correlated with HDL-cholesterol." PLoS One **6**(9): e23949.

Gerencser, A. A., C. Chinopoulos, M. J. Birket, M. Jastroch, C. Vitelli, D. G. Nicholls and M. D. Brand (2012). "Quantitative measurement of mitochondrial membrane potential in cultured cells: calcium-induced de- and hyperpolarization of neuronal mitochondria." J Physiol **590**(Pt 12): 2845-2871.

Gesta, S., O. Bezy, M. A. Mori, Y. Macotela, K. Y. Lee and C. R. Kahn (2011). "Mesodermal developmental gene Tbx15 impairs adipocyte differentiation and mitochondrial respiration." Proc Natl Acad Sci U S A **108**(7): 2771-2776.

Gibson, T. C., E. S. Horton and E. B. Whorton (1975). "Interrelationships of insulin, glucose, lipid and anthropometric data in a natural population." Am J Clin Nutr **28**(12): 1387-1394.

Gill, A. L., M. Frederickson, A. Cleasby, S. J. Woodhead, M. G. Carr, A. J. Woodhead, M. T. Walker, M. S. Congreve, L. A. Devine, D. Tisi, M. O'Reilly, L. C. Seavers, D. J. Davis, J. Curry, R. Anthony, A. Padova, C. W. Murray, R. A. Carr and H. Jhoti (2005). "Identification of novel p38alpha MAP kinase inhibitors using fragment-based lead generation." J Med Chem **48**(2): 414-426.

Gillet, V. J., P. Willett and J. Bradshaw (2003). "Similarity searching using reduced graphs." J Chem Inf Comput Sci **43**(2): 338-345.

Goldfinger, M., M. Shmuel, S. Benhamron and B. Tirosh (2011). "Protein synthesis in plasma cells is regulated by crosstalk between endoplasmic reticulum stress and mTOR signaling." Eur J Immunol **41**(2): 491-502.

Gong, J., C. Cai, X. Liu, X. Ku, H. Jiang, D. Gao and H. Li (2013). "ChemMapper: a versatile web server for exploring pharmacology and chemical structure association based on molecular 3D similarity method." Bioinformatics **29**(14): 1827-1829.

Gregoire, F. M., C. M. Smas and H. S. Sul (1998). "Understanding adipocyte differentiation." Physiol Rev **78**(3): 783-809.

Gregor, M. F. and G. S. Hotamisligil (2007). "Adipocyte stress: the endoplasmic reticulum and metabolic disease." Journal of Lipid Research **48**(9): 1905-1914.

Gregor, M. F. and G. S. Hotamisligil (2011). "Inflammatory mechanisms in obesity." Annu Rev Immunol **29**: 415-445.

Gregor, M. F., L. Yang, E. Fabbrini, B. S. Mohammed, J. C. Eagon, G. S. Hotamisligil and S. Klein (2009). "Endoplasmic reticulum stress is reduced in tissues of obese subjects after weight loss." Diabetes **58**(3): 693-700.

Griparic, L., N. N. van der Wel, I. J. Orozco, P. J. Peters and A. M. van der Bliek (2004). "Loss of the intermembrane space protein Mgm1/OPA1 induces swelling and localized constrictions along the lengths of mitochondria." J Biol Chem **279**(18): 18792-18798.

Grollman, A. P. and M. T. Huang (1973). "Inhibitors of protein synthesis in eukaryotes: tools in cell research." Fed Proc **32**(6): 1673-1678.

Grzywocz, P., K. Mizia-Stec, M. Wybraniec and J. Chudek (2014). "Adipokines and endothelial dysfunction in acute myocardial infarction and the risk of recurrent cardiovascular events." J Cardiovasc Med (Hagerstown).

Guan, K., L. Farh, T. K. Marshall and R. J. Deschenes (1993). "Normal mitochondrial structure and genome maintenance in yeast requires the dynamin-like product of the MGM1 gene." Curr Genet **24**(1-2): 141-148.

Guigas, B., D. Detaille, C. Chauvin, C. Batandier, F. De Oliveira, E. Fontaine and X. Leverve (2004). "Metformin inhibits mitochondrial permeability transition and cell death: a pharmacological in vitro study." Biochem J **382**(Pt 3): 877-884.

Guilherme, A., J. V. Virbasius, V. Puri and M. P. Czech (2008). "Adipocyte dysfunctions linking obesity to insulin resistance and type 2 diabetes." Nat Rev Mol Cell Biol **9**(5): 367-377.

Guillery, O., F. Malka, T. Landes, E. Guillou, C. Blackstone, A. Lombes, P. Belenguer, D. Arnoult and M. Rojo (2008). "Metalloprotease-mediated OPA1 processing is modulated by the mitochondrial membrane potential." Biol Cell **100**(5): 315-325.

Guillod-Maximin, E., A. F. Roy, C. M. Vacher, A. Aubourg, V. Bailleux, A. Lorsignol, L. Penicaud, M. Parquet and M. Taouis (2009). "Adiponectin receptors are expressed in hypothalamus and colocalized with proopiomelanocortin and neuropeptide Y in rodent arcuate neurons." J Endocrinol **200**(1): 93-105.

Gujral, U. P., R. Pradeepa, M. B. Weber, K. M. Narayan and V. Mohan (2013). "Type 2 diabetes in South Asians: similarities and differences with white Caucasian and other populations." Ann N Y Acad Sci **1281**: 51-63.

Guldstrand, M., B. Ahren and U. Adamson (2003). "Improved beta-cell function after standardized weight reduction in severely obese subjects." Am J Physiol Endocrinol Metab **284**(3): E557-565.

Gum, R. J., M. M. McLaughlin, S. Kumar, Z. Wang, M. J. Bower, J. C. Lee, J. L. Adams, G. P. Livi, E. J. Goldsmith and P. R. Young (1998). "Acquisition of sensitivity of stress-activated protein kinases to the p38 inhibitor, SB 203580, by alteration of one or more amino acids within the ATP binding pocket." J Biol Chem **273**(25): 15605-15610.

Gumbs, A. A., I. M. Modlin and G. H. Ballantyne (2005). "Changes in insulin resistance following bariatric surgery: role of caloric restriction and weight loss." Obes Surg **15**(4): 462-473.

Hafner, R. P., G. C. Brown and M. D. Brand (1990). "Analysis of the control of respiration rate, phosphorylation rate, proton leak rate and protonmotive force in isolated mitochondria using the 'top-down' approach of metabolic control theory." Eur J Biochem **188**(2): 313-319.

Halgren, T. A., R. B. Murphy, R. A. Friesner, H. S. Beard, L. L. Frye, W. T. Pollard and J. L. Banks (2004). "Glide: a new approach for rapid, accurate docking and scoring. 2. Enrichment factors in database screening." J Med Chem **47**(7): 1750-1759.

Hall, J. P. and R. J. Davis (2002). "Inhibition of the p38 pathway upregulates macrophage JNK and ERK activities, and the ERK, JNK, and p38 MAP kinase pathways are reprogrammed during differentiation of the murine myeloid M1 cell line." J Cell Biochem **86**(1): 1-11.

Han, J., J. D. Lee, L. Bibbs and R. J. Ulevitch (1994). "A MAP kinase targeted by endotoxin and hyperosmolarity in mammalian cells." Science **265**(5173): 808-811.

Hara, K., T. Yamauchi and T. Kadowaki (2005). "Adiponectin: an adipokine linking adipocytes and type 2 diabetes in humans." Curr Diab Rep **5**(2): 136-140.

Harte, A. L. and P. G. McTernan (2013). "Response to comment on: Harte et al. High fat intake leads to acute postprandial exposure to circulating endotoxin in type 2 diabetic subjects. Diabetes Care 2012;35:375-382." Diabetes Care **36**(3): e43.

Harte, A. L., M. C. Varma, G. Tripathi, K. C. McGee, N. M. Al-Daghri, O. S. Al-Attas, S. Sabico, J. P. O'Hare, A. Ceriello, P. Saravanan, S. Kumar and P. G. McTernan (2012). "High fat intake leads to acute postprandial exposure to circulating endotoxin in type 2 diabetic subjects." Diabetes Care **35**(2): 375-382.

Heida, N. M., J. P. Muller, I. F. Cheng, M. Leifheit-Nestler, V. Faustin, J. Riggert, G. Hasenfuss, S. Konstantinides and K. Schafer (2010). "Effects of obesity and weight loss on the functional properties of early outgrowth endothelial progenitor cells." J Am Coll Cardiol **55**(4): 357-367.

Himpens, J., J. Dobbeleir and G. Peeters (2010). "Long-term results of laparoscopic sleeve gastrectomy for obesity." Ann Surg **252**(2): 319-324.

Honda, S., T. Aihara, M. Hontani, K. Okubo and S. Hirose (2005). "Mutational analysis of action of mitochondrial fusion factor mitofusin-2." J Cell Sci **118**(Pt 14): 3153-3161.

Hoppins, S., L. Lackner and J. Nunnari (2007). "The machines that divide and fuse mitochondria." Annu Rev Biochem **76**: 751-780.

Hotamisligil, G. S. (2006). "Inflammation and metabolic disorders." Nature **444**(7121): 860-867.

Hotamisligil, G. S. (2007). "Endoplasmic reticulum stress and inflammation in obesity and type 2 diabetes." Novartis Found Symp **286**: 86-94; discussion 94-88, 162-163, 196-203.

Hotamisligil, G. S. (2008). "Inflammation and endoplasmic reticulum stress in obesity and diabetes." Int J Obes (Lond) **32 Suppl 7**: S52-54.

Hotamisligil, G. S. and E. Erbay (2008). "Nutrient sensing and inflammation in metabolic diseases." Nat Rev Immunol **8**(12): 923-934.

Hsieh, C. J., S. W. Weng, C. W. Liou, T. K. Lin, J. B. Chen, M. M. Tiao, Y. T. Hung, I. Y. Chen, W. T. Huang and P. W. Wang (2011). "Tissue-specific differences in mitochondrial DNA content in type 2 diabetes." Diabetes Res Clin Pract **92**(1): 106-110.

Huang, P., C. A. Galloway and Y. Yoon (2011). "Control of mitochondrial morphology through differential interactions of mitochondrial fusion and fission proteins." PLoS One **6**(5): e20655.

Huang, P. I., Y. C. Chou, Y. L. Chang, Y. Chien, K. H. Chen, W. S. Song, C. H. Peng, C. H. Chang, S. D. Lee, K. H. Lu, Y. J. Chen, C. H. Kuo, C. C. Hsu, H. C. Lee and M. C. Yung (2011). "Enhanced Differentiation of Three-Gene-Reprogrammed Induced Pluripotent Stem Cells into Adipocytes via Adenoviral-Mediated PGC-1alpha Overexpression." Int J Mol Sci **12**(11): 7554-7568.

Huang, X., K. F. Eriksson, A. Vaag, M. Lehtovirta, M. Hansson, E. Laurila, T. Kanninen, B. T. Olesen, I. Kurucz, L. Koranyi and L. Groop (1999). "Insulin-regulated mitochondrial gene expression is associated with glucose flux in human skeletal muscle." Diabetes **48**(8): 1508-1514.

Hummasti, S. and G. S. Hotamisligil (2010). "Endoplasmic reticulum stress and inflammation in obesity and diabetes." Circ Res **107**(5): 579-591.

Huong, P. T., D. O. Moon, S. O. Kim, K. E. Kim, S. J. Jeong, K. W. Lee, K. S. Lee, J. H. Jang, R. L. Erikson, J. S. Ahn and B. Y. Kim (2011). "Proteasome inhibitor-I enhances tunicamycin-induced chemosensitization of prostate cancer cells through regulation of NF-κB and CHOP expression." Cell Signal.

Ingerman, E., E. M. Perkins, M. Marino, J. A. Mears, J. M. McCaffery, J. E. Hinshaw and J. Nunnari (2005). "Dnm1 forms spirals that are structurally tailored to fit mitochondria." J Cell Biol **170**(7): 1021-1027.

Ishihara, N., Y. Eura and K. Mihara (2004). "Mitofusin 1 and 2 play distinct roles in mitochondrial fusion reactions via GTPase activity." J Cell Sci **117**(Pt 26): 6535-6546.

Ishihara, N., Y. Fujita, T. Oka and K. Mihara (2006). "Regulation of mitochondrial morphology through proteolytic cleavage of OPA1." EMBO J **25**(13): 2966-2977.

Iwabu, M., T. Yamauchi, M. Okada-Iwabu, K. Sato, T. Nakagawa, M. Funata, M. Yamaguchi, S. Namiki, R. Nakayama, M. Tabata, H. Ogata, N. Kubota, I. Takamoto, Y. K. Hayashi, N. Yamauchi, H. Waki, M. Fukayama, I. Nishino, K. Tokuyama, K. Ueki, Y. Oike, S. Ishii, K. Hirose, T. Shimizu, K. Touhara and T. Kadowaki (2010). "Adiponectin and AdipoR1 regulate PGC-1alpha and mitochondria by Ca(2+) and AMPK/SIRT1." Nature **464**(7293): 1313-1319.

Iwasawa, R., A. L. Mahul-Mellier, C. Datler, E. Pazarentzos and S. Grimm (2011). "Fis1 and Bap31 bridge the mitochondria-ER interface to establish a platform for apoptosis induction." EMBO J **30**(3): 556-568.

James, D. I., P. A. Parone, Y. Mattenberger and J. C. Martinou (2003). "hFis1, a novel component of the mammalian mitochondrial fission machinery." J Biol Chem **278**(38): 36373-36379.

Jeng, J. Y., T. S. Yeh, J. W. Lee, S. H. Lin, T. H. Fong and R. H. Hsieh (2008). "Maintenance of mitochondrial DNA copy number and expression are essential for preservation of mitochondrial function and cell growth." J Cell Biochem **103**(2): 347-357.

Jheng, H. F., P. J. Tsai, S. M. Guo, L. H. Kuo, C. S. Chang, I. J. Su, C. R. Chang and Y. S. Tsai (2012). "Mitochondrial fission contributes to mitochondrial dysfunction and insulin resistance in skeletal muscle." Mol Cell Biol **32**(2): 309-319.

Jiang, Y., H. Gram, M. Zhao, L. New, J. Gu, L. Feng, F. Di Padova, R. J. Ulevitch and J. Han (1997). "Characterization of the structure and function of the fourth mem-

ber of p38 group mitogen-activated protein kinases, p38delta." J Biol Chem **272**(48): 30122-30128.

Jiang, Y., Z. Li, E. M. Schwarz, A. Lin, K. Guan, R. J. Ulevitch and J. Han (1997). "Structure-function studies of p38 mitogen-activated protein kinase. Loop 12 influences substrate specificity and autophosphorylation, but not upstream kinase selection." J Biol Chem **272**(17): 11096-11102.

Julia, C., S. Czernichow, N. Charnaux, N. Ahluwalia, V. Andreeva, M. Touvier, P. Galan and L. Fezeu (2014). "Relationships between adipokines, biomarkers of endothelial function and inflammation and risk of type 2 diabetes." Diabetes Res Clin Pract.

Jung, C., A. S. Martins, E. Niggli and N. Shirokova (2008). "Dystrophic cardiomyopathy: amplification of cellular damage by Ca2+ signalling and reactive oxygen species-generating pathways." Cardiovasc Res **77**(4): 766-773.

Jung, U. J. and M. S. Choi (2014). "Obesity and its metabolic complications: the role of adipokines and the relationship between obesity, inflammation, insulin resistance, dyslipidemia and nonalcoholic fatty liver disease." Int J Mol Sci **15**(4): 6184-6223.

Kaaman, M., L. M. Sparks, V. van Harmelen, S. R. Smith, E. Sjolin, I. Dahlman and P. Arner (2007). "Strong association between mitochondrial DNA copy number and lipogenesis in human white adipose tissue." Diabetologia **50**(12): 2526-2533.

Kamohara, S., R. Burcelin, J. L. Halaas, J. M. Friedman and M. J. Charron (1997). "Acute stimulation of glucose metabolism in mice by leptin treatment." Nature **389**(6649): 374-377.

Kaneko, S., R. H. Iida, T. Suga, T. Fukui, M. Morito and A. Yamane (2011). "Changes in triacylglycerol-accumulated fiber type, fiber type composition, and biogenesis

in the mitochondria of the soleus muscle in obese rats." Anat Rec (Hoboken) **294**(11): 1904-1912.

Kar, R., N. Mishra, P. K. Singha, M. A. Venkatachalam and P. Saikumar (2010). "Mitochondrial remodeling following fission inhibition by 15d-PGJ2 involves molecular changes in mitochondrial fusion protein OPA1." Biochem Biophys Res Commun **399**(4): 548-554.

Kayali, A. G., D. A. Austin and N. J. Webster (2000). "Stimulation of MAPK cascades by insulin and osmotic shock: lack of an involvement of p38 mitogen-activated protein kinase in glucose transport in 3T3-L1 adipocytes." Diabetes **49**(11): 1783-1793.

Keller, M. P., Y. Choi, P. Wang, D. B. Davis, M. E. Rabaglia, A. T. Oler, D. S. Stapleton, C. Argmann, K. L. Schueler, S. Edwards, H. A. Steinberg, E. Chaibub Neto, R. Kleinhanz, S. Turner, M. K. Hellerstein, E. E. Schadt, B. S. Yandell, C. Kendziorski and A. D. Attie (2008). "A gene expression network model of type 2 diabetes links cell cycle regulation in islets with diabetes susceptibility." Genome Res **18**(5): 706-716.

Kelley, D. E., J. He, E. V. Menshikova and V. B. Ritov (2002). "Dysfunction of mitochondria in human skeletal muscle in type 2 diabetes." Diabetes **51**(10): 2944-2950.

Kelly, R. D., A. Mahmud, M. McKenzie, I. A. Trounce and J. C. St John (2012). "Mitochondrial DNA copy number is regulated in a tissue specific manner by DNA methylation of the nuclear-encoded DNA polymerase gamma A." Nucleic Acids Res **40**(20): 10124-10138.

Kennedy, G. C. (1953). "The role of depot fat in the hypothalamic control of food intake in the rat." Proc R Soc Lond B Biol Sci **140**(901): 578-596.

Khazen, W., P. M'Bika J, C. Tomkiewicz, C. Benelli, C. Chany, A. Achour and C. Forest (2005). "Expression of macrophage-selective markers in human and rodent adipocytes." FEBS Lett **579**(25): 5631-5634.

Kim, I., C. W. Shu, W. Xu, C. W. Shiau, D. Grant, S. Vasile, N. D. Cosford and J. C. Reed (2009). "Chemical biology investigation of cell death pathways activated by endoplasmic reticulum stress reveals cytoprotective modulators of ASK1." J Biol Chem **284**(3): 1593-1603.

Kim, J., Y. S. Choi, S. Lim, K. Yea, J. H. Yoon, D. J. Jun, S. H. Ha, J. W. Kim, J. H. Kim, P. G. Suh, S. H. Ryu and T. G. Lee (2010). "Comparative analysis of the secretory proteome of human adipose stromal vascular fraction cells during adipogenesis." Proteomics **10**(3): 394-405.

Kim, J. Y., E. van de Wall, M. Laplante, A. Azzara, M. E. Trujillo, S. M. Hofmann, T. Schraw, J. L. Durand, H. Li, G. Li, L. A. Jelicks, M. F. Mehler, D. Y. Hui, Y. Deshaies, G. I. Shulman, G. J. Schwartz and P. E. Scherer (2007). "Obesity-associated improvements in metabolic profile through expansion of adipose tissue." J Clin Invest **117**(9): 2621-2637.

Kimata, Y. and K. Kohno (2010). "Endoplasmic reticulum stress-sensing mechanisms in yeast and mammalian cells." Curr Opin Cell Biol.

Kita, T., H. Nishida, H. Shibata, S. Niimi, T. Higuti and N. Arakaki (2009). "Possible role of mitochondrial remodelling on cellular triacylglycerol accumulation." J Biochem **146**(6): 787-796.

Kitamura, M. (2011). "Control of NF-κB and Inflammation by the Unfolded Protein Response." Int Rev Immunol **30**(1): 4-15.

Knights, A. J., A. P. Funnell, R. C. Pearson, M. Crossley and K. S. Bell-Anderson (2014). "Adipokines and insulin action: A sensitive issue." Adipocyte **3**(2): 88-96.

Koliaki, C. and M. Roden (2014). "Do mitochondria care about insulin resistance?" Mol Metab **3**(4): 351-353.

Kornmann, B. (2014). "Quality control in mitochondria: use it, break it, fix it, trash it." F1000Prime Rep **6**: 15.

Kos, K., A. L. Harte, N. F. da Silva, A. Tonchev, G. Chaldakov, S. James, D. R. Snead, B. Hoggart, J. P. O'Hare, P. G. McTernan and S. Kumar (2007). "Adiponectin and resistin in human cerebrospinal fluid and expression of adiponectin receptors in the human hypothalamus." J Clin Endocrinol Metab **92**(3): 1129-1136.

Koshiba, T., S. A. Detmer, J. T. Kaiser, H. Chen, J. M. McCaffery and D. C. Chan (2004). "Structural basis of mitochondrial tethering by mitofusin complexes." Science **305**(5685): 858-862.

Kozlowska, A. and I. Kowalska (2006). "[The role of adiponectin in pathogenesis of metabolic syndrome and cardiovascular disease]." Endokrynol Pol **57**(6): 626-632.

Kraunsoe, R., R. Boushel, C. N. Hansen, P. Schjerling, K. Qvortrup, M. Stockel, K. J. Mikines and F. Dela (2010). "Mitochondrial respiration in subcutaneous and visceral adipose tissue from patients with morbid obesity." J Physiol **588**(Pt 12): 2023-2032.

Kumar, S., M. S. Jiang, J. L. Adams and J. C. Lee (1999). "Pyridinylimidazole compound SB 203580 inhibits the activity but not the activation of p38 mitogen-activated protein kinase." Biochem Biophys Res Commun **263**(3): 825-831.

Kumar, S., P. C. McDonnell, R. J. Gum, A. T. Hand, J. C. Lee and P. R. Young (1997). "Novel homologues of CSBP/p38 MAP kinase: activation, substrate specificity and sensitivity to inhibition by pyridinyl imidazoles." Biochem Biophys Res Commun **235**(3): 533-538.

Kusminski, C. M., W. L. Holland, K. Sun, J. Park, S. B. Spurgin, Y. Lin, G. R. Askew, J. A. Simcox, D. A. McClain, C. Li and P. E. Scherer (2012). "MitoNEET-driven alterations in adipocyte mitochondrial activity reveal a crucial adaptive process that preserves insulin sensitivity in obesity." Nat Med **18**(10): 1539-1549.

Labrousse, A. M., M. D. Zappaterra, D. A. Rube and A. M. van der Bliek (1999). "C. elegans dynamin-related protein DRP-1 controls severing of the mitochondrial outer membrane." Mol Cell **4**(5): 815-826.

Landes, T., L. J. Emorine, D. Courilleau, M. Rojo, P. Belenguer and L. Arnaune-Pelloquin (2010). "The BH3-only Bnip3 binds to the dynamin Opa1 to promote mitochondrial fragmentation and apoptosis by distinct mechanisms." EMBO Rep **11**(6): 459-465.

Lappas, M. (2014). "Effect of pre-existing maternal obesity, gestational diabetes and adipokines on the expression of genes involved in lipid metabolism in adipose tissue." Metabolism **63**(2): 250-262.

Las, G. and O. S. Shirihai (2014). "Miro1: new wheels for transferring mitochondria." EMBO J **33**(9): 939-941.

Lau, E. and Z. A. Ronai (2012). "ATF2 - at the crossroad of nuclear and cytosolic functions." J Cell Sci **125**(Pt 12): 2815-2824.

Lee, J. C., S. Kumar, D. E. Griswold, D. C. Underwood, B. J. Votta and J. L. Adams (2000). "Inhibition of p38 MAP kinase as a therapeutic strategy." Immunopharmacology **47**(2-3): 185-201.

Lee, K. P. and F. Sicheri (2011). "Principles of IRE1 Modulation Using Chemical Tools." Methods Enzymol **490**: 271-294.

Lee, Y. J., S. Y. Jeong, M. Karbowski, C. L. Smith and R. J. Youle (2004). "Roles of the mammalian mitochondrial fission and fusion mediators Fis1, Drp1, and Opa1 in apoptosis." Mol Biol Cell **15**(11): 5001-5011.

Legros, F., A. Lombes, P. Frachon and M. Rojo (2002). "Mitochondrial fusion in human cells is efficient, requires the inner membrane potential, and is mediated by mitofusins." Mol Biol Cell **13**(12): 4343-4354.

Lehr, S., S. Hartwig and H. Sell (2012). "Adipokines: a treasure trove for the discovery of biomarkers for metabolic disorders." Proteomics Clin Appl **6**(1-2): 91-101.

Lemoine, A. Y., S. Ledoux, I. Queguiner, S. Calderari, C. Mechler, S. Msika, P. Corvol and E. Larger (2012). "Link between adipose tissue angiogenesis and fat accumulation in severely obese subjects." J Clin Endocrinol Metab **97**(5): E775-780.

Levy, P., M. Fried, F. Santini and N. Finer (2007). "The comparative effects of bariatric surgery on weight and type 2 diabetes." Obes Surg **17**(9): 1248-1256.

Li, C. and L. M. Colosi (2013). "Improving the usefulness of molecular similarity-based chemical prioritization strategies." SAR QSAR Environ Res **24**(8): 679-694.

Li, Z., Y. Jiang, R. J. Ulevitch and J. Han (1996). "The primary structure of p38 gamma: a new member of p38 group of MAP kinases." Biochem Biophys Res Commun **228**(2): 334-340.

Liang, S. H., W. Zhang, B. C. McGrath, P. Zhang and D. R. Cavener (2006). "PERK (eIF2alpha kinase) is required to activate the stress-activated MAPKs and induce the expression of immediate-early genes upon disruption of ER calcium homoeostasis." Biochem J **393**(Pt 1): 201-209.

Lidell, M. E. and S. Enerbäck (2010). "Brown adipose tissue--a new role in humans?" Nat Rev Endocrinol **6**(6): 319-325.

Lidell, M. E., E. L. Seifert, R. Westergren, M. Heglind, A. Gowing, V. Sukonina, Z. Arani, P. Itkonen, S. Wallin, F. Westberg, J. Fernandez-Rodriguez, M. Laakso, T. Nilsson, X. R. Peng, M. E. Harper and S. Enerback (2011). "The adipocyte-expressed forkhead transcription factor Foxc2 regulates metabolism through altered mitochondrial function." Diabetes **60**(2): 427-435.

Liesa, M., M. Palacin and A. Zorzano (2009). "Mitochondrial dynamics in mammalian health and disease." Physiol Rev **89**(3): 799-845.

Liesa, M. and O. S. Shirihai (2013). "Mitochondrial dynamics in the regulation of nutrient utilization and energy expenditure." Cell Metab **17**(4): 491-506.

Liew, C. W., J. Boucher, J. K. Cheong, C. Vernochet, H. J. Koh, C. Mallol, K. Townsend, D. Langin, D. Kawamori, J. Hu, Y. H. Tseng, M. K. Hellerstein, S. R. Farmer, L. Goodyear, A. Doria, M. Bluher, S. I. Hsu and R. N. Kulkarni (2013). "Ablation of TRIP-Br2, a regulator of fat lipolysis, thermogenesis and oxidative metabolism, prevents diet-induced obesity and insulin resistance." Nat Med **19**(2): 217-226.

Lin, E., S. S. Davis, J. Srinivasan, J. F. Sweeney, T. R. Ziegler, L. Phillips and N. Gletsu-Miller (2009). "Dual mechanism for type-2 diabetes resolution after Roux-en-Y gastric bypass." Am Surg **75**(6): 498-502; discussion 502-493.

Linnane, A. W., S. Marzuki, T. Ozawa and M. Tanaka (1989). "Mitochondrial DNA mutations as an important contributor to ageing and degenerative diseases." Lancet **1**(8639): 642-645.

Lipinski, C. F. L., F. , Beryl W. Dominy, B and Feeney, P.J. (1997). "Experimental and computational approaches to estimate solubility and permeability in drug discovery and development settings." Advanced Drug Delivery Reviews **23**(1-3): 3-25.

Lisnock, J., A. Tebben, B. Frantz, E. A. O'Neill, G. Croft, S. J. O'Keefe, B. Li, C. Hacker, S. de Laszlo, A. Smith, B. Libby, N. Liverton, J. Hermes and P. LoGrasso (1998). "Molecular basis for p38 protein kinase inhibitor specificity." Biochemistry **37**(47): 16573-16581.

Liu, D., Y. Lin, T. Kang, B. Huang, W. Xu, M. Garcia-Barrio, M. Olatinwo, R. Matthews, Y. E. Chen and W. E. Thompson (2012). "Mitochondrial dysfunction and adipogenic reduction by prohibitin silencing in 3T3-L1 cells." PLoS One **7**(3): e34315.

Liu, M., L. Guo, Y. Liu, Y. Pei, N. Li, M. Jin, L. Ma, Z. Li, B. Sun and C. Li (2014). "Adipose stromal-vascular fraction-derived paracrine factors regulate adipogenesis." Mol Cell Biochem **385**(1-2): 115-123.

Liu, Q., L. Chen, L. Hu, Y. Guo and X. Shen (2010). "Small molecules from natural sources, targeting signaling pathways in diabetes." Biochim Biophys Acta **1799**(10-12): 854-865.

Liu, Q., L. Chen, L. Hu, Y. Guo and X. Shen (2010). "Small molecules from natural sources, targeting signaling pathways in diabetes." Biochim Biophys Acta **1799**(10-12): 854-865.

Lodhi, I. J., L. Yin, A. P. Jensen-Urstad, K. Funai, T. Coleman, J. H. Baird, M. K. El Ramahi, B. Razani, H. Song, F. Fu-Hsu, J. Turk and C. F. Semenkovich (2012). "Inhibiting adipose tissue lipogenesis reprograms thermogenesis and PPARgamma activation to decrease diet-induced obesity." Cell Metab **16**(2): 189-201.

Loiseau, D., A. Chevrollier, C. Verny, V. Guillet, N. Gueguen, M. A. Pou de Crescenzo, M. Ferre, M. C. Malinge, A. Guichet, G. Nicolas, P. Amati-Bonneau, Y. Malthiery, D. Bonneau and P. Reynier (2007). "Mitochondrial coupling defect in Charcot-Marie-Tooth type 2A disease." Ann Neurol **61**(4): 315-323.

Loson, O. C., Z. Song, H. Chen and D. C. Chan (2013). "Fis1, Mff, MiD49, and MiD51 mediate Drp1 recruitment in mitochondrial fission." Mol Biol Cell **24**(5): 659-667.

Lovy, A., A. J. Molina, F. M. Cerqueira, K. Trudeau and O. S. Shirihai (2012). "A faster, high resolution, mtPA-GFP-based mitochondrial fusion assay acquiring kinetic data of multiple cells in parallel using confocal microscopy." J Vis Exp(65): e3991.

Lowell, B. B. and G. I. Shulman (2005). "Mitochondrial dysfunction and type 2 diabetes." Science **307**(5708): 384-387.

Ma, X. L., S. Kumar, F. Gao, C. S. Louden, B. L. Lopez, T. A. Christopher, C. Wang, J. C. Lee, G. Z. Feuerstein and T. L. Yue (1999). "Inhibition of p38 mitogen-activated protein kinase decreases cardiomyocyte apoptosis and improves cardiac function after myocardial ischemia and reperfusion." Circulation **99**(13): 1685-1691.

Macias, A. T., M. Y. Mia, G. Xia, J. Hayashi and A. D. MacKerell, Jr. (2005). "Lead validation and SAR development via chemical similarity searching; application to compounds targeting the pY+3 site of the SH2 domain of p56lck." J Chem Inf Model **45**(6): 1759-1766.

Maekawa, T., W. Jin and S. Ishii (2010). "The role of ATF-2 family transcription factors in adipocyte differentiation: antiobesity effects of p38 inhibitors." Mol Cell Biol **30**(3): 613-625.

Magalhaes, J., P. Venditti, P. J. Adhihetty, J. J. Ramsey and A. Ascensao (2014). "Mitochondria in health and disease." Oxid Med Cell Longev **2014**: 814042.

Mah, E. and R. S. Bruno (2012). "Postprandial hyperglycemia on vascular endothelial function: mechanisms and consequences." Nutr Res **32**(10): 727-740.

Malet, H., B. Coutard, S. Jamal, H. Dutartre, N. Papageorgiou, M. Neuvonen, T. Ahola, N. Forrester, E. A. Gould, D. Lafitte, F. Ferron, J. Lescar, A. E. Gorbalenya, X. de Lamballerie and B. Canard (2009). "The crystal structures of Chikungunya and Venezuelan equine encephalitis virus nsP3 macro domains define a conserved adenosine binding pocket." J Virol **83**(13): 6534-6545.

Malka, F., O. Guillery, C. Cifuentes-Diaz, E. Guillou, P. Belenguer, A. Lombes and M. Rojo (2005). "Separate fusion of outer and inner mitochondrial membranes." EMBO Rep **6**(9): 853-859.

Mansour, S. J., K. A. Resing, J. M. Candi, A. S. Hermann, J. W. Gloor, K. R. Herskind, M. Wartmann, R. J. Davis and N. G. Ahn (1994). "Mitogen-activated protein (MAP) kinase phosphorylation of MAP kinase kinase: determination of phosphorylation sites by mass spectrometry and site-directed mutagenesis." J Biochem **116**(2): 304-314.

Marechal-Drouard, L., M. Sissler and I. Tarassov (2014). "Mitochondria: an organelle for life." Biochimie **100**: 1-2.

Mari, A., M. Manco, C. Guidone, G. Nanni, M. Castagneto, G. Mingrone and E. Ferrannini (2006). "Restoration of normal glucose tolerance in severely obese patients after bilio-pancreatic diversion: role of insulin sensitivity and beta cell function." Diabetologia **49**(9): 2136-2143.

Matsukawa, J., A. Matsuzawa, K. Takeda and H. Ichijo (2004). "The ASK1-MAP kinase cascades in mammalian stress response." J Biochem **136**(3): 261-265.

Matsuzawa, A., H. Nishitoh, K. Tobiume, K. Takeda and H. Ichijo (2002). "Physiological roles of ASK1-mediated signal transduction in oxidative stress- and endoplasmic reticulum stress-induced apoptosis: advanced findings from ASK1 knockout mice." Antioxid Redox Signal **4**(3): 415-425.

Matthews, D. R., J. P. Hosker, A. S. Rudenski, B. A. Naylor, D. F. Treacher and R. C. Turner (1985). "Homeostasis model assessment: insulin resistance and beta-cell

function from fasting plasma glucose and insulin concentrations in man." Diabetologia **28**(7): 412-419.

Medeiros, D. M. (2008). "Assessing mitochondria biogenesis." Methods **46**(4): 288-294.

Medina-Gomez, G., S. L. Gray, L. Yetukuri, K. Shimomura, S. Virtue, M. Campbell, R. K. Curtis, M. Jimenez-Linan, M. Blount, G. S. Yeo, M. Lopez, T. Seppanen-Laakso, F. M. Ashcroft, M. Oresic and A. Vidal-Puig (2007). "PPAR gamma 2 prevents lipotoxicity by controlling adipose tissue expandability and peripheral lipid metabolism." PLoS Genet **3**(4): e64.

Meeusen, S., R. DeVay, J. Block, A. Cassidy-Stone, S. Wayson, J. M. McCaffery and J. Nunnari (2006). "Mitochondrial inner-membrane fusion and crista maintenance requires the dynamin-related GTPase Mgm1." Cell **127**(2): 383-395.

Mercer, T. R., S. Neph, M. E. Dinger, J. Crawford, M. A. Smith, A. M. Shearwood, E. Haugen, C. P. Bracken, O. Rackham, J. A. Stamatoyannopoulos, A. Filipovska and J. S. Mattick (2011). "The human mitochondrial transcriptome." Cell **146**(4): 645-658.

Metz, J. T., E. F. Johnson, N. B. Soni, P. J. Merta, L. Kifle and P. J. Hajduk (2011). "Navigating the kinome." Nat Chem Biol **7**(4): 200-202.

Michel, S., A. Wanet, A. De Pauw, G. Rommelaere, T. Arnould and P. Renard (2012). "Crosstalk between mitochondrial (dys)function and mitochondrial abundance." J Cell Physiol **227**(6): 2297-2310.

Miczke, A., M. Szulinska, P. Bogdanski and D. Pupek-Musialik (2006). "[Does a relationship exist between plasma adiponectin concentration and selected parameters of metabolic syndrome?]." Pol Merkur Lekarski **21**(122): 170-172; discussion 173.

Miller, F. J., F. L. Rosenfeldt, C. Zhang, A. W. Linnane and P. Nagley (2003). "Precise determination of mitochondrial DNA copy number in human skeletal and cardiac muscle by a PCR-based assay: lack of change of copy number with age." Nucleic Acids Res **31**(11): e61.

Mingrone, G., M. Manco, M. Calvani, M. Castagneto, D. Naon and A. Zorzano (2005). "Could the low level of expression of the gene encoding skeletal muscle mitofusin-2 account for the metabolic inflexibility of obesity?" Diabetologia **48**(10): 2108-2114.

Mitra, R., D. P. Nogee, J. F. Zechner, K. Yea, C. M. Gierasch, A. Kovacs, D. M. Medeiros, D. P. Kelly and J. G. Duncan (2012). "The transcriptional coactivators, PGC-1alpha and beta, cooperate to maintain cardiac mitochondrial function during the early stages of insulin resistance." J Mol Cell Cardiol **52**(3): 701-710.

Moffett, K., Z. Konteatis, D. Nguyen, R. Shetty, J. Ludington, T. Fujimoto, K. J. Lee, X. Chai, H. Namboodiri, M. Karpusas, B. Dorsey, F. Guarnieri, M. Bukhtiyarova, E. Springman and E. Michelotti (2011). "Discovery of a novel class of non-ATP site DFG-out state p38 inhibitors utilizing computationally assisted virtual fragment-based drug design (vFBDD)." Bioorg Med Chem Lett **21**(23): 7155-7165.

Mojiminiyi, O. A., N. A. Abdella, M. Al Arouj and A. Ben Nakhi (2007). "Adiponectin, insulin resistance and clinical expression of the metabolic syndrome in patients with Type 2 diabetes." Int J Obes (Lond) **31**(2): 213-220.

Monte, S. V., J. A. Caruana, H. Ghanim, C. L. Sia, K. Korzeniewski, J. J. Schentag and P. Dandona (2012). "Reduction in endotoxemia, oxidative and inflammatory stress, and insulin resistance after Roux-en-Y gastric bypass surgery in patients with morbid obesity and type 2 diabetes mellitus." Surgery **151**(4): 587-593.

Morel, C., G. Ibarz, C. Oiry, E. Carnazzi, G. Berge, D. Gagne, J. C. Galleyrand and J. Martinez (2005). "Cross-interactions of two p38 mitogen-activated protein (MAP) kinase inhibitors and two cholecystokinin (CCK) receptor antagonists

with the CCK1 receptor and p38 MAP kinase." J Biol Chem **280**(22): 21384-21393.

Morris, M. J., E. Velkoska and T. J. Cole (2005). "Central and peripheral contributions to obesity-associated hypertension: impact of early overnourishment." Exp Physiol **90**(5): 697-702.

Mouli, P. K., G. Twig and O. S. Shirihai (2009). "Frequency and selectivity of mitochondrial fusion are key to its quality maintenance function." Biophys J **96**(9): 3509-3518.

Mudhasani, R., V. Puri, K. Hoover, M. P. Czech, A. N. Imbalzano and S. N. Jones (2010). "Dicer is required for the formation of white but not brown adipose tissue." J Cell Physiol.

Mueller, E. (2013). "Understanding the variegation of fat: Novel regulators of adipocyte differentiation and fat tissue biology." Biochim Biophys Acta.

Murholm, M., K. Dixen, K. Qvortrup, L. H. Hansen, E. Z. Amri, L. Madsen, G. Barbatelli, B. Quistorff and J. B. Hansen (2009). "Dynamic regulation of genes involved in mitochondrial DNA replication and transcription during mouse brown fat cell differentiation and recruitment." PLoS One **4**(12): e8458.

Murray, A. J., M. A. Cole, C. A. Lygate, C. A. Carr, D. J. Stuckey, S. E. Little, S. Neubauer and K. Clarke (2008). "Increased mitochondrial uncoupling proteins, respiratory uncoupling and decreased efficiency in the chronically infarcted rat heart." J Mol Cell Cardiol **44**(4): 694-700.

Mustelin, L., K. H. Pietilainen, A. Rissanen, A. R. Sovijarvi, P. Piirila, J. Naukkarinen, L. Peltonen, J. Kaprio and H. Yki-Jarvinen (2008). "Acquired obesity and poor physical fitness impair expression of genes of mitochondrial oxidative phosphorylation in monozygotic twins discordant for obesity." Am J Physiol Endocrinol Metab **295**(1): E148-154.

Nagata, Y., N. Takahashi, R. J. Davis and K. Todokoro (1998). "Activation of p38 MAP kinase and JNK but not ERK is required for erythropoietin-induced erythroid differentiation." Blood **92**(6): 1859-1869.

Nakada, K., K. Inoue, T. Ono, K. Isobe, A. Ogura, Y. I. Goto, I. Nonaka and J. I. Hayashi (2001). "Inter-mitochondrial complementation: Mitochondria-specific system preventing mice from expression of disease phenotypes by mutant mtDNA." Nat Med **7**(8): 934-940.

Natoudi, M., S. G. Panousopoulos, N. Memos, E. Menenakos, G. Zografos, E. Leandros and K. Albanopoulos (2014). "Laparoscopic sleeve gastrectomy for morbid obesity and glucose metabolism: a new perspective." Surg Endosc **28**(3): 1027-1033.

Nawrocki, A. R., M. W. Rajala, E. Tomas, U. B. Pajvani, A. K. Saha, M. E. Trumbauer, Z. Pang, A. S. Chen, N. B. Ruderman, H. Chen, L. Rossetti and P. E. Scherer (2006). "Mice lacking adiponectin show decreased hepatic insulin sensitivity and reduced responsiveness to peroxisome proliferator-activated receptor gamma agonists." J Biol Chem **281**(5): 2654-2660.

Neff, K. J. H. a. l. R., C.W (2013). "Obesity: The diagnosis and Candidate selection." J Clin Pathol. **66**(2): 90-98.

Nesher, R., L. Della Casa, Y. Litvin, J. Sinai, G. Del Rio, B. Pevsner, Y. Wax and E. Cerasi (1987). "Insulin deficiency and insulin resistance in type 2 (non-insulin-dependent) diabetes: quantitative contributions of pancreatic and peripheral responses to glucose homeostasis." Eur J Clin Invest **17**(3): 266-274.

Nicholls, D. (2002). "Mitochondrial bioenergetics, aging, and aging-related disease." Sci Aging Knowledge Environ **2002**(31): pe12.

Nicholls, D. G., L. Johnson-Cadwell, S. Vesce, M. Jekabsons and N. Yadava (2007). "Bioenergetics of mitochondria in cultured neurons and their role in glutamate excitotoxicity." J Neurosci Res **85**(15): 3206-3212.

Nijhawan, S., W. Richards, M. F. O'Hea, J. P. Audia and D. F. Alvarez (2013). "Bariatric surgery rapidly improves mitochondrial respiration in morbidly obese patients." Surg Endosc **27**(12): 4569-4573.

Niskanen, L., M. Uusitupa, H. Sarlund, O. Siitonen, L. Paljarvi and M. Laakso (1996). "The effects of weight loss on insulin sensitivity, skeletal muscle composition and capillary density in obese non-diabetic subjects." Int J Obes Relat Metab Disord **20**(2): 154-160.

Nunnari, J. and A. Suomalainen (2012). "Mitochondria: in sickness and in health." Cell **148**(6): 1145-1159.

Nystad, T., M. Melhus, M. Brustad and E. Lund (2010). "Ethnic differences in the prevalence of general and central obesity among the Sami and Norwegian populations: the SAMINOR study." Scand J Public Health **38**(1): 17-24.

Oelkrug, R., M. Kutschke, C. W. Meyer, G. Heldmaier and M. Jastroch (2010). "Uncoupling protein 1 decreases superoxide production in brown adipose tissue mitochondria." J Biol Chem **285**(29): 21961-21968.

Oikawa, D. and Y. Kimata (2011). "Experimental Approaches for Elucidation of Stress-Sensing Mechanisms of the IRE1 Family Proteins." Methods Enzymol **490**: 195-216.

Okamoto, K. and J. M. Shaw (2005). "Mitochondrial morphology and dynamics in yeast and multicellular eukaryotes." Annu Rev Genet **39**: 503-536.

Olichon, A., L. J. Emorine, E. Descoins, L. Pelloquin, L. Brichese, N. Gas, E. Guillou, C. Delettre, A. Valette, C. P. Hamel, B. Ducommun, G. Lenaers and P. Belenguer

(2002). "The human dynamin-related protein OPA1 is anchored to the mitochondrial inner membrane facing the inter-membrane space." FEBS Lett **523**(1-3): 171-176.

Olichon, A., T. Landes, L. Arnaune-Pelloquin, L. J. Emorine, V. Mils, A. Guichet, C. Delettre, C. Hamel, P. Amati-Bonneau, D. Bonneau, P. Reynier, G. Lenaers and P. Belenguer (2007). "Effects of OPA1 mutations on mitochondrial morphology and apoptosis: relevance to ADOA pathogenesis." J Cell Physiol **211**(2): 423-430.

Ortega Martinez de Victoria, E., X. Xu, J. Koska, A. M. Francisco, M. Scalise, A. W. Ferrante, Jr. and J. Krakoff (2009). "Macrophage content in subcutaneous adipose tissue: associations with adiposity, age, inflammatory markers, and whole-body insulin action in healthy Pima Indians." Diabetes **58**(2): 385-393.

Osellame, L. D., T. S. Blacker and M. R. Duchen (2012). "Cellular and molecular mechanisms of mitochondrial function." Best Pract Res Clin Endocrinol Metab **26**(6): 711-723.

Otera, H., C. Wang, M. M. Cleland, K. Setoguchi, S. Yokota, R. J. Youle and K. Mihara (2010). "Mff is an essential factor for mitochondrial recruitment of Drp1 during mitochondrial fission in mammalian cells." J Cell Biol **191**(6): 1141-1158.

Owen, M. R., E. Doran and A. P. Halestrap (2000). "Evidence that metformin exerts its anti-diabetic effects through inhibition of complex 1 of the mitochondrial respiratory chain." Biochem J **348 Pt 3**: 607-614.

Palaniyandi, S. S., X. Qi, G. Yogalingam, J. C. Ferreira and D. Mochly-Rosen (2010). "Regulation of mitochondrial processes: a target for heart failure." Drug Discov Today Dis Mech **7**(2): e95-e102.

Palmer, C. S., L. D. Osellame, D. Laine, O. S. Koutsopoulos, A. E. Frazier and M. T. Ryan (2011). "MiD49 and MiD51, new components of the mitochondrial fission machinery." EMBO Rep **12**(6): 565-573.

Pao, G. M. and M. H. Saier, Jr. (1994). "The N-terminal, putative, mitochondrial targeting domain of the mitochondrial genome maintenance protein (MGM1) in yeast is homologous to the bacterial ribonuclease inhibitor, barstar." Mol Biol Evol **11**(6): 964-965.

Pargellis, C., L. Tong, L. Churchill, P. F. Cirillo, T. Gilmore, A. G. Graham, P. M. Grob, E. R. Hickey, N. Moss, S. Pav and J. Regan (2002). "Inhibition of p38 MAP kinase by utilizing a novel allosteric binding site." Nat Struct Biol **9**(4): 268-272.

Park, S. and K. Schulten (2004). "Calculating potentials of mean force from steered molecular dynamics simulations." J Chem Phys **120**(13): 5946-5961.

Parra, V., H. E. Verdejo, M. Iglewski, A. Del Campo, R. Troncoso, D. Jones, Y. Zhu, J. Kuzmicic, C. Pennanen, C. Lopez-Crisosto, F. Jana, J. Ferreira, E. Noguera, M. Chiong, D. A. Bernlohr, A. Klip, J. A. Hill, B. A. Rothermel, E. D. Abel, A. Zorzano and S. Lavandero (2014). "Insulin stimulates mitochondrial fusion and function in cardiomyocytes via the Akt-mTOR-NFkappaB-Opa-1 signaling pathway." Diabetes **63**(1): 75-88.

Patel, S. B., P. M. Cameron, S. J. O'Keefe, B. Frantz-Wattley, J. Thompson, E. A. O'Neill, T. Tennis, L. Liu, J. W. Becker and G. Scapin (2009). "The three-dimensional structure of MAP kinase p38beta: different features of the ATP-binding site in p38beta compared with p38alpha." Acta Crystallogr D Biol Crystallogr **65**(Pt 8): 777-785.

Peinado, J. R., Y. Jimenez-Gomez, M. R. Pulido, M. Ortega-Bellido, C. Diaz-Lopez, F. J. Padillo, J. Lopez-Miranda, R. Vazquez-Martinez and M. M. Malagon (2010). "The stromal-vascular fraction of adipose tissue contributes to major differences between subcutaneous and visceral fat depots." Proteomics **10**(18): 3356-3366.

Pelleymounter, M. A., M. J. Cullen, M. B. Baker, R. Hecht, D. Winters, T. Boone and F. Collins (1995). "Effects of the obese gene product on body weight regulation in ob/ob mice." Science **269**(5223): 540-543.

Peng, J. Y., C. C. Lin, Y. J. Chen, L. S. Kao, Y. C. Liu, C. C. Chou, Y. H. Huang, F. R. Chang, Y. C. Wu, Y. S. Tsai and C. N. Hsu (2011). "Automatic morphological subtyping reveals new roles of caspases in mitochondrial dynamics." PLoS Comput Biol **7**(10): e1002212.

Perry, B. and Y. Wang (2012). "Appetite regulation and weight control: the role of gut hormones." Nutr Diabetes **2**: e26.

Petersen, K. F., S. Dufour, D. Befroy, R. Garcia and G. I. Shulman (2004). "Impaired mitochondrial activity in the insulin-resistant offspring of patients with type 2 diabetes." N Engl J Med **350**(7): 664-671.

Picard, M. and D. M. Turnbull (2013). "Linking the metabolic state and mitochondrial DNA in chronic disease, health, and aging." Diabetes **62**(3): 672-678.

Pich, S., D. Bach, P. Briones, M. Liesa, M. Camps, X. Testar, M. Palacin and A. Zorzano (2005). "The Charcot-Marie-Tooth type 2A gene product, Mfn2, up-regulates fuel oxidation through expression of OXPHOS system." Hum Mol Genet **14**(11): 1405-1415.

Pidoux, G., O. Witczak, E. Jarnaess, L. Myrvold, H. Urlaub, A. J. Stokka, T. Kuntziger and K. Tasken (2011). "Optic atrophy 1 is an A-kinase anchoring protein on lipid droplets that mediates adrenergic control of lipolysis." EMBO J **30**(21): 4371-4386.

Piya, M. K., A. L. Harte and P. G. McTernan (2013). "Metabolic endotoxaemia: is it more than just a gut feeling?" Curr Opin Lipidol **24**(1): 78-85.

Pories, W. J. (2008). "Bariatric surgery: risks and rewards." J Clin Endocrinol Metab **93**(11 Suppl 1): S89-96.

Pories, W. J., K. G. MacDonald, Jr., E. J. Morgan, M. K. Sinha, G. L. Dohm, M. S. Swanson, H. A. Barakat, P. G. Khazanie, N. Leggett-Frazier, S. D. Long and et al. (1992). "Surgical treatment of obesity and its effect on diabetes: 10-y follow-up." Am J Clin Nutr **55**(2 Suppl): 582S-585S.

Pories, W. J., M. S. Swanson, K. G. MacDonald, S. B. Long, P. G. Morris, B. M. Brown, H. A. Barakat, R. A. deRamon, G. Israel, J. M. Dolezal and et al. (1995). "Who would have thought it? An operation proves to be the most effective therapy for adult-onset diabetes mellitus." Ann Surg **222**(3): 339-350; discussion 350-332.

Pournaras, D. J., A. Osborne, S. C. Hawkins, R. P. Vincent, D. Mahon, P. Ewings, M. A. Ghatei, S. R. Bloom, R. Welbourn and C. W. le Roux (2010). "Remission of type 2 diabetes after gastric bypass and banding: mechanisms and 2 year outcomes." Ann Surg **252**(6): 966-971.

Prada, P. O., E. R. Ropelle, R. H. Mourão, C. T. de Souza, J. R. Pauli, D. E. Cintra, A. Schenka, S. A. Rocco, R. Rittner, K. G. Franchini, J. Vassallo, L. A. Velloso, J. B. Carvalheira and M. J. Saad (2009). "EGFR tyrosine kinase inhibitor (PD153035) improves glucose tolerance and insulin action in high-fat diet-fed mice." Diabetes **58**(12): 2910-2919.

Praefcke, G. J. and H. T. McMahon (2004). "The dynamin superfamily: universal membrane tubulation and fission molecules?" Nat Rev Mol Cell Biol **5**(2): 133-147.

Priault, M., B. Salin, J. Schaeffer, F. M. Vallette, J. P. di Rago and J. C. Martinou (2005). "Impairing the bioenergetic status and the biogenesis of mitochondria triggers mitophagy in yeast." Cell Death Differ **12**(12): 1613-1621.

Puigserver, P., J. Rhee, J. Lin, Z. Wu, J. C. Yoon, C. Y. Zhang, S. Krauss, V. K. Mootha, B. B. Lowell and B. M. Spiegelman (2001). "Cytokine stimulation of energy ex-

penditure through p38 MAP kinase activation of PPARgamma coactivator-1." Mol Cell **8**(5): 971-982.

Puigserver, P. and B. M. Spiegelman (2003). "Peroxisome proliferator-activated receptor-gamma coactivator 1 alpha (PGC-1 alpha): transcriptional coactivator and metabolic regulator." Endocr Rev **24**(1): 78-90.

Qi, Y., N. Takahashi, S. M. Hileman, H. R. Patel, A. H. Berg, U. B. Pajvani, P. E. Scherer and R. S. Ahima (2004). "Adiponectin acts in the brain to decrease body weight." Nat Med **10**(5): 524-529.

Quiros, P. M., A. J. Ramsay, D. Sala, E. Fernandez-Vizarra, F. Rodriguez, J. R. Peinado, M. S. Fernandez-Garcia, J. A. Vega, J. A. Enriquez, A. Zorzano and C. Lopez-Otin (2012). "Loss of mitochondrial protease OMA1 alters processing of the GTPase OPA1 and causes obesity and defective thermogenesis in mice." EMBO J **31**(9): 2117-2133.

Raghavendra, A. S. and G. M. Maggiora (2007). "Molecular basis sets - a general similarity-based approach for representing chemical spaces." J Chem Inf Model **47**(4): 1328-1340.

Raingeaud, J., A. J. Whitmarsh, T. Barrett, B. Derijard and R. J. Davis (1996). "MKK3- and MKK6-regulated gene expression is mediated by the p38 mitogen-activated protein kinase signal transduction pathway." Mol Cell Biol **16**(3): 1247-1255.

Rajala, M. W. and P. E. Scherer (2003). "Minireview: The adipocyte--at the crossroads of energy homeostasis, inflammation, and atherosclerosis." Endocrinology **144**(9): 3765-3773.

Rao, R. S., R. Yanagisawa and S. Kini (2012). "Insulin resistance and bariatric surgery." Obes Rev **13**(4): 316-328.

Ravussin, E. (2010). "The presence and role of brown fat in adult humans." Curr Diab Rep **10**(2): 90-92.

Regan, J., S. Breitfelder, P. Cirillo, T. Gilmore, A. G. Graham, E. Hickey, B. Klaus, J. Madwed, M. Moriak, N. Moss, C. Pargellis, S. Pav, A. Proto, A. Swinamer, L. Tong and C. Torcellini (2002). "Pyrazole urea-based inhibitors of p38 MAP kinase: from lead compound to clinical candidate." J Med Chem **45**(14): 2994-3008.

Remy, G., A. M. Risco, F. A. Inesta-Vaquera, B. Gonzalez-Teran, G. Sabio, R. J. Davis and A. Cuenda (2010). "Differential activation of p38MAPK isoforms by MKK6 and MKK3." Cell Signal **22**(4): 660-667.

Ren, J., L. Pulakat, A. Whaley-Connell and J. R. Sowers (2010). "Mitochondrial biogenesis in the metabolic syndrome and cardiovascular disease." J Mol Med (Berl) **88**(10): 993-1001.

Richardson, D. K., S. Kashyap, M. Bajaj, K. Cusi, S. J. Mandarino, J. Finlayson, R. A. DeFronzo, C. P. Jenkinson and L. J. Mandarino (2005). "Lipid infusion decreases the expression of nuclear encoded mitochondrial genes and increases the expression of extracellular matrix genes in human skeletal muscle." J Biol Chem **280**(11): 10290-10297.

Risco, A. and A. Cuenda (2012). "New Insights into the p38gamma and p38delta MAPK Pathways." J Signal Transduct **2012**: 520289.

Robertson, M. (2014). "Mitochondria--metabolism and beyond." BMC Biol **12**: 37.
Rong, J. X., Y. Qiu, M. K. Hansen, L. Zhu, V. Zhang, M. Xie, Y. Okamoto, M. D. Mattie, H. Higashiyama, S. Asano, J. C. Strum and T. E. Ryan (2007). "Adipose mitochondrial biogenesis is suppressed in db/db and high-fat diet-fed mice and improved by rosiglitazone." Diabetes **56**(7): 1751-1760.

Rosen, E. D. and B. M. Spiegelman (2006). "Adipocytes as regulators of energy balance and glucose homeostasis." Nature **444**(7121): 847-853.

Ross, H., C. G. Armstrong and P. Cohen (2002). "A non-radioactive method for the assay of many serine/threonine-specific protein kinases." Biochem J **366**(Pt 3): 977-981.

Rossetti, L., D. Massillon, N. Barzilai, P. Vuguin, W. Chen, M. Hawkins, J. Wu and J. Wang (1997). "Short term effects of leptin on hepatic gluconeogenesis and in vivo insulin action." J Biol Chem **272**(44): 27758-27763.

Russell, A. P., V. C. Foletta, R. J. Snow and G. D. Wadley (2014). "Skeletal muscle mitochondria: a major player in exercise, health and disease." Biochim Biophys Acta **1840**(4): 1276-1284.

Saada, A. (2014). "Mitochondria: mitochondrial OXPHOS (dys) function ex vivo--the use of primary fibroblasts." Int J Biochem Cell Biol **48**: 60-65.

Saely, C. H., K. Geiger and H. Drexel (2010). "Brown versus White Adipose Tissue: A Mini-Review." Gerontology.

Sanchis-Gomar, F. and C. Perez-Quilis (2014). "The p38-PGC-1alpha-irisin-betatrophin axis: Exploring new pathways in insulin resistance." Adipocyte **3**(1): 67-68.

Santel, A., S. Frank, B. Gaume, M. Herrler, R. J. Youle and M. T. Fuller (2003). "Mitofusin-1 protein is a generally expressed mediator of mitochondrial fusion in mammalian cells." J Cell Sci **116**(Pt 13): 2763-2774.

Santos, J. M. and R. A. Kowluru (2011). "Role of mitochondria biogenesis in the metabolic memory associated with the continued progression of diabetic retinopathy and its regulation by lipoic acid." Invest Ophthalmol Vis Sci **52**(12): 8791-8798.

Sarzynski, M. A., P. Jacobson, T. Rankinen, B. Carlsson, L. Sjostrom, L. M. Carlsson and C. Bouchard (2011). "Association of GWAS-based candidate genes with HDL-cholesterol levels before and after bariatric surgery in the Swedish obese subjects study." J Clin Endocrinol Metab **96**(6): E953-957.

Sato, M. and K. Sato (2011). "Degradation of paternal mitochondria by fertilization-triggered autophagy in C. elegans embryos." Science **334**(6059): 1141-1144.

Satoh, M., T. Hamamoto, N. Seo, Y. Kagawa and H. Endo (2003). "Differential sublocalization of the dynamin-related protein OPA1 isoforms in mitochondria." Biochem Biophys Res Commun **300**(2): 482-493.

Satoh, T., N. Abiru, M. Kobayashi, H. Zhou, K. Nakamura, G. Kuriya, H. Nakamura, Y. Nagayama, E. Kawasaki, H. Yamasaki, L. Yu, G. S. Eisenbarth, E. Araki, M. Mori, S. Oyadomari and K. Eguchi (2011). "CHOP deletion does not impact the development of diabetes but suppresses the early production of insulin autoantibody in the NOD mouse." Apoptosis.

Satterfield, M. C. and G. Wu (2011). "Brown adipose tissue growth and development: significance and nutritional regulation." Front Biosci **16**: 1589-1608.

Saxena, M. and T. Mustelin (2000). "Extracellular signals and scores of phosphatases: all roads lead to MAP kinase." Semin Immunol **12**(4): 387-396.

Scarpulla, R. C., R. B. Vega and D. P. Kelly (2012). "Transcriptional integration of mitochondrial biogenesis." Trends Endocrinol Metab **23**(9): 459-466.

Schafer, K., M. Halle, C. Goeschen, C. Dellas, M. Pynn, D. J. Loskutoff and S. Konstantinides (2004). "Leptin promotes vascular remodeling and neointimal growth in mice." Arterioscler Thromb Vasc Biol **24**(1): 112-117.

Schauer, P. R., B. Burguera, S. Ikramuddin, D. Cottam, W. Gourash, G. Hamad, G. M. Eid, S. Mattar, R. Ramanathan, E. Barinas-Mitchel, R. H. Rao, L. Kuller and D. Kelley (2003). "Effect of laparoscopic Roux-en Y gastric bypass on type 2 diabetes mellitus." Ann Surg **238**(4): 467-484; discussion 484-465.

Scherer, P. E. (2006). "Adipose tissue: from lipid storage compartment to endocrine organ." Diabetes **55**(6): 1537-1545.

Scherer, P. E., S. Williams, M. Fogliano, G. Baldini and H. F. Lodish (1995). "A novel serum protein similar to C1q, produced exclusively in adipocytes." J Biol Chem **270**(45): 26746-26749.

Schwartz, M. W. and D. Porte, Jr. (2005). "Diabetes, obesity, and the brain." Science **307**(5708): 375-379.

Schwartz, M. W., S. C. Woods, D. Porte, Jr., R. J. Seeley and D. G. Baskin (2000). "Central nervous system control of food intake." Nature **404**(6778): 661-671.

Scopinaro, N. (2002). "Outcome evaluation after bariatric surgery." Obes Surg **12**(2): 253.

Selness, S. R., R. V. Devraj, B. Devadas, J. K. Walker, T. L. Boehm, R. C. Durley, H. Shieh, L. Xing, P. V. Rucker, K. D. Jerome, A. G. Benson, L. D. Marrufo, H. M. Madsen, J. Hitchcock, T. J. Owen, L. Christie, M. A. Promo, B. S. Hickory, E. Alvira, W. Naing, R. Blevis-Bal, D. Messing, J. Yang, M. K. Mao, G. Yalamanchili, R. Vonder Embse, J. Hirsch, M. Saabye, S. Bonar, E. Webb, G. Anderson and J. B. Monahan (2011). "Discovery of PH-797804, a highly selective and potent inhibitor of p38 MAP kinase." Bioorg Med Chem Lett **21**(13): 4066-4071.

Semple, R. K., V. C. Crowley, C. P. Sewter, M. Laudes, C. Christodoulides, R. V. Considine, A. Vidal-Puig and S. O'Rahilly (2004). "Expression of the thermogenic nuclear hormone receptor coactivator PGC-1alpha is reduced in the adipose tissue of morbidly obese subjects." Int J Obes Relat Metab Disord **28**(1): 176-179.

Sethi, J. K. and A. J. Vidal-Puig (2007). "Thematic review series: Adipocyte biology - Adipose tissue function and plasticity orchestrate nutritional adaptation." Journal of Lipid Research **48**(6): 1253-1262.

Sharma, G. D., J. He and H. E. Bazan (2003). "p38 and ERK1/2 coordinate cellular migration and proliferation in epithelial wound healing: evidence of cross-talk activation between MAP kinase cascades." J Biol Chem **278**(24): 21989-21997.

Sharp, T. A., G. K. Grunwald, K. E. Giltinan, D. L. King, C. J. Jatkauskas and J. O. Hill (2003). "Association of anthropometric measures with risk of diabetes and cardiovascular disease in Hispanic and Caucasian adolescents." Prev Med **37**(6 Pt 1): 611-616.

Shay, J. W., D. J. Pierce and H. Werbin (1990). "Mitochondrial DNA copy number is proportional to total cell DNA under a variety of growth conditions." J Biol Chem **265**(25): 14802-14807.

Sheng, Z. H. and Q. Cai (2012). "Mitochondrial transport in neurons: impact on synaptic homeostasis and neurodegeneration." Nat Rev Neurosci **13**(2): 77-93.

Shenouda, S. M., M. E. Widlansky, K. Chen, G. Xu, M. Holbrook, C. E. Tabit, N. M. Hamburg, A. A. Frame, T. L. Caiano, M. A. Kluge, M. A. Duess, A. Levit, B. Kim, M. L. Hartman, L. Joseph, O. S. Shirihai and J. A. Vita (2011). "Altered mitochondrial dynamics contributes to endothelial dysfunction in diabetes mellitus." Circulation **124**(4): 444-453.

Sheridan, R. P. (2007). "Chemical similarity searches: when is complexity justified?" Expert Opin Drug Discov **2**(4): 423-430.

Sheridan, R. P. and S. K. Kearsley (2002). "Why do we need so many chemical similarity search methods?" Drug Discov Today **7**(17): 903-911.

Shimomura, I., K. Maeda, T. Nakamura and T. Funabashi (2006). "[Metabolic syndrome and adiponectin]." Masui **55 Suppl**: S11-17.

Shore, G. C., F. R. Papa and S. A. Oakes (2010). "Signaling cell death from the endoplasmic reticulum stress response." Curr Opin Cell Biol.

Shulman, G. I. (1999). "Cellular mechanisms of insulin resistance in humans." Am J Cardiol **84**(1A): 3J-10J.

Shulman, G. I. (2000). "Cellular mechanisms of insulin resistance." J Clin Invest **106**(2): 171-176.

Siersbaek, R., R. Nielsen and S. Mandrup (2010). "PPARgamma in adipocyte differentiation and metabolism--novel insights from genome-wide studies." FEBS Lett **584**(15): 3242-3249.

Simha, V. and A. Garg (2009). "Inherited lipodystrophies and hypertriglyceridemia." Curr Opin Lipidol **20**(4): 300-308.

Simonetti, S., X. Chen, S. DiMauro and E. A. Schon (1992). "Accumulation of deletions in human mitochondrial DNA during normal aging: analysis by quantitative PCR." Biochim Biophys Acta **1180**(2): 113-122.

Sjostrom, C. D. (2005). "Systematic review of bariatric surgery." JAMA **293**(14): 1726; author reply 1726.

Sjostrom, L., A. K. Lindroos, M. Peltonen, J. Torgerson, C. Bouchard, B. Carlsson, S. Dahlgren, B. Larsson, K. Narbro, C. D. Sjostrom, M. Sullivan, H. Wedel and G. Swedish Obese Subjects Study Scientific (2004). "Lifestyle, diabetes, and cardiovascular risk factors 10 years after bariatric surgery." N Engl J Med **351**(26): 2683-2693.

Skrekas, G., K. Antiochos and V. K. Stafyla (2011). "Laparoscopic gastric greater curvature plication: results and complications in a series of 135 patients." Obes Surg **21**(11): 1657-1663.

Skulachev, V. P. (2001). "Mitochondrial filaments and clusters as intracellular power-transmitting cables." Trends Biochem Sci **26**(1): 23-29.

Smirnova, E., L. Griparic, D. L. Shurland and A. M. van der Bliek (2001). "Dynamin-related protein Drp1 is required for mitochondrial division in mammalian cells." Mol Biol Cell **12**(8): 2245-2256.

Smirnova, E., D. L. Shurland, S. N. Ryazantsev and A. M. van der Bliek (1998). "A human dynamin-related protein controls the distribution of mitochondria." J Cell Biol **143**(2): 351-358.

Song, Z., H. Chen, M. Fiket, C. Alexander and D. C. Chan (2007). "OPA1 processing controls mitochondrial fusion and is regulated by mRNA splicing, membrane potential, and Yme1L." J Cell Biol **178**(5): 749-755.

Soriano, F. X., M. Liesa, D. Bach, D. C. Chan, M. Palacin and A. Zorzano (2006). "Evidence for a mitochondrial regulatory pathway defined by peroxisome proliferator-activated receptor-gamma coactivator-1 alpha, estrogen-related receptor-alpha, and mitofusin 2." Diabetes **55**(6): 1783-1791.

Spak, E., P. Bjorklund, H. F. Helander, M. Vieth, T. Olbers, A. Casselbrant, H. Lonroth and L. Fandriks (2010). "Changes in the mucosa of the Roux-limb after gastric bypass surgery." Histopathology **57**(5): 680-688.

Sparks, L. M., H. Xie, R. A. Koza, R. Mynatt, M. W. Hulver, G. A. Bray and S. R. Smith (2005). "A high-fat diet coordinately downregulates genes required for mitochondrial oxidative phosphorylation in skeletal muscle." Diabetes **54**(7): 1926-1933.

Stemmer, K., M. Bielohuby, B. E. Grayson, D. P. Begg, A. P. Chambers, C. Neff, S. C. Woods, R. G. Erben, M. H. Tschop, M. Bidlingmaier, T. L. Clemens and R. J. Seeley (2013). "Roux-en-Y gastric bypass surgery but not vertical sleeve gastrectomy decreases bone mass in male rats." Endocrinology **154**(6): 2015-2024.

Stojanovski, D., O. S. Koutsopoulos, K. Okamoto and M. T. Ryan (2004). "Levels of human Fis1 at the mitochondrial outer membrane regulate mitochondrial morphology." J Cell Sci **117**(Pt 7): 1201-1210.

Suganami, T. and Y. Ogawa (2010). "Adipose tissue macrophages: their role in adipose tissue remodeling." J Leukoc Biol **88**(1): 33-39.

Sun, K., C. M. Kusminski and P. E. Scherer (2011). "Adipose tissue remodeling and obesity." J Clin Invest **121**(6): 2094-2101.

Swamidass, S. J. and P. Baldi (2007). "Mathematical correction for fingerprint similarity measures to improve chemical retrieval." J Chem Inf Model **47**(3): 952-964.

Swida-Barteczka, A., A. Woyda-Ploszczyca, F. E. Sluse and W. Jarmuszkiewicz (2009). "Uncoupling protein 1 inhibition by purine nucleotides is under the control of the endogenous ubiquinone redox state." Biochem J **424**(2): 297-306.

Szewczyk, A. and L. Wojtczak (2002). "Mitochondria as a pharmacological target." Pharmacol Rev **54**(1): 101-127.

Taguchi, N., N. Ishihara, A. Jofuku, T. Oka and K. Mihara (2007). "Mitotic phosphorylation of dynamin-related GTPase Drp1 participates in mitochondrial fission." J Biol Chem **282**(15): 11521-11529.

Tajtakova, M., D. Petrasova, J. Petrovicova, M. Pytliak and Z. Semanova (2006). "Adiponectin as a biomarker of clinical manifestation of metabolic syndrome." Endocr Regul **40**(1): 15-19.

Tedesco, L., A. Valerio, M. Dossena, A. Cardile, M. Ragni, C. Pagano, U. Pagotto, M. O. Carruba, R. Vettor and E. Nisoli (2010). "Cannabinoid receptor stimulation impairs mitochondrial biogenesis in mouse white adipose tissue, muscle, and liver: the role of eNOS, p38 MAPK, and AMPK pathways." Diabetes **59**(11): 2826-2836.

Tejerina, S., A. De Pauw, S. Vankoningsloo, A. Houbion, P. Renard, F. De Longueville, M. Raes and T. Arnould (2009). "Mild mitochondrial uncoupling induces 3T3-L1 adipocyte de-differentiation by a PPARgamma-independent mechanism, whereas TNFalpha-induced de-differentiation is PPARgamma dependent." J Cell Sci **122**(Pt 1): 145-155.

Thaler, J. P. and D. E. Cummings (2009). "Minireview: Hormonal and metabolic mechanisms of diabetes remission after gastrointestinal surgery." Endocrinology **150**(6): 2518-2525.

Tice, J. A., L. Karliner, J. Walsh, A. J. Petersen and M. D. Feldman (2008). "Gastric banding or bypass? A systematic review comparing the two most popular bariatric procedures." Am J Med **121**(10): 885-893.

Todaro, G. J. and H. Green (1963). "Quantitative studies of the growth of mouse embryo cells in culture and their development into established lines." J Cell Biol **17**: 299-313.

Toldo, S., A. Severino, A. Abbate and A. Baldi (2011). "The Role of PDI as a Survival Factor in Cardiomyocyte Ischemia." Methods Enzymol **489**: 47-65.

Toledo, F. G., S. Watkins and D. E. Kelley (2006). "Changes induced by physical activity and weight loss in the morphology of intermyofibrillar mitochondria in obese men and women." J Clin Endocrinol Metab **91**(8): 3224-3227.

Tong, L., S. Pav, D. M. White, S. Rogers, K. M. Crane, C. L. Cywin, M. L. Brown and C. A. Pargellis (1997). "A highly specific inhibitor of human p38 MAP kinase binds in the ATP pocket." Nat Struct Biol **4**(4): 311-316.

Trayhurn, P. and I. S. Wood (2004). "Adipokines: inflammation and the pleiotropic role of white adipose tissue." Br J Nutr **92**(3): 347-355.

Tschritter, O., A. Fritsche, C. Thamer, M. Haap, F. Shirkavand, S. Rahe, H. Staiger, E. Maerker, H. Haring and M. Stumvoll (2003). "Plasma adiponectin concentrations predict insulin sensitivity of both glucose and lipid metabolism." Diabetes **52**(2): 239-243.

Tseng, Y. H., A. M. Cypess and C. R. Kahn (2010). "Cellular bioenergetics as a target for obesity therapy." Nat Rev Drug Discov **9**(6): 465-482.

Twig, G., A. Elorza, A. J. Molina, H. Mohamed, J. D. Wikstrom, G. Walzer, L. Stiles, S. E. Haigh, S. Katz, G. Las, J. Alroy, M. Wu, B. F. Py, J. Yuan, J. T. Deeney, B. E. Corkey and O. S. Shirihai (2008). "Fission and selective fusion govern mitochondrial segregation and elimination by autophagy." EMBO J **27**(2): 433-446.

Twig, G., B. Hyde and O. S. Shirihai (2008). "Mitochondrial fusion, fission and autophagy as a quality control axis: the bioenergetic view." Biochim Biophys Acta **1777**(9): 1092-1097.

van de Laar, A., L. de Caluwe and B. Dillemans (2011). "Relative outcome measures for bariatric surgery. Evidence against excess weight loss and excess body mass index loss from a series of laparoscopic Roux-en-Y gastric bypass patients." Obes Surg **21**(6): 763-767.

Van den Bogert, C., H. De Vries, M. Holtrop, P. Muus, H. L. Dekker, M. J. Van Galen, P. A. Bolhuis and J. W. Taanman (1993). "Regulation of the expression of mitochondrial proteins: relationship between mtDNA copy number and cytochrome-c oxidase activity in human cells and tissues." Biochim Biophys Acta **1144**(2): 177-183.

Vankoningsloo, S., A. De Pauw, A. Houbion, S. Tejerina, C. Demazy, F. de Longueville, V. Bertholet, P. Renard, J. Remacle, P. Holvoet, M. Raes and T. Arnould

(2006). "CREB activation induced by mitochondrial dysfunction triggers triglyceride accumulation in 3T3-L1 preadipocytes." J Cell Sci **119**(Pt 7): 1266-1282.

Vankoningsloo, S., M. Piens, C. Lecocq, A. Gilson, A. De Pauw, P. Renard, C. Demazy, A. Houbion, M. Raes and T. Arnould (2005). "Mitochondrial dysfunction induces triglyceride accumulation in 3T3-L1 cells: role of fatty acid beta-oxidation and glucose." J Lipid Res **46**(6): 1133-1149.

Vasseur, F., D. Meyre and P. Froguel (2006). "Adiponectin, type 2 diabetes and the metabolic syndrome: lessons from human genetic studies." Expert Rev Mol Med **8**(27): 1-12.

Veeraveedu, P. T., S. S. Palaniyandi, K. Yamaguchi, Y. Komai, R. A. Thandavarayan, V. Sukumaran and K. Watanabe (2010). "Arginine vasopressin receptor antagonists (vaptans): pharmacological tools and potential therapeutic agents." Drug Discov Today **15**(19-20): 826-841.

Vigouroux, C., M. Caron-Debarle, C. Le Dour, J. Magre and J. Capeau (2011). "Molecular mechanisms of human lipodystrophies: from adipocyte lipid droplet to oxidative stress and lipotoxicity." Int J Biochem Cell Biol **43**(6): 862-876.

Villareal, D. T., M. R. Banks, B. W. Patterson, K. S. Polonsky and S. Klein (2008). "Weight loss therapy improves pancreatic endocrine function in obese older adults." Obesity (Silver Spring) **16**(6): 1349-1354.

Virtue, S. and A. Vidal-Puig (2010). "Adipose tissue expandability, lipotoxicity and the Metabolic Syndrome--an allostatic perspective." Biochim Biophys Acta **1801**(3): 338-349.

Vlassov, V. V. (2005). "Long-term outcome of bariatric surgery." N Engl J Med **352**(14): 1495-1496; author reply 1495-1496.

Vogtherr, M., K. Saxena, S. Hoelder, S. Grimme, M. Betz, U. Schieborr, B. Pescatore, M. Robin, L. Delarbre, T. Langer, K. U. Wendt and H. Schwalbe (2006). "NMR characterization of kinase p38 dynamics in free and ligand-bound forms." Angew Chem Int Ed Engl **45**(6): 993-997.

Wai, T., A. Ao, X. Zhang, D. Cyr, D. Dufort and E. A. Shoubridge (2010). "The role of mitochondrial DNA copy number in mammalian fertility." Biol Reprod **83**(1): 52-62.

Waki, H. and P. Tontonoz (2007). "Endocrine functions of adipose tissue." Annual Review of Pathology-Mechanisms of Disease **2**: 31-56.

Wallace, T. M., J. C. Levy and D. R. Matthews (2004). "Use and abuse of HOMA modeling." Diabetes Care **27**(6): 1487-1495.

Wang, L., X. Ye, Q. Zhao, Y. Zhu, Q. Chen and L. Liu (2014). "Drp1 is dispensable for mitochondria biogenesis in induction to pluripotency but required for differentiation of embryonic stem cells." Stem Cells Dev.

Wang, P. W., T. K. Lin, S. W. Weng and C. W. Liou (2009). "Mitochondrial DNA variants in the pathogenesis of type 2 diabetes - relevance of asian population studies." Rev Diabet Stud **6**(4): 237-246.

Wang, X., C. O. Eno, B. J. Altman, Y. Zhu, G. Zhao, K. E. Olberding, J. C. Rathmell and C. Li (2011). "ER stress modulates cellular metabolism." Biochem J.

Wang, Z., B. J. Canagarajah, J. C. Boehm, S. Kassisa, M. H. Cobb, P. R. Young, S. Abdel-Meguid, J. L. Adams and E. J. Goldsmith (1998). "Structural basis of inhibitor selectivity in MAP kinases." Structure **6**(9): 1117-1128.

Watanabe, M., K. Morimoto, S. M. Houten, N. Kaneko-Iwasaki, T. Sugizaki, Y. Horai, C. Mataki, H. Sato, K. Murahashi, E. Arita, K. Schoonjans, T. Suzuki, H. Itoh and J.

Auwerx (2012). "Bile acid binding resin improves metabolic control through the induction of energy expenditure." PLoS One **7**(8): e38286.

Weckbecker, D. and J. M. Herrmann (2013). "Methods to study the biogenesis of membrane proteins in yeast mitochondria." Methods Mol Biol **1033**: 307-322.

Weisberg, S. P., D. McCann, M. Desai, M. Rosenbaum, R. L. Leibel and A. W. Ferrante, Jr. (2003). "Obesity is associated with macrophage accumulation in adipose tissue." J Clin Invest **112**(12): 1796-1808.

Weston, C. R., D. G. Lambright and R. J. Davis (2002). "Signal transduction. MAP kinase signaling specificity." Science **296**(5577): 2345-2347.

White, A., C. A. Pargellis, J. M. Studts, B. G. Werneburg and B. T. Farmer, 2nd (2007). "Molecular basis of MAPK-activated protein kinase 2:p38 assembly." Proc Natl Acad Sci U S A **104**(15): 6353-6358.

Whitmarsh, A. J. and R. J. Davis (1999). "Signal transduction by MAP kinases: regulation by phosphorylation-dependent switches." Sci STKE **1999**(1): PE1.

Wild, P. and I. Dikic (2010). "Mitochondria get a Parkin' ticket." Nat Cell Biol **12**(2): 104-106.

Wilson, K. P., P. G. McCaffrey, K. Hsiao, S. Pazhanisamy, V. Galullo, G. W. Bemis, M. J. Fitzgibbon, P. R. Caron, M. A. Murcko and M. S. Su (1997). "The structural basis for the specificity of pyridinylimidazole inhibitors of p38 MAP kinase." Chem Biol **4**(6): 423-431.

Wilson-Fritch, L., A. Burkart, G. Bell, K. Mendelson, J. Leszyk, S. Nicoloro, M. Czech and S. Corvera (2003). "Mitochondrial biogenesis and remodeling during adipogenesis and in response to the insulin sensitizer rosiglitazone." Mol Cell Biol **23**(3): 1085-1094.

World Health Organization. Global status report on noncommunicable diseases. Geneva, Switzerland, World Health Organization: v.

Wu, C. A., Y. Chao, S. G. Shiah and W. W. Lin (2013). "Nutrient deprivation induces the Warburg effect through ROS/AMPK-dependent activation of pyruvate dehydrogenase kinase." Biochim Biophys Acta **1833**(5): 1147-1156.

Wu, Y. T., S. B. Wu and Y. H. Wei (2014). "Roles of Sirtuins in the Regulation of Antioxidant Defense and Bioenergetic Function of Mitochondria under Oxidative Stress." Free Radic Res.

Xia, Z., M. Dickens, J. Raingeaud, R. J. Davis and M. E. Greenberg (1995). "Opposing effects of ERK and JNK-p38 MAP kinases on apoptosis." Science **270**(5240): 1326-1331.

Xing, L., H. S. Shieh, S. R. Selness, R. V. Devraj, J. K. Walker, B. Devadas, H. R. Hope, R. P. Compton, J. F. Schindler, J. L. Hirsch, A. G. Benson, R. G. Kurumbail, R. A. Stegeman, J. M. Williams, R. M. Broadus, Z. Walden and J. B. Monahan (2009). "Structural bioinformatics-based prediction of exceptional selectivity of p38 MAP kinase inhibitor PH-797804." Biochemistry **48**(27): 6402-6411.

Xu, C. Y., B. Bailly-Maitre and J. C. Reed (2005). "Endoplasmic reticulum stress: cell life and death decisions." Journal of Clinical Investigation **115**(10): 2656-2664.

Yamauchi, T., J. Kamon, Y. Ito, A. Tsuchida, T. Yokomizo, S. Kita, T. Sugiyama, M. Miyagishi, K. Hara, M. Tsunoda, K. Murakami, T. Ohteki, S. Uchida, S. Takekawa, H. Waki, N. H. Tsuno, Y. Shibata, Y. Terauchi, P. Froguel, K. Tobe, S. Koyasu, K. Taira, T. Kitamura, T. Shimizu, R. Nagai and T. Kadowaki (2003). "Cloning of adiponectin receptors that mediate antidiabetic metabolic effects." Nature **423**(6941): 762-769.

Yamauchi, T., J. Kamon, H. Waki, Y. Imai, N. Shimozawa, K. Hioki, S. Uchida, Y. Ito, K. Takakuwa, J. Matsui, M. Takata, K. Eto, Y. Terauchi, K. Komeda, M. Tsunoda, K. Murakami, Y. Ohnishi, T. Naitoh, K. Yamamura, Y. Ueyama, P. Froguel, S. Kimura, R. Nagai and T. Kadowaki (2003). "Globular adiponectin protected ob/ob mice from diabetes and ApoE-deficient mice from atherosclerosis." J Biol Chem **278**(4): 2461-2468.

Yoon, Y., K. R. Pitts and M. A. McNiven (2001). "Mammalian dynamin-like protein DLP1 tubulates membranes." Mol Biol Cell **12**(9): 2894-2905.

Yoshii, S. R., C. Kishi, N. Ishihara and N. Mizushima (2011). "Parkin mediates proteasome-dependent protein degradation and rupture of the outer mitochondrial membrane." J Biol Chem **286**(22): 19630-19640.

Yu, C., Y. Chen, G. W. Cline, D. Zhang, H. Zong, Y. Wang, R. Bergeron, J. K. Kim, S. W. Cushman, G. J. Cooney, B. Atcheson, M. F. White, E. W. Kraegen and G. I. Shulman (2002). "Mechanism by which fatty acids inhibit insulin activation of insulin receptor substrate-1 (IRS-1)-associated phosphatidylinositol 3-kinase activity in muscle." J Biol Chem **277**(52): 50230-50236.

Yu, T., J. L. Robotham and Y. Yoon (2006). "Increased production of reactive oxygen species in hyperglycemic conditions requires dynamic change of mitochondrial morphology." Proc Natl Acad Sci U S A **103**(8): 2653-2658.

Zechner, D., R. Craig, D. S. Hanford, P. M. McDonough, R. A. Sabbadini and C. C. Glembotski (1998). "MKK6 activates myocardial cell NF-kappaB and inhibits apoptosis in a p38 mitogen-activated protein kinase-dependent manner." J Biol Chem **273**(14): 8232-8239.

Zhang, H., T. J. Schulz, D. O. Espinoza, T. L. Huang, B. Emanuelli, K. Kristiansen and Y. H. Tseng (2010). "Cross talk between insulin and bone morphogenetic protein signaling systems in brown adipogenesis." Mol Cell Biol **30**(17): 4224-4233.

Zhang, H., Y. Wang, J. Zhang, B. J. Potter, J. R. Sowers and C. Zhang (2011). "Bariatric surgery reduces visceral adipose inflammation and improves endothelial function in type 2 diabetic mice." Arterioscler Thromb Vasc Biol **31**(9): 2063-2069.

Zhang, X., K. S. Lam, H. Ye, S. K. Chung, M. Zhou, Y. Wang and A. Xu (2010). "Adipose tissue-specific inhibition of hypoxia-inducible factor 1{alpha} induces obesity and glucose intolerance by impeding energy expenditure in mice." J Biol Chem **285**(43): 32869-32877.

Zhang, Y., R. Proenca, M. Maffei, M. Barone, L. Leopold and J. M. Friedman (1994). "Positional cloning of the mouse obese gene and its human homologue." Nature **372**(6505): 425-432.

Zhang, Z., N. Wakabayashi, J. Wakabayashi, Y. Tamura, W. J. Song, S. Sereda, P. Clerc, B. M. Polster, S. M. Aja, M. V. Pletnikov, T. W. Kensler, O. S. Shirihai, M. Iijima, M. A. Hussain and H. Sesaki (2011). "The dynamin-related GTPase Opa1 is required for glucose-stimulated ATP production in pancreatic beta cells." Mol Biol Cell **22**(13): 2235-2245.

Zhao, J., T. Liu, S. Jin, X. Wang, M. Qu, P. Uhlen, N. Tomilin, O. Shupliakov, U. Lendahl and M. Nister (2011). "Human MIEF1 recruits Drp1 to mitochondrial outer membranes and promotes mitochondrial fusion rather than fission." EMBO J **30**(14): 2762-2778.

Zhu, J. H., A. M. Gusdon, H. Cimen, B. Van Houten, E. Koc and C. T. Chu (2012). "Impaired mitochondrial biogenesis contributes to depletion of functional mitochondria in chronic MPP+ toxicity: dual roles for ERK1/2." Cell Death Dis **3**: e312.

Zhuang, S., J. T. Demirs and I. E. Kochevar (2000). "p38 mitogen-activated protein kinase mediates bid cleavage, mitochondrial dysfunction, and caspase-3 activation during apoptosis induced by singlet oxygen but not by hydrogen peroxide." J Biol Chem **275**(34): 25939-25948.

Ziccardi, P., F. Nappo, G. Giugliano, K. Esposito, R. Marfella, M. Cioffi, F. D'Andrea, A. M. Molinari and D. Giugliano (2002). "Reduction of inflammatory cytokine concentrations and improvement of endothelial functions in obese women after weight loss over one year." Circulation **105**(7): 804-809.

Zick, M., S. Duvezin-Caubet, A. Schafer, F. Vogel, W. Neupert and A. S. Reichert (2009). "Distinct roles of the two isoforms of the dynamin-like GTPase Mgm1 in mitochondrial fusion." FEBS Lett **583**(13): 2237-2243.

Zorzano, A., M. Liesa and M. Palacin (2009). "Mitochondrial dynamics as a bridge between mitochondrial dysfunction and insulin resistance." Arch Physiol Biochem **115**(1): 1-12.

Zorzano, A., M. Liesa and M. Palacin (2009). "Role of mitochondrial dynamics proteins in the pathophysiology of obesity and type 2 diabetes." Int J Biochem Cell Biol **41**(10): 1846-1854.

Zou, M. H., S. S. Kirkpatrick, B. J. Davis, J. S. Nelson, W. G. t. Wiles, U. Schlattner, D. Neumann, M. Brownlee, M. B. Freeman and M. H. Goldman (2004). "Activation of the AMP-activated protein kinase by the anti-diabetic drug metformin in vivo. Role of mitochondrial reactive nitrogen species." J Biol Chem **279**(42): 43940-43951.

Zuegel, N. P., R. A. Lang, T. P. Huttl, M. Gleis, M. Ketfi-Jungen, I. Rasquin and M. Kox (2012). "Complications and outcome after laparoscopic bariatric surgery: LAGB versus LRYGB." Langenbecks Arch Surg **397**(8): 1235-1241.

Zungu, M., J. Schisler and M. S. Willis (2011). "All the little pieces. -Regulation of mitochondrial fusion and fission by ubiquitin and small ubiquitin-like modifer and their potential relevance in the heart." Circ J **75**(11): 2513-2521.